Characterization of the in vivo functions of PrimPol, a novel TLS primase-polymerase

Irena Stevanović

Doctoral thesis

University Pompeu Fabra 2013

Director: **Travis Stracker, PhD**

Tutor: **Francesc Posas Garriga, PhD**

Institute for Research in Biomedicine, Barcelona

Genomic Instability and Cancer Laboratory

Acknowledgments

This dissertation is dedicated most of all to my parents and my two brothers for the infinite love, understanding and support they have given me throughout my life; to my boyfriend Jordi Caparrós Fernández, for his love, devotion, care and all the illustrations we made together; to Hilary C. Robinson and Dunja Zungri Sijan for being wonderful, trusting friends; to my brilliant colleagues and friends Marko Marjanovic, Peter Jung and Jelena Urosevic for guidance and encouragement; to the PhD Symposium crew of 2011: Sabine, Jordi, Mili, Laura, Manuel, Selma Radek, Andrey, Kader, Eva, Lara; for the unforgettable experience of being logistical "Ocean 12" scientific package; to Helea, Rubi, Sylwia, Constanze, Petra, Pablo, Joost, Michael, Thomas and the Argentinian family for making this Barcelona experience unique and beautiful; to Nenad Bozinovic for being the initial sparkle of all this whimsical chaos; to the amazing IRB director, Joan Guinovart, for giving us the opportunity to explore our talents in a cutting edge scientific institute, and for giving us the chance to even go beyond the bench and find out where else we can be superb; to all the wonderful scientific minds at the IRB that I have come into contact with, especially Travis Stracker and Eduard Batlle for their inspiring passion for science; to my mentor Travis Stracker for giving me an opportunity to work on such challenging project, as well for supporting me in independent working and thinking, thus enabling me to discover my potential. I have matured scientifically in last four years, but also personally. Finally, this thesis is dedicated to those who will figure out how to boost the scientific budget to what it used to be, if not more. We need funds now, because only now is that special moment to explore beyond.

"In 5 billion years, the expansion of the universe will have progressed to the point where all other galaxies will have receded beyond detection. Indeed, they will be receding faster than the speed of light, so detection will be impossible. Future civilizations will discover science and all its laws, and never know about other

galaxies or the cosmic background radiation. They will inevitably come to the wrong conclusion about the universe..... We live in a special time, the only time, where we can observationally verify that we live in a special time.."

Lawrence M. Krauss, 2009.

Abstract

We have identified PrimPol, a yet uncharacterized protein that can act *in vitro* as a low processivity polymerase able to bypasses thymine dimers in DNA. PrimPol localizes to both the nucleus and mitochondria. In order to investigate functional role of this enzyme we have generated genetrap mice, with a LacZ reporter gene under control of the endogenous promoter, and knock out mice where PrimPol expression is abolished. In cells lacking PrimPol, we can see increased genomic instability even in the absence of damage, indicating that it may suppress expression of common fragile sites. Upon UV damage and aphidicolin treatment, there was a significant increase in chromosomal aberrations, followed by sustained phosphorylation of Chk1 and p53 in *PrimPol*$^{-/-}$ MEFs. In genetrap embryos e14.5, PrimPol expression pattern was ectoderm and eye specific. This was confirmed in the skin of adult mice by LacZ staining and qPCR where we see PrimPol being most highly expressed in the skin compared to other tissues. Xeroderma pigmentosum (XP) is a disease caused by mutation of TLS polymerase Pol η responsible for the repair of TT dimers. XP is associated with increased incidence of sunlight-induced skin cancers. Depletion of Pol η in *PrimPol*$^{-/-}$ MEFs leads to increased sensitivity to UV damage. To validate the *in vivo* function of PrimPol, we observed histological changes in the skin of mice upon acute UV dose treatment for 5 days. *PrimPol*$^{-/-}$ damaged skin showed marked epidermal hyperplasia compared to WT. We have also observed in aged *PrimPol*$^{-/-}$ mice, and in young mice damaged by UV, upregulation of mitochondrial DNA copy number across different tissues, implying that PrimPol may be dealing with the repair of oxidative damage as well. In accordance with these findings, we hypothesize that PrimPol acts as a translesion polymerase that can bypass bulky lesions generated by UV and reactive oxygen to promote the integrity of nuclear and mitochondrial DNA and promote normal aging. PrimPol deficient animals provide a model system for understanding the etiology of sunlight induced skin cancers and the role of mitochondrial DNA integrity in aging.

Resumen

Hemos identificado PrimPol, una proteína no caracterizada que actua *in vitro* como una polimerasa de bajo procesamiento que es capaz de evitar (*bypass*) los dímeros de timina del ADN. PrimPol se localiza tanto en el núcleo como en las mitocondrias. Para poder investigar la función de este enzima, hemos generado ratones *genetrap*, usando LacZ como gen marcador (*reporter gene*) bajo el control de un promotor endógeno y ratones *knock out* en los cuales se ha abolido la expression de PrimPol. En las células que no expresan PrimPol podemos observar un aumento de la inestabilidad genómica incluso en ausencia de daño, indicando que podría suprimir la expression de sitios frágiles comunes. Tras inducir daño mediante radiación ultravioleta (UV) y tratamiento con afidicolina se observó un aumento significativo de aberraciones cromosómicas, seguido de una fosforilación sostenida de Chk1 y p53 en fibroblastos embrionarios de ratones (MEFs) *PrimPol*$^{-/-}$. En embriones *genetrap* de 14.5 días el patrón de expresión era específico de ectodermo y ojos. Dicha expresión se pudo confirmar en piel de ratones adultos mediante tinción de LacZ y qPCR donde pudimos ver que PrimPol está altamente expresado en piel en comparación con otros tejidos. Xeroderma pigmentosum (XP) es una enfermedad causada por una mutación en el gen Pol η, una TLS (*trans lesion*) polimerasa responsable de la reparación de los dímeros de timina. XP se asocia con un aumento de la incidencia de casos de cáncer de piel por exposición solar. La depleción de Pol η en MEFs *PrimPol*$^{-/-}$ produce un aumento en la sensibilidad al daño por UV. Para validar la función de PrimPol *in vivo*, observamos cambios histológicos en la piel de ratones tras ser tratados con una dosis aguda de UV durante 5 días. La piel dañada en ratones *PrimPol*$^{-/-}$ mostró una marcada hiperplasia epidérmica en comparación con los ratones salvajes. También hemos observado que en ratones *PrimPol*$^{-/-}$ de edad avanzada y en ratones jóvenes con lesiones por UV hay un aumento del número de copias de ADN mitocondrial en diferentes tejidos, lo que sugiere que PrimPol podría estar también implicada en la reparación del daño oxidativo. De acuerdo con estos descubrimientos nos planteamos la hipótesis de que PrimPol pueda actuar como una TLS polimerasa que puede saltarse (*bypass*) grandes lesiones inducidas por UV y especies reactivas de oxígeno y así promover la integridad del ADN nuclear y mitocondrial además de un normal envejecimiento. Los animales deficientes en PrimPol proporcionan un modelo para entender la etiología de los cánceres de piel inducidos por la luz solar y el papel de la integridad del ADN mitocondrial en el envejecimiento.

Preface

Fifteen years ago, the polymerase field was at a turning point. Many new enzymes able to catalyze DNA synthesis were discovered, as were the novel functions that they can perform. It became clear that the eukaryotic cell uses the diverse roles of many polymerases in the maintenance of its DNA. As far as we know at this point, the cell is utilizing at least 15 distinct polymerases for the duplication and repair of DNA. It was speculated recently that additional polymerases exist, but the pace of initial discoveries was followed by an uneventful interval, in which our knowledge of the functional properties of polymerases continued to expand without the identification of new molecules. In this dissertation we report the discovery and characterization of novel eukaryotic primase-polymerase named for its functional properties, PrimPol. There were no reports in the literature on this enzyme when we started investigating its functional roles. To obtain a thorough perspective on its biological significance, we tackled this project from several sides. We generated a mouse model and tried to corroborate observed phenotypes in cellular models. This project has been very challenging as there was no any literature available, no experimental tools developed in a newly set laboratory and no available antibody for the endogenous isoform of mouse PrimPol. However, we have managed to uncover some of the roles this protein performs and we propose that PrimPol is an important polymerase that is required for genomic stability. We demonstrate that PrimPol is involved in UV induced lesion tolerance pathways and it is specialized to deal particularly with UV 6-4 photoproducts. This is potentially significant since this enzyme can promote the clearance of highly mutagenic lesions and therefore, we suppose, it can protect the skin from UV induced mutations that can lead to tumor initiation in the skin. In addition, PrimPol is important for mitochondrial biogenesis. We demonstrate that loss of PrimPol may result in oxidative imbalances that are compensated by hyperproliferation of mitochondrial DNA. Considering all of these data, we propose that the loss of PrimPol can impact on the overall wellbeing of the organism by predisposing it to a loss of genomic integrity and accelerated aging. We have opened many questions in this thesis and we hope that with the help of experimental tools we have developed in our laboratory they will soon be answered.

Abbreviations

6-4 PP	Pyrimidine (6-4) pyrimidone photoproduct
8-oxo-G	8-oxo-2'-deoxyguanosine
A	Adenine
AEP	Archaeo-eukaryotic primase
APS	Ammonium persulpha
ATR	Ataxia-telangiectasia mutated and Rad3-related
ATM	Ataxia-telangiectasia mutated
BER	Base excision repair
BLAST	Basic Local Alignment Search Tool
bp	base pair
BRCA2	Breast cancer type 2 susceptibility protein
BRCT	Breast cancer type 1 susceptibility protein (BRCA1) carboxyl-terminus
BLAST	Basic Local Alignment Search Tool
BSA	Bovine serum albumin
C	Cytosine
CBMSO	Centro de Biología Molecular Severo Ochoa
CCDC111	Coiled-coil domain containing 111
CDC	Cell division cycle
cDNA	Complementary DNA
CFS	Common fragile sites
Chk1	Checkpoint kinase 1
Chk2	Checkpoint kinase 2
Co-ip	Co-immunoprecipitation
CPD	Cyclobutane pyrimidine dimer
C-terminus	Carboxyl-terminus
CSR	Class switch recombination
DAPI	4',6-diamidino-2-phenylindole
DDT	Dichlorodiphenyltrichloroethane
DMSO	Dimethyl sulfoxide

DNA	Deoxyribonucleic acid
dCMP	Deoxycytidine monophosphate
dNTP	Deoxynucleotide 5' triphosphate
dRP	5'-deoxyribose phosphate
DSB	Double strand break
EDTA	Ethylenediaminetetra-acetic acid
EGTA	Ethyleneglycoltetra-acetic acid
FBS	Foetal bovine serum
FRT	Flp Recombinase Target
G	Guanine
G1	Growth phase 1
G2	Growth phase 2
GFP	Green fluorescent protein
GT	Gene trap
H_2O_2	Hydrogen peroxide
HA	Haemagglutinin (influenza)
HEK-293	Human embryonic kidney-293
HEPES	4-(2-Hydroxyethyl)piperazine-1-ethanesulfonic acid
HR	Homologous recombination
HRP	Horseradish peroxidase
Hs	Homo sapiens
HU	Hydroxyurea
IF	Immunfluorescence
IPTG	Isopropyl !-D-1-thiogalactopyranoside
IR	Ionising radiation
kb	Kilobase pair
kDa	Kilo Dalton
KO	Knock-out
LOH	Loss of heterozygosity
M	Mitosis
Mb	Megabase pair
MEFs	Mouse embryonic fibroblasts
MCM	Minichromosome maintenance

MMR	Mismatch repair
MMS	Methyl methanesulfonate
MMC	Mitomycin C
mRNA	messenger ribonucleic acid
mtDNA	Mitochondrial DNA
NER	Nucleotide excision repair
NHEJ	Non-homologous end joining
NLS	Nuclear localization sequence
N-terminus	Amino-terminus
NTP	Nucleotide triphosphate
ORC	Origin recognition complex
ORF	Open reading frame
PAGE	Polyacrylamide gel electrophoresis
PCNA	Proliferating cell nuclear antigen
PCR	Polymerase chain reaction
PEI	Polyethylenimine
PI	Propidium iodide
PIPES	Piperazine-N,N"-bis(2-ethanesulfonic acid)
PMSF	Phenylmethylsulfonylfluoride
Pol	DNA-dependant DNA polymerase
Pre-RC	Pre-replication complex
Prim1	DNA primase polypeptide 1
Prim2	DNA primase polypeptide 2
PrimPol	DNA-dependant primase-polymerase
PVDF	Polyvinyladine fluoride
RAD	Radiation (gene)
REV	Reversionless (gene)
RFC	Replication factor C
ROS	Reactive oxygen species
RPA	Replication protein A
RNA	Ribonucleic acid
RPE	Retinal pigment epithelial
SHM	Somatic hypermutation

siRNA	Small interfering ribonucleic acid
S-phase	Synthesis-phase
SDS	Sodium dodecyl sulfate
SNP	Single nucleotide polymorphism
SV40	Simian Virus 40
Tm	Melting temperature
TUNEL	Terminal deoxynucleotidyl transferase dUTP nick end labelling
TLS	Translesion synthesis
U2OS	US-osteosarcoma
WT	Wild type
UV	Ultra violet
XP	Xeroderma pigmentosum
XP-A	Xeroderma pigmentosum complementation group A
XP-V	Xeroderma pigmentosum variant

Table of contents

Abstract **1**

Resumen **2**

Preface **3**

Abbreviations **4**

Table of contents **8**

List of figures **12**

List of tables **14**

Introduction **15**

1. DNA Polymerases **16**

1.1. Overview of eukaryotic DNA Polymerases **16**

1.2. DNA Polymerases involved in the genome duplication **18**

- DNA replication in the nucleus 20
- DNA replication in the mitochondria 21

1.3. DNA Polymerases involved in the DNA repair and DNA damage tolerance **22**

- DNA repair in the nucleus 22
- DNA repair in the mitochondria 25

1.4. DNA damage tolerance **26**

1.5. Bypass of DNA damage caused by UV irradiation **28**

- The UV Induced DNA Damage Response 29

1.6. The overview of Y-family polymerases and DNA polymerase ζ **30**

- DNA polymerase η 32
- DNA polymerase ι 34
- DNA polymerase κ 36
- REV1 37
- DNA polymerase ζ 39

1.7. Fidelity of TLS polymerases **40**

1.8. Distinct functions of TLS polymerases **42**

- Class switch recombination and somatic hypermutation 42

- Common fragile sites stability 44

2. DNA polymerases and diseases 47

2.1. Pol η and Xeroderma Pigmentosum Variant 48

2.2. DNA Pol γ and human diseases 49

2.3. TLS DNA polymerases and genetic instability 52

3. Mouse models 53

3.1. DNA Polymerase η mouse models 54

3.2. DNA Polymerase ι mouse models 55

3.3. DNA Polymerase κ mouse models 55

3.4. REV1 mouse models 56

4. DNA Primases 57

5. PrimPol, novel primase polymerase 60

Materials and methods 63

1. Generation of a PrimPol deficient mouse model 64

1.1. Generation and screening of PrimPol targeting constructs 64

1.2. Genotyping strategy 65

1.3. Real time PCR based assessment of PrimPol expression levels 66

2. Cultured human and mouse cell methods 68

2.1. Cell cultures 68

- Human cell lines 68
- Preparation of mouse embryo fibroblasts (MEFs) 68
- Culture of primary MEFs 69
- Generation and culture of transformed MEFs 69
- 3T3 Proliferation assay 69

2.2. Isolation of genomic DNA for qPCR on mtDNA 69

2.3. Total protein extraction and western blotting 70

- Soluble and insoluble fractions 72

2.4. Purification of Strep-tagged mouse PrimPol from human cultured cells 73

- Subcloning of PrimPol in retroviral vector 73
- Retroviral overexpression 73
- Small scale purification 74

- Affinity purification for mass spectrometry analysis 74
- Silver staining 75

2.5. Knockdown assays 75

- Short hairpin RNA-mediated knockdown 75
- Gene expression profiling 76

2.6. Bioinformatic analysis 76

- Differential expression analysis 76
- Generation of heatmaps 76

2.7. Flow cytometry 77

- BrdU labeling for G_1/S checkpoint assay 77
- G2/M Checkpoint Assay 77

2.8. Clonogenic survival assay 77

- DNA damaging agents and drug treatments 78
- RNA interference 80

2.9. Immunofluorescence microscopy 81

3.0. Metaphase spreads 82

3.1. CPD and 6-4PP ELISA 82

3.2. Isolation of thymocytes for the analysis of differentiation and apoptosis 83

- Isolation of B lymphocytes and stimulation 83
- Class switch recombination (CSR) 84

3. Histological methods 84

3.1. X-gal staining of embryos 84

3.2. Whole mount staining of skin with X-gal 85

3.3. Immunohistochemistry 85

3.4. TUNEL staining of the skin 86

Results 87

Hypothesis and objectives 88

1. Generation and characterization of PrimPol deficient mice 89

1. 1. Strategy and design of *PrimPol* deficient mice 89

1.2. Mapping the expression landscape of PrimPol 94

- PrimPol expression in e13.5 embryos 94
- PrimPol expression in the skin of 6 months old mice 97
- *PrimPol* expression across different tissues 97

1.3. PrimPol deficient mice are susceptible to UV induced damage 98
- Epidermal hyperplasia upon acute UV exposure 99
- Increased persistent damage in skin deficient for *PrimPol* 100

1.4. Analysis of PrimPol requirement in DDR pathways 102
- Sensitivity of PrimPol deficient MEFs to DNA damaging agents 102
- PrimPol functions independently of the ATR pathway in the UV response 104
- Epistasis analysis of PrimPol in UV damage tolerance 108

1.5. *PrimPol* deficiency does not strongly exacerbate cell cycle progression after DNA damage 112

1.6. Loss of PrimPol affects genomic stability 114

1.7. ATR pathway is overactivated in PrimPol deficient MEFs 117

1.8. Loss of PrimPol results in delayed clearance of UV lesions in MEFs 119

1.9. PrimPol and alternative DNA damage response pathways 120

2. *In vitro* studies of PrimPol cellular localization, functions and interactions 125

2.1. PrimPol expression in cultured cells 125

2.2. Immunofluorescent detection of stably and transiently expressed recombinant PrimPol 126

2.3. PrimPol re-localization upon DNA damage 131
- PrimPol assembles into foci in UV-C irradiated cells 131
- PrimPol assembles into foci in cells damaged by ionizing radiation 132
- PrimPol distribution is not altered after oxidative damage 134

2.4. UV regulation of PrimPol expression 134

2.5. Identification of mouse PrimPol interaction partners 136
- Potential PrimPol interacting proteins identified by LC-MS/MS 138
- Validation of PrimPol interacting proteins 140

3. PrimPol is required for mitochondrial homeostasis 143

Discussion 148

1. Introduction 149

1.1. PrimPol is a novel translesion polymerase in the response to UV 149

1.2. PrimPol is required for chromosomal stability: a role at fragile sites? 154

1.3. PrimPol is required for mitochondrial biogenesis 157

2. A unified model for PrimPol functions 161

Conclusions **162**

Bibliography **163**

List of figures

Figure 1. DNA polymerases identified in mammals 17
Figure 2. DNA polymerases are necessary for many cellular events in both the nucleus and mitochondria 19
Figure 3. Sources of DNA damage and mechanisms to repair them 24
Figure 4. Simplified DNA damage tolerance model 27
Figure 5. One or two-polymerase combinations define error-free and error-prone TLS 35
Figure 6. The fidelity of DNA synthesis 41
Figure 7. Origins of common fragile sites 45
Figure 8. Damage of mitochondrial DNA can contribute to developmental diseases and accelerated aging 51
Figure 9. Pol-Prim complex and interacting partners 59
Figure 10. Conserved domains of PrimPol (mus musculus) 61
Figure 11. Alignment of human and mouse PrimPol sequence 90
Figure 12. Schematic of the engineered PrimPol locus. 91
Figure 13. PrimPol gene expression is disrupted in PrimPol$^{-/-}$ (KO) and PrimPol$^{gt/gt}$ (GT) mice 92
Figure 14. Mendelian ratio 92
Figure 15. Weights of mice in the first three months of life 93
Figure 16. Analysis of primary cell growth 93
Figure 17. Expression of PrimPol during embryonic development. 95
Figure 18. Expression of PrimPol in the ectoderm and the eye 95
Figure 19. Expression of PrimPol in the adult the skin and the ear 96
Figure 20. PrimPol expression profile across different tissues. 97
Figure 21. Scheme of experimental setup for UV damage of skin 98
Figure 22. Quantification of epidermal hyperplasia after acute dose of UVB irradiation 99
Figure 23. Quantification of γH2AX positive cells in UVB damaged epidermis 101
Figure 24. Sensitivity to different damaging treatments determined by the clonogenic survival assay 103
Figure 25. Sensitivity to UVC determined by the clonogenic survival assay. 104
Figure 26. Sensitivity to caffeine determined by clonogenic survival assay. 105
Figure 27. Sensitivity to PARP inhibitors determined by clonogenic survival assay 106
Figure 28. Sensitivity to CHK inhibitors determined by clonogenic survival assay 106
Figure 29. Sensitivity to ATR inhibitors determined by clonogenic survival assay 107
Figure 30. Scheme of experimental design for siRNA mediated downregulation of several genes of interest 108

Figure 31. Epistasis analysis between PrimPol and Pol η, Nbs1 or Rev1 in UV sensitivity 109
Figure 32 Sensitivity to UVC for Nbs1$^{\Delta B/\Delta B}$ cell lines 111
Figure 33. Cell cycle distribution 112
Figure 34. Analysis of G1/S checkpoint response upon UVC induced damage 113
Figure 35. Analysis of G2/M checkpoint upon UVC induced damage 113
Figure 36. Metaphase aberrations in exponentially proliferating MEFs 115
Figure 37. Examples of metaphase spreads and aberrations 116
Figure 38. Chromosome distribution per metaphase spread 116
Figure 39. Evaluation of ATR checkpoint signaling upon UVC induced damage 118
Figure 40. Clearance of CPD and 6-4PP lesions over time after UVC damage 119
Figure 41. Differentiation of Thymocytes 121
Figure 42. Viability of thymocytes after X-irradiation 121
Figure 43. Analysis of class switch recombination 123
Figure 44. Proliferation of B cells during maturation 123
Figure 45. Detection by IF of ectopically expressed PrimPol in HEK293 cells 126
Figure 46. Synchronization of mPrimPol$^{C/SF}$ HEK293 cells by nocodazole 127
Figure 47. Localization of ectopically expressed human and mouse isoform PrimPol in HEK293 128
Figure 48. Localization of mouse and human isoform of PrimPol in U2OS cells 129
Figure 49. Prediction of nuclear localization sequence (NLS) in mouse and human PrimPol orthologs 130
Figure 50. PrimPol and RPA co-localization in foci upon UVC irradiation 131
Figure 51. PrimPol and γH2AX co-localization in nuclear foci upon X-irradiation 133
Figure 52. H_2O_2 damage does not induce PrimPol focalization 133
Figure 53. PrimPol and Pol η mRNA expression upon UVC irradiation 135
Figure 54. PrimPol protein levels upon UVC irradiation 136
Figure 55. Affinity purification of stably over-expressed Strep-FLAG tagged mPrimPol from whole cell lysate. 137
Figure 56. mPrimPol co-purifies with RPA and MCM4 141
Figure 57. Validating additional mass spectrometry hits 142
Figure 58. mPrimPol co-purifies with mtSSBP 142
Figure 59. Differential expression of genes upon downregulation of PrimPol in HEK293 143
Figure 60. Validation of the efficiency of PrimPol shRNA downregulation by WB 145
Figure 61. Validation of microarray selected targets by small scale qPCR 145
Figure 62. Oxygen consumption rate in hPrimPol downregulated cell lines 146
Figure 63. Analysis of mitochondrial DNA copy number by qPCR 147
Figure 64. PrimPol is required for DNA damage tolerance 153
Figure 65. PrimPol is required for stability of fragile sites 155
Figure 66. PrimPol is required for mitochondrial homeostasis 160

List of tables

Table 1. PCR reaction conditions 64
Table 2. Screening primer sequences 65
Table 3. Primer combinations and product sizes for long range PCR 65
Table 4. PCR genotyping primers for genomic DNA 66
Table 5. Expected products from indicated alleles (KO, WT, COND or TRAP) 66
Table 6. Genotyping primers for cDNA (by qPCR) 67
Table 7. qPCR conditions 67
Table 8. Primers for qPCR for quantification of mtDNA 70
Table 9. List of primary antibodies 71
Table 10. List of secondary antibodies 72
Table 11. Colony forming assay plating conditions and doses of damaging agents 79
Table 12. siRNA oligonucleotide sequences 80
Table 13. Primers for diagnostic qPCR of downregulated mouse genes (for cDNA) 81
Table 14. The putative interactors of PrimPol 139
Table 15. The list of up- or down-regulated genes in shPP7 cell line 135

Introduction

1. DNA Polymerases

Nature has evolved highly specialized and sophisticated tools that allow DNA to be replicated and maintained so that it can be faithfully passed on from one generation to the next. The replication of DNA requires enzymes called DNA polymerases (DNA pols) that are used for both copying and correcting DNA errors through replication, different types of DNA repair events and DNA recombination. Through these functions, polymerases mediate important physiological processes in diverse cell types including those in the immune system and germline. Since the discovery of DNA pol α in eukaryotic cells by Kornberg and Lehman in 1956 (Bessman et al. 1956), the number of DNA pols identified has grown. Today we know of four different DNA pol families in higher eukaryotic cells containing a total of 15 DNA pols that perform distinct as well as redundant functions, illustrated in Figure 1.

1.1. Overview of eukaryotic DNA Polymerases

The diversification, throughout evolution, from single-cell to multicellular organisms, has required the diversification of cellular functions and the acquisition of more complex levels of regulation to ensure fidelity in the duplication of the genetic information of the cells. Based on sequence homology and structural similarities, eukaryotic DNA pols have been grouped in four different families: A, B, X and Y (Ito and Braithwaite 1991). The exact duplication of the genetic information is achieved through a complex network of enzymes and proteins that constitute the replisome. The core enzymes of the replisome are three different DNA pols that are members of B-family: Pol α (alpha) initiating primase, Pol ε (epsilon) that works on the leading strand and Pol δ (delta) that works on the lagging strand (Garg and Burgers 2005). In contrast, the duplication of the mitochondrial genome requires polymerase γ (gamma), an A-family member that is unique due to the functions it can exert. Pol γ can replicate, repair and act as a proofreading 3'-5' exonuclease and 5' dRP lyase (Kaguni 2004).

DNA pols are also key players in different DNA repair mechanisms, where a certain amount of damaged information has to be replaced with an intact copy. X-family polymerases: β (beta), λ (lambda), μ (mu) are important for maintenance of genome

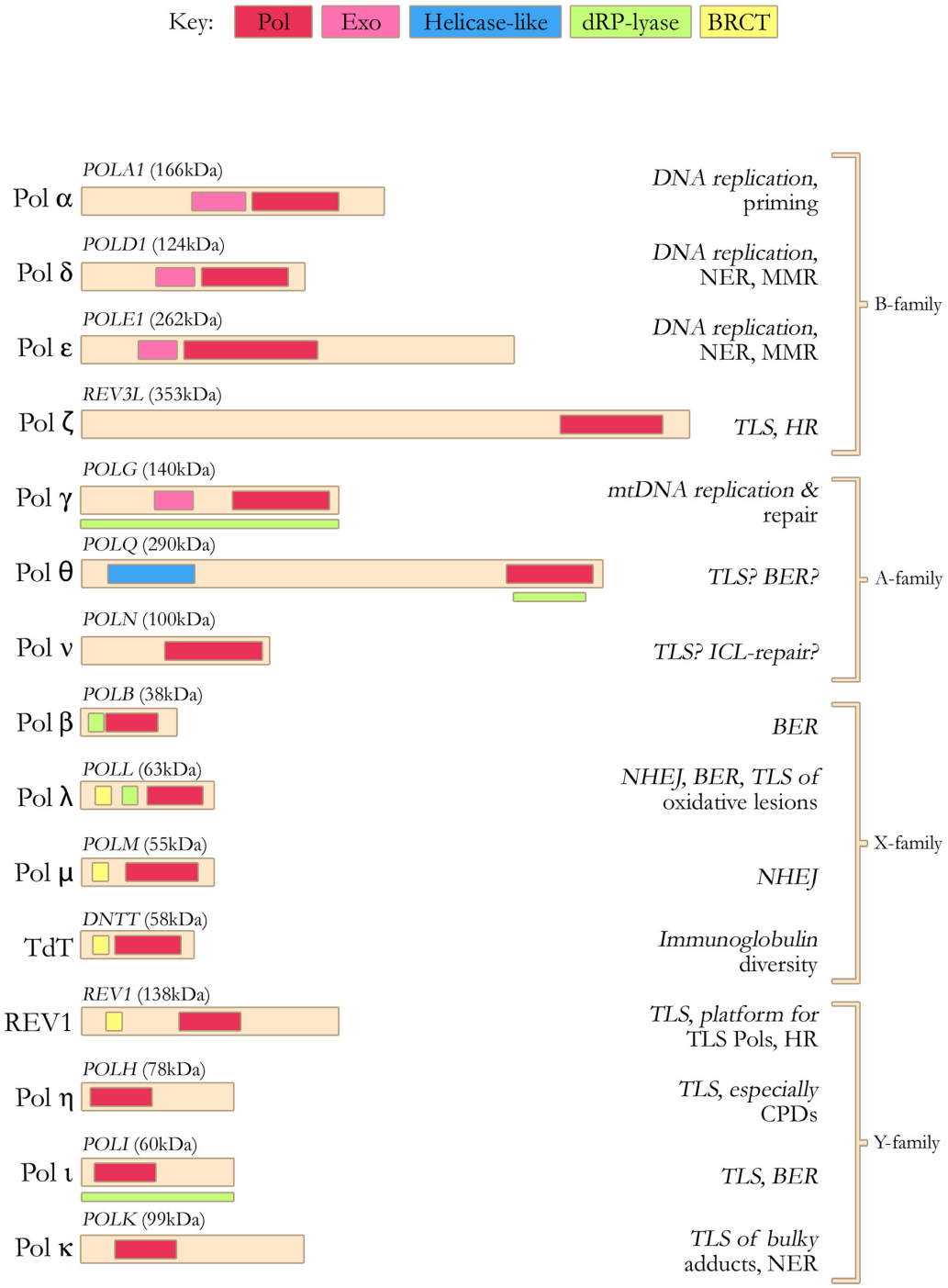

Figure 1. DNA polymerases identified in mammals

There are 15 mammalian DNA polymerases and each is specialized for distinct function (replication or repair, in some cases both). They are classified into 4 families: A, B, X and Y. The main domains are illustrated with different colors: red - polymerase domain, pink – 3'-5' exonuclease domain, blue – helicase like domain, green – deoxyribose phosphate domain (dRP)-lyase domain and yellow – C terminus BRCT1 domain. The figure is adopted from (Lange et al. 2011)

integrity. Pol β is involved in base excision repair, pathway that is essential for the repair of alkylated or oxidized bases and abasic sites (Beard et al. 2006). Pol λ and Pol μ are involved in non-homologous end-joining, a mechanism for rejoining DNA double-strand breaks (Yamtich and Sweasy 2010). An X-family member exception, Terminal Transferase (TdT), is expressed only in lymphoid tissues and is involved in V(D)J recombination to promote immunological diversity (Bentolila et al. 1997; Marshall et al. 1998).

Many polymerases also play a role in DNA damage tolerance through the activity of translesion DNA synthesis (TLS). This is carried out by different specialized DNA pols from the Y-family that have evolved unconventional catalytic properties to selectively bypass particular DNA lesions that stall the polymerases of the replisome. Polymerases η (eta), ι (iota), kappa(k) and REV1 (Y-family) are capable of synthesizing DNA opposite DNA lesions that would otherwise stall a replicative DNA polymerase, thus allowing completion of replication in the presence of DNA damage and promoting DNA damage tolerance (Sale et al. 2012). An overview of the diverse functions that polymerases are required for in the mammalian cell is illustrated in Figure 2.

Although DNA pols from different families are quite dissimilar in terms of their primary sequence that reflects some of their specific properties and functions, all eukaryotic DNA pols share a common structural "core" module (Hubscher et al. 2002), with distinct subdomains (palm, finger, thumb) which can be recognized also in prokaryotic and viral DNA polymerases, testifying their evolutionary diversification from a common ancestral enzyme.

1.2. DNA Polymerases involved in the genome duplication

The principal role of DNA pols is the duplication of the genetic material. Genomic duplication in eukaryotic cell takes place in two different compartments: the nucleus and the mitochondria, where different mechanisms and enzymes are employed. Replication in the nucleus is highly regulated in the context of the cell cycle and occurs in a tightly defined stage, termed the DNA synthesis S-phase. Nuclear replication has been studied in depth and it is known that it involves various protein complexes that are highly regulated,

temporally and spatially. To the contrary, the current knowledge of mitochondrial replication remains in its infancy. Duplication of mitochondrial DNA occurs independently of the cell cycle stage and likely depends in part on the metabolic status of the cell. The core replisome of the mitochondria has been established but the precise mechanisms of

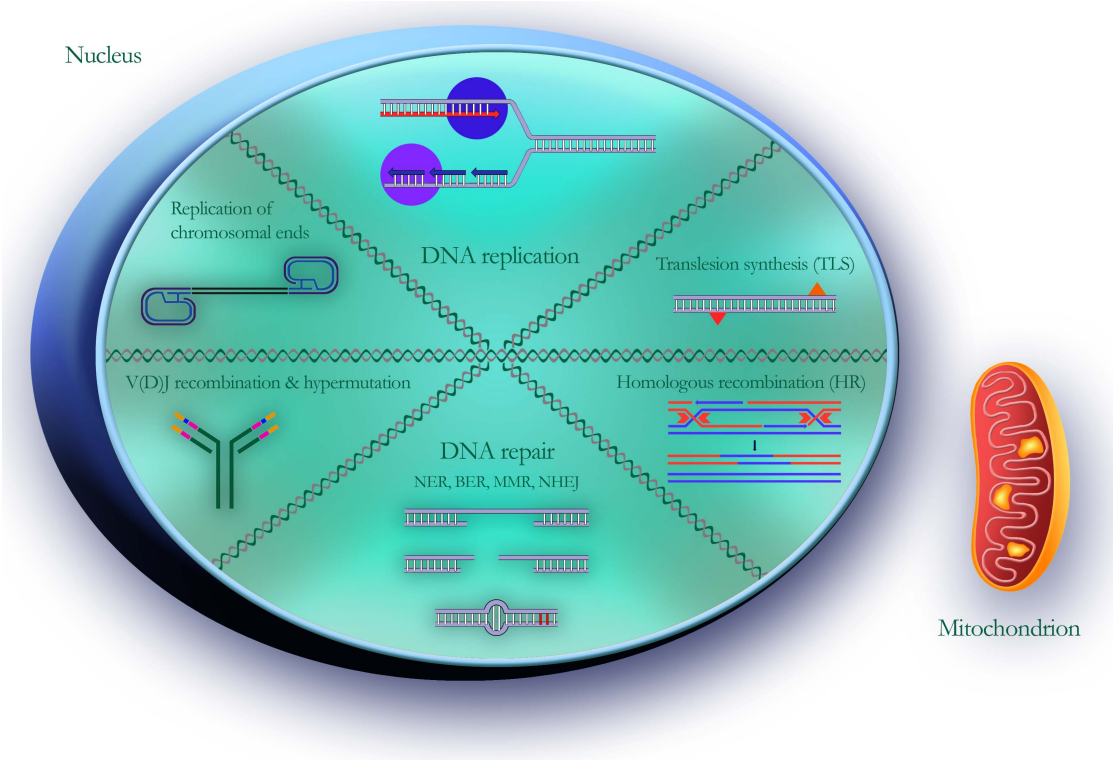

Figure 2. DNA polymerases are necessary for many cellular events in both the nucleus and mitochondria

Essential cellular functions like DNA replication, DNA repair, maintenance of telomerase ends or V(D)J recombination all rely on DNA synthesis carried out by DNA polymerases. The identification of novel polymerases led to the discovery that these enzymes are involved in many aspects of cellular physiology that are not limited only on duplication of genetic information, but also in the protection of it, through several mechanisms.

mitochondrial genome duplication and its regulation remains largely unclear. However there are several proposed mechanisms suggesting that the process and regulation of replication in mitochondria is complex and differs significantly from that of the nuclear DNA (Holt and Reyes 2012).

➢ DNA replication in the nucleus

Nuclear DNA replication proceeds in three enzymatically catalyzed and coordinated steps: initiation, elongation and termination. Initiation takes place during late mitosis and G1 phase at particular points in the DNA, known as "origins". Origins are targeted by protein complexes, known as origin recognition complexes (ORCs), that are required to recruit additional proteins needed to initiate DNA synthesis. There is an excess of origins in the human genome, which in contrast to yeast, have no clear sequence consensus, and only a subset are fired per cell cycle, during S-phase, to allow complete genome duplication (Mechali 2010). Once the origin has been located by the ORC complex, additional proteins are recruited to form the pre-replication complex (pre-RC: CDC6, CDT1 and MCM2-7 complex), which unzips, or separates, the DNA strands at the origin (Nasheuer et al. 2002). Cyclin dependent kinase (CDK) activity initiates DNA replication at the primed preRC. The replication fork is initiated at activated origins (figure 1.3), and the branching structure consists of single stranded DNA prongs that will serve as a template for leading and lagging strands. Meanwhile leading strand being synthesized in a largely continuous manner, synthesis of the lagging strand ensues in a discontinuous manner using ~200 nucleotide Okazaki fragments primed by RNA primers (Okazaki et al. 1967).

The first DNA polymerase binding at the unwound origin is Pol alpha (α). Pol α is associated with DNA primase to form a four subunit complex (Frick and Richardson 2001) and, as a consequence, is the only known eukaryotic enzyme able to start DNA synthesis de novo. Due to presence of primase subunit, the major role of the DNA polymerase alpha-primase complex (Pol-Prim) is the initiation of DNA replication (Muzi-Falconi et al. 2003). The asynchronous nature of replication forks has led to labor division of polymerases δ and ε at the leading and lagging strand. Pol δ and ε are both multi-subunit enzymes of high processivity that have 3'-5' exonuclease proofreading activity ensuring high fidelity of synthesis (Nick McElhinny et al. 2008). On the lagging strand, Pol δ synthesizes each Okazaki fragment up until the RNA-DNA primer of the next Okazaki fragment, then the process of Okazaki fragment maturation occurs with the combined activities of the flap endonuclease FEN1 and DNA Ligase I (Waga and Stillman 1998). Pol ε participates in leading strand synthesis and it will synthesize DNA in a continuous

manner until the replication fork converges with an adjacent replicon. The termination of DNA replication is less well understood than initiation and elongation. It has been proposed that termination occurs randomly in E. Coli (Santamaria et al. 2000). On the other hand it was found that in budding yeast replication terminates at regions containing replication pausing elements (Fachinetti et al. 2010).

➢ DNA replication in the mitochondria

The mitochondrial DNA (mtDNA) polymerase (Pol γ), is currently the only known polymerase able to replicate mtDNA. Due to its 3' – 5' proofreading exonuclease activity, this enzyme is intrinsically a high-fidelity polymerase that can utilize a variety of nucleic acid substrates (Wernette et al. 1988). There are two strands on circular mtDNA, referred to as heavy and light, and each has its own origin of replication (figure 1.4). The mechanism of mtDNA replication is still under debate as there are three proposed replication models. In the asymmetric "strand displacement" model, proposed by Clayton, one strand begins to replicate first, displacing the other strand. The second strand begins replicating in the opposite direction at the point when replication is completed on the first strand (Brown et al. 2005). In a second model proposed by Holt, mtDNA replicates symmetrically, with leading- and lagging-strand synthesis progressing from bidirectional replication forks initiated at multiple points within large region (Bowmaker et al. 2003). The third model, RNA incorporation during mtDNA replication (RITOLS), which is a modification of the asynchronous model of replication, argues that large regions of single-stranded DNA do not exist, rather, the lagging-strand template is largely protected by RNA and subsequently converted into DNA (Yasukawa et al. 2006). None of these proposed models has gained universal acceptance and if, as the data suggest, mitochondria utilize multiple mechanisms of replication, then there is no reason a priori why they should necessarily restrict themselves to a single DNA polymerase. A controversial question arising from these replication models is which enzyme performs RNA synthesis in each of the three proposed models? Recently it was discovered that POLRMT can initiate replication of mtDNA by synthesizing primers from the light-strand origin of DNA replication on leading strand (Fuste et al. 2010). However the role of this RNA polymerase fits only in the symmetrical replication model but does not explain primers synthesis on the

lagging strand that is suggested as a major mechanism in the RITOLS model. This implies that there might be distinct mode of DNA priming and additional primases involved in the replication of the mtDNA.

1.3. DNA Polymerases involved in the DNA repair and DNA damage tolerance

DNA polymerases have an essential role in genome duplication, but they are also important for repair of DNA damage. Pathways to restore the integrity of DNA include mismatch repair (MMR), base excision repair (BER), nucleotide excision repair (NER), nonhomologous end-joining (NHEJ), and homologous recombination (HR) (Figure 1.5). Together these pathways rely on at least 10 different DNA pols. Considering their actions in the cellular context, the DNA pols involved in the repair processes, have to switch between different DNA templates and act in concert with replicative DNA pols. The existence of specialized repair polymerases has been described in both compartments, nuclear and mitochondrial, with the former being studied in more depth.

➢ DNA repair in the nucleus

In both normal and cancer cells, DNA is subjected to damage from many sources. By-products of normal cellular metabolism are inescapable and inflict continual alterations to DNA. Reactive oxygen species (ROS) such as superoxide anions, hydrogen peroxide, and hydroxyl radicals, potentially originating from oxidative phosphorylation in the mitochondria, are an abundant source of DNA damage (Murphy 2009). Other sources of exogenous lesions include ultraviolet (UV) radiation from the sun, naturally occurring ionizing radiation and reactive industrial and environmental chemicals, but also those that can arise as natural metabolites.

Every DNA pol is specialized for certain functions that may be involved only in one pathway or in some cases can be used by multiple DNA damage repair pathways. DNA strand breaks generated during replication, or through physiological processes, utilize

NHEJ and HR pathways to repair these lesions and prevent aberrant recombination events. The distinct DNA repair pathways, such as BER and NER, can minimize the toxic and mutagenic consequences of such damage by repairing base lesions and adducts. Errors occurring during DNA replication, either due to misincorporation by the replicative polymerases or due to mis-coding DNA lesions, are repaired by MMR.

DNA double-strand breaks (DSBs) with blunt or blocked DNA ends can be ligated directly by NHEJ. Trimming of blocked ends and resynthesis of bases is required to join breaks and some polymerases are implicated in this process. NHEJ is a major mode of DSB repair in mammalian somatic cells, it can repair a DSB at any time during the cell cycle and it is also a major pathway for generating diversity in the immune system through V(D)J recombination. The X-family enzymes Pol λ, Pol μ and TdT have all been implicated in immunoglobulin V(D)J gene recombination (Bertocci et al. 2006). An additional strategy for DSB repair is HR. Cells utilize HR only in late S or G2 phase of the cell cycle when a double-stranded copy of the sequence is accessible. Pol β is required for normal meiotic synapsis and functions in the processing of DSBs in an early stage of meiosis (Kidane et al. 2010).

The adducts and abasic sites that result from byproducts of cellular metabolism can lead to mutations that can be repaired by BER throughout the cell cycle. Depending on the extent of the lesion, cells can use short patch BER and long patch BER. In the short patch pathway Pol β is the main enzyme that mediates not only insertion of the correct nucleotide but also the removal of the sugar-phosphate residue that is produced by the action of an AP endonuclease. Pol β can accomplish this because it possesses a dRP lyase domain (Almeida and Sobol 2007). In mitochondria, the replicative polymerase Pol γ is responsible for gap filling in BER (Copeland 2010). Other DNA polymerases like Pol ι (Bebenek et al. 2001), Pol λ (Braithwaite et al. 2005) and Pol θ (Prasad et al. 2009) have been proposed as backup enzymes for BER since they can perform dRP lyase activity as

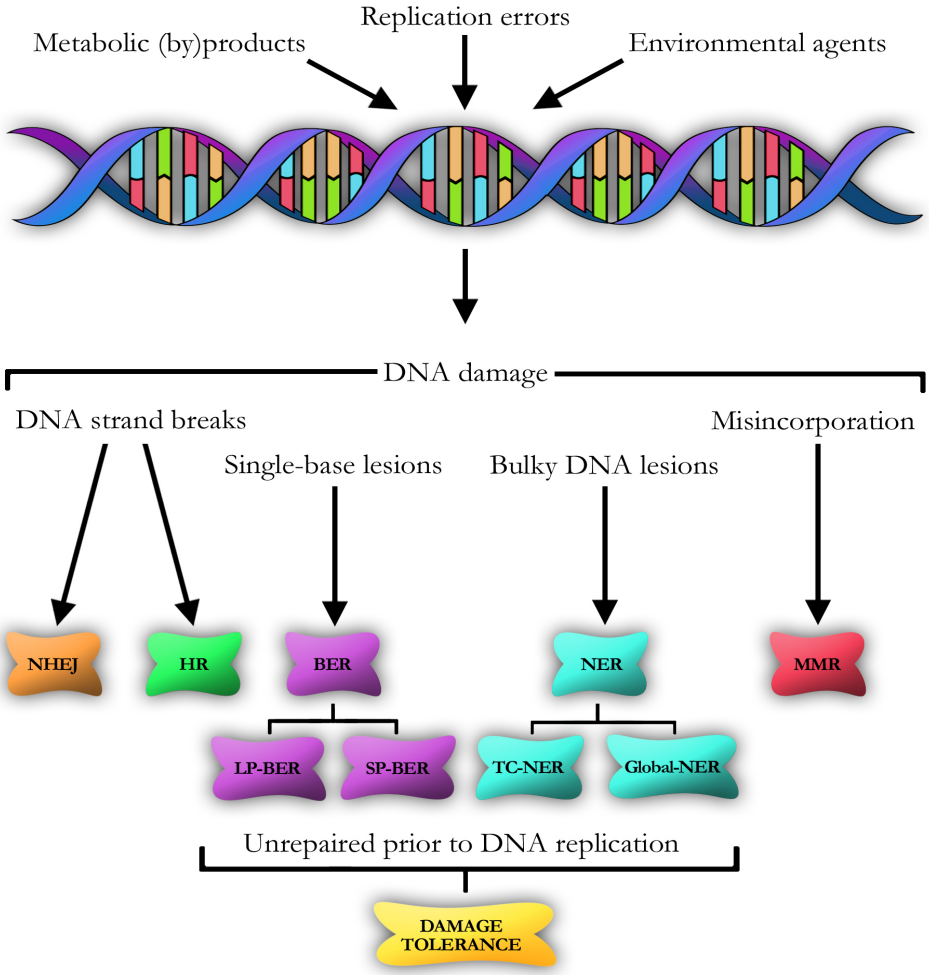

Figure 3. Sources of DNA damage and mechanisms to repair them

There are thousands of damaging events per day, originating from both external (exogenous) and internal metabolic (endogenous) processes. The lesions in DNA can vary depending on the extent of the damage. Double strand breaks are repaired through HR (homologous repair) or NHEJ (nonhomologous end-joining). Single strand breaks and single base lesions can be repaired through short and long patch base excision repair (SP or LP-BER), but if those lesions asignificantly distort the DNA structure then nucleotide excision repair (NER) is employed. Global NER is used for repair of lesions in the transcriptionally active and silent genes while transcription coupled NER (TC-NER) deals only with genes undergoing transcription. If there is no time for BER or NER, as is the case during replication, cells can use DNA damage tolerance and repair the damage later. Misincorporations during replication are rare events but they can be also repaired through mismatch repair (MMR). Adopted and modified from (Shiloh 2003)

well. In long patch BER gap-filling is performed by Pol ε and Pol δ (Stucki et al. 1998).

NER is the most utilized DNA repair mechanism because it can deal with a wide spectrum of structurally diverse DNA alterations. Different types of damage induced by carcinogenic and chemotherapeutic agents, such as psoralen, cisplatin and UV radiation, cause significant helical distortion, in addition to a change in the DNA chemistry, are resolved through NER. The NER process involves the action of at least 20–30 proteins in successive 'cut-and-paste' steps that consist of damage recognition, local opening of the DNA double helix around the injury, and incision of the damaged strand on either side of the lesion.

The resulting gap is filled by subsequent action of polymerases proceeded by ligation as the last step (de Boer and Hoeijmakers 2000). In mammalian cell extracts *in vitro*, either Pol ε or Pol δ can synthesize DNA to fill the gap that is produced during NER. A second form of NER gap filling uses a combination of Pol δ and Pol κ. It was proposed that cells can use the second combination of polymerases when deoxynucleotide concentrations are low, as is the case in non-cycling cells (Ogi et al. 2010). Mutations leading to nonfunctional components of NER (XPA-XPG) are reported to be the main cause of the inherited disease xeroderma pigmentosum (Lehmann 2003). An overview of DNA damage repair mechanisms is given in Figure 3.

➢ DNA repair in the mitochondria

DNA repair research has focused primarily on the nuclear compartment. However, it was shown in the last two decades that mitochondria also possess effective DNA repair mechanisms, and the understanding of how these mechanisms function has notably increased in the last few years. The BER pathway was the first DNA repair pathway that was described to be involved in the repair of mitochondrial DNA in mammalian cell. At present, it is accepted that other DNA repair mechanisms that were thought to take place solely in the nucleus have been recently described to occur as well in mammalian mitochondria such as MMR (de Souza-Pinto et al. 2009) and the long-patch BER (Akbari et al. 2008). Pol γ was the only identified polymerase in mitochondria that can act in repair pathways and it is responsible for the gap filling step in BER (Copeland 2010).

Despite the increased knowledge of mtDNA repair mechanisms, there are still many questions and possible new mitochondrial repair proteins to be identified. It is still not known if there are precise mechanisms for the repair of some specific lesions in mtDNA, like DNA double-strand breaks or bulky lesions, such as T-T dimers generated by UV radiation. It was found that UV photoproducts are persistent in mitochondrial genomes (Clayton et al. 1974) and that *in vitro*, Pol γ most often stalls at thymine dimers, however randomly it can bypass this type of lesions and it can do so in error free or error prone way (Kasiviswanathan et al. 2012). These investigations suggested the existence of a short term DNA damage tolerance pathway for UV-induced mtDNA damage that could be mutagenic, consistent with the observations regarding UV-induced mtDNA mutagenesis. However, to date, no TLS activities have been identified in the mammalian mitochondria.

1.4. DNA damage tolerance

DNA is often chemically altered by environmental agents, such as UV-light, radioactivity, mutagenic chemicals and ROS. Moreover, much endogenous DNA damage is the result of cellular activities, such as hydrolysis, oxidation or lipid peroxidation. It is estimated that ten thousand to one hundred thousand alterations occur per cell per day. Even though the cell is equipped with sophisticated DNA repair mechanisms, some DNA damage escapes repair and can stall the replication machinery. Stalled DNA replication forks are fragile, and if not resolved, they can collapse into structures that cause DNA double strand break (DSB) to be formed, thereby increasing genomic instability and preventing the completion of replication.

The main strategy by which cells are able to tolerate DNA damage during replication is by synthesizing DNA past the damaged bases (Figure 4). The replicative DNA polymerases are the least tolerant against modified DNA (Schmitt et al. 2009). To bypass these replication stalling lesions, cells use TLS, in which specialized error-prone DNA polymerases bypass the blocking lesions (Ohmori et al. 2001). TLS occurs in a two-polymerase reaction: first one or two bases, depending on the lesions, are inserted opposite the damage and, second, an extension from this lesion has to be carried out. Insertion can vary in accuracy depending on TLS polymerase that is chosen to carry out this step.

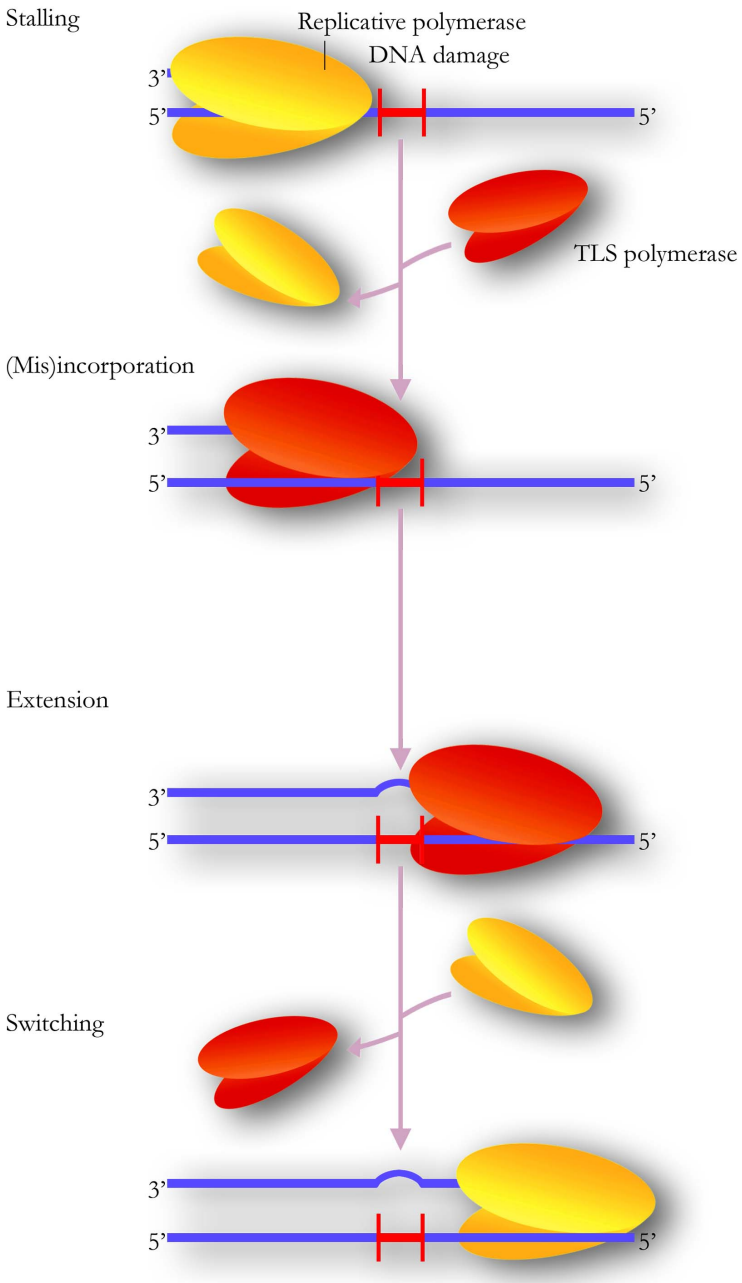

Figure 4. Simplified DNA damage tolerance model

Highly accurate replication polymerases cannot read through errors in DNA and therefore their progress during DNA synthesis can be arrested. To avoid the stalling of replication forks, cells can use low fidelity TLS polymerases that can synthesize across diverse DNA lesions, mostly in an error-prone manner. In critical moments of replication, when it is crucial to continue DNA synthesis, cells can bypass lesions by replacing the main replication polymerases with selected TLS polymerase. Once the lesion is bypassed the replication polymerase returns to replication forks and continues DNA synthesis. Adopted from Sale et al, 2012.

Pol η, Pol ι and Pol κ are polymerases that can perform insertions. Extension mainly relies on Pol ζ and in some cases on Pol κ. Based on these two roles that TLS polymerases can perform, they were classified as inserters or extenders (Livneh et al. 2010). Consequently this division of roles results in an interplay, also called a DNA switch, between the "inserter" and the "extender" DNA pols. The final outcome is that TLS can be either error-free or error-prone. The latter may lead to mutations in the next replication round. TLS polymerases do not possess proofreading exonuclease activity, however they are involved dealing with DNA lesions. TLS polymerases are actually not repair enzymes per se but they facilitate DNA damage tolerance. Despite extensive study, the precise physiological roles for many TLS pols has not been established (Loeb and Monnat 2008).

Each TLS polymerase is "optimized" to deal with certain lesion which include UV induced dimers (CPD and 6-4PP) or oxidative lesions (8-oxoG), bulky adducts that can be caused by benzo[a]pyrene diol epoxide (BPDE) and chemotherapeutic agents (such as cisplatin and mitomycin C (MMC)), as well abasic sites (AP) and thymine glycol residues caused by ionizing radiation.

1.5. Bypass of DNA damage caused by UV irradiation

Irradiation of DNA or cells with ultraviolet light (UV) induces the formation of several types of mutagenic DNA lesions. UVA has the longer wavelength range where most absorption is through highly reactive chemical intermediates, oxygen and hydroxyl radicals, which indirectly cause damage to macromolecules. The shorter wavelengths of UVB and UVC are directly absorbed by DNA and proteins (Kielbassa et al. 1997). Molecular changes induced in DNA by the absorption of UV energy could affect single bases, interactions between adjacent and nonadjacent bases, as well interactions between DNA and proteins.

The major photoproducts produced by UVB are dimers between adjacent pyrimidines, predominantly represented by two lesions, the *cis–syn* cyclobutane pyrimidine dimer (CPD) and the pyrimidine-6/4-pyrimidone (6-4PP). The relative proportions of their induction can vary depending on the UV wavelength. Base sequence, secondary structure, and DNA-

protein interactions can affect he distribution of both photoproducts in DNA (Pfeifer et al. 2005). The 6-4PP undergoes additional photochemical reactions after UV resulting in production of a photoisomer, the Dewar pyrimidinone. The most abundant photoproduct is the CPD, which constitutes ~80% of the total lesions. Although the 6-4PP is less frequent (20% of total lesions), this adduct is of high biological importance and known to be much more mutagenic than CPDs (Lommel and Hanawalt 1993).

CPD lesions can be removed by global NER or by a transcription repair coupled (TCR) mechanism. In transcriptionaly active genes, CPD clearance is faster due to the TCR mechanism. On the other hand, studies showed that the 6-4PPs are removed in an equally efficient manner from all over the genome without any bias from the transcriptional state (Vreeswijk et al. 1994). Therefore it appears that 6-4PPs are repaired via general genome repair pathways without transcriptional coupling. The differences observed between the removal of CPDs and 6-4PPs in DNA raise the possibility that these two lesions are processed by distinct repair pathways (Balajee et al. 1999). When UV induced dimers occur in DNA and distort the helix, cells utilize nucleotide excision repair (NER) or recruit by-pass polymerases to the lesion. Pol η can accurately and efficiently bypass CPDs, however in the absence of this TLS polymerase, alternative DNA pols can take over and by-pass the lesion (Yoon et al. 2009). Xeroderma pigmentosum variant syndrome (XP-V) is human disorder where severe truncations of the protein Pol η results in a strong susceptibility to sunlight-induced skin cancers (Kannouche and Stary 2003). XP-V was the first and remains the best-defined model for the study of the relevance of TLS activity in DNA damage tolerance after UV exposure.

➢ The UV Induced DNA Damage Response

Cell cycle events have to be coordinated temporally and spatially in order to ensure the high fidelity transmission of the genetic information and successful cell duplication. During replication, complex interactions between signaling and repair proteins act to keep these processes from going awry, despite random events that can cause interruption and failures. Activation of cell cycle checkpoints requires the action of DNA damage sensors and signal transducers. In the last 15 years it has become evident that there is a link between DNA

pols and cell cycle checkpoint control.

Exposure to UV can lead to direct damage resulting in thymine dimers and other pyrimidine dimers between adjacent bases or to indirect damage and induction of free radicals and reactive oxygen species. Both types of damage result in DNA lesions and have been linked to malignant melanoma (Narayanan et al. 2010; Rastogi et al. 2010). If left unrepaired, these lesions can stall progression of replication forks and lead to the activation of checkpoint mediated cell cycle arrest. Uncoupling of the replicative DNA helicase from replicative DNA pols activates a checkpoint mediated cell cycle arrest dependent on the conserved ATM and Rad3 like kinase, ATR (Byun et al. 2005). The uncoupling of DNA unwinding and polymerization results in the accumulation of ssDNA that gets coated by replication protein A (RPA). RPA itself can activate the checkpoint and does that by recruiting Rad17, a component of the alternate clamp loader (Zou and Elledge 2003). In addition to uncoupling, RNA synthesis by the primase subunit of Polα is also required for efficient checkpoint activation (Michael et al. 2000).

In addition, TopBP1 independently recruits the Rad17-RFC and Rad9-Rad1-Hus1 (9-1-1) protein complexes to fully activate the checkpoint response (Zou et al. 2002). Once activated, ATR phosphorylates a number of mediators, including histone H2AX Ser139, p53 at s15, the Chk1 kinase at Ser345 and RPA at s4/s8. Phosphorylated Chk1 leads to the phosphorylation of Cdc25A, B and C that subsequently undergo ubiquitin mediated degradation, resulting in G1 and S-phase arrest due to attenuation of CDK activity. Checkpoint signaling is mediated through claspin if DNA damage occurse in G2-phase and it leads to a claspin-dependent activation of Chk1/2, followed by $SCF^{\beta TrcP}$ mediated degradation of CDK-activating phosphatase Cdc25A and cell cycle arrest (Furnari et al. 1999; Mailand et al. 2000; Mailand et al. 2002)

1.6. The overview of Y-family polymerases and DNA polymerase ζ

The first speculation that an error-prone polymerase may exist, functioning in gap filling of damaged DNA, came in early 1970 from Radman(Villani et al. 1978). It turned out that the

first proposed model where replication polymerases can, under certain circumstances, lower their fidelity and replicate through DNA damage, was faulty. It took more than 2 decades to identify the first TLS polymerase, Polymerase η, that is mutated in the disease XP-V. This discovery opened the door to the identification of a new family of polymerases, the Y family, and in less than 2 years additional polymerases (Pol κ, Pol ι, REV1 and Pol ζ) were subsequently identified. The Y-family of DNA polymerases, together with Pol ζ, are essential for translesion synthesis.

This family of polymerases has unique features that enable them to synthesize DNA past damaged bases that otherwise block replicative polymerases. However, this comes with the cost of a much higher error rate. Nonetheless, as they perform with low fidelity when copying undamaged DNA, it is essential that TLS pols are only pressed into service when they are absolutely required. Several layers of regulation ensure that this is achieved. Y family DNA pols share a common basic structural arrangement. Despite poor sequence conservation with the replicative polymerases, the structures of Y family polymerase catalytic domains revealed a similar overall `right hand' topology. However, their active site is more spacious and accessible than that of the replicative polymerases, with little contacts between the enzyme and the DNA template or the incoming dNTP. This might explain their ability to accommodate a bulky adduct on the template base which are normally excluded by the tighter active site of high fidelity DNA pols. The finger and thumb domains are chunkier which decreases the quality of contact with both the DNA and incoming nucleotide, contributing to their reduced processivity and fidelity (Yang 2003).

The Y-family polymerases have an additional, unique domain of about 100 residues, the 'little finger', also termed the polymerase-associated domain (PAD), which mediates DNA contacts close to the lesion site. This domain has been implicated in polymerase selectivity for certain lesions (Boudsocq et al. 2004). These features allow nucleotide incorporation opposite damaged bases that can be error prone or error free. The benefit of a flexible active site has the disadvantage that it impairs accurate and processive replication, and the mutagenicity of the Y-family polymerases is further aggravated by a lack of the 3′–5′ proofreading exonuclease activity that is characteristic of replicative polymerases. Despite structural similarity, a large degree of functional divergence has occurred, rendering the different members of the Y family highly specialized for the bypass of specific lesions and this will be discussed further for each individual TLS polymerase.

➢ DNA polymerase η

Pol η (POLH, XP-V, Rad30) is the most well characterized TLS DNA pol and mutations of the gene cause hypersensitivity to UV-induced DNA damage. A peculiarity of this translesion polymerase is that it is able to catalyze TLS in an error-free manner and with high efficiency past TT-cyclobutane pyrimidine dimers (CPD), but not past 6-4 photoproducts (Johnson et al. 2000). The relevance of human pol η to mutagenesis *in vivo* is demonstrated by the existence of patients with mutations in the human POLH gene (Johnson et al. 1999; Masutani et al. 1999) that disable specific interactions of the enzyme with the TT-CPD. These patients are affected by the variant form of xeroderma pigmentosum, described in section 2.1. Surprisingly, compared to all characterized TLS polymerases, Pol η has the lowest fidelity on undamaged DNA but highest accuracy in nucleotide insertion opposite CPD dimers (Matsuda et al. 2000). Despite its mutagenic potential, overexpression of Pol η in human cells does not result in elevated mutagenesis (King et al. 2005) while knockdown in human cells or knockouts of Pol η in mouse cells resulted in increased mutagenesis, especially after exposure to UV (Choi and Pfeifer 2005; Busuttil et al. 2008). Besides bypass of CPDs, Pol η is proficient in bypassing 8-oxo-guanine lesion (Lee and Pfeifer 2008), some bulky adducts caused by BPDE and cisplatin (Albertella et al. 2005) and it can also replicate through naturally occurring G-quartets (Betous et al. 2009).

It was shown by immunolocalization studies that this enzyme is associated to the sites of ongoing DNA replication in undamaged cells and it is present in the nucleus at very low levels. Pol η foci are induced upon UV damage and methyl methanesulfonate treatment (Kannouche et al. 2001) and in cells subjected to hydroxyurea-induced replication stress (Albertella et al. 2005; de Feraudy et al. 2007). Pol η was found to colocalize with CPDs, BrdU and PCNA in those foci upon damage (Kannouche et al. 2004), implying that it gets recruited to the sites of stalled replication forks. Nevertheless, it was shown that Pol η can also be recruited to the sites UV damage and act in a DNA damage tolerance pathway independently of cell cycle phase (Soria et al. 2009). Intriguingly, while in *S. cerevisiae* UV damage led to induction of RAD30 transcript expression 3-4 fold (Roush et al. 1998), the same was not observed in mouse. Instead, it has been found that there is transcriptional upregulation of Pol η during cell proliferation (Yamada et al. 2000).

Cellular regulation of Pol η activity is controlled through protein-protein interactions mainly with PCNA, Rad18 and Rev1. It is considered that an interaction with monoubiquitinated PCNA stimulates its TLS activity and accumulation of Pol η foci in response to DNA damage is dependent upon monoubiquitinated PCNA (Plosky et al. 2006). The interactions with PCNA and ubiquitin appear to give Pol η a favorable position over the replicative Pol δ after DNA damage (Yuasa et al. 2006). It was recently proposed that Pol η interacts with FANCD2 and gets recruited to the sites of the damage via PCNA. The interaction with FANCD2 takes place even before that with PCNA (Fu et al. 2013). In the context of cellular regulation, another protein crucial for Pol η recruitment to sites of damage is Rad18, an E3 ubiquitin ligase that mediates PCNA monoubiquitination but also interacts directly with mouse Pol η, independently of DNA damage (Watanabe et al. 2004). By proteomic analysis it was identified in human cells that Pol η copurifies together with Rad18, Rad6 and Rev1 (Yuasa et al. 2006) and this complex is enriched in the chromatin fraction upon UV damage according to the demand for TLS at stalled forks. It was demonstrated that disruption of Nbs1 affects the recruitment of Rad18 to foci upon UV damage and abrogates Rad18-dependent ubiquitinaton of PCNA consequently diminishing Pol η engagement in TLS at UV lesions (Yanagihara et al. 2011). Pol η is phosphorylated at serine 601 by ATR kinase and this posttranlsational modification is necessary for postreplication repair and normal survival of XP-V cells (Bomgarden et al. 2006; Gohler et al. 2011).

Beside its major role in translesion synthesis, numerous additional activities have been reported for Pol η. It is implicated in homologous recombination (Kawamoto et al. 2005; McIlwraith et al. 2005) and somatic hypermutation (SHM) where it acts as a mutator polymerase (Zeng et al. 2001). Additionally, Pol η acts as a reverse transcriptase (Franklin et al. 2004), facilitates the replication of common fragile sites (Rey et al. 2009) and participates in the removal of oxidatively induced clustered DNA lesions in cooperation with MSH2-MSH6 (Zlatanou et al. 2011).

➢ DNA polymerase ι

Pol ι (Rad30b) belongs to Rad30 subfamily of polymerases identified exclusively in eukaryotes (McDonald et al. 1999; Tissier et al. 2000). It is paralog of Pol η (Rad30a) although with distinct biochemical properties and function. In contrast to the wealth of information about Pol η, the role of Pol ι is less well understood. Pol ι contains polymerase and dRP domains and activities. It was suggested that Pol η physically interacts with and recruits Pol ι to replication sites. Pol ι does accumulate with Pol η at stalled replication forks after DNA damaging treatment and colocalizes with the same kinetics as Pol η in nuclear foci (Kannouche et al. 2002). Nonetheless, the functional consequences of such tight cooperation remains unclear, as Pol ι does not complement the UV-sensitivity observed in Pol η deficient cells (Dumstorf et al. 2006).

Pol ι can read efficiently though 6-4 photoproducts *in vitro* and also Dewar isomers, incorporating dAMP opposite these lesions (Johnson et al. 2000; Yamamoto et al. 2008). Pol ι is also able to bypass TT-CPD dimers but this is highly mutagenic (Vaisman et al. 2003). There is evidence that Pol ι is involved in UV-induced mutagenesis in XP-V cell lines (Wang et al. 2007). This discovery suggested the possibility in which even if Pol η is not available, like in XP-V cells, TLS still can still occur but with high mutagenicity and through a dual repair mechanism (Figure 5) where Pol ι inserts opposite the lesion and Pol ζ extends (Livneh et al. 2010). The reports on Pol ι contribution to mutagenesis are controversial as some authors have reported that this polymerase is not important for UV induced mutagenesis while others claim that Pol ι contributes to mutagenesis (Yang et al. 2004; Choi et al. 2006; D'Souza et al. 2008; Vidal and Woodgate 2009). Pol ι deficiency in mouse cells did not result in any gross abnormalities (Dumstorf et al. 2006). In regard to the lack of solid data considering a mutagenic role *in vivo*, loss of Pol ι seems to have little consequence on somatic hypermutation (SHM), as the 129/J strain of mice that possess a nonsense mutation in the Pol ι gene preventing its expression, have a normal immunoglobulin hypermutation profile (McDonald et al. 2003). A recent report investigating the biological significance of Pol ι in human cells has demonstrated that cell lines depleted for Pol ι exhibited enhanced sensitivity to oxidative

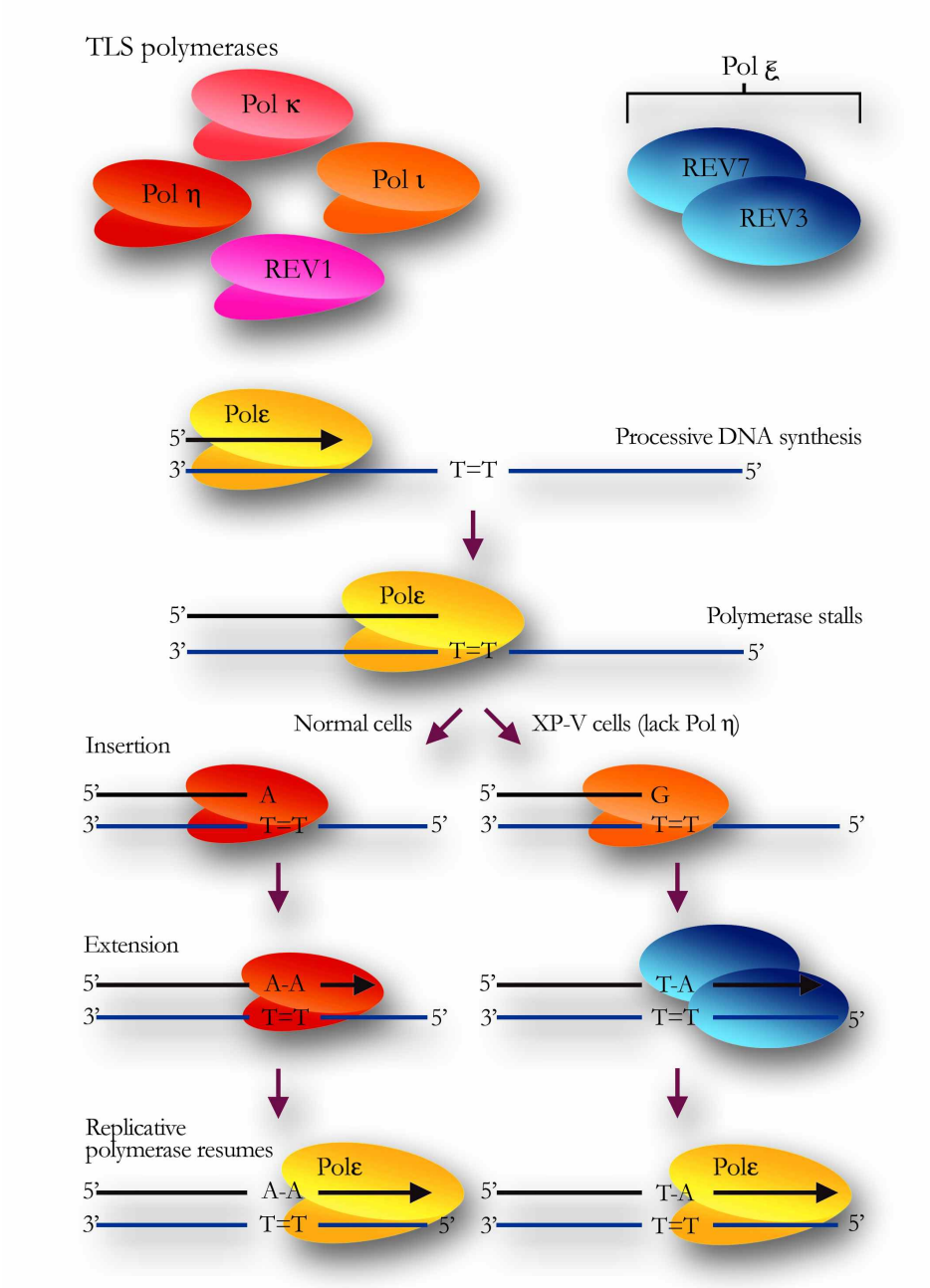

Figure 5. One or two-polymerase combinations define error-free and error-prone TLS

In mammalian cells, at least five TLS polymerases can be recruited to the sites of stalled replication. Depending of the nature of the DNA lesion, cells can use either a one or two polymerase mechanism for bypass. Pol η alone can insert over the lesion (in this illustration over TT dimmers) and extend a few nucleotides beyond in an error-free manner. In the two-Pol model, Pol ι can insert in combination with Pol κ or Pol ζ that further perform extension. The latter model is error-prone and it was proposed that this model is implicated in the repair of CPD lesions when Pol η is not available.

damage. In line with that, it was also found that Pol ι, due to its very narrow active sites, is able to replicate *in vitro* through 8-oxoG lesions in an error-free manner (Kirouac and Ling 2011). This novel role of Pol ι introduced the possibility that Pol ι functions in the repair of DNA damaged by oxidative stress (Petta et al. 2008) consistent with reports that it interacts with the base excision repair factor XRCC1 and is recruited to sites of oxidative DNA damage. Together, with other TLS polymerases, Pol ι can bypass interstrand cross links (ICL), potentially contributing to the repair of oxidative lesions, although in an error-prone way (Ho and Scharer 2010; Smith et al. 2012).

➢ DNA polymerase κ

Like all Y family polymerases Pol κ (DinB) is a low fidelity DNA polymerase, but is the most accurate one (Johnson et al. 2000) and has higher processivity than Pol η or Pol ι (Ohashi et al. 2000). Pol κ can efficiently extend mismatched primer termini, but often generates -1 frameshift deletions through a slippage mechanism (Levine et al. 2001). Pol κ differs from Pol ι and Pol η in its specificity for lesion bypass (Zhang et al. 2000). Pol κ is able to bypass in an error free manner lesions caused by polycyclic aromatic hydrocarbons, like BPDE induced bulky adducts or guanine adducts (Takenaka et al. 2006). This specialized function of Pol κ is potentially related to its high expression in liver, kidney and lung, which are the are major sites of either accumulation or metabolism of polycyclic aromatic hydrocarbons (Stancel et al. 2009).

Surprisingly, Pol κ cannot bypass CPD or 6-4PP UV induced lesions *in vitro* (Zhang et al. 2002), yet cells deficient for Pol κ are sensitive to UV (Ogi and Lehmann 2006). Pol κ appears to be specialized to extend mismatched primer termini and thus seems likely to function as a second "extender" polymerase, as an alternative to Pol ζ, in scenarios where two TLS polymerases are required in concert to bypass a lesion (Carlson et al. 2006; Lone et al. 2007). Recently a possible role for murine Pol κ in nucleotide excision repair (NER) was introduced. It was identified that in Pol κ deficient MEFs, the clearance of 6-4PPs was reduced to 50% of that measured in wild type cells. In addition, transcription coupled repair (TCR) and global genome repair (GGR) were significantly reduced and treatment with hydroxyurea led to diminished repair synthesis in Pol $\kappa^{-/-}$ MEFs (Ogi and Lehmann

2006). Based on these findings it was proposed that Pol κ functions in a separate branch of NER that can be utilized in conditions of low nucleotide concentrations, for example in quiescent cells. The theory of Pol κ involvement in NER was extended to human cells where it was additionally shown that Pol κ is recruited to repair sites together with Pol δ, by ubiquitinated PCNA and XRCC1 (Ogi et al. 2010).

In DNA damage treated organs of mice, protein and mRNA levels for Pol κ were induced. In particular it was observed that transcript levels increased in lung after treatment with 3-methyl methylcholanthrene, a polycyclic aromatic hydrocarbon (Ogi et al. 2001). The increase in mRNA levels was also noted after UV radiation in the skin, upon ionizing radiation in spleen and thymus (Burns and El-Deiry 2003) and by treatment with doxorubicine in kidney, testis, brain, spleen and lung (Velasco-Miguel et al. 2003). Taking into consideration these data, it was concluded that expression of the highly mutagenic Pol κ is kept under tight control and its levels are adapted in conditions of genotoxic stress.

In the absence of DNA damaging treatments, Pol κ deficient cells did not exhibit any phenotype, but the over-expression of Pol κ in mammalian cells led to the alteration of replication fork progression, resulting in genomic instability (Pillaire et al. 2007). In lung cancer where Pol κ overexpression can be significant, it was observed that there was a high incidence of DNA breaks, genetic exchanges and aneuploidy (Bavoux et al. 2005) in line with the proposed role of Pol κ in stress responses.

➢ REV1

REV1 stands out from other TLS polymerases with its particular role in TLS. REV1 mainly acts as a scaffold protein, associating with other TLS polymerases. REV1 is the only member of Y family that does not act as a DNA polymerase but instead as a dCMP transferase, capable of incorporating dCMP opposite templated guanines and some lesions such as abasic sites and adducted G residues (Nair et al. 2005). The carboxyl-terminus of REV1 interacts with all other Y-family polymerases and Pol ζ which was shown by yeast two hybrid and transient transfection assays (Guo et al. 2003; Tissier et al. 2004) and the amino-terminus contains a BRCT (BRCA1 carboxyl-terminus) domain that is important

for PCNA interaction and survival following exposure to UV light (Guo et al. 2006). Thus, multiple protein-protein interaction domains are crucial for the ability of REV1 to provide resistance to DNA-damaging agents and promote mutagenesis. It was proposed based on this that the principal function of Rev1 is to bring postreplication repair proteins to localized mutagenic DNA damage sites, to facilitate translesion synthesis and to assist polymerase switching at the site of a DNA lesion (Friedberg et al. 2005; Lehmann 2005).

Regardless of its incapability to replicate over UV photoproducts *in vitro*, REV1 is required for the bypass of 6-4 TT dimers *in vivo* (Nelson et al. 2000; Zhang et al. 2002; Otsuka et al. 2005). REV1 deficiency in DT40 cells leads to increased genomic instability upon UV induced damage and REV1 depletion sensitized cells to cisplatin and MMS (Simpson and Sale 2003). REV1 is regulated in a cell cycle dependent fashion with the highest levels appearing in G2 phase and during mitosis (Waters and Walker 2006). When ectopically overexpressed, REV1 forms foci in vertebrate cells upon DNA damage (Mukhopadhyay et al. 2004; Murakumo et al. 2006) that colocalize with PCNA and Pol η (Guo et al. 2006). Other reported roles for REV1 include immunoglobulin gene somatic hypermutation (Jansen et al. 2006; Ross and Sale 2006), the replication of G-quadruplex DNA to maintain epigenetic patterns (Sarkies et al. 2010) and HR mediated repair (Sharma et al. 2012).

In *S. Cerevisiae* REV1 localizes to the mitochondria together with Pol ζ. While it is speculated that Pol ζ is responsible for general maintenance of mitochondrial DNA, REV1 plays a role in an alternative way, possibly protecting mtDNA from UV induced lesions. Yeast strains lacking REV1 showed markedly increased mutation frequency in mtDNA upon exposure to UV (Kalifa and Sia 2007). For REV1 it was debated for a long time if it was the most mutagenic TLS polymerases contributing to tumor development. However this speculation was refuted in mouse models (discussed in 3.4.) and in *S. Cerevisiae.* In yeast, it was proposed that mitochondrial dysfunction leads to a nuclear mutator phenotype for which loss of REV1 and Pol ζ function should be the main contributors. On the contrary, loss of these polymerases did not lower the frequency of mutations in DNA caused by mitochondrial dysfunction, pointing out that REV1 and Pol ζ are dispensable for the mutator phenotype in cells suffering mitochondrial dysfuncton (Rasmussen et al. 2003; Zhang et al. 2006).

➢ DNA polymerase ζ

Pol ζ has a special place as a key polymerase in the DNA damage tolerance pathway that acts across all lesions where TLS mechanisms are required, with the exception of CPD lesions bypass. Pol ζ is a member of the B-family polymerases and is a heterodimer composed of the catalytic subunit REV3 (REV3L in higher eukaryotes) and an accessory subunit, REV7. Contrary to DNA pol δ and pol ε, pol ζ lacks a 3'-5' exonuclease proofreading activity (Lawrence 2004) and has relatively low fidelity with a processivity of approximately 2-3 nucleotides.

The best-characterized *in vitro* activity of DNA pol ζ is its role as a general extender in the two-polymerase model during TLS. REV1 is able to bypass TT dimers and glycol lesions but it is considered that it is not a major feature of this enzyme (Nelson et al. 1996; Johnson et al. 2003). Rather, Pol ζ is assigned to extend a bulky DNA lesion, abasic residues or distorted base pairs, such as mismatches, that might result from inaccurate base insertion by a TLS polymerase. It was proposed that Pol ζ could be involved in two distinct TLS pathways. It can act as an extender polymerase in an accurate and efficient manner with the coordinated action of a specialized inserter DNA pol, responsible for the incorporation of a nucleotide opposite the lesion. These observations led to the concept that two-polymerases are necessary to perform TLS (Gueranger et al. 2008). Using this pathway, Pol ζ is able to bypass in an error free manner 6-4PP lesions, a feature that was not assigned to any other TLS polymerases by now (Yoon et al. 2010). In the second proposed pathway, Pol ζ acts alone in a slow and very mutagenic pathway (Shachar et al. 2009).

The *in vitro* lesion bypass activity of Pol ζ has been shown to be stimulated by PCNA (Garg et al. 2005), even though no PCNA binding motifs exist in either REV3 or REV7 and no direct physical interaction has been shown between Pol ζ and PCNA. Rev1 interacts *in vitro* with Pol ζ through REV3-REV1 binding and this interaction strongly stimulates the activity of Pol ζ and probably contributes to its targeting to the replication fork (Acharya et al. 2006). One peculiar difference between Pol ζ and the Y family polymerases is that disruption of the catalytic subunit, REV3L, of the Pol ζ gene is embryonic lethal in mice, thus demonstrating the importance of Pol ζ for mammalian development (Bemark et al.

2000; Esposito et al. 2000; Wittschieben et al. 2000). Most of the functional studies were performed by knocking down REV3 or by deletion of REV3L on a p53 deficient background (Gan et al. 2008). In mice with conditional deletion of Pol ζ in the epidermis, it was surprising to find that the skin of these mice was sensitive to UVB but they do not have an increased incidence of skin tumors. Furthermore, Pol ζ deficient keratinocytes accumulated chromosomal gaps and breaks and exhibited a striking proliferation defect, while the skin was unable to mount a normal regenerative response to UV induced damage (Lange et al. 2013).

Beside TLS function, Pol ζ is involved some pathways of homologous recombination (Sharma et al. 2012), the repair of interstrand DNA crosslinks (Wang et al. 2001; McHugh and Sarkar 2006), somatic hypermutation of immunoglobulin genes and cell-cycle control (Gan et al. 2008). As well, Pol ζ loss in *S. Cerevisiae* resulted in an increased rate of spontaneous mutations in mitochondrial DNA suggesting an alternative role for this enzyme in mitochondria (Kalifa and Sia 2007).

1.7. Fidelity of TLS polymerases

The fidelity of DNA replication depends on the capability of DNA polymerases to select and incorporate into the DNA strand the correct nucleotide over an incorrect or damaged nucleotide. On the basis of selectivity for nucleotides, both during replication and repair, polymerases can be ranked on a fidelity scale (Figure 6). The rate of replication error is very low and it is estimated *in vivo* to be lower than $1x10^{-9}$, due to several mechanisms that are preventing the occurrence of mistakes such as nucleotide selection, proofreading activity and mismatch repair (McCulloch and Kunkel 2008). If there is defect in any of these three processes, the mutation rate may be increased.

DNA pols are not absolutely accurate and an important activity that replicative polymerases possess is 3'-5' exonuclease proofreading activity that reduces the misincorporation rates to a low level and promotes replication fidelity.

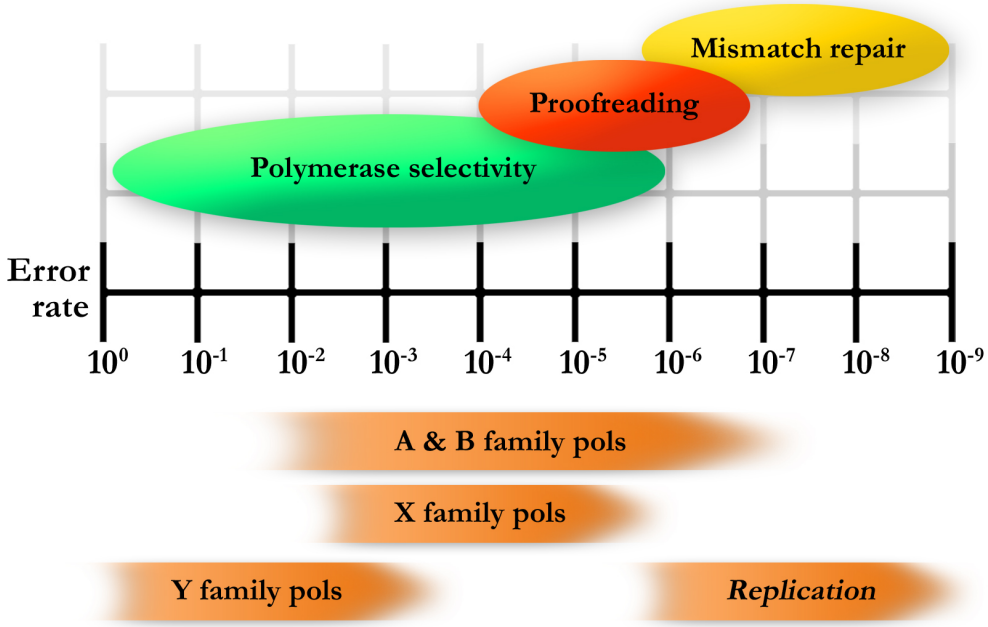

Figure 6. The fidelity of DNA synthesis

Estimated mutation rates of DNA polymerases ranked on a "fidelity scale". The orange bars below the scale illustrate the range of fidelity for each polymerase family. This is determined based on *in vitro* assays and it can differ within each family depending on the type of errors and the polymerase itself. For replication, the mutation rate is estimated based on the *in vivo* fidelity of the whole replication complex and not the individual polymerase. Above the scale in the ovals is the estimated fidelity of the three main mechanisms that polymerases can provide. These ovals are overlapping because there are different competing forces that can affect the fidelity of the polymerase and lead to a decrease or increase in its accuracy. Addopted from McCulloch at al, 2008.

Pol α and pol δ have proofreading activity, but not the initiating Pol ε. If replication fork stalling occurs, it jeopardizes cell survival because it can lead to distortion of the helix and double strand break formation. In this scenario, cells can avoid death or apoptosis by several different mechanisms of DNA damage repair or tolerance. One possibility is TLS that allows lesions to be tolerated until they can be repaired (McCulloch and Kunkel 2008).

Cells employ TLS polymerases that have low catalytic efficiencies, are non-processive, lack proofreading activity and can copy past bulky DNA-template adducts but at cost of much higher error rate (Yang 2003). The accuracy of TLS polymerases on undamaged DNA is decreased by ~10^{-2} compared to replicative DNA polymerases. Two main reasons are lack

of a 3'-5' proofreading domain (Goodman 2002; Kunkel 2004) and the few contacts made with the incoming nucleotide and DNA template. Regarding canonical Watson-Crick base pairing, it has been proposed that some TLS polymerases, like DNA Pol ι and Rev1, have lower fidelity because they have restricted geometry of contact to the template and they use different base pairing rule (Prakash et al. 2005). It was reported that when upregulated or inappropriately regulated, TLS polymerases can lead to a hypermutator phenotype (Baker and Bell 1998; Fujii and Fuchs 2004; Bavoux et al. 2005) which has been observed for Pol ι, the most error prone TLS polymerase (Wang et al. 2007). However, cells also benefit from TLS polymerases by applying their ability to synthesize with low fidelity to the process of immunoglobulin diversification through somatic hypermutation (more in section 1.8.) (Zeng et al. 2001; Faili et al. 2002). The low fidelity of Y family polymerases when copying undamaged DNA needs to be titrated strictly to specific circumstances, or too much error-prone synthesis could lead to accumulation of errors. As a consequence, defects in processes that condition DNA replication fidelity can potentially confer a strong mutator phenotype that can be a driving force for cancer and aging (Arana and Kunkel 2010).

1.8. Distinct functions of TLS polymerases

➢ Class switch recombination and somatic hypermutation

Class switch recombination (CSR) and somatic hypermutation (SHM) are two processes critical for immunoglobulin maturation and the propagation of antibody diversity. A common initiating event contributes to both CSR and SHM. This is the generation of DNA lesions by activation-induced cytidine deaminase (AID) activity. DNA lesions include mismatches, abasic sites, nicks, single-strand and double-strand breaks (DSB) and they can be repaired by NHEJ or HR. In CSR, the constant region portion of the antibody heavy chain is changed and DSBs are critical intermediates in this process (Stavnezer et al. 2008). The variable region does not change during class switching so that antigen specificity is not altered, yet the antibody will interact with different effector molecules. SHM is responsible for the maturation of the antibody's affinity by the programmed mutation in the variable region of the immunoglobulin (Ig) gene, which allows the antibody

to bind a specific foreign antigen with increased affinity. For the most part, mutations are in the form of single base substitutions, with insertions and deletions being less common. These mutations occur often at certain sites in the DNA that are known as hypervariable regions.

Somatic mutations are introduced during error-prone repair of DNA lesions on account of the mutagenic properties of TLS polymerases. The role of REV1, Pol η, Pol ι, Pol κ and Pol ζ in SHM and CSR was extensively analyzed *in vitro* and *in vivo* in available mouse models. Actively hypermutating B cells derived from Pol $\eta^{-/-}$ mice, had lower rates of A:T base pair substitutions in variable and switch regions (Zeng et al. 2001). The same results were obtained from XP-V patients deficient for functional Pol η (Zeng et al. 2004). It was also shown that Pol η physically interacts with the MSH2-6 complex that contributes to A:T mutagenesis (Martomo et al. 2005). Nevertheless, the frequency of somatic mutations was found to be normal and mice lacking Pol η still had a high frequency of C to G mutations. This finding implicated Pol η in SHM even though it is not essential for hypermutagenesis. On the contrary, it was found that in BL2, a Burkitt's lymphoma cell line, where most of SHM is C:G base changes, SHM depends on Pol ι (Faili et al. 2002). This supported the hypothesis that alternative TLS polymerases that can be recruited by the MSH complex to exert hypermutation functions (Delbos et al. 2005). The study in the 129 strain of mice, that bear an inactivating nonsense mutation in Pol ι, contradicted its role in SHM as B cells from these mice did not have any decreased mutation frequency as seen in BL2 (Martomo et al. 2006). In congenic mice lacking functional Pol η and Pol ι, IgG1 production was not affected and B cells were observed with the same mutational spectra as in Pol $\eta^{-/-}$ mice, leaving the actual role of Pol ι controversial (Martomo et al. 2006).

Another candidate for SHM, based on its *in vitro* activities, is Pol κ. However, disruption of *Pol κ* alone had no significant effects on SHM in the mouse (Shimizu et al. 2003), even in combination with Pol ι deficiency(Shimizu et al. 2005). Chicken DT40 B-cells deficient for REV1 showed defects in immunoglobulin gene mutation, indicating that REV1 might be involved in C:G to G:C transversions (Simpson and Sale 2003). Pol ζ was considered as well since the catalytic subunit of REV3L is expressed in the germinal centre of B cells (Winter et al. 2000; Poltoratsky et al. 2001). Moderate reduction of both A:T and G:C

mutations in an immunoglobulin variable gene was observed upon REV3l inhibition by antisense oligonucleotides in the CL-01 cell line (Zan et al. 2001). An identical outcome was reported in transgenic mice expressing *Rev3l* antisense RNA (Diaz et al. 2001). Since the complete disruption of *Rev3l* causes lethality during embryonic development it poses an obstacle for further in-depth study of modest defects observed in SHM in transgenic mice (Bemark et al. 2000).

In summary, the mechanism of SHM is still emerging and several TLS polymerases have been implicated to participate in different stages of the process. Additional experiments using double and triple-gene disruptions should clarify which DNA polymerases are involved and whether they compensate for the function of the others. It has also been suggested that TLS polymerases are recruited to double strand breaks during the process of CSR as frequent mutations are found in S-junction regions (Stavnezer et al. 2008). It might be that recruited DNA polymerases insert mismatched nucleotides and extend the strand to fill in the gap near the DSB ends. In B cells derived from XP-V patients, it was shown that Pol η can also act as an A/T mutator during CSR (Faili et al. 2004). This opens the possibility that TLS polymerases are engaged in both SHM and CSR.

➢ Common fragile sites stability

Common fragile sites (CFS) are 'hot spots' of genomic instability in chromosomes where replication machinery tends to fail if a cell undergoes moderate replication stress. CFRs are expressed as gaps, constrictions and breaks that are mapped based on their appearance on metaphase chromosomes (Ozeri-Galai et al. 2012). CFSs exist in all individuals as normal chromosomal components. A complex network of replication checkpoint and repair responses are necessary for the maintenance of CFS stability (Casper et al. 2002; Durkin and Glover 2007). CFSs are of clinical relevance because there is high correlation with chromosomal breakpoints found in certain tumors (Hecht and Glover 1984) and breaks in fragile sites were found to be involved in deletions of tumor suppressor genes and genomic amplification of oncogenes (Hellman et al. 2002).

There are several hypothesized models on how breakage at CFSs occurs (also referred to as

fragile site expression). CFSs are late replicating regions (Le Beau et al. 1998) with altered epigenetic patterns and one explanation for delayed replication could be that AT-rich repeats lead to the formation of secondary structures that stall replication fork progression (Yu et al. 1997; Hewett et al. 1998), thereby introducing chromosome breaks in regions of unreplicated DNA (Figure 7). Additionally, CFSs are present in very large genes, which can result in delayed termination of replication in S-phase and the collision of transcription and replication machinery (Helmrich et al. 2011). Additional models suggest that there might

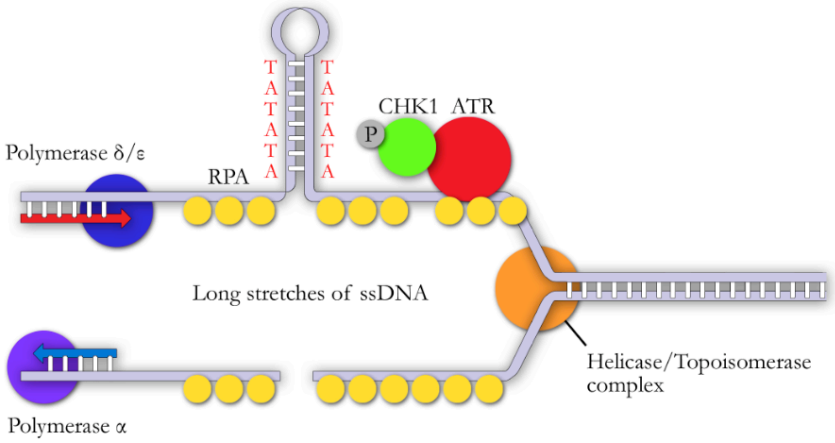

Figure 7. Origins of common fragile sites

Besides a paucity of replication origins and late replicating, large genomic domains, additional explanations for CFS expression are A-T rich sequences that can lead to the formation of secondary structures that can hamper replication fork progression. Prolonged arrest can lead to dissociation of replication polymerases from the helicase complex resulting in the accumulation of single stranded DNA coated with RPA. This eventually triggers the ATR checkpoint pathway responsible for preventng fragile site expression.

be a low density of replication origins and failure to activate additional replication origins under stress (Ozeri-Galai et al. 2011). It was demonstrated that the ATR and Chk1 checkpoint pathway is crucial for the maintenance of stability at common fragile sites and that they result from unreplicated regions where stalled forks have bypassed the replication checkpoint (Casper et al. 2002).

Expression of fragile sites is induced by low concentrations of aphidicolin, an inhibitor of replication polymerase α (Glover et al. 1984; Sheaff et al. 1991). In a study done on

FRA3B, one of the most frequently occurring fragile common sites, it was found that after the aphidicolin treatment, there was double the amount of sister chromatid exchanges at fragile sites compared to gaps and breaks, which indicated that some type of recombinational repair is occurring at these sites (Glover and Stein 1987; Walsh et al. 2013).

It was recently proposed that replication polymerases slow down or even dissociate from the template within CFS sequence and TLS polymerases might facilitate the replication of CFSs in that case. It was proposed that Pol κ is more efficient than Pol δ in synthesizing DNA through the repetitive sequence of CFSs and that Pol κ might function in direct replication within CFSs when Pol δ pauses (Bhat et al. 2013). It was suggested that Pol κ might also function in repair and recombination events downstream of double stranded breaks at CFSs (Walsh et al. 2013). Furthermore, it was reported that REV3, the catalytic subunit of Pol ζ, is required in efficient replication of CFSs during G2/M phase and that the cause of embryonic lethality in REV3 knock out mice could be high fragile site instability (Betous et al. 2009). Bhat et al. found that depletion of REV3, but not REV7, leads to increased CFS expression, elevated chromosomal instability, and arrest of cell division.

Along similar lines, Pol η was proposed to be important for CFS stability during replication in S phase (Rey et al. 2009). Depletion of Pol η led to increased CFS expression and spontaneous chromosome abnormalities, mainly chromatid breaks, however the fork progression rate was unaltered. This was backed up by increased sensitivity of Pol η depleted cell lines to low doses of caffeine, an inhibitor of ATR, especially after UV treatment. Mechanistically, it could be that stalled forks cannot be stabilized in cells where ATR is inhibited and Pol η is absent and that exposure to UV can exacerbate this instability.

Collectively, these discoveries pointed out that TLS polymerases can have fundamentally different functional roles in mammalian cells, one in the context of lesion bypass synthesis and DNA damage tolerance and the other in the context of DNA synthetic events within fragile sites. The mechanism of their action in CFS expression remains unclear but several possibilities are anticipated. It can be that TLS pols are recruited to replicate secondary

non-B DNA structures like G-quadriplexes (Betous et al. 2009). Alternatively TLS pols can be recruited in homologous repair to extend invading strands in D loop (McIlwraith et al. 2005), or to terminate replication of DNA between two converging forks prior to topological resolution (Kawamoto et al. 2005). Understanding the role of TLS polymerases in CFS expression could be crucial for understanding of mechanisms that lead to CFS instability and initiation of tumorigenesis.

2. DNA polymerases and diseases

Since the first discovery of polymerases with major DNA synthetic activity, most of the research focused on the biochemical properties and cellular functions of these molecules. In the last two decades the "polymerase field" was expanded as additional polymerases with non-canonical roles were identified and it became clear that these enzymes might have unanticipated roles in physiology and human diseases. Mutations in DNA polymerases or expression level alterations can lead to the accumulation of errors during DNA replication and repair. If these errors are not properly dealt with, they can result in the accumulation of genomic instability and drive cancer progression or developmental disorders.

Until now, mutations in two DNA polymerase genes are recognized to be the cause of human diseases. Mutations in the catalytic and regulatory domain of the *POLH* gene (encoding Pol η) result in XP-V. Mutations within the *POLG1* gene underlie autosomal and recessive forms of Progressive External Ophthalmoplegia (PEO), Alpers syndrome, Ataxia-Neuropathy or infertility. Single nucleotide polymorhisms (SNP) were identified in most DNA polymerases and many of these SNPs are predicted to result in nonsynonymous amino acid substitutions. Functional consequences of these variants are being currently investigated.

2.1. Pol η and Xeroderma Pigmentosum Variant

XP-V is an autosomal recessive disease caused by molecular alterations in the gene *POLH* that encodes translesion polymerase Pol η. There are an additional 7 groups of Xeroderma Pigmentosum diseases where nucleotide excision repair (NER) is impaired and is caused by a defect in of one of the seven genes belonging to complementation groups (XPA-XPG). The XP disease is characterized by sun sensitivity, cutaneous and ocular deterioration and early onset of neoplastic changes on sun-exposed skin. Overall progress of XP-V is more favorable as the symptoms are less severe and begin later compared to other XP types. Patients with XP-V represent around 20% of all patients with XP.

Unlike NER-defective cells, XP-V cells have functional NER but are deficient in post replication repair (PRR) (Robbins et al. 1975; Lehmann et al. 1977). In contrast to the NER-defective XP cells, which have very marked hypersensitivity to UV, fibroblasts from XP-V patients are just moderately sensitive to UV light. However both NER-defective XP and XP-V cells show high frequency of UV induced mutations (Maher et al. 1976; Myhr et al. 1979; Yagi et al. 1991). XP-V was described first time in 1970 by Ernst G. Jung (Jung 1970), but the responsible gene, mutations and mechanism that results in the development of the disorder were not identified until 1998. It was first discovered that XP-V cells are defective in the repair of UV damaged DNA (Ensch-Simon et al. 1998; Svoboda et al. 1998), specifically in the repair of CPD dimers, which pointed out that TLS is impaired in XP-V patients (Cordonnier et al. 1999) and subsequently the human homolog of the yeast *RAD30* gene, designated as Pol η, was identified as mutated in XP-V patients (Ensch-Simon et al. 1998; Svoboda et al. 1998; Cordonnier et al. 1999; Johnson et al. 1999) Complementation of XP-V cell lines with Pol η corrected the defect in bypass of CPD dimers (Masutani et al. 1999). Mutations in the Pol η gene can be classified in three categories (Broughton et al. 2002). In the first category are null alleles resulting in a severe truncation of the protein. In the second category are missense mutations placed in the conserved catalytic domain of the *Pol η* gene. Cells bearing mutations in the catalytic domain are unable to perform TLS. In the third category are mutations in the C-terminus where the nuclear localization signal (NLS) is located, so these cells are able to carry out TLS but unable to localize to the nucleus or replication foci (Kannouche et al. 2001; Broughton et al. 2002).

2.2. DNA Pol γ and human diseases

Pol γ is the only known mitochondrial DNA polymerase that is involved in replication and repair identified to date. It is encoded by the *POLG* gene and there are about 150 pathogenic mutations mapped to the coding sequence of this gene that are associated with mitochondrial diseases and identified in patients (all listed in Human Polymerase Gamma Mutation Database: http://tools.niehs.nih.gov/polg). Diseases caused by those mutations are highly heterogeneous and mostly identified in compound heterozygotes where each *POLG* allele has one or more different mutations (Stumpf and Copeland 2011). Mutations in *POLG* are associated with various disorders (Figure 8) such as PEO, Alpers syndrome, Ataxia-Neuropathy, dysarthria, premature menopause and infertility (Longley et al. 2005; Chan and Copeland 2009; Copeland 2012).

Progressive external ophthalmoplegia (PEO) is type of muscle dystrophia characterized by progressive weakening of external eye muscle and bilateral ptosis resulting in blepharoptosis and ophthalmoparesis. Affected individuals can also develop progressive weakness of proximal skeletal muscles and exercise intolerance. Apart from one, all mutations causing autosomal dominant forms of PEO were identified in the polymerase domain of Pol γ, mostly resulting in mtDNA depletion and/or accumulation of mtDNA point mutations and deletions (Zeviani et al. 1989; Van Goethem et al. 2001). PEO usually manifests between 18 and 40 years of age. It is characteristic for PEO patients that skeletal muscles show decreased respiratory chain enzyme activity causing a mosaic cytochrome c oxidase (COX) defects in muscles (Suomalainen et al. 1997) and there is typical histopathological changes present in skeletal muscles. For example, by Gomori trichrome staining of muscle fibers it is possible to visualize enlarged mitochondria and as well as "ragged red fibers" visible by dark red staining. This staining is regularly used for PEO differential diagnosis (Yamamoto and Nonaka 1988). However, it is not yet elucidated the mechanism by which impaired function of Pol γ and decreased activity lead to the accumulation of mtDNA defects in muscle cells and to the PEO phenotype. Autosomal recessive forms of PEO are most often identified in compound heterozygous bearing

multiple mutations in POLG that can affect the polymerase and exonuclease domains of the protein or domains necessary for interaction with the accessory subunit p55. These

patients usually have a complex clinical picture because PEO occurs associated with other symptoms like ataxia (Van Goethem et al. 2004), parkinsonism (Davidzon et al. 2006) or profound peripheral neuropathy (Van Goethem et al. 2003).

Ataxia-neuropathy syndrome is manifested in the early teens to late thirties and it is caused by autosomal recessive mutations in POLG resulting in mtDNA deletions. Symptoms are variable and can be manifested as peripheral neuropathy, dysarthria, dysphagia, ophthalmoparesis, encephalopathy, myoclonus and involuntary movemements progressing toward epileptic attacks. Depending on the combination of symptoms and their severity, ataxia can be termed and classified as the following syndromes: mitochondrial-associated ataxia syndrome (MIRAS) (Hakonen et al. 2005; Winterthun et al. 2005), SANDO (sensory ataxic neuropathy, dysarthria, and ophthalmoparesis) (Van Goethem et al. 2003) and SCAE (spinocerebellar ataxia with epilepsy) (Lamperti and Zeviani 2009). The conditions in this group feature a range of similar signs and symptoms, so often is hard to differentiate these syndromes.

Alpers' syndrome is the most severe of POLG-related diseases. It is progressive degenerative disorder of central nervous system with the beginning in the childhood. The symptoms that typically can occur are severe encephalopathy, epileptic seizures, progressive mental retardation, dementia and hepatic failure. The POLG mutations in Alpers patients are recessive and many of the same mutations are present in those affected by arPEO (Nguyen et al. 2006). However there are mapped mutations that lead to mono-allelic expression of POLG and reduced content of mtDNA to 30% of those of wild type as well as undetectable activity of Pol γ in skeletal muscles and liver (Naviaux et al. 1999; Naviaux and Nguyen 2004). These types of mutations are yet not identified in the other mitochondrial diseases.

Premature aging for a long time was considered to be a consequence of mitochondrial dysfunction that led to the accumulation of errors in mitochondrial electron transport and the accumulation of ROS. The occurrence of premature aging was reported in two independently generated mouse models harboring mutations in the exonuclease proofreading domain of POLG (Trifunovic et al. 2004; Kujoth et al. 2005).

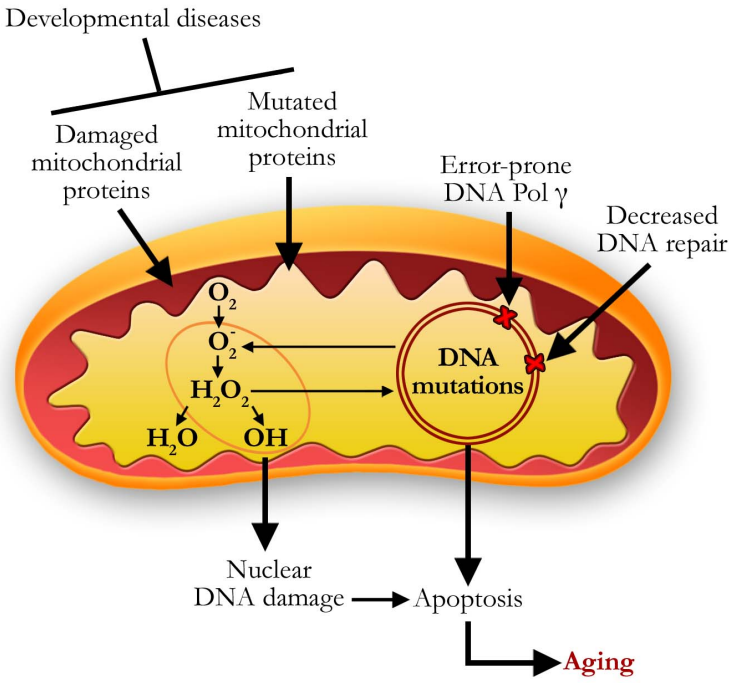

Figure 8. Damage of mitochondrial DNA can contribute to developmental diseases and accelerated aging

Mutations in Pol γ can lead to decreased fidelity and repair of mtDNA. As a result mutated mitochondrial proteins are produced and defects in their functions impact on the TCA cycle. This can lead to increased ROS (superoxide anion, hydrogen peroxide, and hydroxyl radicals), as a by-product of mitochondrial oxidative phosphorylationoxidative disbalance and cause further damage to mitochondrial nucleic acids and proteins. Increased ROS can lead to nuclear DNA damage and activate caspase pathways leading to apoptosis, cell death or accelerated aging. Mutations in mtDNA that lead to impaired function, disfunctional mitochondrial proteins and impaired homeostasis can contribute to the development of pathologies like Alper's syndrome, PEO or Ataxia-neouropathy syndrome. Addopted and modified from Loeb at al, 2005.

It was found that in these mice, mitochondrial mutation rates are elevated by at least 3- to 11-fold in multiple tissues. Both models had similar phenotypes characterized by reduced muscle mass and body fat, hair graying and hair loss, induced incidence of kyphosis, dilated cardiac hypertrophy, loss of fertility and reduced survival. This theory was brought into question when additional mouse models carrying mtDNA deletions of up to 80% were generated (Inoue et al. 2000; Nakada et al. 2004; Kasahara et al. 2006) and they did not

demonstrate almost any of the premature aging features observed in POLG exonuclease mutants. The contribution of mtDNA mutations and deletions to normal aging remains a controversial issue (Figure 8).

2.3. TLS DNA polymerases and genetic instability

Fidelity of DNA replication depends on the ability of a DNA polymerase to select and incorporate correct nucleotides during elongation at replication forks or during repair of DNA damage. Cancer susceptibility is strongly correlated with a course of changes that result from a decrease in replication fidelity (Loeb et al. 2003; Bielas et al. 2006). Loeb et al. suggested that the heterogeneity of cancers could be explained by a mutator phenotype, which implies that normal mutation rates are insufficient for the occurrence of multiple mutations and that there has to be additional mechanisms that initially lead to mutations of genes responsible for fidelity of replication and efficacy of DNA repair. Perturbed regulation of DNA polymerase levels can lead to more frequent imposition of error-prone polymerases from X and Y family at replication forks and temporary replacement of error-free polymerases with error prone TLS pols. Aberrant engagement of the TLS polymerases has been suggested to play a role in tumorigenesis by promoting genetic mutations (Albertella et al. 2005).

Despite the number of studies trying to identify links between cancer and gene expression of TLS polymerases, the exact relationship remains undetermined. Prognostic significance of Pol ζ, Pol κ, Pol η, REV1 and Pol ι were studied in different tumors. It was found in a study on patients with glioma that Pol κ and Pol ι were markedly upregulated and they were associated with shorter survival of patients (Wang et al. 2010). Pol ι was found to also be overexpressed in malignant breast cells (Yang et al. 2004) and in uterus, stomach, prostate and rectum cancers (Albertella et al. 2005). In the same study from Albertella et al. Pol κ was under-expessed in many other tumor samples. However, overexpression of Pol κ was identified in non-small cell lung cancer (NSCLC) and it correlated with the mutation status of *TP53* (J et al. 2001; Wang et al. 2004). In this study it was suggested that Pol κ overexpression in lung tumors was secondary to p53 loss. Pol η was identified as potential prognostic marker in study on NSCLC patients treated with platinum-based chemotherapy

as high Pol η expression levels were brought in relationship with shorter survival of patients (Ceppi et al. 2009). For Pol ζ it was found that the catalytic subunit, REV3L, was upregulated in gliomas (Wang et al. 2009) while in the another study addressing REV3L transcript levels showed that REV3L was expressed uniformly in lung, gastric, colon and renal tumors compared to normal tissues (Kawamura et al. 2001). Pan et al. questioned the link between TLS polymerase overexpression and cancer. In a significant number of specimens from lung, stomach and colorectal cancers they found downregulation of Pol η, Pol κ, Pol ι and Pol ζ, with the exception that Pol η was upregulated in colorectal cancers (Pan et al. 2005).

The variation in the expression levels of TLS pols in these different studies could be explained by a function of tumor stage or by cell-type specificity. Nevertheless, this collection of paradoxical findings illustrates how complex the expression pattern of TLS polymerases in cancer is and shows that it can vary significantly between normal tissue and tumors. Furthermore, it demonstrates that the levels of TLS polymerases are commonly altered in cancer, although additional molecular and epidemiological studies are needed to understand how polymerases affect human health and cancer risk.

3. Mouse models

For the most part, data obtained about *in vitro* functions of TLS polymerases was controversial and prompted several questions. First, why would a mammalian organism need so many specialized enzymes for DNA damage tolerance and what is the bona fide functional relevance *in vivo* for all of these enzymes that are generally error-prone? In addition, the low fidelity of TLS polymerases casts doubt on whether these enzymes are in fact protective or if their faulty nature can be potentially harmful. Based on the conceptual framework built from *in vitro* and model system data, TLS polymerases are predicted to be primarily involved in DNA damage tolerance pathways. However, recent advances made in the last few years have opened up the possibility to many new functions that these enzymes may exert. Given the complexity of this issue and the potential for cell or organ specific

functions, a number of laboratories have generated mouse models for each of the TLS polymerases to identify in their *in vivo* roles.

3.1. DNA Polymerase η mouse models

The first Pol η deficient mouse was generated by the Kucherlapati group on a C57BL/6 background by knocking out exon 4 (Lin et al. 2006) and producing a truncated protein lacking polymerase activity and the C-terminus required for interactions with other proteins. *Polh*$^{-/-}$ mice are fertile and viable, without any phenotypic abnormalities or spontaneous tumor formation during 12 months of observation. After chronic, 2 month treatment with UVB irradiation, *Polh*$^{-/-}$ mice developed severe lesions on their ears and squamous cell carcinomas on the dorsal skin, whereas heterozygous and wild type littermates did not show any of these malignancies. Since *Polh*$^{-/-}$ mice were generated using the J1 embryonic stem cell line derived from 129 mouse strain that is spontaneously deficient for *Poli*, it was possible to test influence of Pol ι on tumor formation in Pol η deficient and 129/OLA wild type counterparts and Pol ι haploinsufficiency did not lead to the exacerbation of skin changes upon chronic UV treatment. Subsequently the Hanaoka group generated mice deficient for both genes but this model will be described in 1.3.4.2. section. Two more groups generated Pol η deficient mice and they investigated if the process of Ig maturation is affected. Martomo et al. designed a knock-out by deleting exon 8 on the C57BL/6 background. B-cell development and CSR was normal in these mice, however SHM was affected since there was decline in A to T mutagenesis in the J_H4 intron and Sμ region (Martomo et al. 2005). The Wang lab generated crosses of *Polh*$^{-/-}$ with catalytically inactive *Rev1* (*Rev1AA*) mice. *Polh*$^{-/-}$ *Rev1AA* mice are viable, fertile, and without apparent abnormalities. B-cell and CSR events were not affected in double mutants but SHM analysis in the J_H4 intron revealed almost no C to G transversions and reduced G to C transversions compared to *Rev1AA* or *Polh*$^{-/-}$ mice (Kano et al. 2012). This study identified the existence of functional and genetic interactions between REV1 and Pol η as well as a novel role for Pol η in SHM.

3.2. DNA Polymerase ι mouse models

It was reported that the commonly used 129/Ola mouse strain is deficient for *Pol ι*, since the gene carries a nonsense mutation in exon 2 that results in the truncation of the Pol ι protein (McDonald et al. 2003). It was supposed that Pol ι has an essential role in SHM based on its low fidelity on undamaged DNA and deficient SHM in the human Burkitt lymphoma cell line (BL2) bearing a homozygous deletion of both *Pol ι* alleles. However analysis done in 129/Ola strain refuted this expectation since the mice had a normal frequency and pattern of mutations in the J_H4 intron (McDonald et al. 2003). This was tested also in the Pol ι knock-out on the C57BL/6 background either alone or crossed to *Polh*$^{-/-}$ mice. Double knock out mice had the same mutation spectrum as *Polh*$^{-/-}$ mice and the SHM frequency of *Poli*$^{-/-}$ was the same as in the matched wild type mice (Martomo et al. 2006). The Hanaoka group generated double deficient *Polh*$^{-/-}$ (exon 8 disrupted) and *Poli*$^{-/-}$ (exon 2 disrupted on 129/OLA background, backcrossed to C57BL/6 for 12 generations) mice and they analyzed the influence of UV irradiation on the skin. Interestingly, while double deficient fibroblasts were not more sensitive than *Polh*$^{-/-}$ fibroblasts to UVC, double knock-out mice showed slightly earlier onset of skin tumor formation and somewhat higher predisposition to tumor development upon chronic treatment with UVB (Ohkumo et al. 2006). Tumors developed in Pol η deficient mice were predominantly epithelial tumors while those formed on Pol ι deficient background were mostly mesenchymal tumors such as sarcomas and hemangiomas. The authors explained this contrast in tumor spectrum by differences in the dynamics of CPD clearance between the epidermis and dermis, demonstrating a supporting role of Pol ι in the delayed phases of CPD clearance that occurs in dermis (Qin et al. 1995). The difference in the incidence of mesenchymal tumors after chronic UV treatment in the Pol ι deficient background was high, demonstrating a controversial ability of Pol ι to act in DNA damage tolerance pathway *in vivo*. This experimental model pointed out that one of the functions of Pol ι is to back up other TLS polymerases in the repair or tolerance of UV induced lesions, protecting mammals from harmful effects of exposure to UV light.

3.3. DNA Polymerase κ mouse models

Mice deficient for Pol κ were generated on a mixed 129/OLA and C57BL/6 background,

by disruption of exon 6 that contains critical catalytic residues (Schenten et al. 2002) and these mice were viable and fertile. Since Pol κ has the highest expression in the seminiferous tubules of the testis, it was supposed that males would be infertile or at least develop abnormalities related to the sperm and testis. However, there were not any histological differences detected in the testes and the shape and mobility of the sperm were comparable to those of wild type. Since Pol κ is an error prone polymerase, it was also supposed that it had a function in SHM, but again this was shown not to be the case. Both SHM and CSR were unaffected and B and T cell populations were present in normal proportions. SHM was addressed in a different mouse model and it was also reported that absence of Pol κ does not affect the efficiency or mutation spectrum during Ig maturation (Shimizu et al. 2003).

It was therefore surprising that *Pol* $\kappa^{-/-}$ mice showed a higher degree of spontaneous mutations in 2 additional studies. Higher mutation rates were detected at two expanded simple tandem repeat (ESTR) loci of *Pol* $\kappa^{-/-}$ mice compared to wild type (Burr et al. 2006). In the model of Big Blue-*Pol* $\kappa^{-/-}$ mice with the lambda cII mutagenesis reporter gene, increased frequency of mutations was recorded in lung, kidney and liver (Stancel et al. 2009). *Pol* $\kappa^{-/-}$ MEFs also showed increased sensitivity to benzo[a]pyrene-dihydrodiol epoxide (BPDE) consistent with the proposed role of Pol κ in TLS past dG adducts in DNA. The higher degree of mutations in the absence of Pol κ can be explained by the fact that liver, kidney and lung accumulate DNA base damages caused by naturally occurring polycyclic aromatic hydrocarbons more than other organs and that Pol κ is expressed in these organs because of its protective role. The biological significance of Pol κ was strengthened by finding that Pol κ is important for accurate and efficient by-pass of benzo[a]pyrene (B[a]P)-adducted guanine (Ogi et al. 2002). Benzo[a]pyrene (B[a]P) is an environmental carcinogen that is present in cigarette smoke and air pollutants and is considered as one of main etiological factors for lung tumor development.

3.4. REV1 mouse models

REV1 deficient mice were generated by deletion of exon 10 that contains part of the catalytic domain. *Rev1*$^{-/-}$ mice could not be obtained beyond an F2 backcross into C57BL/6

mice, whereas the same was not true in 129/OLA mice but it was unrelated to Pol ι deficiency (Jansen et al. 2006) and *Rev1* deletion resulted in reduced growth. By SHM analysis it was shown that mice displayed normal mutation frequency but a complete absence of C to G transversions and a slight decrease in G to C transversions. It was shown that *Rev1*$^{-/-}$ MEFs have significantly reduced DNA synthesis at 6-4PP lesions in contrast to CPD lesions where DNA synthesis reduction was modest (Jansen et al. 2009). The authors proposed that depending on the domain involved, REV1 could mediate early or late mode of DNA damage bypass and the BRCT domain of REV1 is necessary for the initial progression of stalled forks at UV damaged sites. Mice generated with a truncated *Rev1* BRCT domain showed elevated instability upon UVC, reduced mutagenesis at *Hprt* sites and also less mutations at TT dimers compared to wild type cells (Jansen et al. 2005). Since the mutation phenotype was opposite to the one seen in XP-V cells, the authors suggested that in the Pol η deficient scenario, REV1 is the possible factor driving carcinogenesis by promoting error-prone TLS. To test this hypothesis they generated mice on an NER deficient background by crossing *Xpc*$^{-/-}$ with hypomorphic *Rev1* BRCT mice. Surprisingly, chronic treatment with low dose of UVB in *Rev1*$^{b/b}$*Xpc*$^{-/-}$ mice led to earlier manifestation of squamous cell carcinoma (SCC) compared to *Xpc*$^{-/-}$ mice (Tsaalbi-Shtylik et al. 2009). Signs of inflammation marked by acanthosis and Il-6 expression were more pronounced in the epidermis of *Rev1*$^{b/b}$*Xpc*$^{-/-}$ mice treated with UV compared to controls. These results indicated that error-prone REV1 is necessary to suppress UV-induced carcinogenic effects even at the expense of high load of mutations and that the final role of REV1 is beneficial.

4. DNA Primases

A key function of DNA primases is to start the synthesis of new DNA strands by synthesizing short RNA–oligonucleotides on single stranded DNA. These short fragments will serve as starting sites, or primers, for replication polymerases that are not capable themselves of initiating replication *de novo* (Ogawa et al. 1985; van der Ende et al. 1985). In all eukaryotic species analyzed to date, DNA primase comprises two subunits of

approximately 58kDA (Prim2) and 49 kDa (Prim1), and is tightly bound to the 180-kDa pol α (Foiani et al. 1997). The pol α–primase complex also contains a fourth subunit whose molecular weight varies between 70 and 90 kDa, depending upon the organism (Figure 9). This complex is responsible for initiation of synthesis of nuclear DNA. In contrast to the nucleus, no DNA primase has been characterized in the mitochondria. The activity of a putative mitochondrial primase was reported by Clayton's group in 1980 (Wong and Clayton 1985; Wong and Clayton 1986) but the protein responsible was never identified. However, it was eventually shown that the mitochondrial RNA polymerase (POLRMT) is necessary for priming DNA synthesis in mitochondria (Wanrooij et al. 2008; Fuste et al. 2010).

Several distinct primase families exist but they do not share a sequence relationship between the families, even though they share common catalytic features. This difference in families is explained by the possibility that primases emerged more than once during evolution. Structurally, two groups of primase superfamilies can be distinguished and classified into the DnaG-like superfamily and the archaeo-eukaryotic primase (AEP)-like superfamily (Kuchta and Stengel 2010). The DnaG-like superfamily is identified in eubacteria, phages and some plasmids. These primases consist of a single unit that is involved in replication and it is usually associated with helicases that drastically increases their synthetic efficiency (Frick and Richardson 2001). The AEP–like superfamily includes eukaryotes, herpes viruses, and archae (Iyer et al. 2005). These are heteromeric enzymes that normally consist of small catalytic subunits and a large accessory subunit. In eukaryotic organisms, AEP family primases normally associate with polymerase α in a four-subunit complex. The small subunit p49 (Prim1) from this complex is a homologue of other AEP family members and represents the catalytic core of this complex (Muzi-Falconi et al. 2003).

To date, there is no high-resolution structural data for eukaryotic primases and, therefore, a combination of bioinformatic sequence analysis and mutagenesis studies have been used to identify residues important for primase functions. Eukaryotic primases are homologous to the X-family of polymerases in several catalytic particles. Particularly the AEP primase is comparable to polymerase β that is involved in DNA repair (Holm and Sander 1995). The three essential acidic residues found in the active site of other nucleotide polymerases,

analogous to those in the p49 subunit, are aspartates D109, D111 and D306. They are essential for phosphodiester bond formation and are thought to form the metal-binding core of the active site (Copeland and Tan 1995). In a number of AEP primases, a zinc-binding motif is present and the same can be identified in the bacterial DnaG primase family with the difference that this motif is placed in different domains between these two families (Pan and Wigley 2000). It is speculated that analogous to the functional role established in bacterial primases, this motif is required in AEPs for binding to ssDNA. Compared with other template-dependent DNA and RNA polymerases, the eukaryotic primase exhibits the lowest fidelity and it is the most error-prone polymerase known (Sheaff and Kuchta 1994). However, fidelity of replication is not compromised due to high error frequency of primase since the RNA primer is degraded by cellular nucleases and replaced with DNA.

The Pol α-primase complex (referred to as Pol-Prim henceforth) interacts with a broad network of proteins, consistent with the fact that replication is highly regulated and involves a multitude of players. It was suggested that interaction with Cdc45, RPA and PARP can influence the activity of the Pol-Prim complex. RPA binds the p180, p58 and

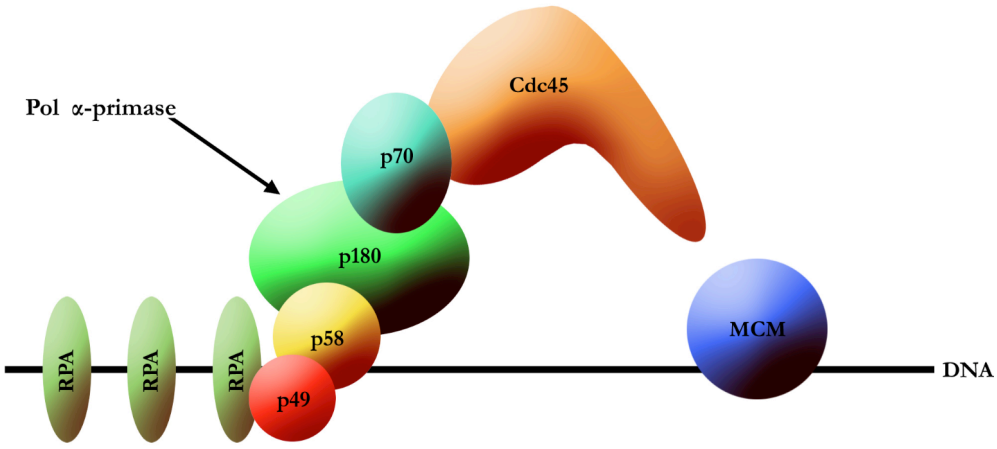

Figure 9. Pol-Prim complex and interacting partners

Pol-Prim complex consists of four subunits: 58kDA (Prim2) and 49 kDa (Prim1) primase subunits tightly bound to polymerase α (subunits 180kDa and 70kDa). The interaction with Cdc45 and MCM thorugh p70 subunit are proposed to regulate recruitment of Pol-Prim complex to replication origins. RPA can interact with p49, p58 and p180 and it can inhibit the function of Pol-Prim complex, potentially playing a role in repair signaling. Adopted from Arezi and Kuchta, 2000.

p49 subunits and it is involved in the inhibition of Pol-Prim because ssDNA coated with RPA is an inadequate substrate (Weisshart et al. 2000). Cdc45, that is found at origins of replication, interacts with the p70 subunit and also with MCM helicase complex. It is suggested that p70-Cdc45-MCM interactions (Figure 9) might recruit pol α–primase to origins of replication to allow primer synthesis on RPA-coated DNA (Kukimoto et al. 1999; Labib et al. 2000). PARP interaction was also confirmed by co-immunoprecipitation experiments (Dantzer et al. 1998) but it is not clear if PARP inhibits the primase activity of the Pol-Prim complex or if it is immobilizing this complex to lesions. In Xenopus the activation of checkpoint signaling requires accumulation of chromatin bound Cdc45-Pol-Prim complex (Michael et al. 2000) while in yeast containing a mutation of the p49 subunit, cell cycle progression was altered in response to DNA damage (Marini et al. 1997). Aside from its major role in replication and proposed possible role in repair, primases are also required for the maintenance of telomeres (Diede and Gottschling 1999) and have been proposed to function in the restart of stalled forks. *In vitro* it was identified that bacterial primases can co-ordinate DnaG-dependent priming downstream of the lesion on both the leading and lagging strand to facilitate the reactivation of stalled forks (Heller and Marians 2006).

5. PrimPol, novel primase polymerase

The laboratories of Doherty and Shuman (Zhu and Shuman 2006; Zhu et al. 2012) identified an AEP domain in the *M. Tuberculosis* ligase gene, *LigD*, and named this primase/polymerase domain PolDom (Doherty et al. 2001; Weller et al. 2002). Both groups demonstrated that this enzyme functions in NHEJ repair in bacteria (Pitcher et al. 2006; Pitcher et al. 2007). The function of AEPs in bacterial repair propelled the idea that uncharacterized AEPs may exist in eukaryotes as well. Iyer and colleagues performed phylogenetic analysis of all enzymes across different cellular systems that were homologous in AEP catalytic domains and *CCDC111* was the only eukaryotic gene that contained this domain (Iyer et al. 2005). In an attempt to identify the activity and function of this novel eukaryotic enzyme, Doherty and colleagues started an *in vitro* characterization and identified

that CCDC111 can act as an RNA and DNA template-dependent primase and polymerase *in vitro*. For this reason a new name was coined for this enzyme that embraces both functions: PrimPol. The *PrimPol* gene encodes a putative primase-polymerase and is found in both human and mouse.

PrimPol is present in a range of unicellular and multicellular eukaryotes, however it is not conserved throughout all eukaryotes. PrimPol is absent from *Drosophila, C. elegans* and all but one fungus, the parasitic *B. dendrobatidis*. Additionally, PrimPol has not been identified in prokaryotic and archaeal genomes.

The mouse *PrimPol* gene is located on chromosome 8. There are several conserved regions in the *PrimPol* sequence, generaly divided into two domains (Figure 10); the first is a catalytic AEP domain towards the amino-terminus, thus identifying PrimPol as a member of the AEP superfamily (Figure 10).The *PrimPol* AEP domain contains the three catalytic motifs, annotated as motif I, II and II that are conserved in all AEP-like enzymes. Residues in motif I and III are predicted to be required for binding of divalent metal ions and motif II required for nucleotide binding (Copeland and Tan 1995; Lao-Sirieix and Bell 2004). The

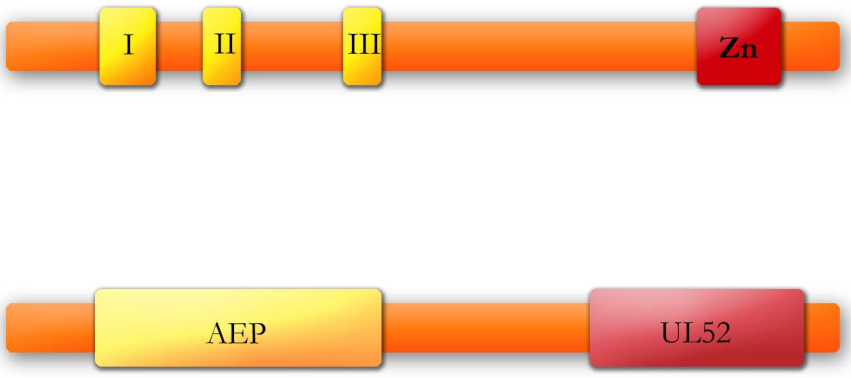

Figure 10. Conserved domains of PrimPol (*Mus musculus*)

PrimPol contains two conserved domains, AEP (archaeo-eukaryotic primase) and the UL52 domain. The N-terminal AEP domain is identified by three catalytic motifs predicted to be crucial for the binding of divalent metal ions (motif I and III) and dNTP binding (motif II). The C-terminal domain is homologous to that of the UL52 herpesvirus protein that is part of a replicative helicase-primase complex. This domain contains a Zinc binding motif potentially important for primer synthesis and DNA binding.

second conserved region among PrimPol homologues is a motif with homology to the human herpesvirus (HHV) UL52 subunit of the helicase-primase complex and is predicted to be a zinc-finger domain that plays a role in primer synthesis and DNA binding (Biswas and Weller 1999; Biswas and Weller 2001).

The main focus of this dissertation is the functional characterization of the novel primase-polymerase, PrimPol. The introductory chapter of the thesis was designed to give the reader a thorough and up-to-date introduction to TLS polymerases, DNA damage tolerance and DNA primases. In the first part of results, I will describe the generation of a PrimPol deficient mouse model and the functional characterization of PrimPol *in vitro* and *in vivo*. The second part of the results section is dedicated to the identification of PrimPol cellular localization and potential interacting partners. In the last chapter the biological significance, putative roles of PrimPol and its potential connection to human pathology will be discussed.

Materials and methods

1. Generation of a PrimPol deficient mouse model

Design and construction of a PrimPol-targeting vector, ES cell transfection, identification of correctly targeted cell clones, ES microinjection into pre-implantation stage mouse embryos and chimera generation were done by Mouse Mutant Core Facility at IRB Barcelona.

1.1. Generation and screening of PrimPol targeting constructs

The *PrimPol* (*CCDC111*) knock out first targeting construct was generated using standard pRed/ET recombineering methods in the IRB Mutant Mouse Core facility. The genomic locus of *PrimPol* was captured from a BAC clone (bMQ227f06) that was obtained from Sanger gene service and screened by PCR. A Zeo/pheS and LoxP flanked EM7-Kanamycin cassette were sequentially recombineered into the BAC up and downstream of exon 5 and the modified genomic locus recombineered into a capture vector. The EM7-Kanamycin cassette was deleted by Cre expression, leaving a single LoxP site 3' of exon 5. A Gateway reaction was then carried out to swap the Zeo/pheS cassette for a LacZ/Neo Trap cassette containing a LoxP site upstream of exon 5. ES cells were targeted by electroporation of the AsiSI linearized construct followed by selection with Neomycin. Positive clones were screened by long range PCR using DNA isolated from targeted ES cell clones as substrate.

Table 1. PCR reaction conditions

Genomic DNA	1µl
Buffer 10X	2.5µl
dNTPS 10X	2.5µl
MgSO4	2µl
KOD-HS TAQ	0.5µl
Primer 1	0.75µl
Primer 2	0.75µl
Betaine 5X	5µl
Water	10µl

Table 2. Screening primer sequences

CDS Test F	AAGCCAGAAGAACCATCCTCC
GF3	GTGAGCGTCAGCTGAGCGATAGGTTGGCTG
Screen O 3.1	AACATCTTCGGCTGAGCACT
GR3	CTGGAGAGTGATAACTGATACTACATAC
GR4	CACTAACAGACAGGAGAAGGAACAAG
UR5	AGGGCTGTTCAGGCTGCTGTATAA
LAR3	CACAACGGGTTCTTCTGTTAGTCC
KO cass diag rev3	GGCCACCCAACTGACCTTGGG
3'PNF	ATCCGGGGGTACCGCGTCGAG

Table 3. Primer combinations and product sizes for long range PCR

For 5' side		
CDS test F	UR5	1457
CDS test F	LAR3	5043
CDS test F	KO cass diag rev3	5098
GF3	UR5	2633
GF3	LAR3	6219
GF3	KO cass diag rev3	6274
For 3' side		
Ccdc111 screen O 3.1	3' PNF	6013
GR3	3' PNF	7338
GR4	3' PNF	7134

1.2. Genotyping strategy

For the purpose of genotyping we have designed primers for PCR that allowed us to distinguish with high accuracy wild type, gene trap and knock out alleles based on unique amplification products. PCR reaction conditions are in Table 1. Primer sequences are provided in Table 4. and Table 5. Genomic DNA used for genotyping was isolated from

the tails of the mice and extracted by digestion with proteinase K over night at 56ºC, followed by isopropanol precipitation. The buffer used for genomic DNA extraction has next composition: 0.1M Tris/HCl, 200mM NaCl, 0.2% SDS and 5mM EDTA.

Table 4. PCR genotyping primers for genomic DNA

Ccdc111-LoxP-F1	GAGATGGCGCAACGCAATTAA
Ccdc111-DR	ACTCTGAGGCCAGATGAGCAC
Ccdc111_GenR2	TGAGAAACCTTCACCCAGCCC
3'U PNF	ATCCGGGGGTACCGCGTCGAG
Ccdc-GenF1	TGCACAAGAGGATGTAGTCCGTCA
Ccdc-GenF2-R	TCCAGAAGTCCTGCGTTCAGTTCT
Ccdc111-COND-F1	GAAGGCGCATAACGATACCACGAT
Ccdc111_GenR2	TGAGAAACCTTCACCCAGCCC
Ccdc111-COND-F1	GAAGGCGCATAACGATACCACGAT
Ccdc111-DR	ACTCTGAGGCCAGATGAGCAC

Table 5. Expected products from indicated alleles (KO, WT, COND or TRAP)

Forward primer	Reverse Primer	Amplicon
Cdc111-LoxP-F1	Ccdc111-DR	3' LoxP 341 bp, WT no product
3'U PNF	Ccdc111_GenR2	Trap 380, WT no product
Ccdc-GenF1	Ccdc-GenF2-R	WT 204 bp, Trap no product
Ccdc111-COND-F1	Ccdc111_GenR2	Cond 422 bp, WT, Trap no product
Ccdc111-COND-F1	Ccdc111-DR	KO 590 bp, WT, Trap, Cond no product

1.3. Real time PCR based assessment of PrimPol expression levels

In order to assess the endogenous transcript levels in gene trap and knock out mice as well

as in siRNA experiments, we have developed a quantitative/real-time PCR (qPCR) assay for both the human and mouse *PrimPol* genes. qRT-PCR was performed using comparative CT method and a Step-One-Plus Applied Biosystems Instrument. Amplification was performed using SYBR Green Expression Assay following manufacturer's instruction. Primer sequences are given in the Table 6. and qRT-PCR reaction conditions are given in the Table 7. All assays were done in triplicates and Gapdh or Beta Actin primers were used as an endogenous control for normalization. Data are means ± standard deviation of at least 3 experiments.

Table 6. Genotyping primers for cDNA (by qPCR)

Tested gene	**Housekeeping gene**
PrimPol (exon3-5)	**Gapdh**
Fw:TAACAAATTGGCCAACCCAGGAG Rv: ACCTTAGCTTCATCATCCTCGGC	Fw: GCACAGTCAAGGCCGAGAAT Rv: GCCTTCTCCATGGTGGTGAA

Table 7. qPCR conditions

Step	**Temperature**	**Time**
Holding stage	95ºC	10min
Cycling stage	95ºC 60ºC repeat these 2 steps 40 times	15sec 1min
Melt Curve Stage	95ºC 60ºC 95ºC	15sec 1min 15sec

2. Cultured human and mouse cell methods

2.1. Cell cultures

The cell media, supplements, and antibiotics, were purchased from Gibco Invitrogen. Cell culture flasks, plates, dishes, and cryotubes were purchased from Nunc and BD Falcon. All cells were grown in a 37ºC incubator with a humidified atmosphere containing 5 % CO2.

➢ Human cell lines

Osteosarcoma U2OS and human embryonic kidney HEK293 cells were cultured in Dulbecco's modified Eagle Medium (DMEM, Invitrogen) supplemented with 10 % (v/v) foetal calf serum (FCS) and 100 U/ml penicillin/streptomycin (Gibco). Strep-FLAG-PrimPol-HEK-293 cells, engineered for stable expression of epitope tagged PrimPol, were cultured in the same media containing selection antibiotic 10 μg/ml Puromycin.

➢ Preparation of mouse embryo fibroblasts (MEFs)

Mouse embryonic fibroblasts were isolated from pregnant females at E14.5. Uterine horns were removed and placed into a petri dish with PBS. Intact embryos were taken out from uterine horns into fresh PBS, embryos were then released from yolk sac and placenta and moved to fresh PBS. Heads and viscera were removed and tails were taken for the genotyping. Carcasses were washed in fresh PBS and kept over night at 4ºC in the 5ml trypsin in 15ml Falcon tubes. Upon obtaining genotyping results, selected embryos were processed further. Trypsin volume was reduced in tubes and carcasses were incubated in 1ml of remaining trypsin at 37ºC for 20 minutes. 5ml of DMEM media was added to each carcass and they were minced by pipetting up and down with a 5ml serological pipette. The supernatant containing cells were plated in 3 x 10 cm plates and further propagated as necessary.

➢ Culture of primary MEFs

Primary MEFs (p0-p5) were cultured in Dulbecco's modified Eagle Medium (DMEM) supplemented with 10 % (v/v) foetal calf serum (FCS), 2mM L-glutamine and 100 U/ml penicillin. Cells were used for experiments until passage 5 while still in the log phase of growth.

➢ Generation and culture of transformed MEFs

Primary MEFs were transformed in two ways.

a) The primary mouse embryonic fibroblast cells were replated every 3 days at the rigid density of 1 x 10^6 cells per 10-cm dish. The spontaneously immortalized cells with a stable growth rate were established after 20-30 generations in culture.
b) The primary MEFs were transfected with linearized p129 plasmid (origin-less SV40 genome) using the AMAXA nucleofector (MEF solution 2) protocol . Immortalized cells were selected after 3-5 passages.

3T3 and SV40 transformed cells were cultured in Dulbecco's modified Eagle Medium (DMEM) supplemented with 10 % (v/v) foetal calf serum (FCS) and 100 U/ml penicillin.

➢ 3T3 Proliferation assay

Primary MEFs were continuously replated every 3 days at rigid density of 1 x 10^6 cells per 10-cm dish. The cells were counted each passage until spontaneous immortalization. For analysis of long-term growth, total cell numbers in each passage was plotted on a log scale, against passage numbers on a linear scale.

2.2. Isolation of genomic DNA for qPCR on mtDNA

This protocol was used on MEF, U2OS and HEK293 cells. Cells were plated at 10cm plates at 106 cells/plate density. Next day cells were washed by PBS and harvested with 500 µl of buffer containing: 75mM of NACl, 50mM EDTA, 0.2% SDA and 0.4mg/ml of Proteinase K. Cells were incubated over night at 50ºC and next day isopropanol precipitated, resuspended in 200ul of TE and stored at -20ºC for further usage. Primers

used for qPCR are listed in Table 8.

Table 8. Primers for qPCR for quantification of mtDNA

NUCLEAR GENES	
GAPDH	**H19**
Fw:GCGCGAAAGTAAAGAAGCCC Rv: AGCGGCCCGGAGTCTTAAGTATTAG	Fw:GTCCACGAGACCAATGACTG Rv: GTACCCACCTGTCGTCC
MITOCHONDRIAL GENES	
COX1	**CYTB**
Fw: CTGAGCGGGAATAGTGGGTA Rv: TGGGGCTCCGATTATTAGTG	Fw: ATTCCTTCATGTCGGACGAG Rv: ACTGAGAAGCCCCCTCAAAT

2.3. Total protein extraction and western blotting

Cells were lysed with a TNG-150 buffer containing 50mM Tris/Hcl, 150mM NaCl, 1% Tween-20, 0.5%NP-40, 1x Sigma protease and phosphatase inhibitors. Protein samples were quantified using The Bio-Rad *DC* Protein Assay, separated by standard SDS-PAGE on 6%, 8%, 12% or 15% polyacrylamide gel (90V, 20min + 120 V, 90 min) and transferred (1hr, 95V) to PVDF membrane (Immobilon-P, Millipore). The primary antibodies used are listed in the table 9. and secondary antibodies are in Table 10.

Table 9. List of primary antibodies

Species recognized	Antibody	Species raised	Source	Dilution
Mouse	H2AXg (S139)	Mouse	Millipore (05-636)	IF 1:500, IHC 1:600
Human	Chk1 (FL-476)	Rabbit	Santa Cruz (sc7898)	WB 1:500
	p-Chk1 (s345)	Rabbit	Cell Signaling (2341S)	WB 1:500
	p-RPA32 (s4/s8)	Rabbit	Bethyl (A300-245A)	WB 1:1000
	RPA32/RPA2 (9h8)	Mouse	Abcam (ab2175)	WB 1:500, IF 1:500
	α-tubulin	Mouse	Sigma (T5168)	WB 1:16000
	p53 (1c12)	Mouse	Cell Signaling (2524)	WB 1:6000
	p-p53 (s15)	Rabbit	Cell Signaling (9284s)	WB 1:2000
	ATR	Rabbit	Abcam (2905)	WB 1:1000
	ATM (MAT3)	Mouse	Sigma (A1106-200UL)	WB 1:3000
	MCM4	Mouse	Santa Cruz (sc-48407)	WB 1:1000
	MCM2	Rabbit	Santa Cruz (sc-10771)	WB 1:1000
	PCNA (F-2)	Mouse	Santa Cruz (sc-7907)	WB 1:1000
	BrdU	Mouse	Becton Dickinson (347580)	FACS 1:50
	Histone3 serine10	Rabbit	Milipore (06-570)	FACS 1:200
	PrimPol	Rabbit	Doherty lab, GDSC,	WB 1:1000
	SSBP1	Rabbit	Brighton	WB 1:1000
	CPD (TDM-2)	Mouse	Sigma (HPA002866)	ELISA 1:1000
	6-4PP (64M-2)	Mouse	Cosmo Bio Co.	ELISA 1:1500
Tags	FLAG	Mouse	(NMDN001)	WB 1:2000, IF 1:500
	c-Myc	Mouse	Cosmo Bio Co	WB 1:3000
			(NMDN002)	
			Sigma (F3165)	
			Sigma (M4439)	

Table 10. List of secondary antibodies

Antibody	Source	Dilution
Rabbit HRP	Thermo Scientific	WB 1:30000
Mouse HRP	Thermo Scientific	WB 1:30000
Rabbit Alexa Fluor 488 (green)	Invitrogen	IF 1:500
Rabbit Alexa Fluor 594 (red)	Invitrogen	IF 1:500
Mouse Alexa Fluor 488 (green)	Invitrogen	IF 1:500
Mouse Alexa Fluor 594 (red)	Invitrogen	IF 1:500
FITC-Anti Rabbit IgG (H+L)	Jackson ImmunoResearch	FACS 1:200
Biotin-XX F(ab) fragment of IgG (H+L)	Life Technologies	ELISA 1:2000

➢ Soluble and insoluble fractions

The fractionation protocol was modified from Groth et al, 2008. Fractionation of HEK293 cells over-expressing PrimPol required two confluent 15 cm dish per condition in order to detect chromatin bound PrimPol. Plates were washed 2 times in ice cold PBS and incubated at 4ºC for 10 minutes in 10 ml of buffer E without phospho or protease inhibitors, containing 20mM HEPES-KOH, 5mM Potassium Acetate, 0.5mM $MgCl_2$, 0.5mM DTT. In this step cells will get swollen. The buffer gets removed and replaced with fresh cold buffer E containing phosphatase and protease inhibitors and cells are incubated additional 10 minutes at 4ºC. After incubation is over, buffer is removed and plates are drained. Cells are scraped and transferred into Wheaton 1ml douncer where they get homogenized by pestle (25-30 strokes/sample). The disrupted cells are transferred then to tubes and centrifuged for 5minutes at 1500g. Pellet contains nuclei while the supernatant can be cleared by additional spinning at 13.000g for 15min and used as cytosolic fraction that contains cytoplasmic and soluble nuclear proteins. Nuclear pellet is further resuspended in buffer N that contains buffer E, 540mM NaCl and 10% Glycerol. Chromatin and nuclear bound proteins are extracted by end-over-end rotation for 90 min at 4ºC. Afterwards samples are spun at maximum speed for 15 minutes and the supernatant is used for further analysis of chromatin bound proteins.

2.4. Purification of Strep-tagged mouse PrimPol from human cultured cells

➢ Subcloning of PrimPol in retroviral vector

Mouse and human isoforms of PrimPol were subcloned in D-TOPO vector (from Invitrogen) with primers assigned below. From this vector mPrimPol was subcloned by LR clonase reaction (Invitrogen) into PLPC backbone or PcDNA3.0-*Strep*-FLAG (provided by Dr. Ueffing's laboratory, Helmholtz Zentrum Munchen). Later two were used for transient or stable transfections.

Human PrimPol:

Forward primer: 5'-CACCATGAATAGAAAATGGGAAGCAAAAC-3'

Reverse primer: 3'-CTAATTATAGAAGTATTACAAGAG-5'

Mouse PrimPol:

Forward primer: 5'- CACCATGTTGAGGAAATGGGAGGCAA-3'

Reverse primer: 3'- GCAGCTATTCTGGTAAAGCTTCT

➢ Retroviral overexpression

For production of retrovirus, HEK293t packaging cells were transfected with the gene of interest subcloned in pLPC backbone and with retroviral vectors (VSVG and GagPol) using PEI (1mg/ml) and NaCl (150mM). Viral supernatants were harvested 48 and 72 hours post transfection, filtered (0.45um) and placed directly on fresh split HEK293 cells. Infection was done in presence of polybrene (10 μg/ml) for 24 hours in 2 cycles. Cells were then recovered with fresh media and selected with 10 μg/ml of puromycin for several days.

➢ Small scale purification

For small-scale affinity purification of *Strep-FLAG*-tagged mouse PrimPol from human cultured cells, HEK293 cells stably overexpressing PrimPol-FLAG-*Strep* were seeded at in two 150mm plates (Corning) and on a day when 90% confluence was reached, cells were harvested for purification and protein extraction. Cells were lysedfor 20 minutes at 4ºC, in 1ml of buffer containing 1x TBS, 0.5% NP-40, Roche protease inhibitor cocktail and mix 2 and 3 of phosphatase inhibitors (Sigma). The lysate was cleared by centrifugation (10 000 g, 10 minutes, 4 ^{O}C) and by filtration through syringe filters (0.22μm, Millipore). Concentration of protein was measured and in total 5mg of protein per sample was used for small-scale purification. 500ug was retained as input and the rest of lysate was incubated at overhead tumbler, with 100ul Strep-Tactin superflow resin (IBA) for 1hour. Resin was transferred to miscrospin columns (GE Healthcare) where they were washed three times with buffer containing 1x TBS, 0.1% NP-40, Roche protease inhibitor cocktail and mix 2 and 3 of phosphatase inhibitors (Sigma). Resin was then eluted with 500μl of 1x desthiobiotin elution buffer (IBA) containing 2mM desthiobiotin, incubated for 15 minutes at 4ºC and mixed every few minutes. Elute was either used immediately for western blot analysis or it was further purified with FLAG peptide. In additional purification step, protein was incubated for 1hour at 4ºC with 50 μl of anti-FLAG-M2-agarose (Sigma) in micro-spin columns. Upon incubation protein lysates were washed with 1x TBS buffer 2 times and incubated for additional 15 minutes at 4ºC with FLAG peptide (Sigma) resuspended in 1xTBS buffer at 200 μg/ul. Elute was extracted on the magnet from the beads and analyzed by western blot.

➢ Affinity purification for mass spectrometry analysis

For mass spectrometry analysis it was necessary to provide sufficient amount of purified protein. In our experimental setup that was around 100-150 μg of protein. Since mouse PrimPol is expressed at low level in HEK293 cells, for mass spectrometry we used 10 times more protein than for small-scale purifications. The starting amount was around 50mg of protein harvested from 20 150mm plates (Corning) with 90% confluent HEK293 cells stably overexpressing mPrimPol. 50mg of protein was divided into batches of 5mg protein that were processed at the same time with amounts of reagents annotated in 2.3.3.1. Only one purification step was carried out. Elutes were run on 8% SDS PAGE and silver

stained.

➢ Silver staining

After electrophoresis the gel was fixed for 1 hour in solution containing 10% acetic acid and 40% ethanol. Upon fixation gel was washed gently twice in 20% ethanol for 20 minutes and two more times in water for 10 minutes. Gel was then sensitized by soaking for one minute in 0.8mM sodium thiosulfate and then washed again twice in water. Impregnation was done with 12mM silver nitrate for 30 minutes. After this step gel was placed in developer, containing citric acid and 0.1% formaldehyde. When the adequate degree of staining is achieved reaction needs to be stopped by adding solution containing 4% Tris and 2% acetic acid. Gel is washed for several times and bands of interest are cut.

2.5. Knockdown assays

➢ Short hairpin RNA-mediated knockdown

Short hairpins against PrimPol were purchased from the Functional Genomics Core Facility at IRB Barcelona. HEK293t were transfected with the shRNA and lentiviral vectors (VSVG, RSV and RRE) using PEI (1mg/ml) and NaCl (150mM). Viral supernatants were harvested 48 and 72 hours post transfection, filtered (0.45um) and placed directly on fresh split HEK293 cells. Infection was done in presence of polybrene (10 μg/ml) for 24 hours in 2 cycles. Cells were then recovered with fresh media and selected with 10 μg/ml of puromycin for several days. shRNAsequences are listed below:

shPP5 against PrimPol:
CCGGGTCAGGTTCTCAGATACTTTACTCGAGTAAAGTATCTGAGAACCTGACTTTTTTG
shPP7 against PrimPol:
CCGGCTTGTGACAACCTATGCTGAACTCGAGTTCAGCATAGGTTGTCACAAGTTTTTTG

➢ Gene expression profiling

RNA from shRNA infected HEK293 cells was isolated two passages after puromycin selection was finalized. RNA's were isolated by TRIZOL (Invitrogen) and in the final step they were purified through RNeasy Mini kit (Qiagen) columns. For expression profiling 1μg of total RNA was provided per sample and samples were submitted in duplicates to the Functional Genomics Core Facility at IRB Barcelona. cDNA for each sample was hybridized to the geneChip Human Genome U133Plus 2.0 Array (Affymetrix, USA). RNA integrity evaluation and microarray hybridization were performed in the Functional Genomics Core Facility.

2.6. Bioinformatic analysis

All the data from the arrays was analyzed by the Biostatistics and Bioinformatic Core facility.

➢ Differential expression analysis

All microarray statistical analyses were performed using Bioconductor. Background correction, quantile normalization and median polish summarization was performed as implemented in bioconductor's affy package2. A semi-parametric empirical Bayes procedure based on moderated t-tests3 (as implemented in the limma package) was performed to obtain a posterior probability for differential expression. We set the Bayesian FDR at 5% level4. Additionally, only genes with an absolute fold change value bigger than 2.5 were considered differentially expressed.

➢ Generation of heatmaps

The Heatmap was obtained with Pearson distance and complete linkage for columns and rows. The genes selected for the Heatmap were the ones that were considered differentially expressed (fold change bigger than 2.5 and fdr bellow 0.05). (Irizarry et al. 2003; Gentleman et al. 2004)(Irizarry et al. 2003; Gentleman et al. 2004)(Irizarry et al. 2003; Gentleman et al. 2004).

2.7. Flow cytometry

➢ BrdU labeling for G_1/S checkpoint assay

$1x10^6$ primary passage 2 MEFs were plated on 10 cm plates. Media was removed and they were exposed to varying doses of UVC ($5J/m^2$, $10J/m^2$ or $15J/m^2$) using a Stratalinker (Stratagene). 14 hours after UVC exposure, MEFs were pulsed with 10uM BrdU (Sigma) for 4 hours. Cells were washed in PBS, trypsinized and fixed over night with 70% ethanol. Cells were washed in PBS and DNA was denaturated by incubation in 0.1M HCl and by 100ºC heat. Cells were stained with BrdU-FITC antibody (Sigma) and were resuspended in 300ul of PBS with 10 μg /ml of propidium iodide (PI) and 10 μg /ml of RNaseA. The percentage of S-phase cells was determined by flow cytometry and normalized to untreated cells (S-phase ratio).

➢ G2/M Checkpoint Assay

Primary MEFs in passage 2 were mock treated or damaged with $15J/m^2$ of UVC. 1 hour after damage, cells were harvested in PBS and fixed over night with 70% ethanol. Cells were washed and stained for one hour at room temperature with rabbit anti-H3ser10 at 1:200 dilution (table 1.3). Following several washes they were incubated 1 hour with secondary anti- IgG-FITC at 1:200 dilution. All washes and incubations with primary and secondary antibodies were done in dilution buffer containing 1% FBS and 0.1% Triton X-100 in PBS. Cells were resuspended in 300ul of PBS with the addition of 10ug/ml of propidium iodide (PI) and 10ug/ml of RNaseA. The percentage of mitotic cells was determined by flow cytometry and normalized to untreated cells (G2M-phase ratio).

2.8. Clonogenic survival assay

The ability of SV40 immortalized MEFs to form colonies upon damage was tested by clonogenic colony forming assay (CFA). Cells were plated either after the treatment (X-irradiation induced damage) or before the treatment (UVC, etoposide, camptothecin. MMS, caffeine and PARP/Chk/ATR inhibitors). Cells were plated on 6 cm plates in duplicates. The number of cells for seeding was adjusted to the plating efficiency and the

toxicity of the treatment. Details are provided in the Table 1.9. Cells were kept in a CO_2 incubator at 37°C for 10 days until cells in control plates formed visible colonies (50 cells per colony is the minimum for scoring). Colonies were stained with crystal violet (Sigma-Aldrich) and counted. Based on the colony number, plating efficiency (PE=number of colonies formed/number of colonies seeded x 100%) and surviving fraction (SF=number of colonies formed after treatment/number of cells seeded x PE) were calculated and plotted.

➢ DNA damaging agents and drug treatments

UV-C irradiation at 254 nm was performed with a germicidal lamp using a Stratalinker. Cells plated in dishes were aspirated of their medium, washed with PBS, and with no liquid present in the dish and lid removed, exposed to the desired dose of UV-C radiation. Pre-warmed media was then added to the cells before returning to the incubator for the appropriate recovery time. Exposure of cells to ionising radiation was performed with 200 kV X-rays at 4.5 mA with a dose rate of 0.025 Gy/s. Cells were irradiated in suspension and plated following damage. Camptothecin stock solution was dissolved in DMSO 1mM stock concentration and added to cell medium to a final concentration of 40, 80 or 120 nM for 24 hours for the clonogenic assay (CFA). Etoposide was dissolved in DMSO to 50mM stock concentration and added to cell medium to a final concentration of 50, 150 or 300 nM for 24 hours for CFA. MMS was applied for 24hrs at final concentration of 2, 4 or 8 μg/ml (CFA). Aphidicolin was prepared in DMSO and added to cell medium to a final concentration of 300 nM for 36 hours (metaphase spreads) or 20 μM for 30minutes (western blotting). ATR inhibitors were kind gift from the Oscar Capetillo-Fernandez group (Toledo et al. 2011). ATR inhibitor was reconstituted in DMSO prior to the experiment at a concentration of 5mM and it was added to cells at 5 μM 30minutes before UVC treatment and for an additional 7 hours after the treatment for CFAs. PARP inhibitors (Seleckchem) were dissolved in DMSO at a concentration of 100mM and added to the media at 5 μM following UVC treatment and left on the plates for 10 days. Chk inhibitors (Seleckchem) were dissolved in DMSO at a concentration of 20mM and were added upon UVC treatment at 100nM concentration and left on the plates for 10 days. Details of plating conditions and doses used for CFAs are given in Table 11.

Table 11. Colony forming assay plating conditions and doses of damaging agents

Etoposide		Camptothecin		MMS	Cells/6cm plate
Mock		Mock		Mock	500
50nM		40nM		2ug/ml	1000
150nM		80nM		4ug/ml	2000
300nM		120nM		8ug/ml	4000

X irradiation	Cells/6cm plate		UVC	Cells/6cm plate
Mock	500		Mock	400
2Gy	750		$5J/m^2$	800
4Gy	1000		$10J/m^2$	1600
8Gy	3000		$15J/m^2$	2400

Chk1 inhibitor +UVC		PARP inhibitors +UVC		ATR inhibitors +UVC	Cells/6cm plate
100nM + UV Mock		5uM + UV Mock		5uM + UV Mock	800
100nM + $5J/m^2$		5uM + $5J/m^2$		5uM + $5J/m^2$	1600
100nM + $10J/m^2$		5uM + $10J/m^2$		5uM + $10J/m^2$	3200

➢ RNA interference

Small interfering (si)RNA duplexes targeting PrimPol, Nbs1 and Rev1 mRNA were designed using tools found at the http://sirna.wi.mit.edu/ web site and they were manufactured by Invitrogen as Stealth RNAi siRNA. For each gene at least 3 primer sets were tested for the most efficient downregulation. The sequences of the siRNA duplexes are detailed in the Table 12. SV40 transformed MEFs were transfected using Lipofectamine RNAiMAX (Invitrogen); 7.5 µl RNAiMAX was added to a well of a 6-well plate containing 350 µl OPTI-MEM medium (Invitrogen) with 10 nM siRNA duplex (final concentration). To this a 400 µl suspension of 3 x 10^5 cells was added and returned to the incubator. Twenty-four hours later a transfection mix composed of 350 µl OPTI-MEM, 7.5 µl RNAiMAX, and 10 nM siRNA (final) was added to the well before returning to the incubator. Usually, a well became confluent 48 hours after seeding and initial transfection, and required passaging into an appropriate size dish; experiments were typically performed the following day (72 hours from the starting point). The number of wells seeded was scaled up as required. Mock transfections that contained water instead of siRNA were performed alongside as a control. The efficiency of downregulation was evaluated with qPCR using diagnostic primers listed in table 13.

Table 12. siRNA oligonucleotide sequences

Gene	Fw siRNA oligonucleotide	Rv siRNA oligonucleotide
Nbs1	GGUCAUUGGUUGUCAGUAA [dT] [dT]	UUACUGACAACCAAUGACC [dT] [dT]
PrimPol	GGAUCUAGGAGUGUAUACA [dT] [dT]	UGUAUACACUCCUAGAUCC [dT] [dT]
Rev1	GGUUCCUGCUAAUUCAAAU [dT] [dT]	AUUUGAAUUAGCAGGAACC [dT] [dT]
Pol Eta	CCAGAUGCCAAUCCGUAAA [dT] [dT]	UUUACGGAUUGGCAUCUGG [dT] [dT]

Table 13. Primers for diagnostic qPCR of downregulated mouse genes (for cDNA)

Gene	First primer set	Second primer set
Nbs1	Fw- TGGTCTTCAGGACAGCAGTG Rv- AGGAAATGTCGCCTTCTTGA	Fw- CAGCAGCAGAACTCCATCAA Rv- CTGATGCTCCTTGCTTTTCC
PrimPol	Fw- TGTGTCTTTGGAGGTTGCTG Rv- TAAAACACTCAGCCCGCTTT	Fw- TAAGACCCGGAAAACCCTCT Rv- AACATCTTCGGCTGAGCACT
Rev1	Fw- GAGAGCCACGTGGAAAGAAG Rv- GAATGCTGGAAGGGCAATTA	Fw- ATGATGTTGCATGGAGGTCA Rv- CAGCTTTGATGCTTTCCACA
Pol Eta	Fw- CACCAAGTACCGGGAAGCTA Rv- AAGTGCTTGGCAGCAAATCT	Fw- AAAAGCTGCCAAAAAGCAGA Rv- GTCAGGAGCCGCAGAGTTAC
House keeping genes	**First primer set**	**Second primer set**
Beta actin	Fw: TGTTACCAACTGGGACGACA Rv:TCTCCAGGGAGGAAGAGGAT	Fw: TACAGCTTCACCACCACAGC Rv: AAGGAAGGCTGGAAAAGAGC
Gapdh	Fw:GCACAGTCAAGGCCGAGAAT Rv:GCCTTCTCCATGGTGGTGAA	Fw:GTGTGAACGGATTTGGCCGTATTG GGCG Rv:GCCCATCACCATCTTCCAGGAGCGA

2.9. Immunofluorescence microscopy

Primary and secondary antibodies used in this thesis for immunofluorescence analysis are detailed in Tables 1.3 and 1.4 respectively. Cells were grown on glass cover slips, which for HEK293 cells were poly-L-lysine coated (Invitrogen), in typically 3.5cm dishes with 2-3 cover slips per dish. Cell medium was removed and cells washed in PBS before fixing in 4 % formaldehyde (in PBS) for 10 minutes at room temperature. Following fixation, dishes of fixed cells were often stored at 4ºC in PBS until immunofluorescent staining. Cells were permeabilised with 0.2 % Triton X-100 (in PBS) for 5 minutes, then washed with PBS before blocking with 3 % BSA (in PBS) for at least 30 minutes. Primary antibodies were

diluted in blocking buffer and added dropwise to the surface of the cover slips, and incubated for at least 1 hour at room temperature. Cells were then washed with PBS before incubation with the secondary antibody and 4',6-diamidino-2-phenylindole (DAPI) also diluted in blocking buffer, for at least 30 minutes in the dark. Following further washes with PBS, the excess PBS was removed from the cover slip before mounting onto a glass slide with Prolong Gold anti-fade (Invitrogen). Nail varnish was then used to coat the edge of the cover slips to create a seal and the slides were stored at 4°C until analysis. If slides were to be scored, they were analysed on a Leica spectral confocal microscope (SPE) with a 40x and 63x oil immersion objective.

3.0. Metaphase spreads

A mitotic population of primary MEFs in log phase growth was enriched by colcemid treatment for 1 or 2 hours at $2x10^{-7}$M concentrations. Cells were harvested, swollen with 0.075M KCL for 15 minutes at 37ºC and fixed over night with dropwise added ice-cold methanol: glacial acetic acid (3:1). Cells were resuspended in 300 μl of fixative and 30ul was spread over the glass slide that was then inverted over 80ºC water bath for 7 seconds and dried on the hot lid. Slides were stained in 5% Giemsa solution for 10 minutes and examined under oil immersion at 100X magnification, using a white light source. 50 spreads were counted per sample and the number of chromosomes per spread and aberrations per spread were recorded.

3.1. CPD and 6-4PP ELISA

SV40 transformed MEFs were damaged by 30 J/m^2 of UVC as previously described. Cells were trypsin harvested, washed and spinned at different time points upon 30 J/m^2 UVC damage and cell pellets were frozen at -80ºC until all samples were collected. Genomic DNA was isolated using Life Science kit PureLink (#K1820-01), DNA samples were diluted with PBS to a concentration of 4 μg/ml (for 6-4PP protocol) or 0.2 μg/ml (for CPD protocol). DNA was denatured for 10 minutes at 100ºC and 50 ul was plated on a well of 96-well plate precoated with 0.003% protamine-sulfate. Samples were incubated

over night at 37ºC. DNA coated plates were washed next day with PBS containing 0.05% Tween-20 for five times and then blocking step was 30 minutes with 200 μl of PBS containing 2%FBS. 100ul of each primary antibody, CPD and 6-4PP (listed in the Table 1.3), were incubated in wells for 1hr. Secondary antibody Biotin-F(ab')$_2$ fragment of antimouse IgG (H+L) was incubated for 30 minutes at 100ul volume/well. Afterwards 1:10000 Peroxidase-Streptavidin was added at 100 μl and incubated additional 30 minutes. Final staining step was done with substrate solution composed of H_2O_2 and o-Phenylene diamine in citrate-phosphate buffer (pH 5.0), kept on wells for 30 minutes at 100 μl volume. To stop the reaction 50 μl of 2M of H_2SO_4 was added to each well and the absorbance at 492nm was determined by spectrophotometer. All incubations were done at 37ºC and between each step wells were washed five times with 150 μl of PBS containing 0.05% Tween-20. All samples were plated in triplicates.

3.2. Isolation of thymocytes for the analysis of differentiation and apoptosis

The thymus was isolated from 8 week old mice. The organ was ground in media chilled on ice with a 5ml syringe barrel and splenocytes were segregated by pipetting through a 40 μM filter into a 50 ml conical tube. 10^6 of cells in 100ul volume of media were plated in the wells of a 96-well plate in RPMI-1640 media enriched with 15% FBS. For assessment of T-cell differentiation, cells were stained for CD4, CD8 and CD3 markers and analyzed by flow cytometry. Additional cells were damaged with different doses of X-irradiation (1.25 Gy, 2.5 Gy and 5 Gy), incubated for an additional 16 hours and stained for apoptotic marker Annexin V and propidium iodide (PI). Cells were analyzed by flow cytometry to determine the number of viable (double negative) cells.

➢ Isolation of B lymphocytes and stimulation

Isolation of B cells was done from 8 weeks old mice. Isolation was performed according to the instruction of the manufacturer (Miltenyi Biotec) and it was based on magnetic beads

labeling of non-B cells, which were depleted, in subsequent steps from B cell population by magnetic separation with LS and MS columns. From the portion of isolated splenocytes $2x10^9$ were kept for B cell isolation. First step is magnetic labeling of the cells. Cells was washed and pelleted, then resuspended in 50μl/10^7 cells buffer containing Biotin-Antibody Cocktail (diluted 1:5) and incubated 15 minutes at 4ºC. Then 50 μl of Anti-Biotin MicroBeads (Anti-Biotin-APC (Miltenyi 130-090-856) diluted 1:2) was added and incubated at 4ºC for additional 15 minutes. Cells were washed 2 times and resuspended in 500 μl of buffer containing PBS, 0.5% BSA and 2mM EDTA. Cell suspension was then applied to MACS column attached to magnetic separator. Buffer was passed 3 times through columns and total effluent, containing unlabeled cells, was collected. These cells represent B cell fraction that will be used further for downstream experiments.

- **Class switch recombination (CSR)**

Isolated B lymphocytes were plated on 6 well plates and cultured in RPMI 1640 media. Cells were stimulated for CSR by next: 25 μg/ml LPS for IgG1, IgM or 5 μg/ml IL-4 and 25 μg/ml LPS for IgG2b. CSR events were analyzed by flow cytometry on day 1 and day 4 following stimulus or mock treatment. For labeling, the following antibodies were used: IgG1-Biotin (Miltenyi 130-095-879), IgG1-Biotin isotype control (Miltenyi 130-093-018), IgG2b-Biotin (BD Pharmingen 550333), IgG2b-Biotin isotype control (Miltenyi 130-092-466), IgM-APC (Miltenyi 130-095-910), IgM isotype control (Miltenyi 130-093-176), and CD45R (B220)-FITC (Miltenyi 130-091-829). All antibodies were used at 1:10 dilution and samples were incubated for 15 minutes at 4ºC.

3. Histological methods

3.1. X-gal staining of embryos

The embryos at e13.5 were isolated, embedded in OCT and frozen at -80ºC. Sagittal sections of 9 μm thickness were fixed for 10 minutes at room temperature in X-gal buffer

containing 0.2% glutaraldehyde, washed 3 times in buffer containing 0.01% of sodium deoxycholate and 0.02% NP-40 and stained for 36 hours at 37ºC in X-gal solution. This solution contains X-gal at final concentration 1mg/ml, 5mM of $K_3Fe(CN)_6$ and 5mM $K_4Fe(CN)_6$. Sections were counterstained for 1 minute in Nuclear Fast Red (NFR) and mounted with DPX.

3.2. Whole mount staining of skin with X-gal

Pieces of skin, isolated from the shaved back of sacrificed mice, were stained for X-gal. Pieces of 6x8 mm surface were fixed in 4% paraformaldehyde (PFA) for 4 hours at 4ºC. Staining was done in X-gal solution for 36 hours at r.t on the rotator. Skin pieces were placed in Falcon tubes and protected from the light. Skin was fixed one more time for additional 2 hours in 4% PFA and then incubated over night in 20% sucrose solution. Skin portions were mounted in OCT, frozen at -80ºC and cut with cryostat to sections of 3um thickness. Sections were counterstained with Nuclear Fast Red (Sigma) and mounted with DPX (Sigma).

3.3. Immunohistochemistry

Portions of skin were taken from animals exposed to UVB at a dose of X for 5 consecutive days. Animals were sacrificed and skin was fixed in 10% formalin over night at 4ºC and paraffin embedded. Sections were made at 3 um thickness and staining for hematoxylin and eosin (H&E), Ki67 and γH2AX was performed in the facility for immunohistochemistry at IRB Barcelona. Pictures were taken using E600 Nikon epifluorescence microscope equipped with 40x NA 0.75 objective lens and a charge-coupled Olympus DP72 device camera.

3.4. TUNEL staining of the skin

Terminal deoxynucleotidyl transferase dUTP nick end labelling (TUNEL) was performed to detect DNA strand breaks in the skin damaged by UVB, using the Fluorescein *In Situ* Cell Death Detection Kit (Roche). Skin was fixed and mounted on microscope slides as described for immunofluorescence microscopy (section 3.8.) and the TUNEL staining was performed according to the manufacturer's instructions.

Results

Hypothesis and objectives

Hypothesis:

We hypothesize that PrimPol, a novel AEP primase polymerase, acts as a translesion polymerase to bypass bulky base adducts generated by UV and reactive oxygen in order to maintain the integrity of nuclear and mitochondrial DNA. We propose that the activities of PrimPol are required for the response to UV damage and to promote normal aging.

Objectives:

1. Generation of a conditional knockout mouse model to determine the functions of PrimPol in primary cells and *in vivo*.
2. Phenotypic characterization of primary and transformed cells lacking PrimPol in the presence or absence of DNA damage.
3. Analysis of protein-protein interactions and subcellular localization of PrimPol in the presence or absence of DNA damage.
4. Characterization of the effect of PrimPol loss on mitochondrial homeostasis.

1. Generation and characterization of PrimPol deficient mice

In order to study the *in vivo* functions of PrimPol we have generated a knockout-first conditional allele. In the initial configuration, *PrimPol* expression is blocked by a genetrap expressing a beta-galactosidase reporter gene. Expression of the FLP recombinase excises the cassette, generating a conditional allele. Subsequent expression of Cre leads to the deletion of a critical exon and the complete loss of mRNA and protein expression. The AEP (archaeo-eukaryotic primase) domain of PrimPol is a highly conserved domain containing residues predicted to be essential for polymerase activity because they are required for binding of divalent metal ions. Since motif III of the AEP domain (Figure 11) is encoded in exon 5 of the mouse *PrimPol* gene we decided to target this exon in order to ensure that if residual protein was made following Cre expression, it would be non-functional. We achieved this by introducing LoxP sites on either side of exon 5 so that Cre expression would lead to its deletion.

1. 1. Strategy and design of *PrimPol* deficient mice

A principal element of the gene trap vector is the trapping cassette, consisting of a splice acceptor (SA) followed by a promoterless reporter *LacZ* gene that expresses beta galactosidase and a downstream transcriptional termination sequence (polyadenylation sequence; polyA or pA). This cassette is followed by a selectable neomycin marker used for the selection of targeted ES cells. The cassette is inserted into the intron between exons 4 and 5 of the *PrimPol* gene and successful trapping of the gene allows the gene trap cassette to be transcribed from the endogenous promoter of that gene in the form of a fusion transcript in which the exons upstream of the insertion site are spliced in frame to the reporter gene. Since transcription is terminated prematurely at the inserted polyadenylation site, the processed fusion transcript encodes a truncated and non-functional version of the cellular protein and the reporter which will be refered to as the gene trap (GT) allele. The GT cassette is flanked by FRT sites so the expression of the FLP recombinase *in vitro* or *in vivo* should restore normal expression of the wild type (WT) gene in the context of the conditional allele (COND). In this allele, exon 5 is flanked by LoxP sites rendering it

Figure 11. Alignment of human and mouse PrimPol sequence

There is 68% identity between human and mouse sequence. The three motifs of the AEP domain are labeled with yellow squared boxes while catalytic residues required for polymerase activity are labeled as lilac and purple stars. Exon boundaries and exons are annotated by purple bars and letters. UL52 domain is labeled with red square And residues essential for Zn chelation are lebaled with green stars.

susceptible to Cre recombinase mediated deletion, leading to the loss of critical residues and a frameshift mutation that should generate mRNA that will be degraded by the nonsense mediated mRNA decay machinery. This allele is designated as knockout (KO). Any mRNA that is made and translated would lead to the generation of truncated nonfunctional protein. The configuration of the construct is shown in Figure 12.

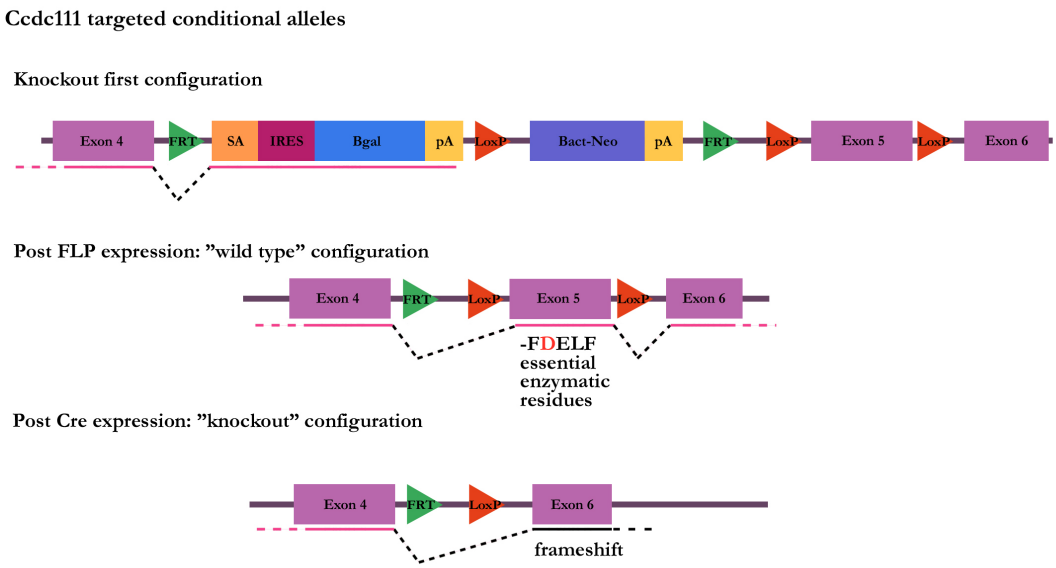

Figure 12. Schematic of the engineered PrimPol locus.

The PrimPol gene trap was generated by introducing the cassette, between exon 4 and 5, containing an FRT (flippase recognition target) recombination site, SA (splicing acceptor), IRES (internal ribosome entry site), β gal (β galactosidase reporter gene), pA (poly(A) tail), LoxP (locus of X-over P1 recombination site), and a Bact-Neo (Neomycin selection marker). The genetrap configuration can be reverted to "wild type" after a Flp (Flippase) mediated recombination event. From this configuration, a complete PrimPol knock out, lacking essential catalytic residues FDELF, can be obtained by recombination with Cre. This ultimate step leads to excision of exon 5 and a frameshift so that no functional protein can be produced.

Genotyping of the *PrimPol* alleles was performed by PCR using allele specific primers that generate differential fragment sizes or amplify products specific to particular alleles. The *PrimPol* deficient mice were maintained on a (129/Ola × C57BL/6) mixed genetic background. As we did not have antibodies that recognized the mouse isoform of PrimPol, we established conditions and primers for quantitative RT-PCR to analyze the inactivation of the *PrimPol* gene. The primers were used to amplify *PrimPol* transcripts from e13.5 primary MEFs using a primer set with one primer in exon 5 so that no product should be detectable in the KO homozygous mice (Figure 13).

Both male and female *PrimPol*$^{gt/gt}$ (GT) and *PrimPol*$^{-/-}$ (KO) mutants were fertile and litter sizes did not differ significantly from wild-type (WT) littermate mice (data not shown). No anatomic abnormalities were observed in embryos isolated at e14.5 but PrimPol$^{-/-}$ mice on

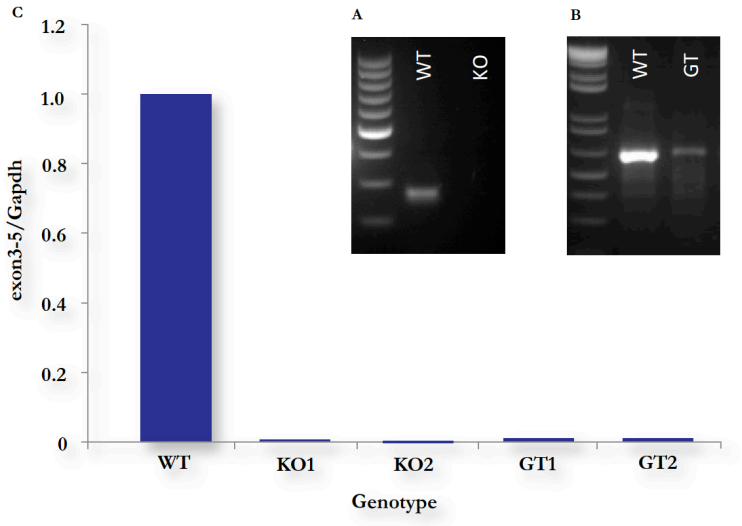

Figure 13. *PrimPol* gene expression is disrupted in *PrimPol*$^{-/-}$ (KO) and *PrimPol*$^{gt/gt}$ (GT) mice

A) The example of PCR genotyping of genomic DNA from offspring from *PrimPol*$^{+/-}$ (HET) intercross. The WT product corresponds to PrimPol wild-type allele and the KO product corresponds to the modified, disrupted allele. Expected band is around 200bp, size is compared to 100bp Biotools DNA ladder. B) The example of PCR genotyping of genomic DNA from offspring from *PrimPol*$^{gt/+}$ intercross. The GT product corresponds to the modified, disrupted allele. Expected band is around 200bp, size is compared to 1kb Plus Invitrogen ladder. C) qPCR (quantitative real-time PCR) on cDNA from primary MEFs, with primers annealing in exon 3 and downstream of exon 5, respectively. Values are normalized to housekeeping gene Gapdh and samples were used as triplicates. GT stands for *PrimPol*$^{gt/gt}$, KO stands for *PrimPol*$^{-/-}$ and WT for *PrimPol*$^{+/+}$.

a mixed C57BL/6 × 129 inbred mouse strain background were born at lower than expected Mendelian ratio, potentially indicating that some mutant embryos perish during embryogenesis prior to e14.5 (Figure 14).

Chi^2=0.14	PrimPol$^{+/+}$	PrimPol$^{+/-}$	PrimPol$^{-/-}$
Expected	16	34	8
Observed	14.5	29	14.5

Figure 14. Mendelian ratio

Observed versus expected Mendelian ratio for e13.5 embryos from PrimPol heterozygous intercrosses.

To determine if development progressed normally, we measured the weight of mice in the first three months of life. There was no significant difference observed in the weights among female or male cohorts of WT and KO animals (Figure 15).

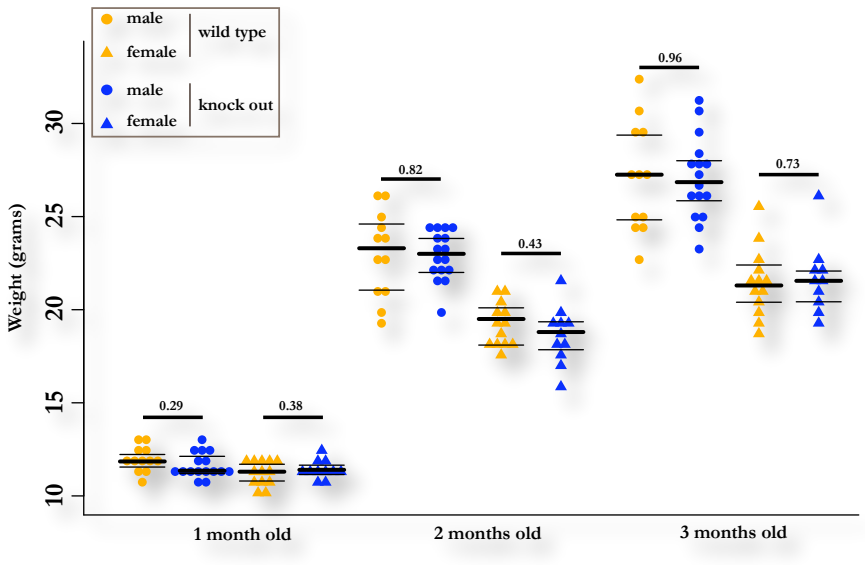

Figure 15. Weights of mice in the first three months of life

WT is indicated in orange, KO in blue; males are designated with circles and females with triangles. The P value is assigned above every cohort and was calculated using the T-test. Modest differences observed between genotypes does not appear to be significant.

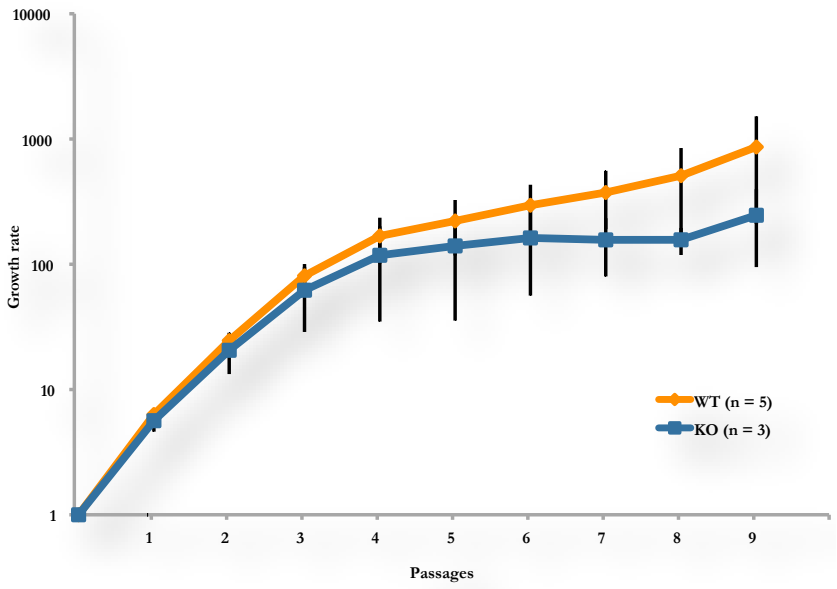

Figure 16. Analysis of primary cell growth

The growth of primary MEFs of the indicated genotypes was analyzed using a modified 3T3 protocol. KO cell cultures showed little or no difference in proliferation compared to WT cells. Results from N representative experiments performed in duplicates are shown. Error bars indicate standard deviation mean.

To determine if *PrimPol* deficiency had an effect on cell proliferation, primary MEFs were isolated from embryos at e13.5e and replated for at least 25 passages until spontaneous immortalization. We observed relatively normal growth rates of cells lacking *PrimPol* compared to their WT littermates (Figure 16).

1.2. Mapping the expression landscape of PrimPol

Since no reliable information was available for *PrimPol* expression in the mouse, we decided to investigate the expression pattern in *PrimPol*$^{gt/gt}$ embryos at e13.5 and in adult animals. The advantage of the gene trap mouse model is that trapped *PrimPol* allele contains the *LacZ* reporter gene, which is expressed under control of the endogenous promoter. Therefore β -galactosidase expression can be can be considered as indicative for expression of *PrimPol*. LacZ activity is detected by X gal staining. The gene product, β –Galactosidase, cleaves X-gal substrate into galactose and 5-bromo-4-chloro-3-hydroxyindole. The latter compound is then oxidized into 5,5 -dibromo-4,4 -dichloro-indigo producing a final product that is blue in color, providing a visual assay of LacZ activity that can be observed in tissue sections.

➢ PrimPol expression in e13.5 embryos

In order to check expression of *PrimPol* during embryonic development, we have stained sagital cryosections of mouse *PrimPol*$^{gt/gt}$ (GT) embryos with X-gal. The highest expression of *PrimPol* was observed in the superficial layer of the eye (A) and the ectoderm (B). Staining was also present in the other parts of the embryos but at very low levels compared to the ectodermal layer (Figure 17). X-gal positive staining was specific for GT samples as no staining was observed in wild type samples. This was interesting as X-gal positive structures are those that will develop and differentiate into skin, sclera, retina and vitrous body (Figure 18). These organs represent the first barrier to UV irradiation and for this reason they should be armed with additional mechanisms to deal with UV damage. The expression pattern of *PrimPol* suggested the possibility that PrimPol might be involved in the DNA damage response to UV induced lesions.

Figure 17. Expression of PrimPol during embryonic development.

Sagittal cryosections (9um thick) of e13.5 whole embryos were stained with X-gal. The staining was weak so the expression of PrimPol is highlighted with a blue line. It can be observed in the ectoderm and in the eye. Image was taken by 4x objective.

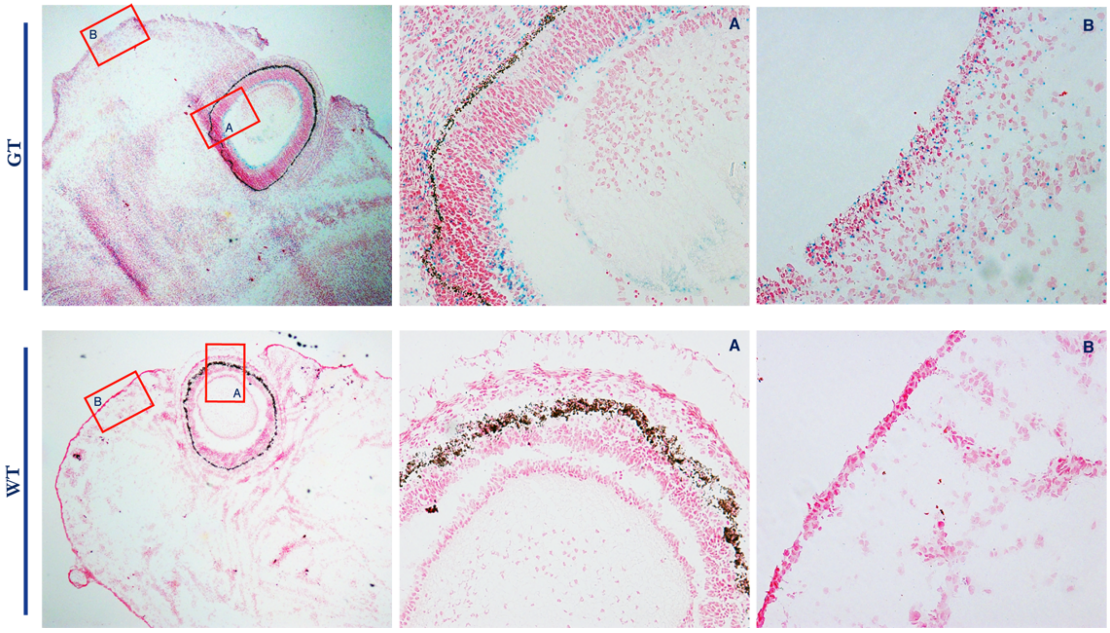

Figure 18. Expression of PrimPol in the ectoderm and the eye

Sagittal cryosections (9um thick) of E13.5 embryos were stained with Xgal. In the first picture (taken with a 10x objective) is the whole sagittal section of the head and read squares are indicating regions that are magnified in A and B (taken by 40x objective). A) Example of β – Galactosidase activity in the eye. In GT several layers are positive for Xgal staining while in WT no staining is visible. B) Example of β – Galactosidase activity in the superficial layer of the ectoderm that will develop in skin.

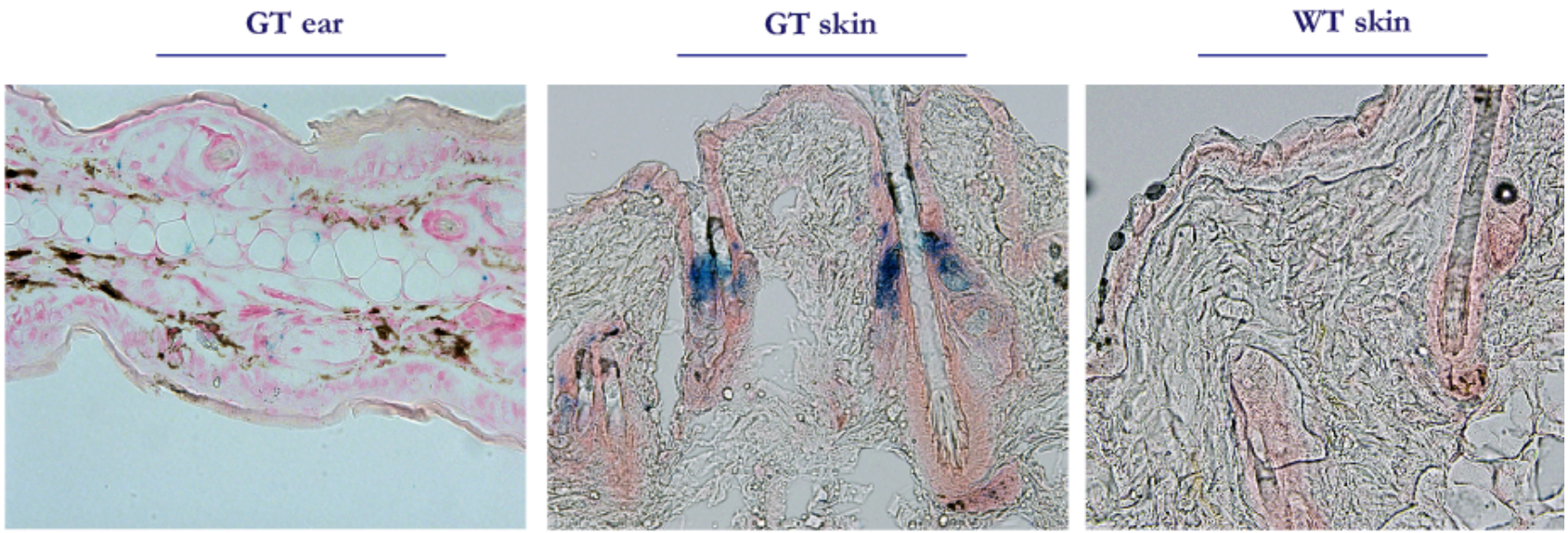

Figure 19. Expression of PrimPol in the adult the skin and the ear

Tissue sections of 3um thickness were stained by whole mount X-gal staining and counter-stained with Nuclear Fast Red. Examples shown are for X-gal positive staining in auricular cartilage (GT ear) or epidermis and sebaceous glands (GT skin). No positive staining was observed in WT samples. Pictures were taken using the 20x objective of a light microscope.

➢ PrimPol expression in the skin of 6 months old mice

To test if we could observe the *PrimPol* expression pattern in adult tissues, we performed whole mount skin staining with X-gal. Skin was isolated from the backs of 6 months old animals and stained with X-gal. X-gal positive staining was again specific for GT samples, as no staining was observed in WT samples. *PrimPol* is expressed in the epidermis of adult skin and around the hair follicle, potentially in the sebaceous gland or bulge. We observed high *PrimPol* expression in the ear of the same animals around auricular cartilage (Figure 19). There were no clear histological difference between skin samples from GT and WT animals.

➢ *PrimPol* expression across different tissues

To more quantitatively assess the expression of *PrimPol* in different tissues, we have analyzed its expression across different organs from five months old, WT mouse. For this purpose we have isolated mRNA and we used quantitative PCR and comparative Ct

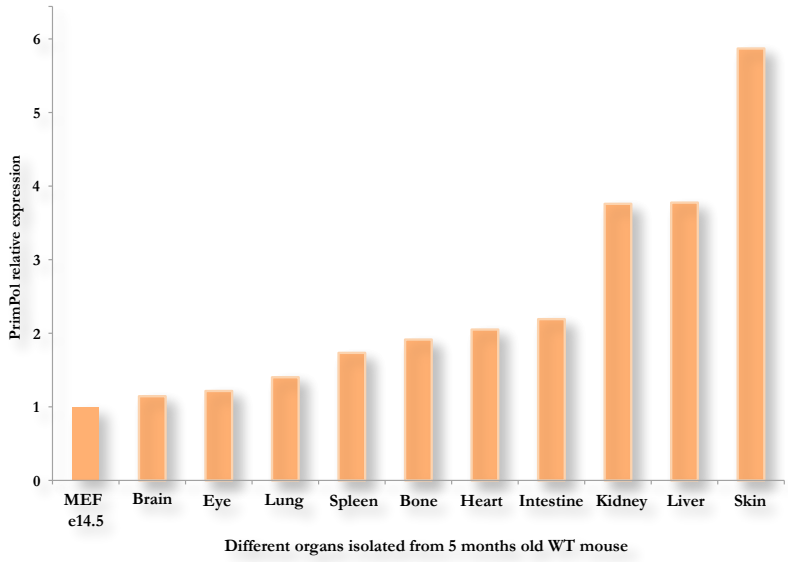

Figure 20. *PrimPol* expression profile across different tissues.

RNA was isolated from different organs of a 5 month old WT mouse. Transcript expression of *PrimPol* was measured by qPCR. The values were quantified by comparative Ct method and normalized to housekeeping gene *beta Actin*. Results from one qPCR experiment performed in triplicates are shown.

method to quantify the expression values that were then normalized to the housekeeping gene *beta Actin*. *PrimPol* was expressed in all of the organs that we isolated and tested for its expression. Most of the other organs had similar expression levels of *PrimPol* with the exception of skin where the levels of *PrimPol* were very high, consistent with the LacZ reporter staining (Figure 20). In addition, the kidney and liver had two fold higher *PrimPol* expression levels compared to the other organs.

1.3. PrimPol deficient mice are susceptible to UV induced damage

We suspected, based on the expression patterns of *PrimPol* as well as biochemical data from our collaborators, that this enzyme might be necessary for the protection of skin and the eyes against environmental damage, as these two organs are the first physical defense barrier. UV radiation is the main component of solar light to which skin and eyes are regularly exposed. The effect of UV irradiation can be immediate and prolonged exposure to UV irradiation can lead to a systemic response in the organism, affecting immunity and hormonal levels. Therefore we wondered how the absence of *PrimPol* would affect the UV damage response. To examine this, we have subjected 2 cohorts of mice (*PrimPol*$^{-/-}$ and *PrimPol*$^{+/+}$) to acute UVB irradiation treatment regimens. Each cohort contained three mice of each genotype that were sex and age (6 weeks) matched. Mice were irradiated for 4 days, every 24 hours with 2kJ/m2 of UVB as illustrated in Figure 21. On the fifth day, 24 hours after the last dose, mice were sacrificed and the dorsal skin was isolated for histological analysis.

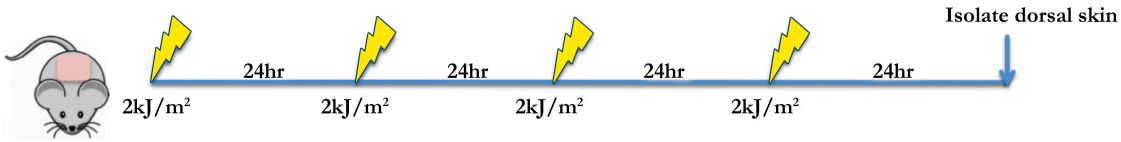

Figure 21. Scheme of experimental setup for UV damage of skin

Irradiation of mice with 4 doses of UVB. Each dose was 2kJ/m^2 and delivered every 24 hours. On the fifth day dorsal skin and ears were isolated. There were 3 animals per genotype.

After the acute UVB treatment we observed that the animals of both genotypes developed notable histopathological changes as expected. Epidermal hyperplasia, hyperkeratosis, intercellular edema and dermal cell infiltration were present in epidermis and dermis, while in the hypodermis we noticed signs of inflammation and the presence of macrophages and neutrophils based on H&E staining.

➢ Epidermal hyperplasia upon acute UV exposure

Protection from UV irradiation is important to avoid cell damage and death, specifically in the highly exposed, outermost part of the epidermis. Surviving cells may acquire gene

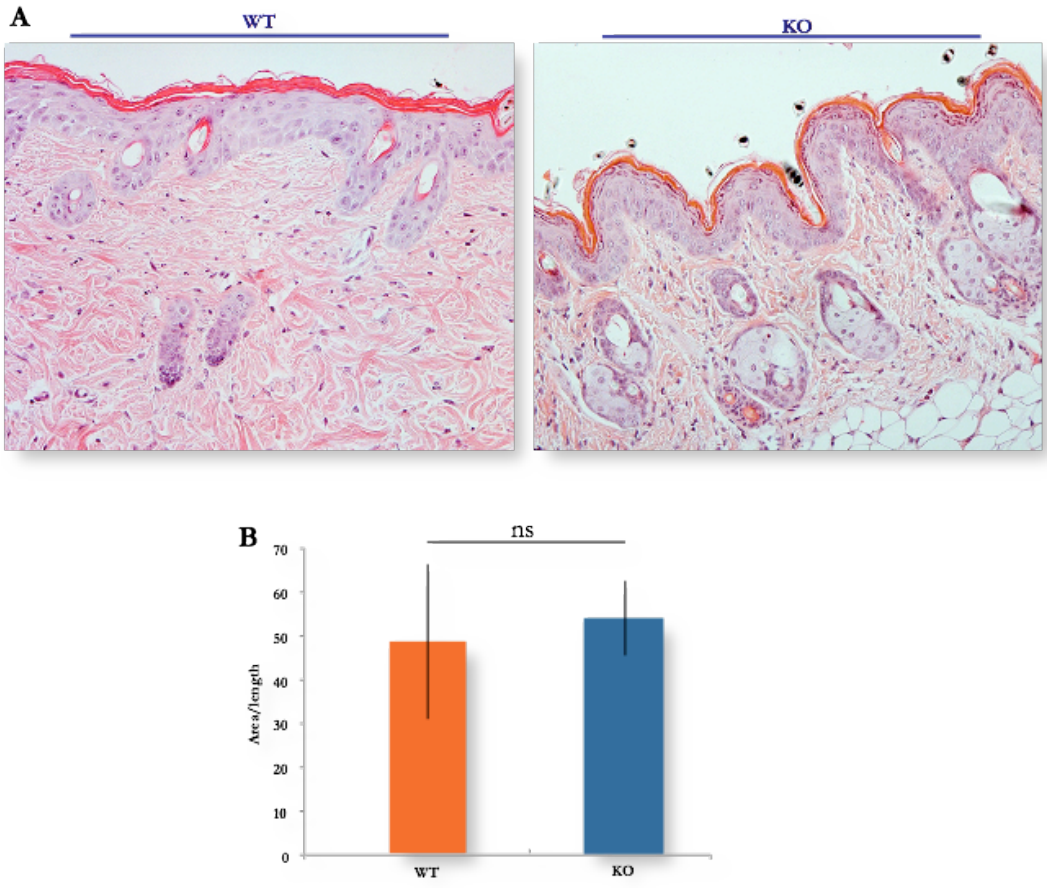

Figure 22. Quantification of epidermal hyperplasia after acute dose of UVB irradiation

A) Representative H&E-stained skin sections from 5 weeks old mice irradiated by UVB. B) Quantification of epidermal thickness per epidermal length (p=0.28). Data points are mean ± SEM (n=3).

mutations and these alterations may give rise to cancer so the surveillance of UV induced damage is crucial for preventing disease. One of the first adaptive responses that skin employs to limit further damage from UV exposure is epidermal thickening or hyperplasia. This is result of increased rate of cell division in lower epidermis that eventually leads to thickening of the whole epidermis including stratum corneum (the most superficial layer).

To analyze the response of KO skin to acute UV radiation, we have quantified the extent of epidermal hyperplasia in the epidermis by measuring the surface of the epidermis and dividing it by the length of the epidermis. WT skin seemed slightly more hyperplastic than wild type skin but the variability in wild type was high and this difference was not statistically significant (Figure 22).

➢ Increased persistent damage in skin deficient for *PrimPol*

Upon UV induced damage there is an accumulation of pyrimidine dimers, CPD and 6-4PPs, that can stall the progression of replication forks. If these lesions are left unrepaired this can lead to prolonged replication arrest and replication forks can collapse leading to double DNA double strand breaks (DSB) formation. DSBs lead to the rapid phosphorylation of histone H2AX on serine 139, one of several variants of the nucleosome core histone H2A, yielding a modified phosphorylated histone H2AX (referred as γH2AX) that is widely used as a sensitive DSB marker. It was reported in XP-V cell line that UV irradiation could lead to enhanced DSB formation and γH2AX foci accumulation (Limoli et al. 2002). We have analyzed if there is accumulation of DSBs in skin samples damaged by UVB. While in the undamaged skin samples from WT and KO there were no γH2AX positive cells, we have observed many positive cells in damaged samples of both genotypes. Interestingly, significantly higher number of γH2AX positive cells was present in KO skin samples than in WT samples (Figure 23). This indicated that skin deficient for *PrimPol* is more susceptible to UV induced damage and that PrimPol might be involved in the specialized DNA damage pathways that respond to UV lesions.

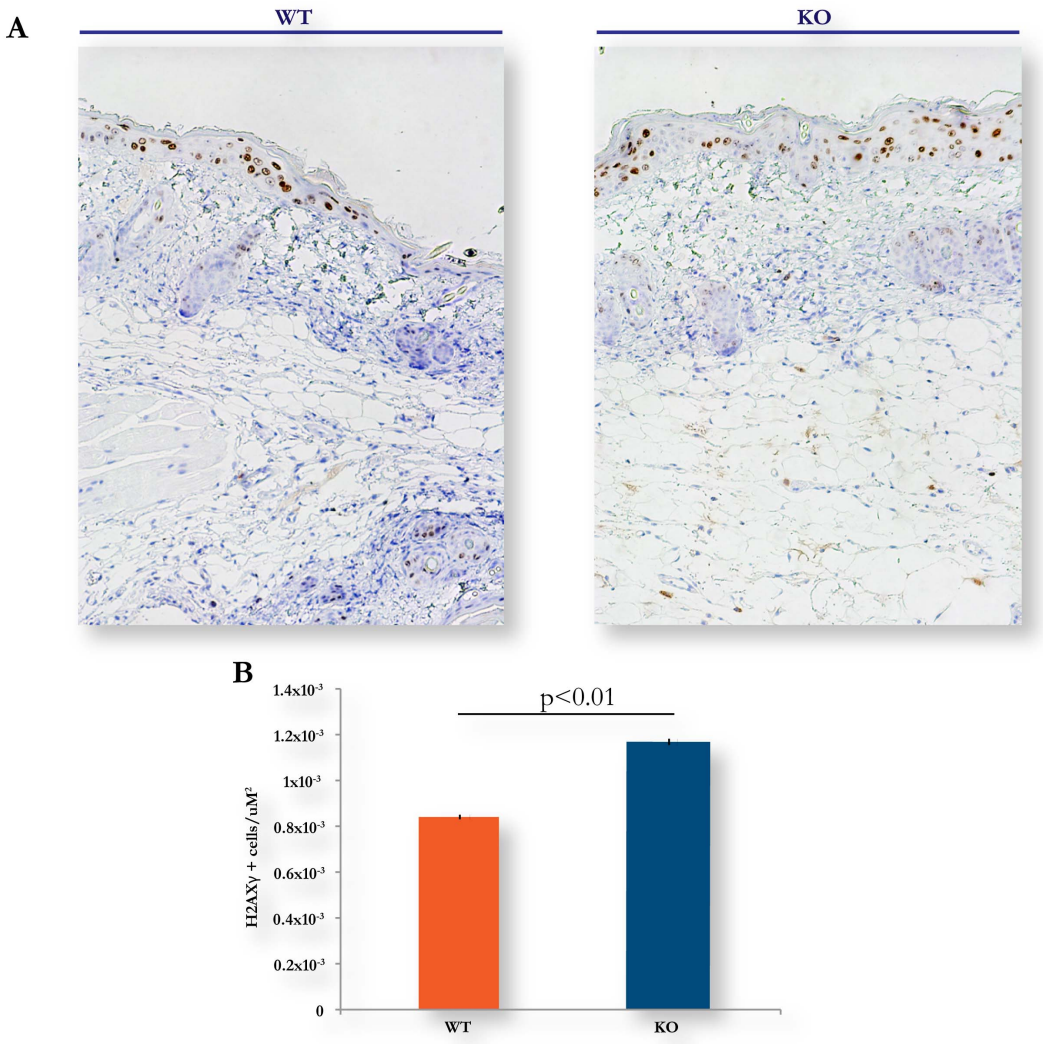

Figure 23. Quantification of γH2AX positive cells in UVB damaged epidermis

A) Representative γH2AX stained skin sections from 5 weeks old mice irradiated with UVB. B) Quantification of γH2AX positive cells (stained brown in A) per epidermal surface ($p<0.01$). Data points are mean ± SEM (n=3).

1.4. Analysis of PrimPol requirement in DDR pathways

➢ Sensitivity of PrimPol deficient MEFs to DNA damaging agents

In order to test if PrimPol is involved in the DNA damage response (DDR) and to identify the pathways in which PrimPol could have a role, we have tested the sensitivity of MEFs isolated either from GT or KO mice to X-irradiation, MMS, camptothecin, etoposide and UVC using clonogenic survival assays. This reveals the ability of a cell to survive a particular cytotoxic threat and continue to proliferate indefinitely, forming a large colony (>50 cells) visible to the naked eye following contrast staining.

The loss of functional PrimPol did not exacerbate sensitivity to any of the double strand break predisposing agents, X-irradiation, MMS, or topoisomerase inhibitors (camtpthotecin or etoposide) (Figure 24). The differences observed for GT and WT cell lines, in the experiments done with camptothecin or etoposide, were not significant.

Next we investigated whether PrimPol contributed to cell survival following UVC irradiation in SV40 immortalized fibroblasts, using the clonogenic survival assay. We have tested both alleles, GT and KO, because we suspected that some amount of protein may be generated from the GT allele as some mRNA production could be observed as faint GT band can be observed (Figure 13B). Consistent with this possibility, we observed minor sensitivity in the KO line, showing statistical significance at $5J/m^2$ of UVC, but not in the GTs.

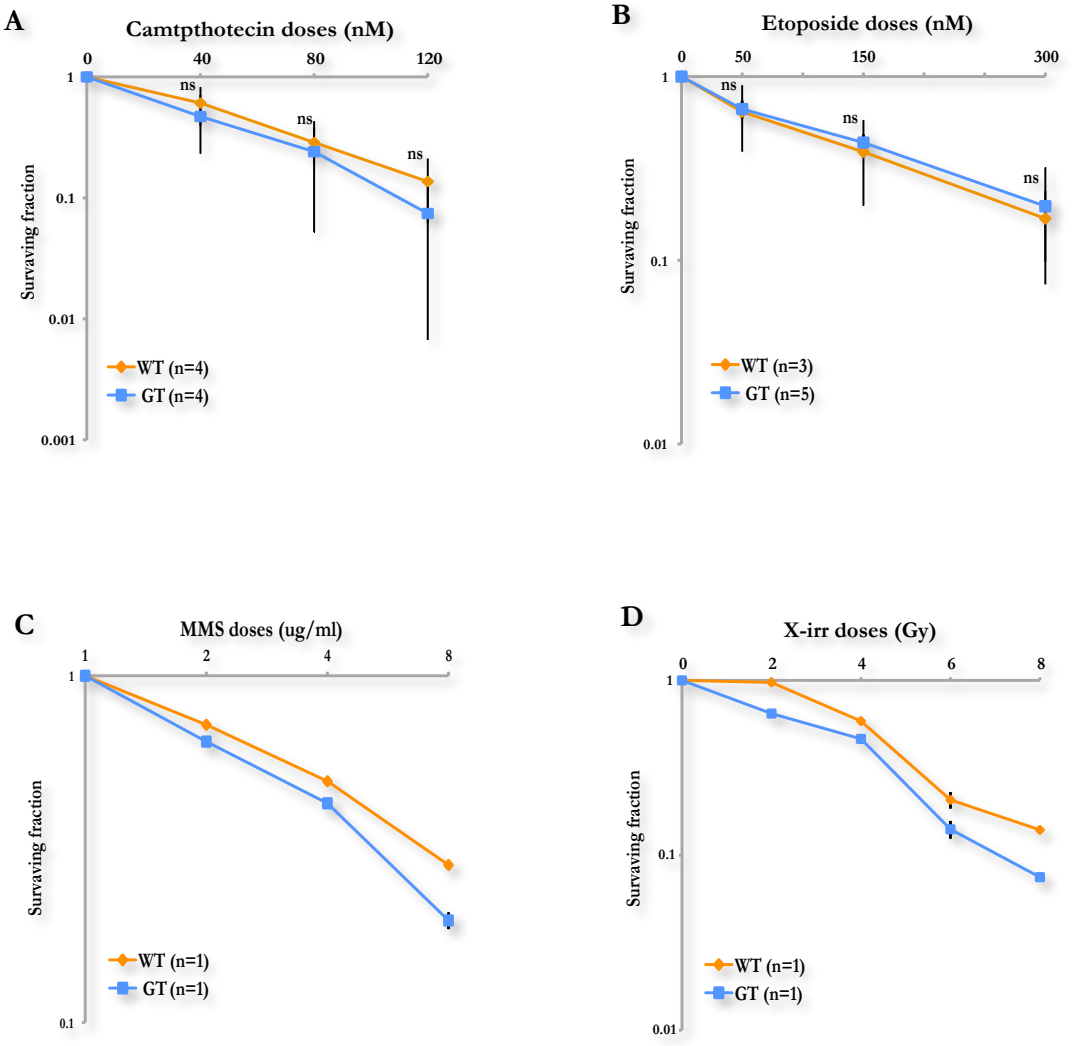

Figure 24. Sensitivity to different damaging treatments determined by the clonogenic survival assay

SV40-transformed MEF cultures were treated with A) campthotecin (CPT), B) etoposide, C) MMS, D) X-irradiation, at the indicated doses and plated for colony formation. Results from N representative experiments performed in triplicates (MMS and X-irr) and in duplicates (CPT and etoposide) are shown. Error bars denote standard deviation mean. Statistical significance was determined by T-test.

➢ PrimPol functions independently of the ATR pathway in the UV response

Given the higher susceptibility to the UV-induced damage of PrimPol deficient skin, we hypothesized that PrimPol is functioning in the UV-induced damage pathway. However, as we did not observe that loss of PrimPol rendered cells more sensitive to UV compared to wild type (Figure 25), we decided to explore the relationship of PrimPol to known UV damage-induced pathways to determine if there was potential redundant functions that may mask its role.

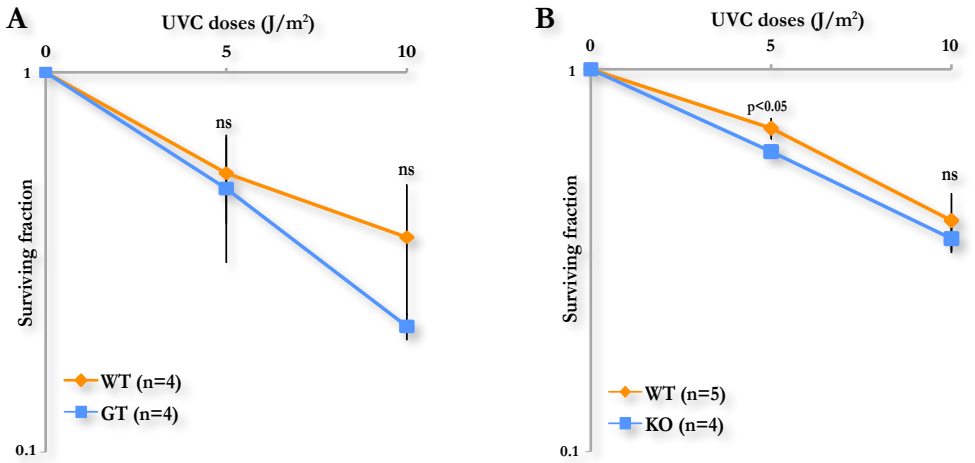

Figure 25. Sensitivity to UVC determined by the clonogenic survival assay.

SV40-transformed MEF cultures were treated with UVC at the indicated doses and plated for colony formation. Results from n representative experiments performed in duplicates are shown. A) Assay performed on GT and WT lines. B) Assay performed on KO and WT lines. Error bars denote standard deviation mean. Statistical significance was determined by T-test.

Caffeine was reported to be potent inhibitor of UV-induced cell cycle checkpoints that are ATR-dependent (Sarkaria et al. 1999). In addition, caffeine inhibits ATM and can induce cell cycle arrest and under some conditions apoptosis. It was also reported that XP-V cells that are mildly sensitive to UVC showed enhanced UV sensitivity upon treatment with low doses of caffeine (Arlett et al. 1975). We have investigated if *PrimPol* deficient fibroblasts would show sensitivity to UVC compared to WT cells in the presence of caffeine. Several titrations of caffeine were tested for sensitivity assays. While we could optimize concentration of caffeine alone, it was difficult to optimize conditions for UVC treatment

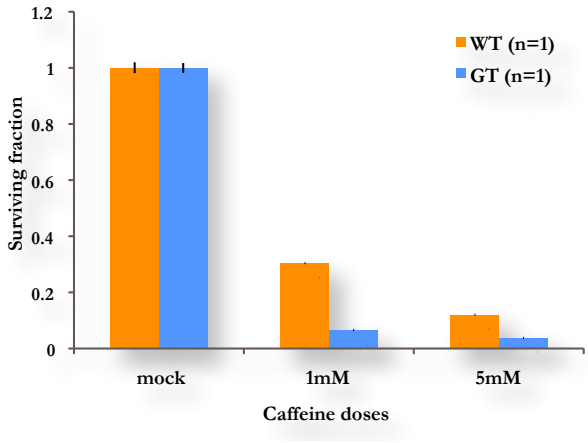

Figure 26. Sensitivity to caffeine determined by clonogenic survival assay.

SV40-transformed MEF cultures were plated for colony formation and treated with caffeine for 24 hours at the indicated doses. Results from 1 representative experiments performed in duplicates is shown. Error bars denote standard deviation mean.

in with caffeine as most doses led to massive cytotoxicity and most fibroblasts were unable to form colonies because they were dying. However we were able to observe the effect of caffeine treatment alone on fibroblasts (Figure 26).

Loss of PrimPol rendered cells more sensitive to caffeine compared to WT cells. This gave us an idea that PrimPol might be acting in parallel to the ATR pathway. To explore this possibility we have tested the UVC sensitivity of WT, GT and KO fibroblasts using additional inhibitors against ATR as well as those for the downstream Chk1 kinase and the poly-ADP ribose polymerase, which are the molecules important for the UV response.

The inhibition of the PARP pathway resulted in increased sensitivity of KO MEFs to lower dose of UVC, although this difference in sensitivity between WT and KO cell lines was lost at higher dose of UVC (Figure 27A). The discrepancy observed at different doses of UVC can be explained by the fact that PARP inhibitors alone already inhibit the growth of KO MEFs substantially as seen in Figure 27B. So the difference seen at 5J/m2 where KO cells are more sensitive than WT cells is not due to synergistic effect of UVC and PARP inhibitors but more likely because of the effect exerted by the drug itself. At higher dose 10J/m2 this difference is lost because of the effect of UVC on cell viability is much stronger than that of the PARP inhibitor. PARP inhibition stalls forks, so this may reflect on a role for PrimPol in fork restart.

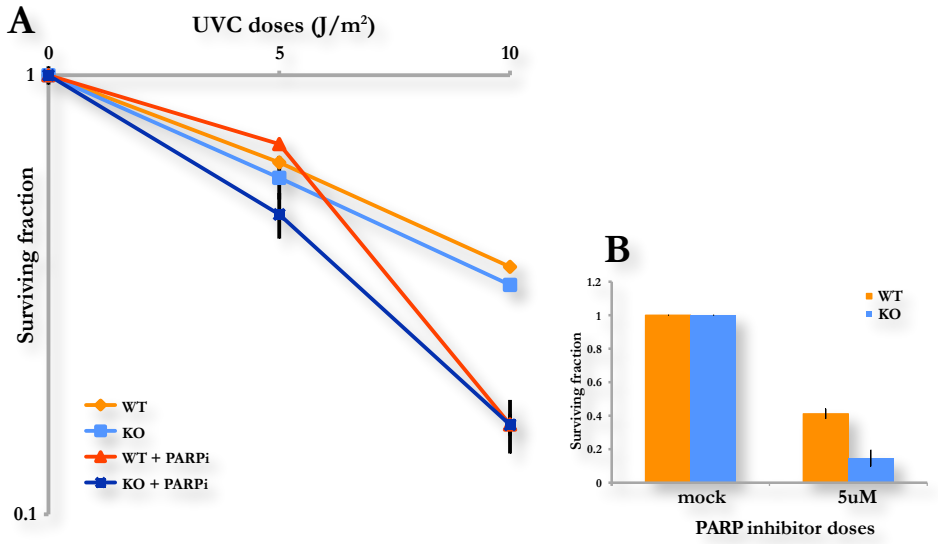

Figure 27. Sensitivity to PARP inhibitors determined by clonogenic survival assay

A) Sensitivity to UVC in the presence of PARP inhibitors was determined by clonogenic survival assay. SV40-transformed MEF cultures were plated for colony formation and treated with PARP inhibitors at the dose 5uM 30minutes before UVC treatment and for 7 hours afterwards. B) The effect of PARP inhibitors alone on proliferation. Results from one experiment performed in duplicates are shown in A and B. Error bars denote standard error mean.

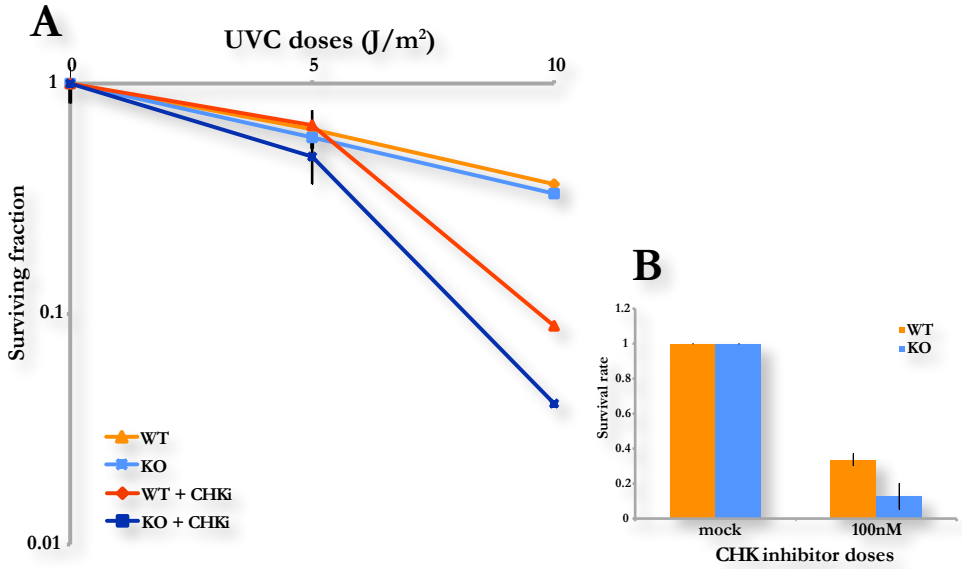

Figure 28. Sensitivity to CHK inhibitors determined by clonogenic survival assay

A) Sensitivity to UVC in the presence of CHK inhibitors was determined by clonogenic survival assay. SV40-transformed MEF cultures were plated for colony formation and treated with CHK inhibitors at the dose 100nM 30 minutes before UVC treatment and left on the cells afterwards. B) The effect of CHK inhibitors alone on survival. Results from 1 representative experiments performed in duplicates are shown in A and B. Error bars denote standard deviation mean.

Downregulation of CHK1 and CHK2 pathway resulted in the increased sensitivity of PrimPol deficient fibroblasts compared to WT (Figure 28A). This drop in survival rate in KO cells was not only because of the effect from CHK inhibitors alone (Figure 28B) but rather because of the combined effect of UVC and the drug.

In the presence of ATR inhibitors we observed that the surviving fraction of GT fibroblasts was decreased more than 2 fold compared to WT cells treated with UVC alone. There was not a clear difference between WT and GT cell lines in sensitivity to ATR inhibitors alone (Figure 29B) suggesting that what we observed in the Figure 29A is a real synergistic effect on sensitivity to UVC and ATR inhibitors and that PrimPol may act in parallel to the ATR pathway.

ATR protein kinase is a crucial transducer of the DDR to single-stranded DNA damage associated with stalled replication forks as well as generated during BER and double strand break repair as DNA repair intermediates. Activated ATR in turn phosphorylates a number

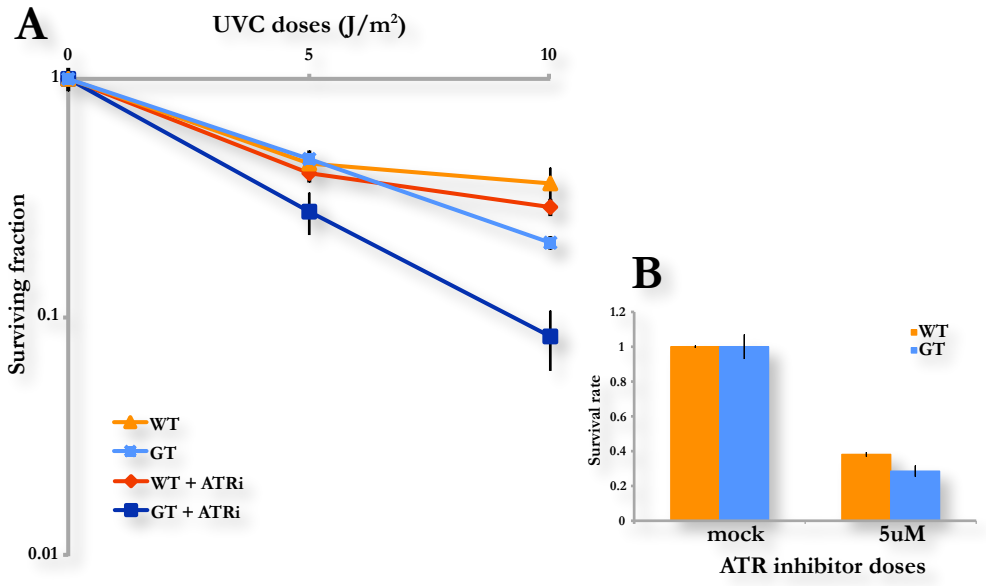

Figure 29. Sensitivity to ATR inhibitors determined by clonogenic survival assay

Sensitivity to UVC in the presence of ATR inhibitors was determined by clonogenic survival assay. SV40-transformed MEF cultures were plated for colony formation and treated with ATR inhibitors at the dose 5uM 30minutes before UVC treatment and for 7 hours afterwards. B) The effect of ATR inhibitors alone on survival. Results from 1 representative experiments performed in duplicates are shown in A and B. Error bars denote standard deviation mean.

of substrates involved in cell cycle regulation, DNA replication, DNA repair and apoptosis. Recently it was reported that ATR dependent phosphorylation of Pol η is important for normal survival and postreplication repair (Gohler et al. 2011). It has been speculated that there can be an additional, not yet characterized TLS polymerase that operates in DNA damage tolerance and compensates potentially for the loss of Pol η in XP-V cells. Based on our results, we hypothesized that PrimPol could be that additional TLS polymerase.

➢ Epistasis analysis of PrimPol in UV damage tolerance

To test if PrimPol can have redundant functions to Pol η or to the other TLS polymerases we decided to use siRNA to downregulate genes shown to be important for DNA damage bypass upon UV exposure. The strategy of downregulation of chosen genes in WT and KO immortalized MEFs and subsequent plating for sensitivity assay to UVC is illustrated in Figure 30.

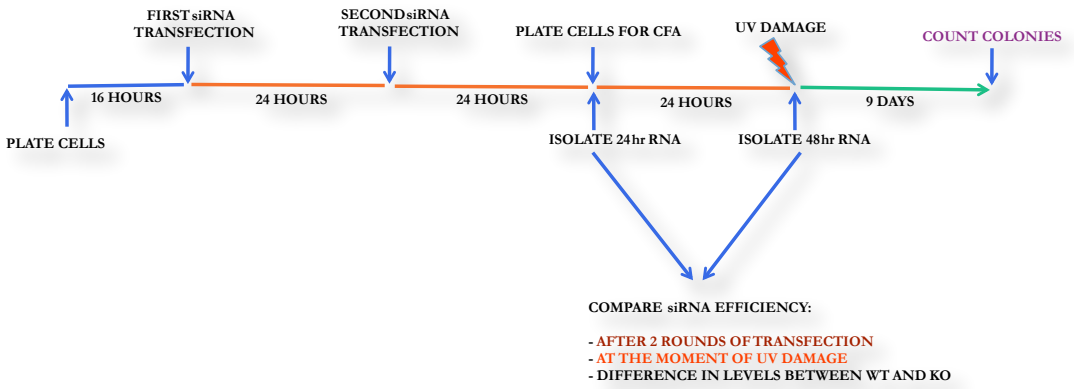

Figure 30. Scheme of experimental design for siRNA mediated downregulation of several genes of interest

KO and WT immortalized MEFs were plated at 3x105 per well on a 6 well plate. After 2 transfections with siRNAs at designated time points, cells were plated for the colony forming assay 24 hours after the last transfection and damaged by UVC 24 hours upon plating. RNA was isolated in 2 rounds, on the day of plating and on the day of UVC damage.

To examine the genetic dependencies of PrimPol in the UV response, we have chosen to deplete Pol η, Nbs1 and Rev1 as these proteins are been implicated in the UV response by

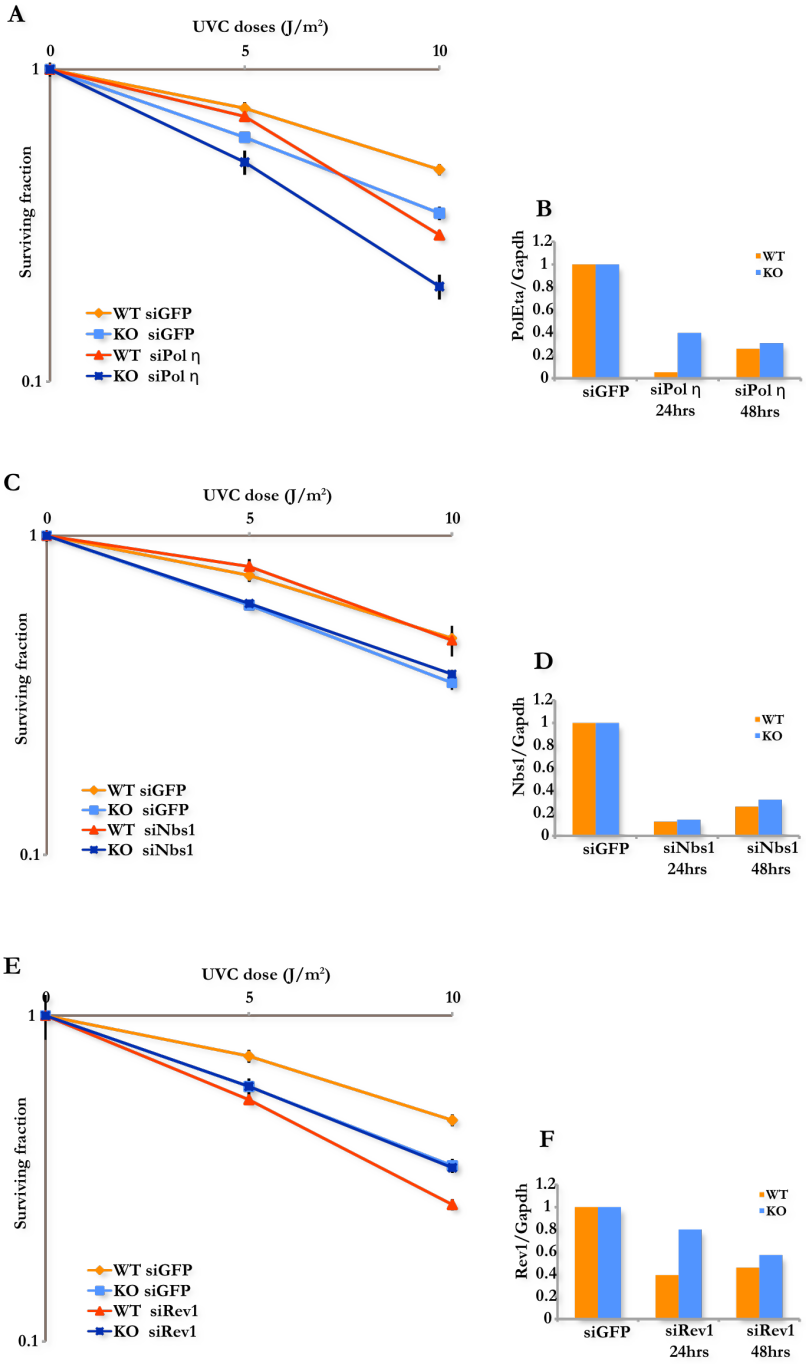

Figure 31. Epistasis analysis between PrimPol and Pol η, Nbs1 or Rev1 in UV sensitivity

SV40-transformed MEF cultures were plated for colony formation and treated as described in the scheme 3.3. In A, C and E are plotted proliferation rates after UVC damage alone or combined with downregulation of gene of interest. In B, D and F are plotted expression levels of assigned genes after siRNA mediated downregulation 24hrs versus 48hrs after the last transfection. The values are obtained by qPCR and normalized to control samples treated by siRNAs against GFP. A and B) siRNA against Pol η; C and D) siRNA against Nbs1; E and F) siRNA against Rev1.Results from 1 representative experiments performed in duplicates are shown. Error bars denote standard deviation mean.

indirectly signaling UV damage or by directly bypassing UV lesions. We suspected that PrimPol may act in the by-pass of UV induced dimers and for that reason we did not see sensitivity to UV alone as PrimPol could act redundantly to other translesion polymerases. So far, Pol η is the best-described TLS polymerase that can read through CPD dimers in an error-free manner. In addition, PolEta has been shown to be regulated by ATR and cells depleted of Pol η showed mild sensitivity to UVC (Gohler et al. 2011). We wanted to test if depletion of Pol η in *PrimPol*$^{-/-}$ cells would sensitize them even more to UV induced damage.

Nbs1, a central component of the Mre11 complex that senses DSBs, was reported to be involved in translesion synthesis by interacting with and recruiting RAD18 to DNA damage sites, regulating in that manner monoubiquitination of PCNA and Pol η recruitment (Yanagihara et al. 2011). By depleting Nbs1 we hypothesized that we would affect Pol η regulated UV damage by-pass and that this would provide an alternative approach to examining potential redundancy between PrimPol and Pol η. In addition, Nbs1 is critical for homology directed repair that has been implicated in the survival of UV lesions (Tauchi et al. 2002; Falck et al. 2012).

Rev1 was proposed to act as a scaffold for other TLS polymerases and to be involved in regulation of TLS in that manner. We hypothesized that depleting Rev1 would affect the recruitment of other TLS polymerases and that we would see if there is redundancy to other described TLS polymerases in addition to Pol η.

The expression levels of *Pol H* were quantified by qPCR 24 hours and 48 hours after the last transfection with siRNAs against Pol Eta (Figure 31B). At the moment of UV damage, levels of *Pol H* were around the same in WT and KO cells, which was 30% of levels observed in controls treated with siRNA against GFP. This means that 70% of *Pol H* expression was down and that was sufficient to affect sensitivity of KO cells since only after both genes were fully or partially inactive we could observe marked sensitivity to UVC (Figure 31A).
Nbs1 knock-downs were efficient (Figure 31D) but there was no difference observed in UVC sensitivity among samples that were siRNA treated and those that were not (Figure 31C). We conclude that either cells have to be completely deficient of Nbs1 to show

sensitivity to UVC or that Nbs1 does not play a major role in UV induced damage pathway. Consistent with this, we have not been able to reproduce published data (Yanagihara et al. 2011)that Nbs1 mutant cells from mice or human patients are UV sensitive (Figure 32).

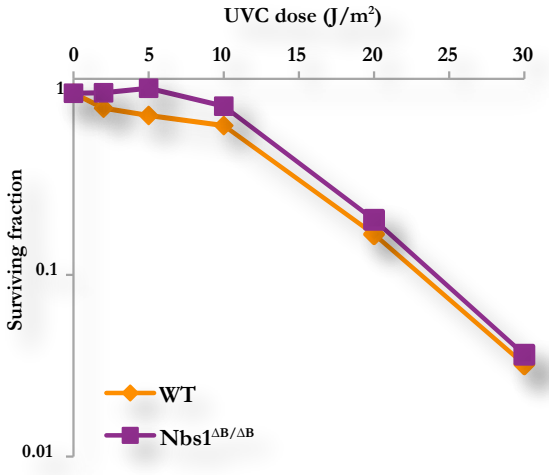

Figure 32. Sensitivity to UVC for Nbs1$^{\Delta B/\Delta B}$ cell lines

SV40-transformed WT and Nbs1$^{\Delta B/\Delta B}$ MEF cultures were treated with UVC at the indicated doses and plated for colony formation assay. Results from one representative experiments performed in triplicates are shown. Error bars denote standard deviation mean.

The siRNA depletion of Rev1 was not very efficient (Figure 31E) and therefore the results were difficult to interpret (Figure 31F) since it turned out that KO lines with or without Rev1 are equally sensitized to UVC while the WT line showed a significant difference in UVC sensitivity depending on whether *Rev1* expression was diminished or not.

We conclude from these results that PrimPol functions in a UV lesion tolerance pathway that is independent from the one of ATR and Pol η and that this novel bypass pathway protects Pol η deficient cells from further UV-C cytotoxicity by compensating for the loss of Pol η function.

1.5. *PrimPol* deficiency does not strongly exacerbate cell cycle progression after DNA damage

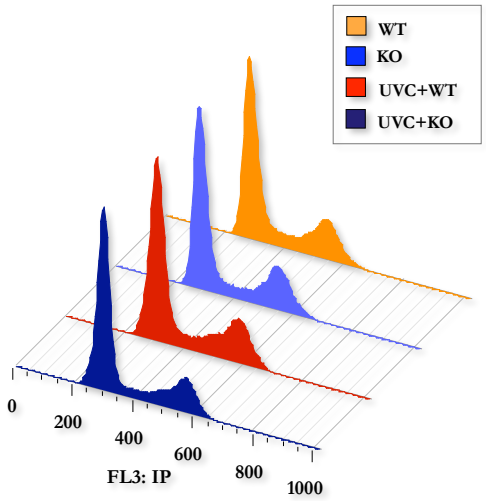

Figure 33. Cell cycle distribution

Histograms of cell cycle distribution in primary MEFs labeled with propidium iodide (IP). Cell cycle profiles were analyzed by flow cytometry and plotted as cell count vs. DNA content. Cells were either undamaged or damaged with 10J/m^2 UVC and let for 14 hours to recover.

To determine if *PrimPol* deficiency affected cell cycle progression following DNA damage, especially after UV, we have analyzed cell cycle distribution in *PrimPol* deficient primary MEFs by propidium iodide incorporation. Undamaged cells were compared to those damaged by 10J/m^2 (Figure 33). No difference in cell cycle distribution was observed compared to WT littermates.

We then analyzed checkpoint responses to UV damage in *PrimPol* deficient MEFs. To examine the G1/S checkpoint, exponentially growing MEFs were exposed to 10J/m^2 of UVC, and the percentage of cells in S phase 14hr post-treatment was measured by BrdU incorporation. PrimPol KO cells incorporated less BrdU compared to WT cells (Figure 34A) indicating that less cells were entering S phase after damage. This result could indicate that DNA damage accumulates in KO cells as it does not get repaired as efficiently as in WT cells, thus blocking the progression of replication forks. This interpretation would fit with previous results in the skin where we observed increased levels of DNA damage after UVB treatment (Figure). A similar effect of UVC on S phase entry was reported in XP-V cells (Bullock et al. 2001). To test this hypothesis we would need to analyze if there are more stalled replication forks in KO cells and if elongation of DNA is affected. One of the ways to check this is by analyzing the amount single stranded DNA by checking phosphorylation of RPA. This analysis was performed and it will be described in the next section.

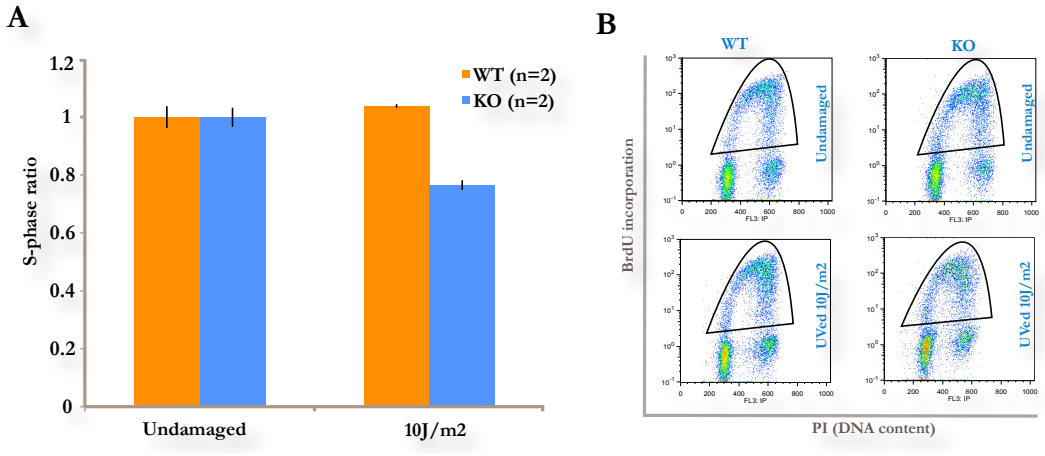

Figure 34. Analysis of G1/S checkpoint response upon UVC induced damage

A) G1/S checkpoint in early-passage MEF cultures. The S phase ratios (%BrdU-positive of damaged or undamaged/average %BrdU-positive undamaged) are plotted. Results are the average of 2 experiments performed in triplicates for each genotype. Error bars denote standard deviation. B) Example of BrdU staining of primary MEFs pulse labeled with BrdU for 4 hours 14 hours after exposure to 10J/m² of UVC. BrdU positive cells are gated.

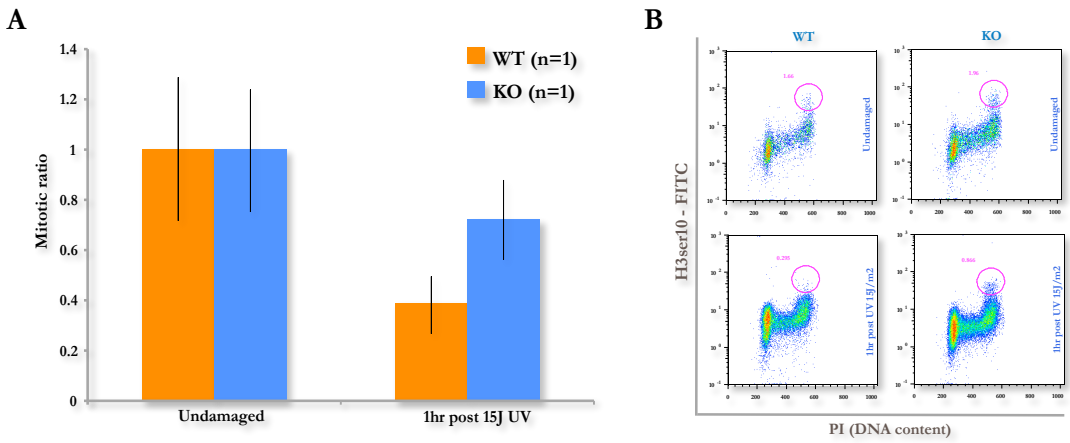

Figure 35. Analysis of G2/M checkpoint upon UVC induced damage

A) G2/M checkpoint responses of exponentially growing murine embryo fibroblasts (MEFs). The mitotic ratios (percentage of H3ser10 positive UVC-damaged cultures, normalized to percentage of undamaged) of UVC treated cells (15J/m²) at 1 hr post UVC treatment are presented. Results are the average of 1 experiment performed in triplicate for each genotype. Error bars denote standard deviation. B) Example of H3ser10 stainings quantified by flow cytometry. Only H3ser10 positive cells were gated.

We next examined the G2/M checkpoint response in *PrimPol* deficient cells as the activation of this DNA-damage-dependent checkpoint is known to be strongly dependent on ATR. As can be observed in Figure 35A KO cells have a higher mitotic index compared to WT cells after 15J/m2 of UV damage indicating that they are accumulating more cells in mitosis due to impaired checkpoint activation or slower mitotic progression. In future experiments we will examine cell cycle distribution upon UVC in PrimPol deficient cells with Pol Eta depletion.

1.6. Loss of PrimPol affects genomic stability

We have analyzed metaphase spreads prepared from KO primary exponential growing MEFs and control WT MEFs to investigate the consequence of PrimPol loss on chromosomal stability. *PrimPol* deficiency in MEFs resulted in a significant increase in cells presenting chromatid breaks in the absence of exogenous DNA damage (Figure 36A). Chromatid breaks and chromosome fragments were the most common abnormalities in all samples analyzed. Overall, metaphase aberrations were 3 fold higher in KO cells than in WT control. After damage with 5J/m^2 of UVC, cells deficient for *PrimPol* had more chromosomal abnormalities compared to control cells that showed mainly chromatid breaks (Figure 36C) 2.5 hours after damage with UV. In the cells that were left to recover longer after UVC we noticed that chromatid breaks accumulated but this increase was proportional in both WT and KO samples. The examples of metaphase spread and aberrations that were scored are presented in Figure 37.

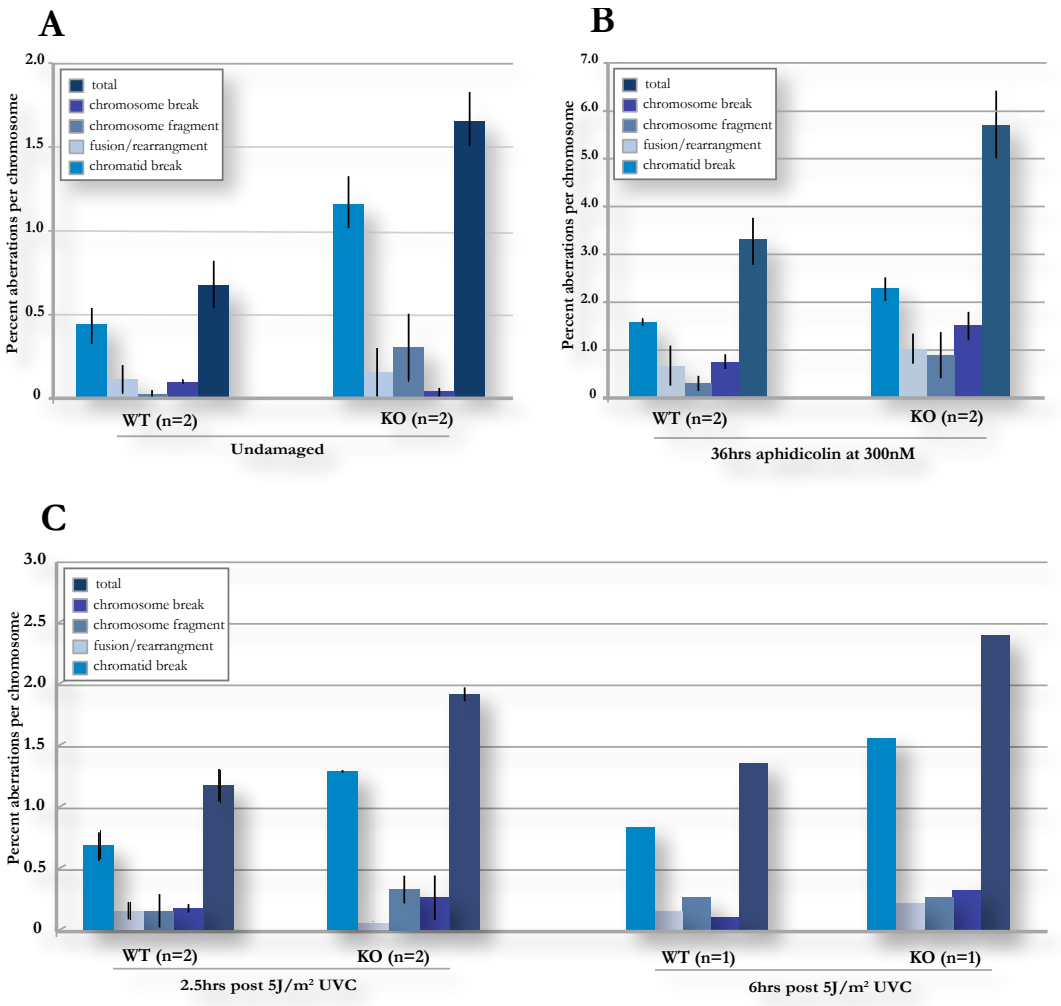

Figure 36. Metaphase aberrations in exponentially proliferating MEFs

The frequency of aberrations in two independent experiments (50 metaphases scored for each) was quantified from Giemsa stained spread metaphase analysis by phase contrast microscopy. MEFs were A) undamaged; B) 300nM aphidicolin treated for 36hours; C) damaged with 5J/m² of UVC and let to recover for 2.5 hours or 6 hours.

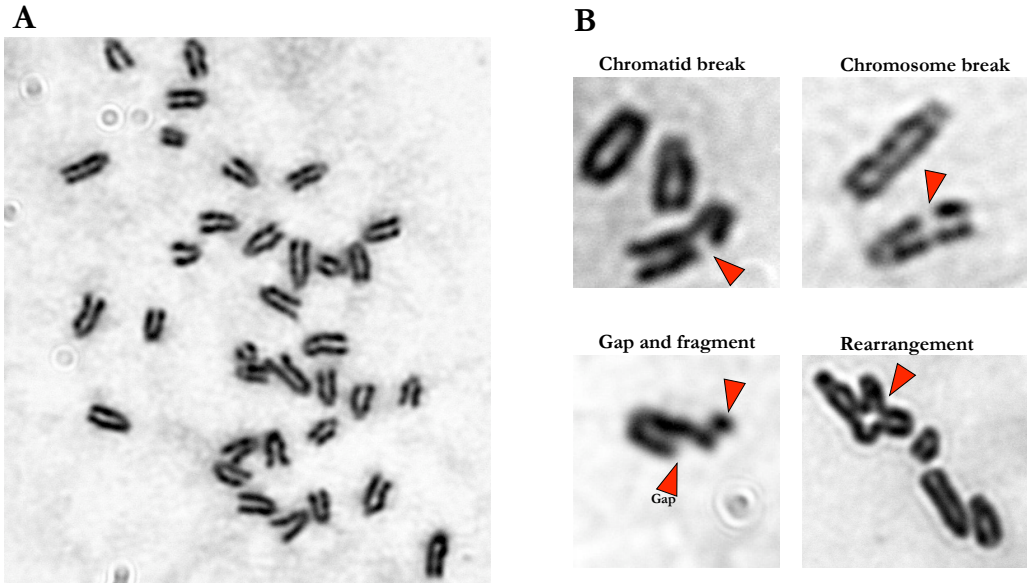

Figure 37. Examples of metaphase spreads and aberrations

Metaphase spreads were Giemsa stained and analyzed by phase contrast microscopy. Examples from KO MEFs are shown in A. Types of aberrations that were scored in our analysis of metaphases are indicated with red arrowheads in B.

We have also observed a substantially higher frequency of aberrant metaphases in *PrimPol* deficient MEFs compared to WT controls, after 36 hours of treatment with low dose (300nM) aphidicolin (Figure 36B). Aphidicolin inhibits polymerase α, causing the dissociation of leading and lagging strands and the accumulation of underreplicated DNA at low doses or the complete inhibition of replication at higher doses. Aphidicolin induces chromatid breaks at high levels in fragile sites (FRA) that have repetitive DNA or potential secondary structures (G-quadraplex for example). After aphidicolin all types of aberrations were expressed at

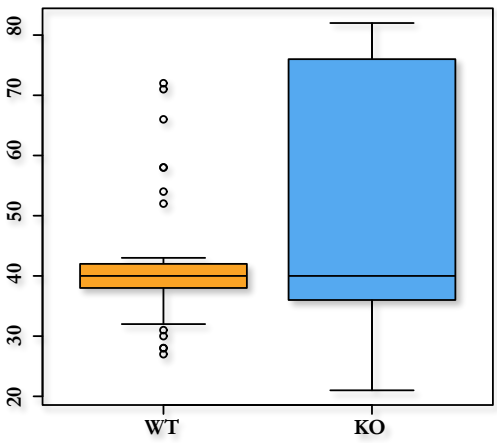

Figure 38. Chromosome distribution per metaphase spread

Distribution of chromosome number per metaphase spread after 36 hours treatment with aphidicolin 300nM.

higher frequencies in KO cell lines compared to WT. Also, the chromosome number per metaphase spread was markedly elevated in KO cells compared to WT treated with aphidicolin (Figure 38). These results indicated that PrimPol may play important roles during DNA replication, particularly at FRA sites. Secondary structure at FRA sites may be analogous to the bulky lesions caused by UV and is known to require TLS polymerases such as Pol η for their efficient replication.

.

1.7. ATR pathway is overactivated in PrimPol deficient MEFs

As these results suggested that PrimPol acts in an ATR independent pathway that monitors replication after UV damage, we decided to investigate the effect of UV on intra-S checkpoint signaling in PrimPol deficient cells. Lesions in DNA incited by UV can lead to uncoupling of the replication polymerase-helicase complex (Byun et al. 2005) and consequently to the accumulation of single stranded DNA (ssDNA) coated with RPA. This serves as a substrate for the ATRIP-ATR complex and leads to the activation of ATR kinase activity (Kaufmann 2010). ATR activation leads to the phosphorylation of the effector kinase, Chk1, and downstream phosphorylation of RPA (Figure 39A). It was shown that UVC damage in XP-V cells resulted in S-phase delay and over-activation of the intra-S checkpoint (Cordeiro-Stone et al. 2002; Cruet-Hennequart et al. 2006).

To determine the effects of PrimPol deficiency we examined the amount of phosphorylated Chk1 on serine 345 (Chk1 S345) that corresponds to the level of its activation (Liu et al. 2000) and as well the level of phosphorylated RPA (S4/S8 RPA32) that correlates with ATR activity and the generation of ssDNA (Binz et al. 2004; Patrick et al. 2005). Exponentially growing primary MEFs were UVC irradiated with a dose of $50J/m^2$or treated with high doses of aphidicolin (20uM) for 30 minutes. Loss of PrimPol resulted in the over-activation of Chk1 one hour after the initial UVC damage and immediately after aphidicolin treatment. Chk1 phosphorylation was persistent but lower 4 hours after UVC damage and remained elevated in KO cells compared to control WT (Figure 39B). Consistent with this, one hour after UV damage the hyperphosphorylated form of RPA32 was detectable and was even more notable 4 hours after damage in both

WT and KO samples. However, hyperphosphorylation of RPA32 was increased in the absence of PrimPol. In contrast, there was no difference in the levels of hyperphosphorylated RPA32 after aphidicolin treatment (Figure 39B). This might be because protein was isolated shortly after the treatment and differences in the levels and the kinetics of phosphorylation may be different at other time points. A similar effect of

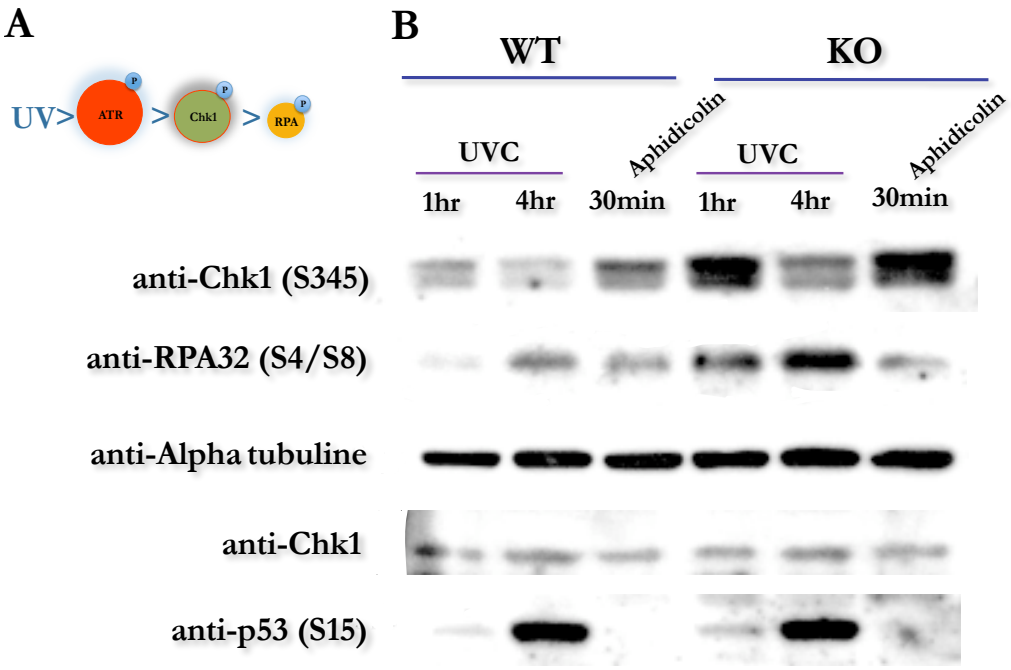

Figure 39. Evaluation of ATR checkpoint signaling upon UVC induced damage

Loss of PrimPol results in over-activation of ATR checkpoint pathway in UVC damaged and aphidicolin treated primary MEFs. A) Scheme of ATR kinase main targets that are phosphorylated upon detection of stalled forks; B) Kinetics of Chk1 phosphorylation on serine 345 (pChk1 S345), RPA p32 subunit on S4/S8 and p53 on S15. Total Chk1 and alpha tubuline were used as loading controls. Exponentially growing MEFs in second passage were irradiated with UVC at 50J/m2 and incubated afterwards for 1 or 4 hours. The second treatment was with 20uM of aphidicolin for 30 minutes. Cells were isolated immediately after the treatment. Experiment was repeated 3 times with the same outcome.

Pol η deficiency on increased hyperphosphorylation of RPA was reported (Cruet-Hennequart et al. 2006). p53 is phosphorylated at serine 15 by ATR upon UV damage (Tibbetts et al. 1999) and it was shown that phosphorylation of this exact residue is marker of high dose of UV (Latonen et al. 2001). It was also reported that p53 phosphorylated at S15 is recruited by ATR after UV damage and it is responsible for NER efficient response to UV and damage clearance by nuclear import of XPA (Li et al. 2011). We observed

slightly higher level of S15 phosphorylated p53 one hour after UVC damage in *PrimPol* deficient MEFs. Four hours after the induced damage there was no obvious difference in the S15 phosphorylated form of p53 between KO and WT cells (Figure 39B).

1.8. Loss of PrimPol results in delayed clearance of UV lesions in MEFs

We have shown that PrimPol is involved in the UV induced DNA damage pathway and that cells, deficient for PrimPol and depleted for Pol η, are more sensitive to UVC than controls. These findings prompted the idea that PrimPol may act as translesion polymerase involved in alternative DNA damage tolerance pathway to Pol η. To test this we have performed an ELISA assay on genomic DNA isolated from MEFs that were either SV40 or 3T3 immortalized. Cells were damaged by 30J/m2 of UVC and genomic DNA was isolated after 30minutes, 1, 2, 3, 6 and 24 hours. The assigned dose was used in order to maximize the occurrence of UV lesions and especially 6-4PP dimers, since those represent only 15-20% of the total dimers occurring. DNA was denaturated, plated and incubated with monoclonal antibodies recognizing specifically the 6-4PP or CPD lesions. Both

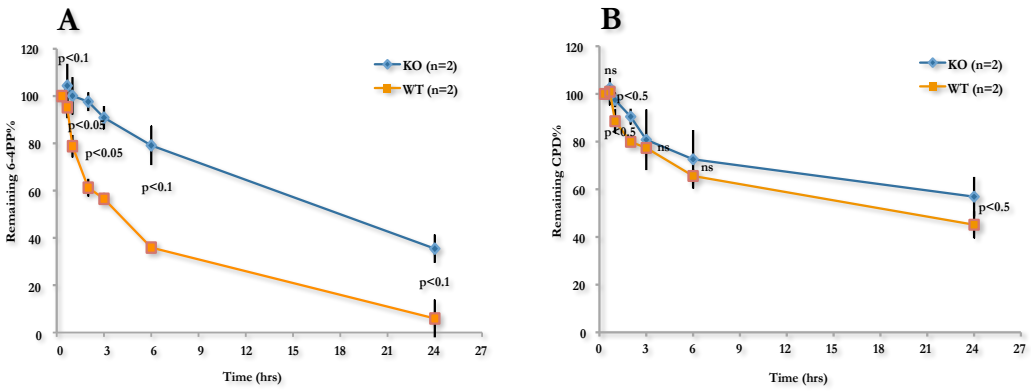

Figure 40. Clearance of CPD and 6-4PP lesions over time after UVC damage

The repair kinetics of 6-4PP (a) and CPD (b) lesions measured by ELISA on genomic DNA from immortalized MEFs. Results from N representative experiments performed in triplicates Error bars denote standard deviation mean. Assay performed on KO and WT lines damaged initially by 30J/m². Statistical significance was quantified by T-test and p values are assigned to each time point.

lesions are induced by UV and can distort the helix and impede replication fork progress if left unrepaired. CPD lesions can be bypassed efficiently and in error-free manner by Pol η, however error free TLS of 6-4 photoproducts is not yet characterized and it is primarily removed by nucleotide excision repair enzymes. At all time points measured, the clearance of 6-4PP lesions in PrimPol deficient cells was not as efficient as in wild type (Figure 40A). Nevertheless, some amount of 6-4PP lesions was removed by 24 hours, probably by nucleotide excision repair machinery or other TLS polymerases. Removal of CPD lesions was delayed as well in PrimPol deficient cells but not to the same extent as for 6-4PPs (Figure 40B). We conclude from this experiment that PrimPol is involved in clearance of UV induced lesions, particularly in 6-4PPs. We suspect that we might see even more pronounced defect in NER or Pol η deficient cells in combination with PrimPol deficiency and this is something that will be topic of future investigation.

1.9. PrimPol and alternative DNA damage response pathways

Several polymerases are involved in the process of differentiation and maturation of T and B immune cells. Pol η and Pol λ are required to fill in single stranded gaps during V(D)J recombination event of BCR and TCR receptors (Hefferin and Tomkinson 2005). TLS polymerases are also implicated in the process of immunoglobulin maturation through somatic hypermutation (SHM) and class switch recombination (CSR) that is described in introduction (section 1.8.). To test if PrimPol is involved in alternative DNA damage response pathways we have studied thymocyte differentiation, apoptosis in thymocytes and class switch recombination in B cells.

We have analyzed the differentiation of thymocytes from 8-weeks old mice. Non-homologous end joining is necessary for rejoining of double strand breaks that occur during TCR receptor rearrangements in T cells. Lack of any of NHEJ factors can affect TCR recombination events thus causing aberrant distribution of T cell subsets. We have analyzed if loss of PrimPol would have an effect on TCR rearrangements but as it can be seen in Figure 41, the distribution of subsets was the same in KO mice as in wild type littermates, implicating that PrimPol does not have a role in NHEJ.

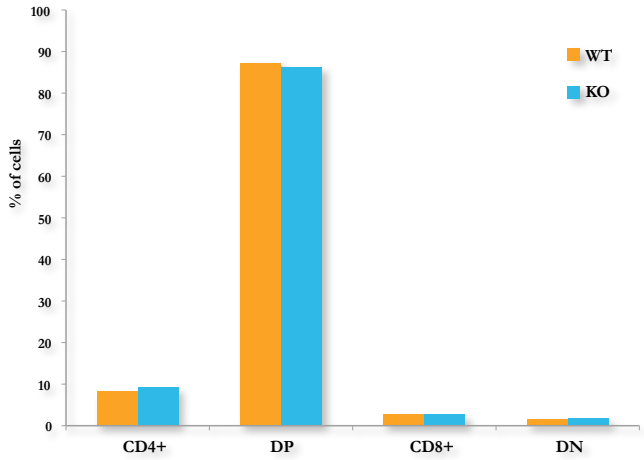

Figure 41. Differentiation of Thymocytes

Percentages of thymocyte subsets isolated from *PrimPol*$^{-/-}$ (KO mice and WT littermates. The bar graphs depict percentages of DN (double negative), DP (double positive) and CD4 or CD8 single positive thymocytes. Flow cytometric analysis of T-cell development was performed from 8-week old mice. Thymocytes were stained with anti–CD4–phycoerithryn (PE), anti–CD8–fluorescein isothyocyanate (FITC) and anti–CD3-APC. Experiment was performed once in duplicates.

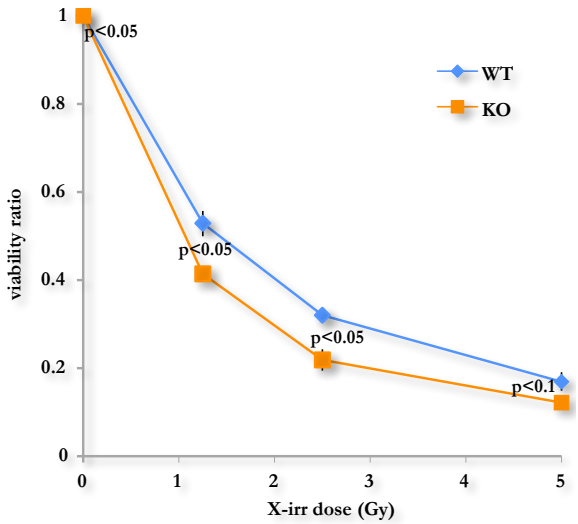

Figure 42. Viability of thymocytes after X-irradiation

Dose response of thymocytes post X-irradiation treatment. Triplicate results from one KO and one WT animals are shown. Apoptosis in irradiated WT and KO thymocytes 20 hr postexposure to the indicated ionizing radiation (IR) dose. Viability ratios are plotted for each dose (% viable cells mock or IR treated divided by % viable cells mock treated). Triplicate results of one representative experiments are plotted. Statistical significance was quantified by T-test and p values are assigned to each time point.

It was described that thymic lymphocytes undergo p53-dependent apoptosis upon γ-irradiation and that p53 activity is tightly controlled in response to ionizing-irradiation *in vivo* (Clarke et al. 1993; MacCallum et al. 1996; Komarova et al. 1997). We investigated if loss of PrimPol would affect induction of apoptosis in thymocytes upon X-irradiation. To obtain a more quantitative view of the apoptotic defect, ionizing-irradiation-induced apoptosis was assessed in PrimPol KO thymocytes *ex vivo* after 3 different doses of irradiation. KO thymocytes appeared slightly more apoptotic compared to wild type control. Since the difference observed is statistically significant we consider that experiment needs to be repeated on additional mice. In this experiment, samples are generated from one mouse of each genotype, which is not sufficient to establish that observed difference reflects biological significance (Figure 42).

Class switch recombination (CSR) is an important event in the maturation of immunoglobulin, directed through series of deletional recombination events, resulting in the creation and propagation of antibodies of different isotypes and effector functions. CSR is initiated with double strand breaks in the switch (S) region of the immunoglobulin genes that are later sealed by a variant NHEJ mechanism. It was shown that Rev1 has important function in CSR by recruiting uracil DNA glycosylase to switch regions, mediated through its scaffolding but not enzymatic function (Zan et al. 2012). On the other hand, Pol η is involved not only in somatic hypermutation but also in CSR, acting as an A/T mutator (Faili et al. 2004). We have investigated if loss of PrimPol will affect immunoglobulin maturation and CSR. We have stimulated B cells for 4 days with LPS and Il-4 and measured on the fourth day the percentage of cells that have switched from IgM to IgG1 or IgG2b isotype. There were no significant differences observed between wild type and KO cells (Figure 43).

Cellular proliferation is essential for the generation of class-switched B cells. It was reported that clonal propagation of B cells undergoing class switching requires cell proliferation and the number of class-switched cells detected after a B cell response will be determined by the degree of this clonal expansion. Since we hypothesized that we would

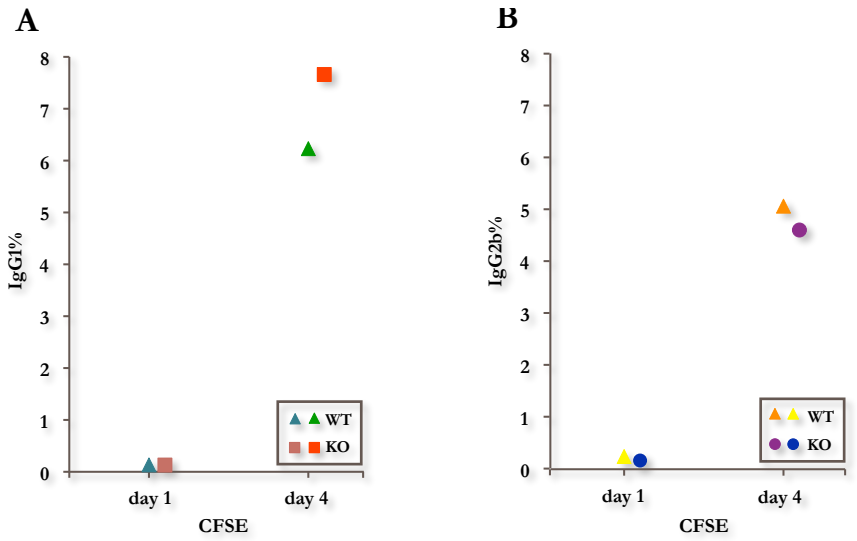

Figure 43. Analysis of class switch recombination

Surface Ig expression of IgG1 and IgG2b isotypes on *in vitro* stimulated B cells. CFSE-stained resting B cells were stimulated for four days *in vitro* with LPS and IL-4, harvested on the forth day and flow cytometric analysis was used to determine surface IgG1 and IgG2b expression. The percentage of B cells expressing IgG1(A) or IgG2b (B) on CFSE stained cells is indicated for KO B cells and WT B cells. Experiment was done in duplicates and results of one representative experiment are shown. Absolute values are plotted.

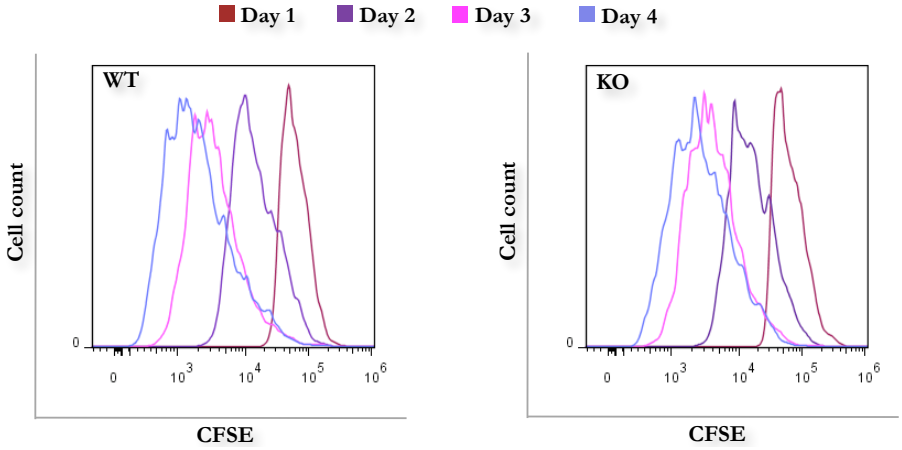

Figure 44. Proliferation of B cells during maturation

Quantitative assessment of clonal expansion of B cells. CFSE staining profiles of KO B cells and WT B cells are presented in the histograms. Resting B-cells were stimulated with LPS and Il-4 for 1-4 days and the dilution of CFSE was quantified by flow cytometry.

see a difference in CSR between WT and KO B cells, we checked if there was a defect in cell proliferation that could affect any difference in the switching of B-cells. We combined cytoplasmic dye dilution with flow cytometric staining of surface Ig isotypes to measure clonal expansion of switched cells. Resting splenic B cells from KO and control mice were labeled with CFSE and activated *in vitro* with LPS and IL-4. At multiple time points after stimulation, cells were harvested and analyzed by flow cytometry. Assessment of cell division was done by quantification of the dilution of intracellular CFSE staining. A modest decrease in cell division was observed in the response of KO B cells to LPS and cytokines, as reflected by a slightly higher proportion of KO cells that had undergone fewer cell divisions as compared with WT cells (Figure 44).

2. *In vitro* studies of PrimPol cellular localization, functions and interactions

2.1. PrimPol expression in cultured cells

Growing knowledge in the polymerase field has brought the realization that many specialized polymerases exist in the cell and that they can function not only in replication but also in DNA damage repair. They are required not only in the nucleus but also in the mitochondria. Currently, there are 14 characterized polymerases in the nucleus and only one in mitochondria.

We wanted to characterize the mouse isoform of PrimPol and its cellular roles. I on order to study spatial and temporal regulation, localization and response to damaging agents we needed tools to analyze PrimPol in cells. Due to the lack of antibody detecting the endogenous isoform, we constructed an expression construct with PrimPol fused to a Strep-FLAG tag. We used HEK293 cells to generate stable cell lines expressing mouse Strep-FLAG tagged PrimPol. We obtained the vector pcDNA3.0 with Strep II-FLAG tags from Dr. Ueffing's laboratory, Helmholtz Zentrum Munchen. The PrimPol cDNA was cloned without a stop codon in frame with tandem Flag and Strep-Tag II epitopes that were fused at C-terminus and this construct was ligated into an expression vector, generating the construct pLPC.mPrimPol/C- FLAG-Strep-Tag II. 293t cells were then transfected with this construct and retroviral packaging vectors (VSVG, RRE and REV). Retrovirus was produced and HEK293 cells were subsequently infected and puromicin selected for those cells that are stably over-expressing mPrimPol$^{C/SF}$.

The tagged version of PrimPol was successfully over-expressed in HEK293 cells and the majority of experiments were performed in these cells. This was the only cell line where we managed to stably express PrimPol. We have also tried PrimPol stable over-expression in additional cell lines including 3T3, Hela, U2OS and MCF7. Stable over-expression did not give rise to cells that could survive the puromycin selection and maintain PrimPol expression. It was possible to transiently over-express PrimPol in Hela and U2OS cells. We

presumed this intolerance of cells for PrimPol indicated that it impaired critical pathways leading to cytotoxicity.

2.2. Immunofluorescent detection of stably and transiently expressed recombinant PrimPol

To study the intercellular localization of the mouse orthologue of PrimPol (mPrimPol) we have generated HEK293 cells stably expressing tagged protein with a Strep-FLAG fused to the C terminus of mPrimPol (mPrimPol$^{C/SF}$). Additionally we have checked PrimPol localization by immunfluorescence (IF) microscopy in other cell lines transiently transfected with mPrimPol$^{C/SF}$. The mPrimPol$^{C/SF}$ protein is localized primarily in the nucleus and in the control cell line over-expressing myc-C/Strep-FLAG we did not see any

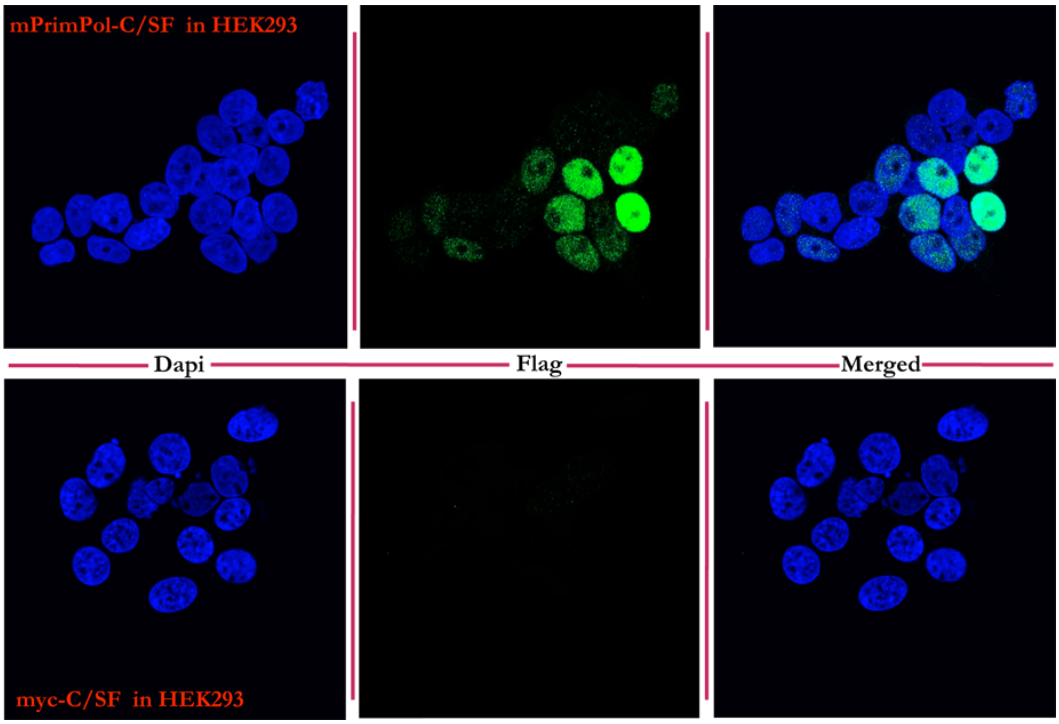

Figure 45. Detection by IF of ectopically expressed PrimPol in HEK293 cells

IF detection of Strep-FLAG tagged mouse isform PrimPol (mPrimPol$^{C/SF}$) in cultured human cells. HEK293 cells were infected by retrovirus and selected for clones stably expressing mPrimPol$^{C/SF}$. Cells over-expressing mPrimPol$^{C/SF}$ were subjected to immunofluorescent analysis with anti-FLAG antibody (green). Following immunofluorescent staining, cells were stained with DAPI to label the nuclei (blue). Image was taken by 60x objective of a confocal microscope, processed in the ImageJ program.

staining with anti-FLAG antibody, indicating that nuclear signal arises specifically from Flag-tagged PrimPol. mPrimPol$^{C/SF}$ appeared unequally distributed in nuclei with a punctuated pattern in some nuclei and a diffuse pattern in others (Figure 45). Those nuclei that were positive for PrimPol, appeared to be cells that had recently divided. This indicated that PrimPol may be specifically stabilized in certain stages of the cell cycle.

We tested if PrimPol would overlap with cell cycle markers like cyclin A, cyclin B or PCNA. Unfortunately we did not obtain any quantifiable results as HEK293 cells were a difficult system to work with due to their poor adherence. The cells were readily detaching and any harsher detergent treatments caused most of the cells to detach. We were surprised that we did not see any cytoplasmic staining for mPrimPol$^{C/SF}$ as it was reported from our collaborators that human ortholog is present in mitochondria.

As we were unable to monitor cell cycle by IF, we decided to analyze PrimPol protein

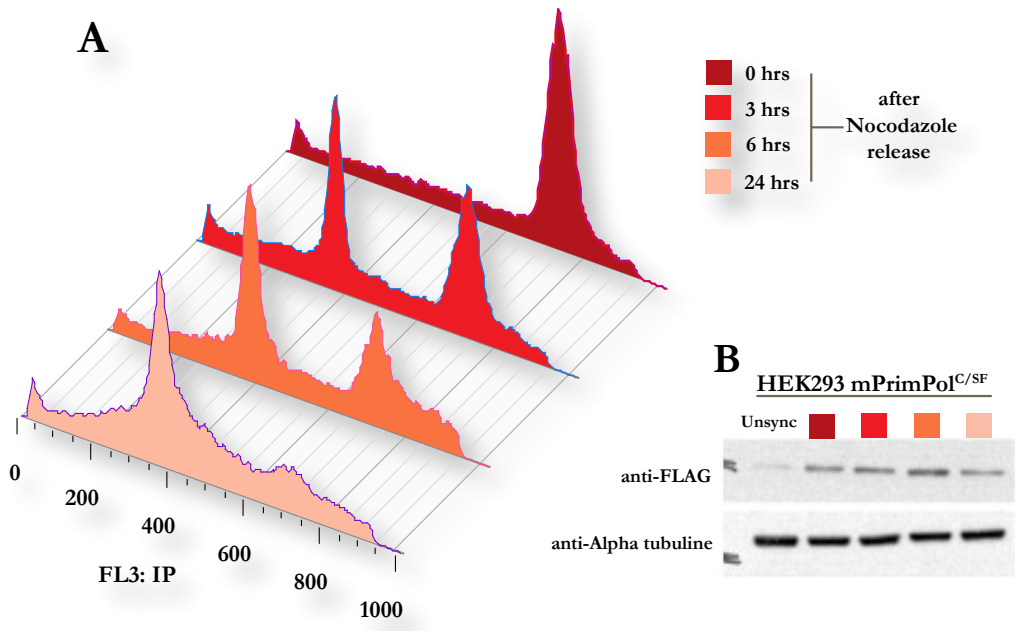

Figure 46. Synchronization of mPrimPol$^{C/SF}$ HEK293 cells by nocodazole

Nocodazole synchronization of HEK293 cells stably expressing mPrimPol$^{C/SF}$. A) Histograms of cell cycle distribution labeled with propidium iodide (IP) after Nocodazole (80ng/ul) release. Cell cycle profiles were analyzed by flow cytometry and plotted as cell count vs. DNA content. B) Protein levels of PrimPol in HEK293 upon mitotic arrest with Nocodazole. Protein was isolated from whole cell lysates. PrimPol was detected by FLAG antibody and alpha tubulin was used as a loading control. Unsync indicates the sample isolated from asynchronous cells.

levels in synchronized cells. We synchronized cells with nocodazole and analyzed the distribution of mPrimPol $^{C/SF}$across cell cycle. It is known that nocodazole arrests cells in the G2-M stage and we observed that synchronization with nocodazole in HEK293 cells was efficient (Figure 46A). We examined the protein level of ectopically expressed PrimPol using the FLAG antibody and we noticed that PrimPol is ubiquitous in all cell cycle stages, however it seems to be accumulating the most 6 hours after mitotic arrest (Figure 46B). This time-point corresponds on cell cycle histogram to distribution of cells that are between S and G2 stage. However, this is performed on whole cell lysates and the real picture could be masked by localization or solubility. For example, we would see different distribution of PrimPol in the chromatin fraction.

We decided to test if there was a difference in expression of human and mouse proteins by transiently expressing each with identical tags in HEK293 cells. Interestingly, human

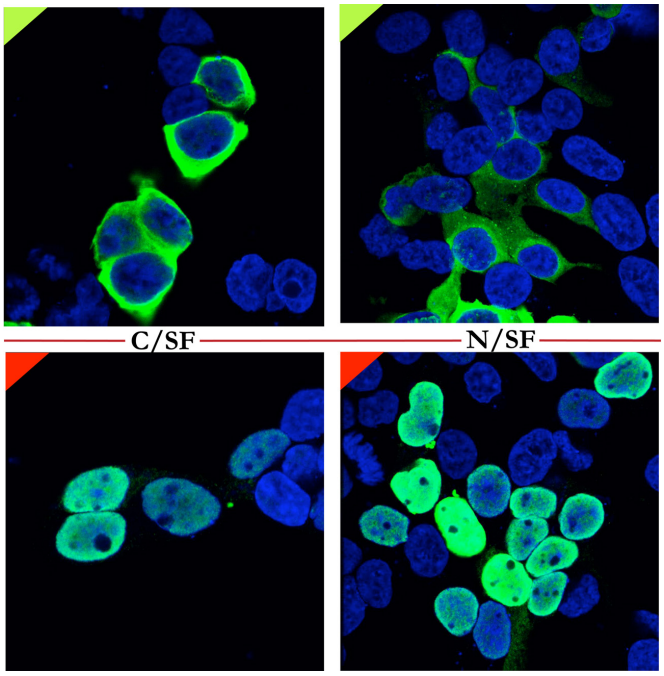

Figure 47. Localization of ectopically expressed human and mouse isoform PrimPol in HEK293

IF detection of Strep-FLAG tagged, N or C terminus fused, mouse and human PrimPol in cultured human cells. HEK293 cells were transiently transfected by PEI. Cells over-expressing mPrimPol^{SF} and hPrimPol^{SF} were subjected to IF analysis with anti-FLAG antibody (green). Following IF staining cells were stained with DAPI to label the nuclei (blue). C/SF stands for Strep-FLAG tag fused to C terminus of *PrimPol* gene, N/SF stands for Strep-FLAG tag fused to N terminus of *PrimPol* gene. A green corner labels images taken from human PrimPol expressing cells, and a red corner labels images taken from mouse PrimPol expressing cells. Images were taken by 60x objective of confocal microscope and processed in the ImageJ program.

PrimPol was present primarily in the cytoplasm and mouse PrimPol was mostly expressed mainly in nuclei with a very small portion in the cytoplasm (Figure 47). We also checked if the position of the Strep-FLAG tag had an effect on the localization of protein, but both N and C fused tags showed the same pattern of expression.

As HEK293 cells have little cytoplasm for IF studies, we decided to test different cell lines where nuclear and cytoplasmic compartments were equally represented. U2OS cells are flatter and more adherent so transiently expressed mouse and human PrimPol^{SF} in this cell line. Again we saw a striking difference in the localization pattern. Mouse PrimPol was almost entirely nuclear while human PrimPol was cytoplasmic. In this experiment we counterstained cells with the DNA intercalating dye DAPI and the mitochondrion-specific dye MitoTracker, to visualize nuclei and mitochondria respectively. We then subjected the

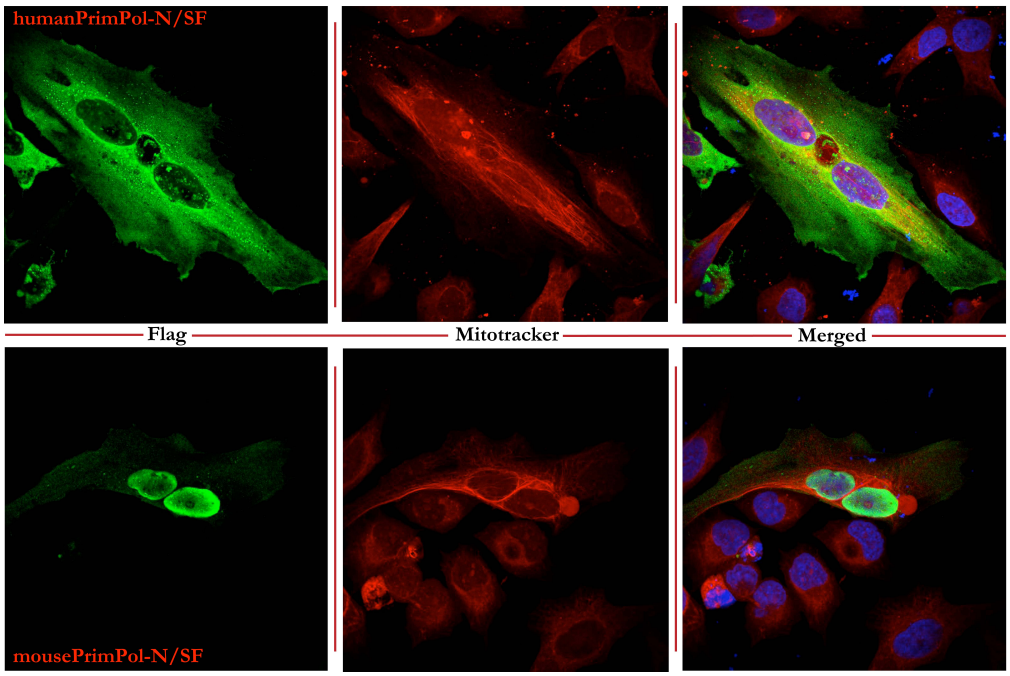

Figure 48. Localization of mouse and human isoform of PrimPol in U2OS cells

IF detection of Strep-FLAG tagged mouse and human isoform PrimPol (mPrimPol$^{N/SF}$, hPrimPol$^{N/SF}$) in cultured human cells. U2OS cells were transiently transfected by PEI. Cells over-expressing mPrimPol$^{N/SF}$ and hPrimPol$^{N/SF}$ were subjected to IF analysis with anti-FLAG antibody (green). Prior to fixation, cells were incubated with MitoTracker Deep Red to stain mitochondria (red) and following IF staining cells were stained with DAPI to label the nuclei (blue). N/SF stands for the Strep-FLAG tag fused to N terminus of *PrimPol* gene. Image was taken with the 40x objective of a confocal microscope and processed in ImageJ program.

cells to immunofluoresence analysis using an anti-FLAG antibody. In U2OS cells it was obvious that human PrimPol was colocalising with mitochondria, yet the colocalisation was not complete, with ample cytoplasmic immunofluoresence visible outside of mitochondrial network that could be due to the high levels of overexpression (Figure 48). When we aligned the sequences of human and mouse PrimPol we noticed that mouse PrimPol has a predicted nuclear localization sequence or NLS (Figure 49). This sequence is also present in Pol η and Pol ι (Kannouche et al. 2003) where it is required for efficient localization into the nucleus and foci formation upon UV damage.

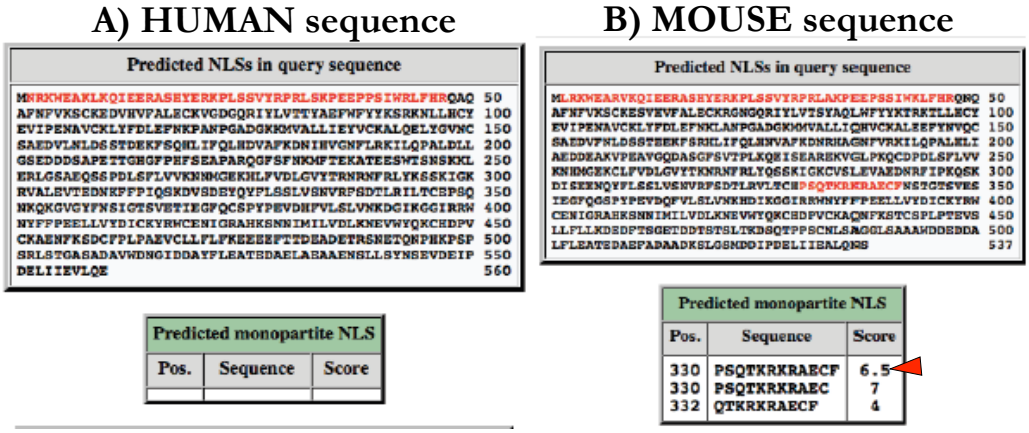

Figure 49. Prediction of nuclear localization sequence (NLS) in mouse and human PrimPol orthologs

A) Human PrimPol sequence has no predicted NLS. B) Mouse PrimPol sequence with identified residues that can be with high probability part of nuclear localization sequence. Prediction of NLS was done by cNLS Mapper software (http://nls-mapper.iab.keio.ac.jp/cgi-bin/NLS_Mapper_form.cgi).

We did not continue further with the analysis of domains regulating subcellular localization but the differences observed suggest that human and mouse PrimPol may be regulated in different ways. Consistent with this, our collaborators have identified putative Cdk phosphorylation sites in human PrimPol that are not present in the mouse protein sequence (Aidan Doherty, unpublished). This could explain the distinct localization pattern and regulation of human and mouse PrimPol orthologs. Another possibility is that mitochondrial localization is achieved by a species-specific interacting proteins as we could not identify a canonical mitochondrial targeting signal in human or mouse PrimPol.

2.3. PrimPol re-localization upon DNA damage

PrimPol is distributed in the nuclei, mitochondria and cytoplasm. The presence of a putative NLS suggests that this enzyme is recruited by certain signals to the nucleus and maybe also to the mitochondria. We tested to determine if DNA damage led to the accumulation or relocalization of PrimPol to any subcellular compartments or structures.

➢ PrimPol assembles into foci in UV-C irradiated cells

HEK293 cells stably expressing PrimPol$^{C/SF}$ were damaged by 10J/m^2 of UVC and after 2, 8 and 24 hours of recovery from the damage cells were fixed, stained and analyzed by IF. In the first set of experiments, we noticed that 20 hours following UVC damage PrimPol accumulated in nuclear foci (data not shown). We did not notice the appearance of PrimPol foci at earlier time-points. At UV-stalled replication forks, uncoupling of helicases and the replicative DNA polymerase results in long tracts of single stranded DNA coated

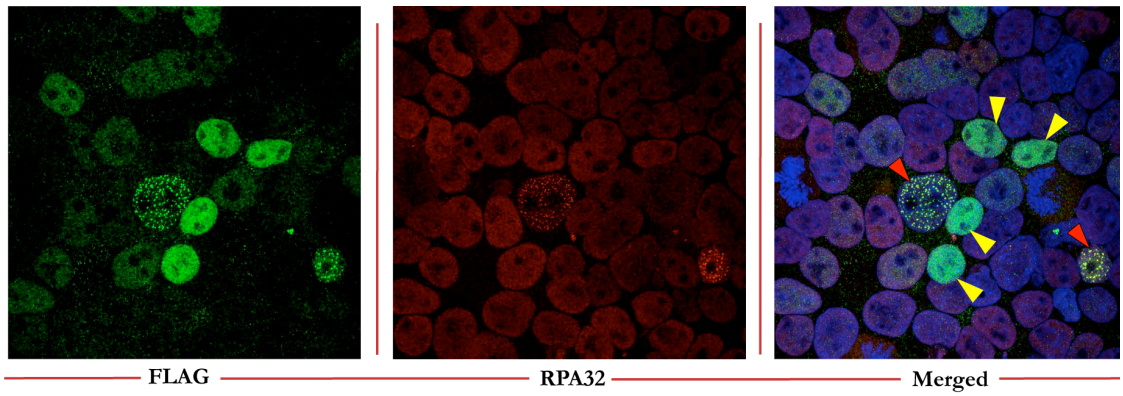

Figure 50. PrimPol and RPA co-localization in foci upon UVC irradiation

IF detection of Strep-FLAG tagged mouse PrimPol (mPrimPol$^{C/SF}$) in cultured human cells. HEK293 cells were infected by retrovirus and selected for clones stably expressing mPrimPol$^{C/SF}$. C/SF stands for Strep-FLAG tag fused to the C terminus of the *PrimPol* gene. Cells were damaged with 10J/m^2 UVC and left to recover for 24 hours. Cells over-expressing mPrimPol$^{C/SF}$ were subjected to IF analysis with anti-FLAG antibody (green) and RPA32 (red). Following IF staining cells were stained with DAPI to label the nuclei (blue). The red arrowheads point to cells with PrimPol/RPA foci. Yellow arrowheads point to cells that look like they just divided and with PrimPol staining distributed all over nucleus. Image was taken with the 60x objective of a confocal microscope and processed in ImageJ.

with RPA, which can trigger TLS repair (Lehmann 2005). To test if PrimPol co-localizes with RPA foci we have performed staining of HEK293 cells, damaged with 10J/m^2 of UVC and left to recover for 24 hours. Following exposure to 10 J/m2 UVC radiation, 24 hours later PrimPol was visible as multiple tiny bright spots within (as we estimated) ~5 % of nuclei (Figure 50). PrimPol was co-localizing in these spots with RPA32 suggesting that PrimPol accumulates at stalled forks. To further test if foci positive for RPA32-PrimPol are chromatin bound, we have tried several *in situ* pre-extractions using either Triton X-100 or modified protocol for chromatin extraction described by Kannouche at. (Kannouche et al. 2004). Unfortunately, in HEK293 cells treated with detergent, it was almost impossible to perform IF due to detachment of cells.

We repeatedly observed cells with PrimPol distributed all over the nucleus and without clear foci formation of RPA32 staining. These cells looked like they just divided and probably FLAG staining observed in those cells was not due to UV induced damage but for some other reason. This will be addressed in future studies of cellular functions of PrimPol. We conclude that PrimPol is recruited to UV damaged sites and in future studies we will analyze if this recruitment is replication dependent.

➢ PrimPol assembles into foci in cells damaged by ionizing radiation

We have also explored other damaging treatments in order to find out if PrimPol foci are UV damage specific. Ionizing radiation is a potent inducer of double and single strand breaks. Phosphorylation of H2AX at ser139 (termed γH2AX) is an indicator of double strand breaks occurring during DNA damage but also of replication stress and fork stalling (Rogakou et al. 1998; Limoli et al. 2002). We have analyzed the response to ionizing radiation of HEK293 cells stably over-expressing PrimPol$^{C/SF}$. We subjected the cells to 5Gy of X-irradiation and left them to recover for 2, 8 or 24 hours. While γH2AX foci were visible immediately after 2 hours and persisted in irradiated cells 20 hours later, PrimPol was visible only after 24 hours. Curiously, PrimPol assembled into foci that perfectly co-localized with γH2AX foci (Figure 51). We concluded that besides being recruited to UV lesions, PrimPol is also recruited to persistent double strand breaks. Possibly we would see these foci at earlier time-points with pre-extraction of chromatin.

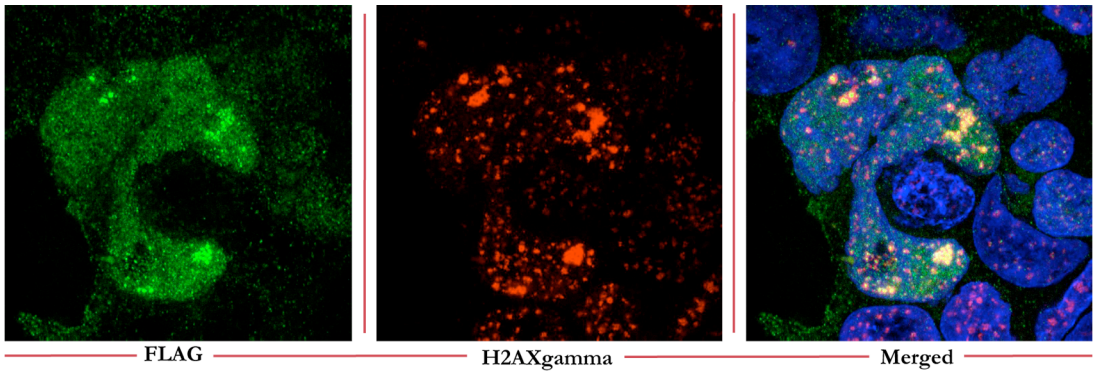

Figure 51. PrimPol and γH2AX co-localization in nuclear foci upon X-irradiation

IF detection of the Strep-FLAG tagged mouse PrimPol (mPrimPol$^{C/SF}$) in cultured human cells. HEK293 cells were infected by retrovirus and selected for clones stably expressing mPrimPol$^{C/SF}$. C/SF stands for Strep-FLAG tag fused to C terminus of *PrimPol* gene. Cells were damaged with 5 Gy of X-irradiation and left to recover for 24 hours. Cells over-expressing mPrimPol$^{C/SF}$ were subjected to IF analysis with anti-FLAG antibody (green) and H2AXγ (red). Following IF staining cells were stained with DAPI to label the nuclei (blue). The red arrowheads point to cells with PrimPol/γH2AX foci. Image was taken with the 40x objective of a confocal microscope and processed in ImageJ.

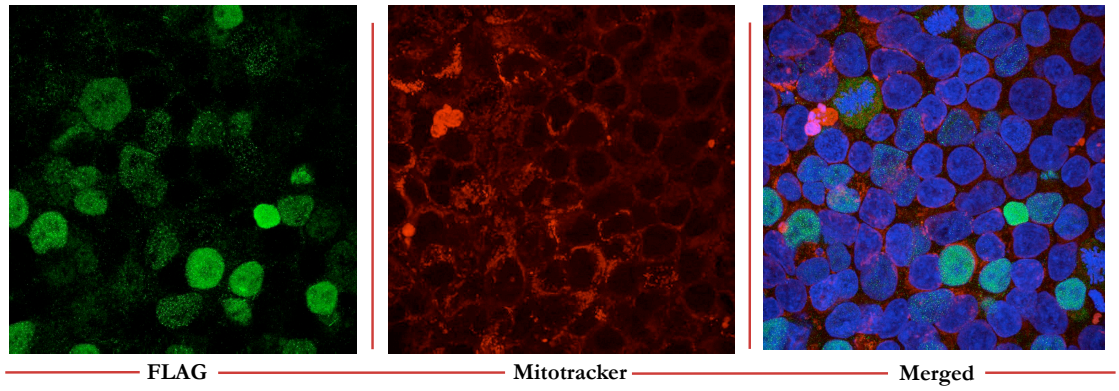

Figure 52. H_2O_2 damage does not induce PrimPol focalization

IF detection of Strep-FLAG tagged mouse PrimPol (mPrimPol$^{C/SF}$) in cultured human cells HEK293. C/SF stands for Strep-FLAG tag fused to C terminus of *PrimPol* gene. Cells were treated with 400nM of H_2O_2 for 2 hours and left to recover for 12 hours. Cells over-expressing mPrimPol$^{C/SF}$ were subjected to IF analysis with anti-FLAG antibody (green) and MitoTracker Deep Red to stain mitochondria (red) and following immunofluorescent staining cells were stained with DAPI to label the nuclei (blue). Image was taken by 60x objective of confocal microscope and processed in ImageJ program.

➢ PrimPol distribution is not altered after oxidative damage

We have tested the distribution of PrimPol in cells upon oxidative damage. H_2O_2 is known to act as signaling molecule but also depending on its concentration, it can cause oxidative damage leading to formation of stress granules in the cytosol and nucleus (Veal et al. 2007; Emara et al. 2012). H_2O_2 results in oxidative base modifications and single strand breaks (Jaruga and Dizdaroglu 1996). Cells were treated with 400nM hydrogen peroxide for 2 hours and left to recover for 12 hours (Figure 52). IF analysis of HEK293 stably expressing PrimPol$^{C/SF}$ revealed no focal accumulation of PrimPol following hydrogen peroxide treatment. This suggests that focal accumulation of PrimPol only occurs following the generation of specific DNA lesions that may cause stalling of replication forks, such as those caused by UV-C and X-irradiation.

2.4. UV regulation of PrimPol expression

In order to determine whether PrimPol is regulated by the UV response, we examined PrimPol mRNA and protein levels after treatment. For Pol η, it was shown previously in murine cells that there is no time or dose correlation at the protein or RNA level with UV damage (Skoneczna et al. 2007). We analyzed the expression levels of both PrimPol and Pol η in exponentially growing MEFs damaged with different doses of UVC. RNA was isolated from these cells 6 hours after UVC exposure. Interestingly at the RNA level, PrimPol expression levels dropped linearly with applied UVC dose (Figure 53).

In contrast, Pol η did not have a definable expression pattern that could be correlated with the applied dose. This data pointed out that PrimPol and Pol η are potentially regulated in a different spatial and temporal manner by the UV damage pathway consistent with our data suggesting that they act in independent pathways. At the protein level we analyzed PrimPol distribution after different UV doses and checked whether PrimPol's association with chromatin was altered. For this purpose we fractionated cells stably over-expressing mPrimPol$^{C/SF}$. The levels of PrimPol were analyzed using the FLAG antibody.

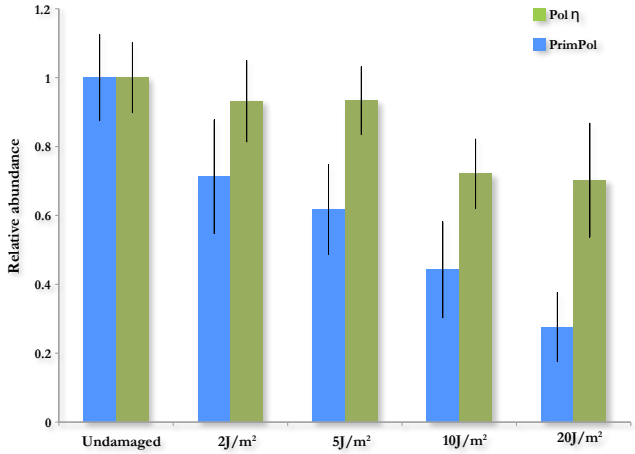

Figure 53. PrimPol and Pol η mRNA expression upon UVC irradiation

PrimPol and Pol η mRNA levels after UVC induced damage. Exponentially growing wild type MEFs were damaged in early passage with assigned doses of UVC. 6 hours later RNA was isolated and expression of PrimPol and Pol η was quantified by qPCR using the ΔCt method. Normalization was done to undamaged samples and as reference we used two housekeeping genes: Gapdh and beta Actin. Result from one experiments performed in triplicates is shown. Error bars denote standard deviation mean.

Cells were unsynchronized and the levels of protein were observed for 30J/m^2 and 90J/m^2 UVC damaged cells and compared to the undamaged. We have used as control HEK293 cells stably over-expressing Myc$^{C/SF}$(Figure 54).

Interestingly we noticed that more PrimPol was in the chromatin fraction than in the soluble nuclear fraction in undamaged cells. This ratio stayed the same in cells damaged by 30J/m^2 UVC. Surprisingly, the chromatin fraction did not get enriched as we expected after UV damage and at 90J/m^2 UVC damage there was less PrimPol in the chromatin fraction (Figure 54). The only thing we could conclude from this result is that PrimPol associates with chromatin. In future experiments we will address the effect of lower UV doses on PrimPol distribution and how the protein levels are changing over the time after induced damage. We will test the same in synchronized cells in order to examine in which stage of the cell cycle is PrimPol enriched.

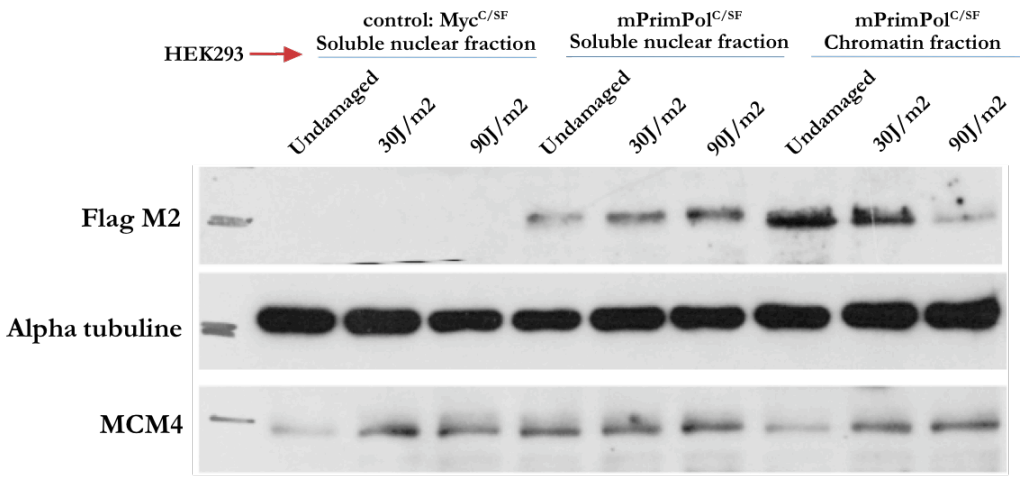

Figure 54. PrimPol protein levels upon UVC irradiation

Over-expressed PrimPol is enriched in chromatin fraction. Unsynchronized HEK293 cells stably over-expressing mPrimPol$^{C/SF}$ or Myc$^{C/SF}$ were assayed for protein expression. Equal amounts of soluble nuclear and chromatin fractions were resolved by 8% SDS-PAGE. Cells were either undamaged or damaged with 30 or 90J/m2 of UVC and 1 hour later protein was isolated. mPrimPol$^{C/SF}$ was detected by FLAG antibody, anti-Alpha tubulin and anti-MCM4 were used as loading control.

2.5. Identification of mouse PrimPol interaction partners

As our data indicated that PrimPol functioned in a potentially new pathway to respond to UV and replicative lesions, we aimed to identify interacting proteins that may shed light on its functions. The principal strategy we employed was to affinity purify mouse PrimPol isoform stably expressing HEK293 cells and to analyze purifications by mass spectrometry. We have used a protocol for tandem affinity purification of proteins tagged with Strep-FLAG allowing single or double tag purification of native proteins (Gloeckner et al. 2009; Gloeckner et al. 2009). Since PrimPol is ectopically expressed at very low levels, we could not use tandem affinity purification because the amount of protein that we isolated was not sufficient for mass spectrometry analysis. We used a single purification using the Strep tag, which has the advantage of the high affinity and specific binding between streptavidin and its natural ligand biotin. Precisely, Strep-Tag II (WSHPQFEK) was used, which allows

affinity purification with the streptavidin derivative Strep-Tactin and elution with desthiobiotin.

As we knew from experiments we performed, and those from the laboratory of our collaborator Aidan Doherty, that PrimPol resides in both the nucleus and mitochondria, our first attempt to purify interacting protein complexes was from whole cell extracts. We started with approximately 50mg of protein to get to 100ug in the final purification step. This amount of protein was resolved on 8% SDS- polyacrylamide gel and silver stained. The difference between bands in control sample and mPrimPol$^{C/SF}$ was not clear, as we had many background bands with the Strep beads alone. Nevertheless we obtained slight

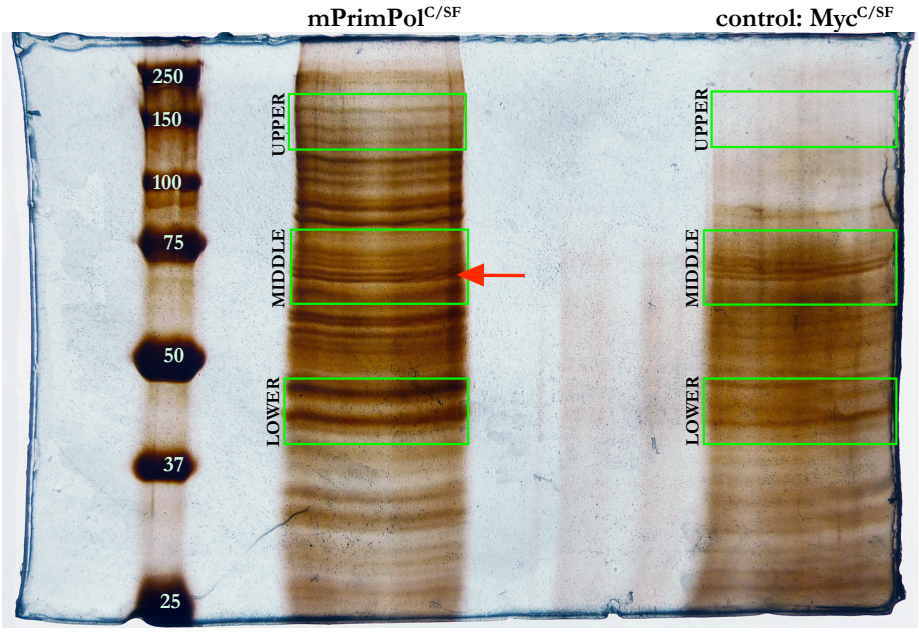

Figure 55. Affinity purification of stably over-expressed Strep-FLAG tagged mPrimPol from whole cell lysate.

mPrimPol$^{C/SF}$ was affinity purified using Strep-Tactin resin from HEK293 cells. Elutions from mPrimPol$^{C/SF}$ and control Myc$^{C/SF}$ were run on 8% SDS-PAGE and silver stained afterwards. Each lane was sliced in 3 squares, labeled in green, that were analyzed separately by mass spectrometry. In the middle square, labeled by red arrow should be band representing PrimPol with the size of 64kDa. On the far left is the protein ladder.

enrichment of the band that was likely PrimPol and we decided to analyze this purification product by mass spectrometry (MS). Both gel lanes, for control and PrimPol sample, were

sliced into 3 equal squares with the middle square corresponding to the area where the PrimPol band should be (Figure 55) and samples were analyzed by The Mass Spectrometry Core Facility at IRB.

Our second attempt to purify potential PrimPol-interaction molecules was modified in two steps. As we had evidence that PrimPol could be involved in UV induced DNA damage tolerance we decided to pull down and compare native protein complexes with mPrimPol$^{C/SF}$ purified from cells that were undamaged or damaged with 30J/m^2 of UVC. In addition to the damage we also applied fractionation and used only the nuclear fraction hoping that we will get more specific hits by MS analysis. The final amount of 170ug of purified protein was not separated by SDS-PAGE but it was submitted in 100ul of elution buffer for liquid chromatography separation and analysis.

A database search was performed with Proteome Discoverer software v1.3 (Thermo) using Sequest search engine and SwissProt database (Human, release 2012_08). Searches were run against targeted and decoy databases to determine the false discovery rate (FDR). Search parameters included trypsin enzyme specificity, allowing for two missed cleavage sites, carbamidomethyl in cysteine as static modification and methionine oxidation as dynamic modifications. Peptide mass tolerance was 10 ppm and the MS/MS tolerance was 0.8 Da. Peptides with a q-value lower than 0.1 and a FDR < 1% were considered as positive identifications with a high confidence level.

➢ Potential PrimPol interacting proteins identified by LC-MS/MS

In both approaches, a large set of proteins was identified. Unfortunately we did not observe large differences between samples that were UVC damaged or undamaged. However, we obtained many distinct hits in the undamaged samples. We have combined the hits we obtained from the first and second experiments and we ended up with the list of 36 putative interactors. The criteria used to select potential interactors was identification of the protein in more than one experiment, the absence of the protein in the control samples and in an additional category, we also included proteins that were substantially

Protein ID	Gene Symbol and description
P33991	DNA replication licensing factor MCM4
Q92499	ATP-dependent RNA helicase DDX1
O75821	Eukaryotic translation initiation factor 3 subunit G EIF3G
Q13263-2	Isoform 2 of Transcription intermediary factor 1-beta TRIM28
P49321	Nuclear autoantigenic sperm protein NASP
Q14566	DNA replication licensing factor MCM6
Q14683	Structural maintenance of chromosomes protein 1A SMC1A
P56192	Methionine--tRNA ligase, cytoplasmic MARS
O75534-2	Isoform Short of Cold shock domain-containing protein E1 CSDE1
Q92973-3	Isoform 3 of Transportin-1 TNPO1
P61081	NEDD8-conjugating enzyme Ubc12 UBE2M
P62191	26S protease regulatory subunit 4 PSMC1
Q9Y5L4	Mitochondrial import inner membrane translocase subunit Tim13 TIMM13
P42167	Lamina-associated polypeptide 2, isoforms beta/gamma TMPO
P40939	Trifunctional enzyme subunit alpha, mitochondrial HADHA
Q9BUJ2-3	Isoform 3 of Heterogeneous nuclear ribonucleoprotein U-like protein HNRNPUL1
Q02790	Peptidyl-prolyl cis-trans isomerase FKBP4
Q00610-2	Isoform 2 of Clathrin heavy chain 1 CLTC
Q5T8P6-5	Isoform 5 of RNA-binding protein 26 RBM26 -
P54136-2	Isoform Monomeric of Arginine--tRNA ligase, cytoplasmic RARS
P55265-5	Isoform 5 of Double-stranded RNA-specific adenosine deaminase ADAR -
Q13148	TAR DNA-binding protein 43 TARDBP
P34897-3	Isoform 3 of Serine hydroxymethyltransferase, mitochondrial SHMT2
O75937	DnaJ homolog subfamily C member 8 DNAJC8
Q09028-4	Isoform 4 of Histone-binding protein RBBP4
P25440	Bromodomain-containing protein 2 BRD2
Q15181	Inorganic pyrophosphatase PPA1
P55060-2	Isoform 2 of Exportin-2 OS= CSE1L -
P00441	Superoxide dismutase [Cu-Zn] SOD1
Q15424	Scaffold attachment factor B1 SAFB
P06454-2	Isoform 2 of Prothymosin alpha PTMA
P53396-2	Isoform 2 of ATP-citrate synthase ACLY
Q8IY67-3	Isoform 3 of Ribonucleoprotein PTB-binding 1 RAVER1
O75369-5	Isoform 5 of Filamin-B FLNB
P68400-2	Isoform 2 of Casein kinase II subunit alpha GN=CSNK2A1 -

Table 14. The putative interactors of PrimPol

In the list are only MS hits that we have observed in both Strep-purification experiments.

enriched in PrimPol purifications but still present at some low percentage in control samples. The control samples were HEK293 cells stably expressing $Myc^{C/FS}$.

Two of the predominant groups identified were nuclear and mitochondrial proteins, which was expected considering the dual localization of PrimPol. It was interesting to find that several mitochondrial proteins that came down are those present in mitochondrial nucleoids, where transcription and DNA replication take place. Notable mitochondrial (Mt) proteins present in PrimPol purifications are LONP1 (targeting specific regulatory Mt proteins for degradation), TUFM (involved in translation of mitochondrial proteins) and LRPPRC (stabilizing Mt mRNA and coordinating mitochondrial translation). Additionally we also pulled down a number of mitochondrial and nuclear importins and exportins, which could explain how PrimPol is traveling in and out of these two compartments.

A large proportion of DNA and nucleotide binding proteins were also present, particularly proteins involved in the regulation of cell cycle, DNA replication and also in DNA damage repair in nucleus (MCM2-6 family, SMC1-2, KAP1, Cullin4a, DDB1, TFII, RPA, PARP1). The list of the most enriched proteins identified is summarized in the Table 14.

➢ Validation of PrimPol interacting proteins

To validate potential PrimPol interacting proteins from the preliminary MS analysis, small-scale affinity purifications of Strep-tagged PrimPol from whole cell lysate were performed and analysed by Western blot. We were especially interested in MCM helicase family and RPA because these are key proteins present at replication forks during replication and DNA damage repair. Confirming an interaction with MCM and RPA would suggest that

PrimPol operates together with or in the vicinity of replication forks. We have confirmed the interaction with RPA in several experiments (Figure 56). From the MCM family we have tested for an interaction with the MCM4 subunit of the helicase complex because that antibody was available in the lab. From 5 repeated experiments MCM4 co-purified 3 times with PrimPol and 2 times we did not detect any band corresponding to MCM4 in the co-immunoprecipitated fraction. We have tried UVC damage of the cells in order to test if we will see stronger interaction. The same amount of RPA and MCM4 was purified from undamaged and UVC damaged cells (Figure 56).

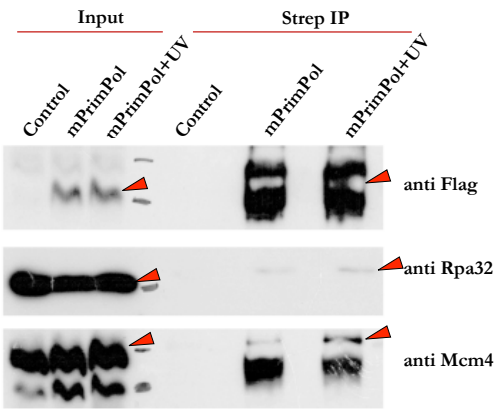

Figure 56. mPrimPol co-purifies with RPA and MCM4

Validating mass spectrometry hits –mPrimPol co-purifies with RPA and MCM4. HEK293 cell generated to stably express mPrimPol$^{C/SF}$ were affinity purified from whole cell lysate using Strep-Tactin resin. Fractions were analyzed by Western blot with the antibodies indicated. Samples were either untreated or UVC (30J/m^2) damaged.

Additional hits of interest included PARP1 and Ku70 that looked like promising targets given their important functions in DNA repair but they did not give specific bands and co-purified in equal amounts in control and PrimPol over-expressed sample (Figure 57). In addition, proteins that were not identified in the mass-spectrometry analysis but were likely candidates for interaction, such as the mtSSB (the mitochondrial ssDNA binding protein analogous to RPA) or EXDL2 (a protein that was shown to colocalize in mitochondria) were probed in Westerns. Co-elution was observed for mtSSB (Figure 58) but not for other mitochondrial protein EXDL2 (data not shown).

Although the preliminary hits obtained from the mass-spectrometry were many, the small-scale purifications have validated some of them as proteins that co-purify with PrimPol, such as the single-stranded DNA binding proteins RPA and mtSSB. It remains to be determined whether these interactions are protein-protein or DNA-mediated.

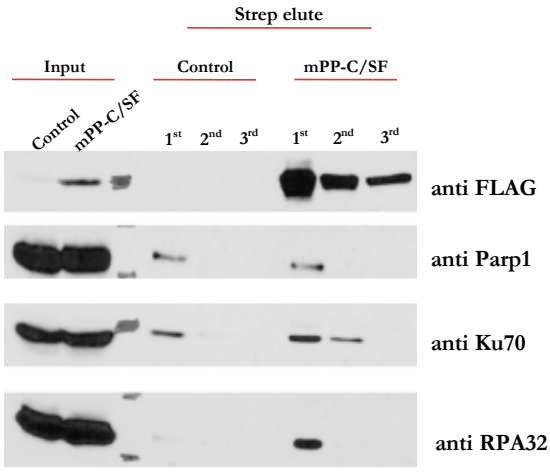

Figure 57. Validating additional mass spectrometry hits

mPrimPol co-purifies with RPA but not with Parp1 and Ku70. HEK293 cell generated to stably express mPrimPol$^{C/SF}$ were affinity purified from whole cell lysate using Strep-Tactin resin. Fractions were analyzed by Western blot with the antibodies indicated. Three subsequent elutions of Strep-Tactin resin were tested for the presence of mPrimPol$^{C/SF}$ and the potential interactors.

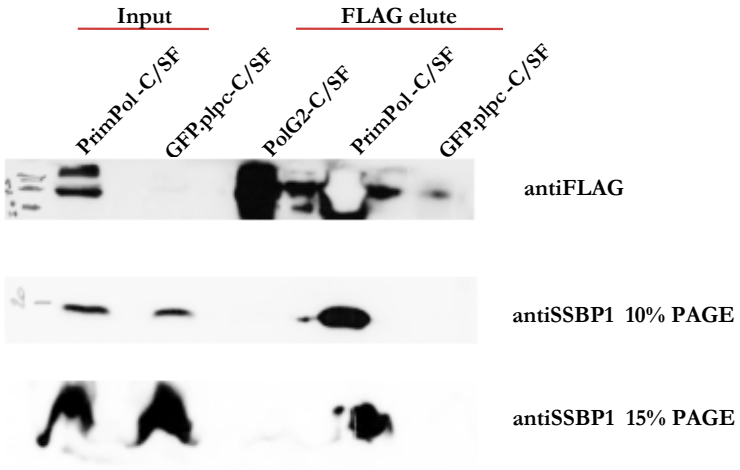

Figure 58. mPrimPol co-purifies with mtSSBP

HEK293 cells, transiently transfected with mPrimPol$^{C/SF}$ were affinity purified from whole cell lysate using FLAG –M2 agarose beads. Fractions were analyzed by Western blot with the anti-mtSSB antibody. Two different concentrations of SDS-PAGE were used, 10% and 15% because mtSSB runs low with the expected size around 17kDa.

3. PrimPol is required for mitochondrial homeostasis

Considering the localization of PrimPol to the mitochondria, we were interested to determine the function of this enzyme in the mitochondrial compartment. In the previous section, I discussed several interesting putative interacting proteins obtained by proteomics analysis, such as the mitochondrial nucleoid core components LRPPRC, LONP1 and TFUM. Additionally we have pulled down TIM13, a protein responsible for chaperone-mediated import of nuclear proteins into the mitochondrial matrix (Chacinska et al. 2002) and several proteins important for the TCA cycle (CS, IDH1, ACLY).

To determine if cells depleted for PrimPol exhibited abnormal transcriptional signatures that could be indicative of mitochondrial stress, we analyzed gene expression in cells depleted of human PrimPol. As cells from knock-out mice were not yet available, we

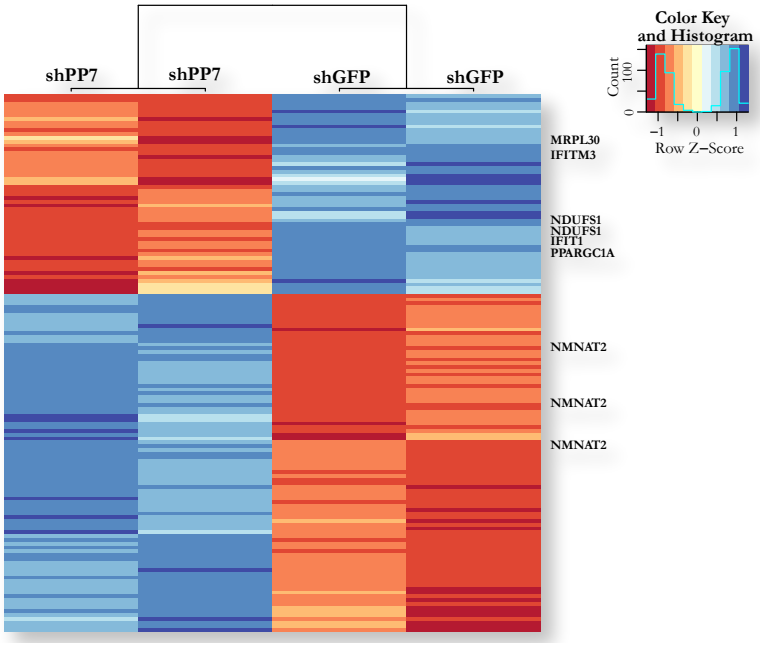

Figure 59. Differential expression of genes upon downregulation of PrimPol in HEK293

Hierarchical clustering of differential expression of genes obtained by microarrays in HEK293 cell line downregulated for PrimPol (shPP7) or shGFP. Only genes with fold change higher than 2.5 and with false discovery rates lower than 0.05 were selected for the heatmap. Each row represents one gene and each column one cell line.Varying levels of expression are represented on a scale from dark orange (lowest PrimPol expressionexpression) to dark blue (highest expression). Genes of interest are annotated on the right side.

transduced HEK293 cells with lentiviruses expressing shRNA (shPP7) to target PrimPol and selected for infected cells. PrimPol expression levels were restored to normal levels after only 4-5 passages so we performed the analysis at early passage after the introduction of the shRNA bearing lentiviruses. RNA samples were sent to the Functional Genomics Core Facility at IRB Barcelona for mRNA profiling by Affymetrix expression arrays. The expression level changes after depletion of PrimPol are shown in Figure 59 and some interesting targets that were significantly altered in expression are selected and summarized in Table 15. Our analysis indicated that several downregulated genes are important for mitochondrial biogenesis (*PGC1-α, NDUFS1, MRLP30*). Interestingly most of the genes that were upregulated are involved in signaling in neuronal and endocrine cells

Upregulated mRNAs of PrimPol knock-downs in HEK293	
Gene Symbol	Fold Change (KD vs. WT)
SCG3	15.8573
CHGB	10.0437
NMNAT2	9.2317
CGA	8.3894
SNAP25	6.0412
CHGA	4.8470
INSM2	4.5591
SYP	3.8535
GABBR2	3.5219

Downregulated mRNAs of PrimPol knock-downs in HEK293	
Gene Symbol	Fold Change (KD vs. WT)
LAMA4	-4.1464
MAML2	-4.1461
IFIT1	-4.3960
NDUFS1	-2.9812
IFITM2	-2.8974
MRPL30	-2.7682
HLA-DPA1	-2.6377
PPARGC1A	-2.5976
IFITM3	-2.5028

Table 15. The list of up- or down-regulated genes in shPP7 cell line

Transcriptomic changes after PrimPol depletion by shRNA (shPP7) in HEK293 cell line.

Of several shRNAs we validate for PrimPol, we chose shPP7 for microarrays because it was the most efficient in downregulating PrimPol. However, for further phenotypic characterization of PrimPol deficient cell lines, we used an additional shRNA, shPP5, and HEK293 infected by shRNA against GFP as a negative control (the latter was also used in the array analysis). Both lines showed no protein expressed (Figure 60) and low levels of PrimPol expression (Figure 61, first row).

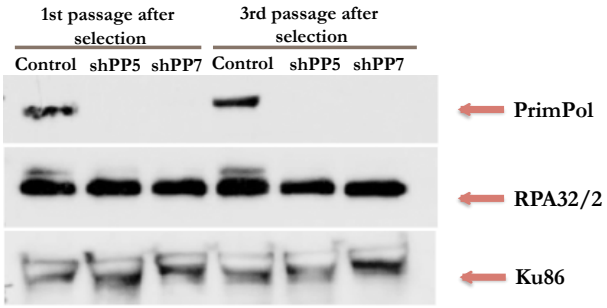

Figure 60. Validation of the efficiency of PrimPol shRNA downregulation by WB

Expression of PrimPol in HEK293 cell line upon lentiviral infection with shPP5 and shPP7 and selection. shPP5 and shPP7 are two different shRNAs against human isoform of PrimPol. Downregulation at the protein level was validated in several passages after puromicin selection.

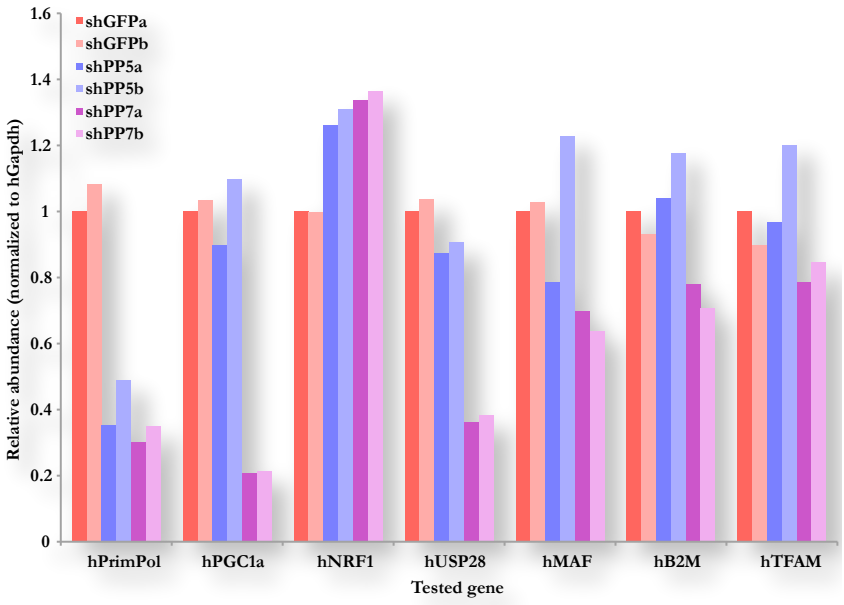

Figure 61. Validation of microarray selected targets by small scale qPCR

Control cell line was produced by shRNA against GFP and experimental lines with shRNA against human isoform PrimPol were shPP5 and shPP7. Results represent two experiments done in triplicates. qPCR was done on cDNA, quantified by the ΔCt method and all values are normalized to house keeping gene Gapdh.

First we attempted to validate some of the expression changes seen in the microarray. We examined the expression of PGC1α, TFAM, NRF1, hMAF and USP28 using real time PCR in the 2 shRNA lines and the control (Figure 61). We did not observe a consistent phenotype between the shRNA lines depleted for PrimPol, despite similar levels of PrimPol depletion, suggesting that the changes could be due to off target effects.

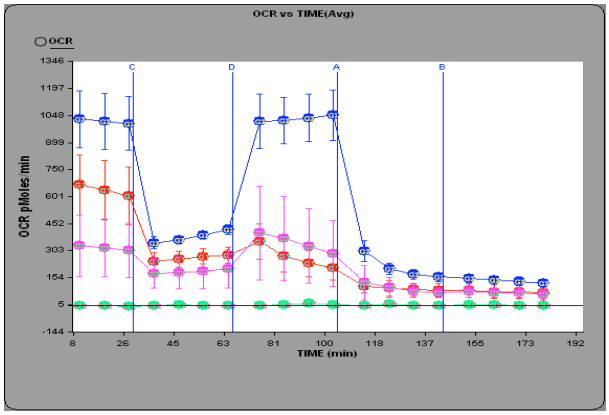

Figure 62. Oxygen consumption rate in hPrimPol downregulated cell lines

The rate of oxygen consumption (OCR) as a rate of mitochondrial respiration measured by Seahorse analyzer. Blue-shPP5, purple- shPP7, red – shGFP, green – temperature control.

Defects in mitochondrial homeostasis are often evident due to differences in oxygen metabolism. We analyzed oxygen consumption rates (OCR) in the two shPP cell lines compared to wild type using the Seahorse bioanalyzer. This instrument can sensitively determine changes in oxygen consumption that can be indicative of mitochondrial funtion. We again observed disparity between the shRNA lines as the shPP7 cell line behaved like the control shGFP cell line, while shPP5 had significantly altered oxygen consumption rates (Figure 62). At this point, we decided that the shRNA approach had too many caveats as we could not distinguish which of the observed phenotypes were the result of off target effects, and these experiments were put on hold.

From the information obtained in HEK293, we tentatively concluded that PrimPol depletion may affect mitochondrial biogenesis. To test this hypothesis in a more reliable system, we analyzed the mitochondrial copy number levels in primary mouse fibroblasts and in different organs from mice lacking PrimPol. In passage 2 primary MEFs we observed mitochondrial copy numbers that were on average 20% higher in KO compared to WT fibroblasts (Figure 63A). In the organs of 6 month old PrimPol deficient mice, we also saw that mitochondrial copy number is upregulated in the heart, liver and intestine, but

not in the brain (Figure 63B). When we analyzed mitochondrial copy number in the organs of 5 week old mice that were irradiated with UVB for 5 consecutive days (described in section 1.3.) we observed that tissues of PrimPol KO mice that were exposed to UV damage have markedly elevated mtDNA copy number (Figure 63C). We concluded from this that PrimPol influences the maintenance of mitochondrial DNA.

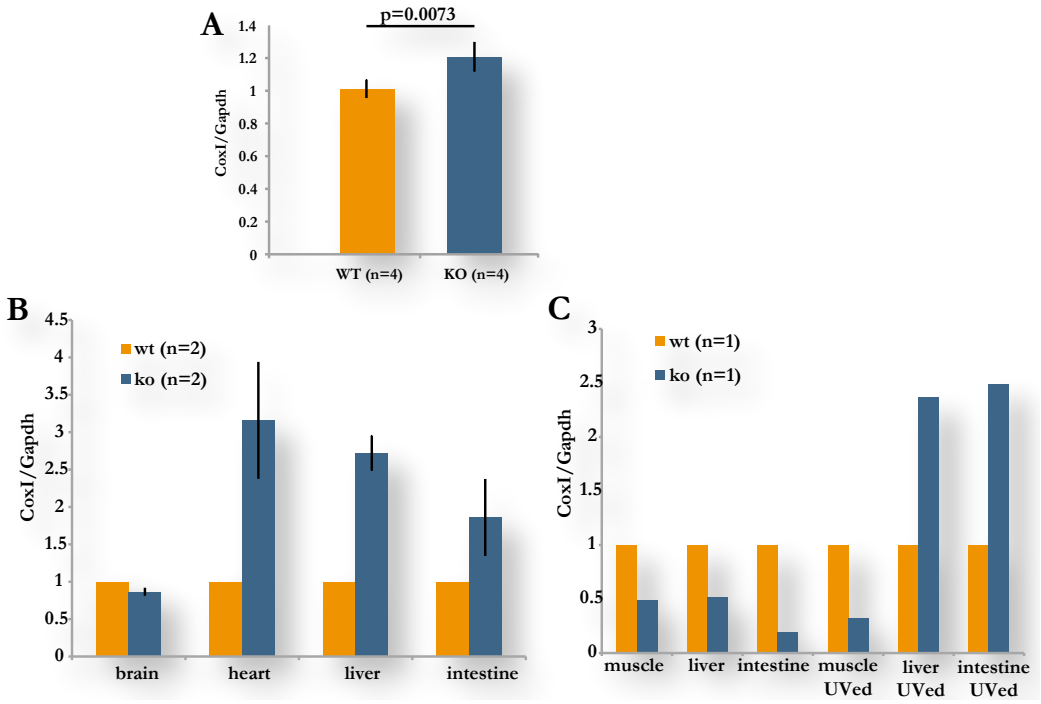

Figure 63. Analysis of mitochondrial DNA copy number by qPCR

Analyzis of mDNA copy number was done on genomic DNA and quantified by ΔCt method. A) From exponentially growing MEFs mtDNA, error bars denote standard deviation mean. Statistical significance was determined by T-test ($p<0.01$). B) From annotated tissues isolated from 6 months old mice. C) From undamaged and UVB damaged tissues from 5 weeks old animals.

Discussion

1. Introduction

The main focus of this dissertation was the characterization of the eukaryotic primase-polymerase *PrimPol* (official symbol: *Ccdc111*). When the project was started, no reports were published regarding the function of this protein, only the *in silico* analysis by Iyer and colleagues (2005) in which they classified this protein as a putative member of the AEP superfamily. The groundwork of biochemical characterization was initiated in the laboratories of our collaborators Aidan Doherty (Sussex University, Brighton) and Luis Blanco (CBMSO, Madrid). They have identified that PrimPol is capable of de novo DNA-dependent DNA/RNA primase and DNA-dependent DNA/RNA polymerase activities *in vitro* (manuscripts under revision). Due to its biochemical primase and polymerase activities, this enzyme was renamed PrimPol. Using a variety of approaches, I have attempted to characterized the functions of PrimPol and determine the consequences of its absence in a mouse model and cultured primary and transformed cells. The data I have collected are consistent with PrimPol being required for the tolerance of naturally occurring DNA damage, such as UV or oxidative lesions, rather than for the initiation of DNA replication or DNA repair. Everything considered, the work I have presented describes a novel role for an eukaryotic AEP.

1.1. PrimPol is a novel translesion polymerase in the response to UV

PrimPol has two conserved domains. It is predicted that the domain closer to N-terminus is an AEP catalytic domain that provides PrimPol the function of nucleotidyl transferase and is required for DNA binding. The second conserved domain is closer to the C-terminus and is homologous to the UL52 domain from the herpesvirus family. It is required for primase activity and as well DNA binding. Based on the domain configuration of PrimPol we have hypothesized that PrimPol is involved in DNA metabolism that would take place in the nucleus and mitochondria. By means of immunofluorescence as well as fractionation that was performed in the Doherty lab, we have confirmed that PrimPol is present in both compartments. Furthermore, PrimPol localizes to foci upon UV damage where it colocalizes with RPA32, a marker of ssDNA. The observation that PrimPol is recruited to the sites of damage provided one of the first insights into possible function of PrimPol and it suggested that PrimPol is involved in DNA damage response to UV.

Consistent with this, we have observed persistent damage in the skin of animals deficient for PrimPol after UV damage. Additionally, PrimPol expression was observed to be highest in UV sensitive organs such as the skin and eyes. All together, our results led us to the conclusion that PrimPol is a candidate gene involved in DNA damage response provoked by UV.

UV damage leads to pyrimidine dimers that distort the DNA helix and impede replication and transcription, resulting in cell death and enhanced mutagenesis (Lehmann 2000; Latonen and Laiho 2005). UV results in the formation of 2 types of pyrimidine dimers, CPDs and 6-4PPs and cells can either repair these lesions with NER or they can bypass them using TLS polymerases. Given its enzymatic functions, we decided to investigate the possibility of PrimPol being required for lesion bypass and damage tolerance. Preliminary evidence from the Doherty group suggested that PrimPol has the unique ability to bypass 6-4PPs *in vitro*, while it could not bypass CPDs. To determine if there was any specificity to the activity of PrimPol in deficient cells from our mouse models, I employed an ELISA assay to measure particular UV induced lesions over time. In PrimPol deficient cells, we observed a notable delay in the clearance of 6-4PPs after UV induced damage. In the same cells, CPD clearance was slightly delayed but to a much lesser extent than that observed for 6-4PPs. We concluded from this, as well as *in vitro* data, that PrimPol has specific affinity for bypassing 6-4PP lesions.

While these data suggested that the main function of PrimPol was in lesion bypass of 6-4PPs, it did not rule out other potential roles and it was unclear how this would affect UV sensitivity. We used clonogenic survival assays to determine if PrimPol loss would cause increased sensitivity and reduced cell survival after UV irradiation. Surprisingly, PrimPol deficient fibroblasts were not sensitized to UV damage more than wild type cells. Knocking down Pol η, which we suspected may have redundant functions to PrimPol, rendered the PrimPol deficient fibroblasts more sensitive to UV than the knockdown of Pol η in a wild type background. This suggested that PrimPol can act as a backup TLS polymerase when Pol η is not available and importantly, that PrimPol is involved in a UV lesion bypass pathway that is non-epistatic with Pol η, consistent with its preference for 6-4PPs.

Chemical inhibition of Chk1 and ATR led to increased UV sensitivity in XP-V cells (mutant for Pol η) compared to wild type fibroblasts. After low doses of UVC, the ATR pathway was over-activated in XP-V cells, suggesting defective lesion repair. Additionally, it was established that ATR plays a crucial role by phosphorylating Pol η that is necessary for its role in postreplication repair and checkpoint control (Despras et al. 2010; Gohler et al. 2011). This work demonstrated that the ATR-Chk1 pathway directly regulated Pol η and was independently involved in stabilizing forks that were stalled by bulky UV lesions. Similar to what was observed with XP-V cells, inhibiting the ATR pathway rendered PrimPol deficient fibroblasts more sensitive to UV induced damage. We have also observed increased sensitivity in PrimPol KO lines after Chk1 inhibition and observed over-activation of the ATR-Chk1 pathway, as hyperphosphorylation of Chk1 and RPA32 were stronger and more persistent compared to WT. However, we used a much higher UV dose ($50J/m^2$) than that used with XP-V cells where this was examined after $2J/m^2$ of UVC. To make a more relevant comparison to Pol η we will address the effect of lower UV doses in future experiments. These data again are consistent with PrimPol functioning in a different pathway than Pol η and suggest that the destabilization of stalled forks may sensitize PrimPol deficient cells to UV damage.

A major factor in the stability of stalled replication forks is PARP1. Inhibition of PARP1, that is involved in mediating fork stability and restart, rendered PrimPol deficient MEFs more sensitive to low dose UV. It is noteworthy that PARP1 inhibition alone had a significant effect on the reduction of survival in cells lacking PrimPol in the absence of UV. It was shown previously that PARP1 is recruited to forks stalled by small gaps and it is required to restart stalled forks by recruiting Mre11 and promoting end resection (Bryant et al. 2009). All things considered, this could be indicative of a role for PrimPol in replication fork restart. In co-immunoprecipitation (co-IP) experiments with HEK293 cell line stably expressing $mPrimPol^{C/SF}$ we identified PARP1 in multiple experiments but it was also present in control samples, so we concluded that PARP1 is likely a contaminant as it has high affinity for nucleic acids. In future experiments we could use more stringent conditions and digest DNA or RNA that may bridge the interaction using benzonase or DNaseA. In IF experiments we observed focal accumulation of PrimPol after UV and X-irradiation and co-localization with RPA and H2AXγ. Both RPA and H2AXγ localize to stalled forks after depletion of dNTP pools by hydroxyurea (HU) (Bianchi et al. 1986).

While the importance of PrimPol for fork restart remains unclear, we could examine this in future experiments using DNA fiber analysis after treatments that stall forks such as UV, HU or aphidicolin (Michalet et al. 1997).

Collectively, our results support a role for PrimPol in the response to UV lesions, particularly 6-4PPs. This is likely to be primarily a role in the bypass of these lesions but additional data suggests that PrimPol may be important for other types of bulky adducts as well as replication fork restart (Figure 64). It was shown previously that clearance of 6-4PP lesions is rapid and in less than 24 hours all 6-4PP lesions are repaired (Volker et al. 2001; Rastogi et al. 2010). 6-4PP lesions are removed faster than CPDs because they occur at a lower frequency than CPDs, approximately one 6-4PP lesion to every 3 CPD lesions (Mitchell 1988). Additionally, the XPA-XPC complex of the NER pathway has a higher affinity for 6-4PP lesions and these lesions are recognized and incised faster than CPDs (Wakasugi and Sancar 1999; Batty et al. 2000). 6-4PP lesions have been shown to be more mutagenic and more cyototoxic, thus efficient and fast removal of these lesions is critical to reduce mutagenicity and cell death (Mitchell 1988). Besides NER, Pol ι, Pol ζ and REV1 have been proposed to be involved in 6-4PP clearance through DNA damage tolerance pathways but this is mostly based on *in vitro* data (reviewed in the introduction).

This begs the important question, why would we see delayed 6-4PP clearance when the cell already possesses other mechanisms to bypass and repair them? There are several ways to explain this. First it is possible that immortalized MEFs are dividing faster and therefore they are more often in S-phase, the interval in which it is critical to repair the damage. Since the NER mechanism is time consuming and "expensive" for the cell, there is no time to employ it for every single lesion or its subunits could be limiting. The solution could be that the cell utilizes PrimPol for lesion bypass to complete replication and then it would have time to repair it later in G2 through multiple mechanisms. Another reason could be that PrimPol is involved in repriming events, providing a new start for replication forks. In that case PrimPol is providing the substrate for later repair. A third explanation can be that in the TLS system, with multiple TLS polymerases potentially performing the same function, cell can choose when and where to use each of available TLS players. In other words, there might be spatial, temporal or tissue specific hierarchies of TLS pols.

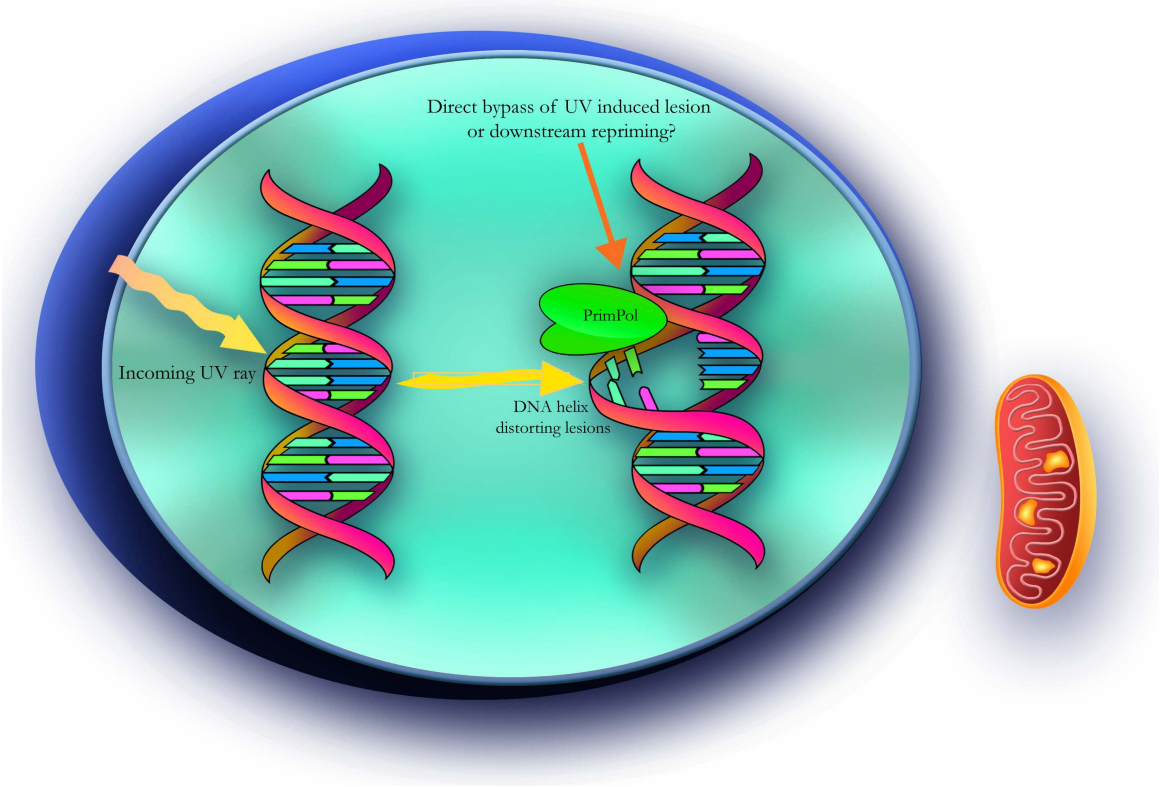

Figure 64. PrimPol is required for DNA damage tolerance

We hypthesize that PrimPol in necessary to deal with UV induced lesions though DNA damage tolerance pathway. PrimPol can either directly bypass helix-distorting dimers or it can provide substrate for restart of replication forks by repriming downstream of the lesion.

1.2. PrimPol is required for chromosomal stability: a role at fragile sites?

Genome instability, a hallmark of cancer cells, is thought in many cases to influence both tumor initiation and tumor progression. The expression of common fragile sites (CFS), regions linked to genomic instability, is correlated with a higher probability of cancer incidence (Gorgoulis et al. 2005; Tsantoulis et al. 2008). CFSs are characterized as "hot spots" where double strand breaks, translocations and sister chromatid exchanges occur more frequently than in any other part of the genome (Durkin and Glover 2007; Debatisse et al. 2012). Genomic integrity depends critically on the fidelity and efficiency of DNA replication. Loss of Pol κ, Pol η and Rev3L leads to elevated genomic instability and expression of CFSs. It was proposed that TLS polymerases could be required to replicate through regions that can stall replicative polymerases such as A-T rich, repetitive sequences (ex. rDNA) or sequence that forms secondary structure (ex. G-quadraplexes).

We have observed in primary cells in the absence of exogenous damage that loss of PrimPol leads to increased chromosomal instability, characterized by a higher percentage of chromatid breaks. Chromatid breaks are indicative of lesions that occur in the S or G2 phases of the cell cycle and can indicate fragile site expression. Fragile site expression can be enhanced using low doses of polymerase inhibitor, aphidicolin. After low dose aphidicolin treatment, the percentage of aberrations in PrimPol KO cells was much higher than that in WT, with chromatid breaks and rearrangements being the most common aberrations identified. We have also observed that the distribution of chromosome number per metaphase spread was unusually high in KO fibroblasts after aphidicolin treatment indicating potential aneuploidy or polyploidy due to mitotic errors. These observations, indicated that most or all chromosomal abnormalities in PrimPol depleted cells are likely to be replication dependent. These results prompted us to speculate that PrimPol might be required for stability of CFSs (Figure 65). An additional hint that encouraged this idea came from the identification of SMC1 as an interacting protein in purifications with mPrimPol$^{C/SF}$. SMC1 (a subunit of the cohesin complex) was shown to suppress CFS expression and its depletion exacerbated the effects of aphidicolin treatment (Musio et al. 2005). Musio et al. proposed a model in which SMC1 would prevent the expression of CFSs by allowing replication strands sufficient time to deal with the lesion that can impede the progression of replication forks.

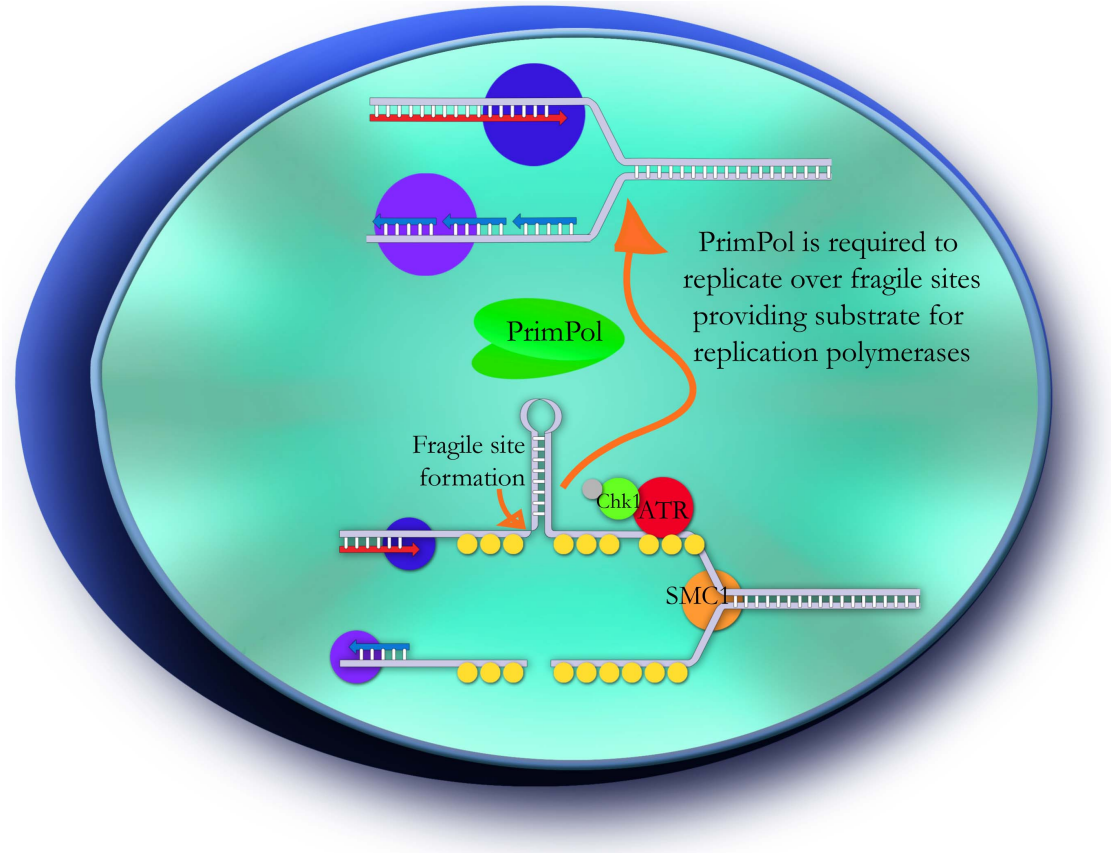

Figure 65. PrimPol is required for stability of fragile sites

In case when failure of replication polymerases to synthesize over difficult regions like CFSs can lead to replication arrest, PrimPol is recruited to replace main replication polymerases and synthesize over fragiles sites. In the absence of PrimPol there is increased expression of fragile sites resulting in high incidence of chromatid breaks.

Upon transient stalling of forks, the ATR axis is activated, leading to phosphorylation of SMC1. We suspect that SMC1 may recruit PrimPol to stalled forks in order to facilitate replication over difficult sequences such as those encountered at CFSs. To test this, we will first try to validate the interaction and then determine if SMC1 depletion in PrimPol deficient cells aggravates genomic instability. We are currently breeding mice *PrimPol*$^{-/-}$ with *Mre11* hypomorphic animals to determine if double knock out cells have higher levels of aberrations. Mre11, a key component of MRN (Mre11-Rad50-Nbs1) complex, is recruited to stalled replication forks by PARP1 where it is required for resection of double strand breaks and restart of stalled replication forks, as well as SMC1 phosphorylation (Bryant et

al. 2009; Ying et al. 2012). Mre11 deficiency alone in MEFs leads to increased spontaneous genomic instability (Buis et al. 2008). Considering the effect of PARP inhibitors on PrimPol deficient MEFs, alone or in combination with UV damage, we anticipate that PrimPol is important for the restart of stalled forks and will interact genetically with the Mre11 mutant.

To determine if the increase in breaks and gaps in PrimPol depleted fibroblasts occurs in CFSs, we will use a FISH approach with probes specific to known CFSs, such as FRA3B, FRA7H, FRA7G, FRA16C, FRA6E (Ozeri-Galai et al. 2012). Additionally, we will analyze proliferating lymphocytes for metaphase aberrations as it was reported that a distinct CFS expression pattern predominates in lymphocytes compared to fibroblasts and levels of CFSs are higher in lymphocytes (Mrasek et al. 2010; Letessier et al. 2011). For example in Pol η deficient fibroblasts, the FRA7H fragile site was characterized and reported as highly expressed under modest replication stress (Rey et al. 2009). In an ATR deficient background, the expression of FRA3B and FRA16D was 7-8 fold higher compared to ATR proficient cells (Casper et al. 2002). Mapping CFSs in PrimPol deficient cells would potentially provide insight into the mechanism of PrimPol action. Each CFS described by now has its own "identity", characterized by different features predisposing to failure of the replication machinery and decreased stability. For example, genomic instability in the FRA3B site is explained by scarcity of replication origins in large portions of this genomic region (Palakodeti et al. 2010). On the other hand, replication in the FRA16C site is getting randomly interrupted even in the absence of replication stress just because this site is AT-sequence rich (Palakodeti et al. 2004; Ozeri-Galai et al. 2011). FRA7H and FRA6E were shown to be late replicating regions where completion of replication can completely fail upon aphidicolin treatment (Hellman et al. 2000; Palumbo et al. 2010).

Discovering CFSs specific for PrimPol would not only help to solidify additional roles for PrimPol but would also give us a clue for potential pathologies or cancers that could be influenced in PrimPol KO mice (besides skin cancers). Many CFSs encode tumor suppressor genes and deletions in these regions are followed by loss of heterozygosity (LOH) that are associated with various cancers. For example in FRA16D, the *WWOX* tumor-suppressor gene and loss of this gene were identified in ovarian cancer and multiple myeloma (Mangelsdorf et al. 2000; Paige et al. 2001). Deletions in FRA4F was associated

with hepatocellular carcinoma (Rozier et al. 2004), while FRA6E encoding the Parkin gene was linked to non-small cell lung cancer (Picchio et al. 2004), ovarian cancer and juvenile parkinsonism (Denison et al. 2003; Denison et al. 2003). Fragile sites are also frequent sites of translocations. It was found that translocation breakpoint in FRA3B site causes loss of FHIT gene function and results in the development of esophageal adenocarcinoma (Fang et al. 2001). In addition CFSs are sites susceptible to random viral integrations, like the human papilloma virus, often found in FRA3B, FRA6C and FRA17D (Thorland et al. 2000).

1.3. PrimPol is required for mitochondrial biogenesis

Most of proteins essential for mitochondrial replication and transcription are encoded in the nucleus and translocated to the mitochondria through a variety of import mechanisms (Holt 2009). Despite its small size, the mitochondrial genome is highly complex at the level of organization and regulation. There is no agreement in the mitochondrial field on the exact mechanism of replication for mitochondrial DNA and only one replication polymerase has been reported, Pol γ. BER is the only major repair mechanism that has been clearly shown to be utilized by mitochondria and it is the major choice for the repair of oxidative lesions that are most frequent. NER and TLS have not yet been clearly observed in the mitochondria with the exception of *S. Cerevisiae* where Pol ζ and Rev1 were found to localize and function there (Alexeyev et al. 2013).

In the first preliminary experiments in the laboratories of our collaborators, PrimPol was identified in the mitochondria by IF (Luis Blanco, Aidan Doherty unpublished). This observation led us to our original working hypothesis that PrimPol was a mitochondrial replication protein, required to prime de novo DNA synthesis. In subsequent experiments, this hypothesis was refuted, as they could not detect any differences in mtDNA replication in the absence of PrimPol. However we still believe that PrimPol plays important roles for overall mitochondrial homeostasis. I will summarize some of the results indicating a role for PrimPol in proper mitochondrial function.

We have tried to detect the localization of PrimPol in mitochondria by electron microscopy but reliable data was not obtained at the time. Nevertheless we have identified some proteins by mass spectrometry that co-purified with PrimPol and are involved in mitochondrial import or are part of the mitochondrial nucleoid core that contains multiple copies of the mtDNA. We identified the mitochondrial import inner membrane translocase subunit (Tim13) in 2 experiments. Interaction with Tim13 could explain how PrimPol, with no clear mitochondrial import signal, gets shuttled into the mitochondria. Several proteins involved in the citrate cycle were also purified with PrimPol including IDH1 (isocitrate dehydrogenase), CS (citrate synthase) and ACLY (ATP citrate lyase). And several Mt proteins that are part of the nucleoid were identified including LONP1 (targeting specific regulatory Mt proteins for degradation), TUFM (involved in translation of mitochondrial proteins) and LRPPRC (stabilizing Mt mRNA and coordinating mitochondrial translation). For us, LRPPRC is especially interesting as mutations in this gene lead to development of Leigh syndrome French Canadian variant, a rare neurodegenerative disease (Cooper et al. 2006). This disorder is characterized by cytochrome c oxidase deficiency and its dysfunction affects hepatic function and metabolism (Xu et al. 2012). LRPPRC was linked in several studies with PGC1-α, master regulator of mitochondrial metabolism (Cooper et al. 2008) where it was shown that it can control its activity in several important metabolic pathways.

To determine if we could identify any metabolic or stress responses indicative of mitochondrial dysfunction, we performed microarray analysis on 293HEK cells where we depleted *PRIMPOL* by shRNA. In these experiments, we observed marked downregulation of *PGC1-α* (main regulator of mitochondrial biogenesis), mitochondrial ribosomal protein L30 (*MRPL30*) and NADH dehydrogenase (*NDUFS1*), the latter gene being important for the TCA cycle and the prevention of leukoencephalopathy (Hoefs et al. 2010; Ferreira et al. 2011). Given the heterogeneity of these results we did not pursue validation of many genes identified in the arrays.

While inconclusive, our results led us to speculate that PrimPol was important for mitochondrial function and therefore we analyzed mitochondrial copy number. In primary PrimPol KO MEFs and tissues of aged, but not young, KO mice, we observed upregulation of mitochondrial copy number using real time PCR. Furthermore, in the

tissues of young mice that were UV irradiated, we observed higher mitochondrial copy number in PrimPol deficient tissues. It is known that in aging tissue with elevated oxidative stress, increases in mitochondrial copy number follow the decline of functional mitochondria. It is considered that cells attempt to compensate for defective mitochondrial function by boosting proliferation of mtDNA (Lee and Wei 2000; Wang et al. 2013). Increased mtDNA copy can be followed by elevated ROS levels and this was reported in aged rats with mitochondria that encoded defective respiratory chain components (Gadaleta et al. 1992) and in late passages of human cells (Shmookler Reis and Goldstein 1983). Our *in vivo* data showed that cells without PrimPol have higher mitochondrial DNA copy numbers in tissues like intestine and liver that have higher metabolic turnover and therefore a higher potential production of ROS. Our primary MEFs are also cultured under slightly hyperoxic conditions (20%), which is known to cause oxidative stress.

Our current hypothesis is that PrimPol is involved in the maintenance of mtDNA by protecting mtDNA from oxidative damage, particularly in the form of the common 8-oxo-G lesion. The Doherty lab showed that PrimPol can read through 8-oxo-G lesions in a random error-free or error-prone way in vitro (manuscript under revision). PrimPol could therefore be performing TLS functions in the mitochondria to facilitate mtDNA replication and subsequent repair by BER. In the absence of PrimPol we would speculate that we would observe increased levels of 8-oxo-G lesions and we could test this using the ELISA approach we employed for 6-4PPs. We speculate that increase in mitochondrial copy number in KO tissues reflects defects in mitochondrial metabolism caused by impaired mitochondrial function due to increased mutagenesis of mtDNA or the accumulation of dysfunctional copies. This could lead to defects in the TCA cycle and elevated oxidative stress that triggers a compensatory response and mtDNA hyperproliferation (Figure 66).

One prediction that follows this proposal is that PrimPol mice may age prematurely due to mitochondrial dysfunction and increased ROS accumulation. To test this, we have been monitoring an aging cohort but thus far have not seen any pathological outcomes consistent with this. In future experiments we will need to profile the cells and tissues of PrimPol deficient animals for increased ROS or other signs of oxidative stress and determine if this is linked to increased mtDNA copy number. Increased ROS has been linked to stem cell aging and dysfunction in the epidermis. As we observed high levels of

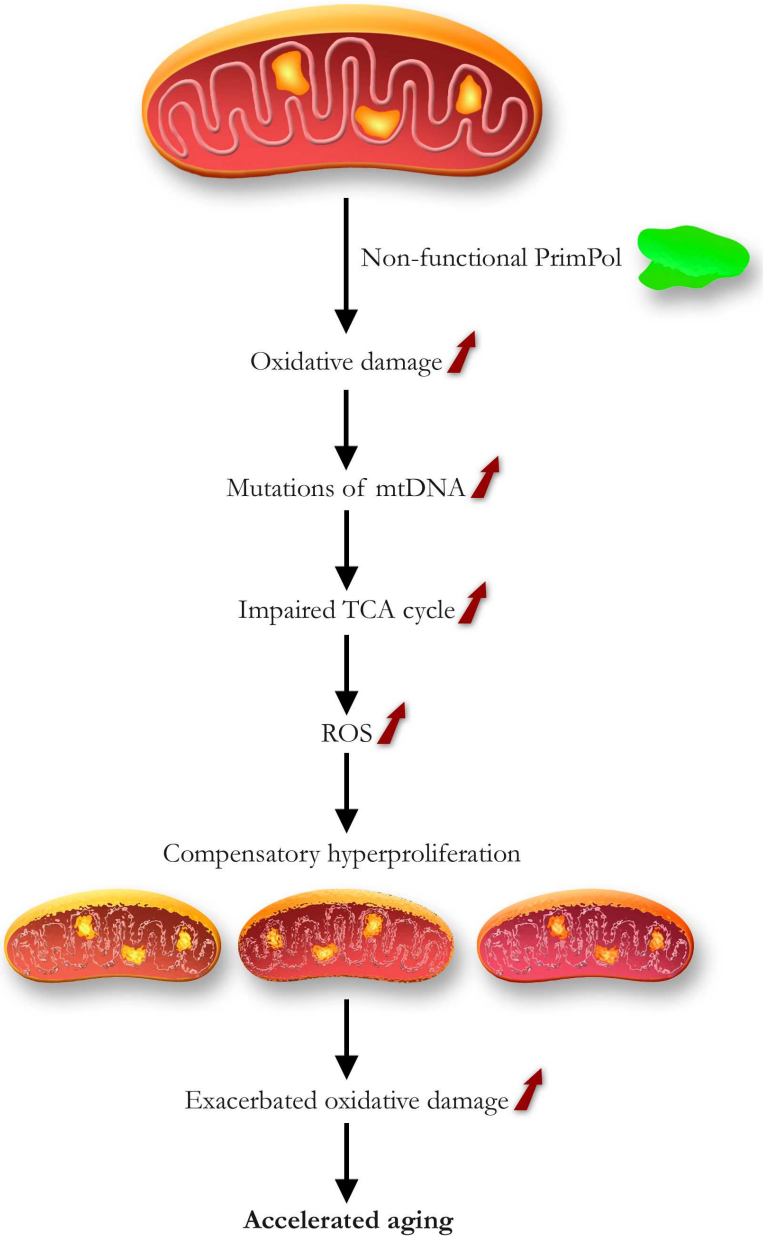

Figure 66. PrimPol is required for mitochondrial homeostasis

We propose a model where disfunction of PrimPol can affect mitochondrial biogenesis, leading to increased oxidative damage that can result in mutations of mtDNA and lead to impaired function of TCA cycle. Defect in metabolism and insufficient energy production for cellular needs can trigger compensatory hyperproliferation of defective mitochondria. This in feedback loop can exacerbate even more already existing oxidative damage and potentially accelerate aging through elevated apoptosis.

PrimPol in the skin, we can determine if age affects both ROS levels and pluripotency of these cells. As PrimPol is expressed across different tissues, it would also be interesting to examine muscle architecture as it was reported that defects in mitochondrial biogenesis strongly affects muscles and can be diagnosed as "red ragged fibers". Finally it would be valuable to determine the quality of mtDNA in aged KO animals by sequencing mtDNA and analyzing the type and frequency of mutations that are present.

2. A unified model for PrimPol functions

The data collected to date firmly establishes a role for PrimPol in the metabolism of UV lesions, implicates it in DNA replication and replication fork restart, particularly at fragile sites and suggests a role in bypassing bulky base lesions caused by oxidative damage in the nucleus and mitochondria. We therefore hypothesize that PrimPol deficiency could have a significant impact on aging related phenotypes as well as cancer predisposition as mice lacking PrimPol would potentially accumulate a higher load of mutations and chromosome aberrations during normal aging. To address this, we have been monitoring a cohort of PrimPol deficient animals but clear pathological outcomes have yet to emerge. As TLS activities may be highly redundant, the phenotypes could be masked by other activities. In addition to crosses with Mre11 deficient animals, we have also initiated crosses with mice lacking Pol η in order to address the effects on the UV response and CFS expression *in vivo* and in primary cells.

Deficiency of Pol η and Pol ι in mice differentially affects tumor initiation and development after UV damage. Pol η deficient mice were susceptible to epithelial tumors (squamous cell carcinoma, adenosquamous cell carcinoma, papilloma), while Pol ι mice developed mesenchymal tumors (sarcomas, hemangiomas) (Ohkumo et al. 2006). This finding highlights the fact that while Pol η and Pol ι may have the same function, that is bypass of CPDs, one enzyme is more important for keratinocytes while the other for fibroblasts. Based on this, we can hypothesize that PrimPol may be necessary for certain types of cells and further analysis of the PrimPol deficient mice using biochemical and genetic approaches will be necessary for clarifying its relevance to human pathology.

Conclusions

1. PrimPol is a novel AEP primase-polymerase that functions in the nucleus and mitochondria.
2. PrimPol is highly expressed in UV sensitive tissues such as the skin and eye in embryos and adults.
3. PrimPol is required for the tolerance of UV lesions, independently of ATR-Pol η.
4. Loss of PrimPol leads to increased chromosomal instability in primary cells.
5. Loss of PrimPol affects mitochondrial homeostasis, leading to increased mitochondrial copy number.

Bibliography

Acharya, N., R. E. Johnson, S. Prakash and L. Prakash (2006). "Complex formation with Rev1 enhances the proficiency of Saccharomyces cerevisiae DNA polymerase zeta for mismatch extension and for extension opposite from DNA lesions." Mol Cell Biol **26**(24): 9555-9563.

Akbari, M., T. Visnes, H. E. Krokan and M. Otterlei (2008). "Mitochondrial base excision repair of uracil and AP sites takes place by single-nucleotide insertion and long-patch DNA synthesis." DNA Repair (Amst) **7**(4): 605-616.

Albertella, M. R., C. M. Green, A. R. Lehmann and M. J. O'Connor (2005). "A role for polymerase eta in the cellular tolerance to cisplatin-induced damage." Cancer Res **65**(21): 9799-9806.

Albertella, M. R., A. Lau and M. J. O'Connor (2005). "The overexpression of specialized DNA polymerases in cancer." DNA Repair (Amst) **4**(5): 583-593.

Alexeyev, M., I. Shokolenko, G. Wilson and S. LeDoux (2013). "The maintenance of mitochondrial DNA integrity--critical analysis and update." Cold Spring Harb Perspect Biol **5**(5): a012641.

Almeida, K. H. and R. W. Sobol (2007). "A unified view of base excision repair: lesion-dependent protein complexes regulated by post-translational modification." DNA Repair (Amst) **6**(6): 695-711.

Arana, M. E. and T. A. Kunkel (2010). "Mutator phenotypes due to DNA replication infidelity." Semin Cancer Biol **20**(5): 304-311.

Arlett, C. F., S. A. Harcourt and B. C. Broughton (1975). "The influence of caffeine on cell survival in excision-proficient and excision-deficient xeroderma pigmentosum and normal human cell strains following ultraviolet-light irradiation." Mutat Res **33**(2-3): 341-346.

Baker, T. A. and S. P. Bell (1998). "Polymerases and the replisome: machines within machines." Cell **92**(3): 295-305.

Balajee, A. S., A. May and V. A. Bohr (1999). "DNA repair of pyrimidine dimers and 6-4 photoproducts in the ribosomal DNA." Nucleic Acids Res **27**(12): 2511-2520.

Batty, D., V. Rapic'-Otrin, A. S. Levine and R. D. Wood (2000). "Stable binding of human XPC complex to irradiated DNA confers strong discrimination for damaged sites." J Mol Biol **300**(2): 275-290.

Bavoux, C., J. S. Hoffmann and C. Cazaux (2005). "Adaptation to DNA damage and stimulation of genetic instability: the double-edged sword mammalian DNA polymerase kappa." Biochimie **87**(7): 637-646.

Bavoux, C., A. M. Leopoldino, V. Bergoglio, O. W. J, T. Ogi, A. Bieth, J. G. Judde, S. D. Pena, M. F. Poupon, T. Helleday, M. Tagawa, C. Machado, J. S. Hoffmann and C. Cazaux (2005). "Up-regulation of the error-prone DNA polymerase {kappa} promotes pleiotropic genetic alterations and tumorigenesis." Cancer Res **65**(1): 325-330.

Beard, W. A., R. Prasad and S. H. Wilson (2006). "Activities and mechanism of DNA polymerase beta." Methods Enzymol **408**: 91-107.

Bebenek, K., A. Tissier, E. G. Frank, J. P. McDonald, R. Prasad, S. H. Wilson, R. Woodgate and T. A. Kunkel (2001). "5'-Deoxyribose phosphate lyase activity of human DNA polymerase iota in vitro." Science **291**(5511): 2156-2159.

Bemark, M., A. A. Khamlichi, S. L. Davies and M. S. Neuberger (2000). "Disruption of mouse polymerase zeta (Rev3) leads to embryonic lethality and impairs blastocyst development in vitro." Curr Biol **10**(19): 1213-1216.

Bentolila, L. A., G. E. Wu, F. Nourrit, M. Fanton d'Andon, F. Rougeon and N. Doyen (1997). "Constitutive expression of terminal deoxynucleotidyl transferase in transgenic mice is sufficient for N region diversity to occur at any Ig locus throughout B cell differentiation." J Immunol **158**(2): 715-723.

Bertocci, B., A. De Smet, J. C. Weill and C. A. Reynaud (2006). "Nonoverlapping functions of DNA polymerases mu, lambda, and terminal deoxynucleotidyltransferase during immunoglobulin V(D)J recombination in vivo." Immunity **25**(1): 31-41.

Bessman, M. J., A. Kornberg, I. R. Lehman and E. S. Simms (1956). "Enzymic synthesis of deoxyribonucleic acid." Biochim Biophys Acta **21**(1): 197-198.

Betous, R., L. Rey, G. Wang, M. J. Pillaire, N. Puget, J. Selves, D. S. Biard, K. Shin-ya, K. M. Vasquez, C. Cazaux and J. S. Hoffmann (2009). "Role of TLS DNA polymerases eta and kappa in processing naturally occurring structured DNA in human cells." Mol Carcinog **48**(4): 369-378.

Bhat, A., P. L. Andersen, Z. Qin and W. Xiao (2013). "Rev3, the catalytic subunit of Polzeta, is required for maintaining fragile site stability in human cells." Nucleic Acids Res **41**(4): 2328-2339.

Bianchi, V., E. Pontis and P. Reichard (1986). "Changes of deoxyribonucleoside triphosphate pools induced by hydroxyurea and their relation to DNA synthesis." J Biol Chem **261**(34): 16037-16042.

Bielas, J. H., K. R. Loeb, B. P. Rubin, L. D. True and L. A. Loeb (2006). "Human cancers express a mutator phenotype." Proc Natl Acad Sci U S A **103**(48): 18238-18242.

Binz, S. K., A. M. Sheehan and M. S. Wold (2004). "Replication protein A phosphorylation and the cellular response to DNA damage." DNA Repair (Amst) **3**(8-9): 1015-1024.

Biswas, N. and S. K. Weller (1999). "A mutation in the C-terminal putative Zn2+ finger motif of UL52 severely affects the biochemical activities of the HSV-1 helicase-primase subcomplex." J Biol Chem **274**(12): 8068-8076.

Biswas, N. and S. K. Weller (2001). "The UL5 and UL52 subunits of the herpes simplex virus type 1 helicase-primase subcomplex exhibit a complex interdependence for DNA binding." J Biol Chem **276**(20): 17610-17619.

Bomgarden, R. D., P. J. Lupardus, D. V. Soni, M. C. Yee, J. M. Ford and K. A. Cimprich (2006). "Opposing effects of the UV lesion repair protein XPA and UV bypass polymerase eta on ATR checkpoint signaling." EMBO J **25**(11): 2605-2614.

Boudsocq, F., R. J. Kokoska, B. S. Plosky, A. Vaisman, H. Ling, T. A. Kunkel, W. Yang and R. Woodgate (2004). "Investigating the role of the little finger domain of Y-family DNA polymerases in low fidelity synthesis and translesion replication." J Biol Chem **279**(31): 32932-32940.

Bowmaker, M., M. Y. Yang, T. Yasukawa, A. Reyes, H. T. Jacobs, J. A. Huberman and I. J. Holt (2003). "Mammalian mitochondrial DNA replicates bidirectionally from an initiation zone." J Biol Chem **278**(51): 50961-50969.

Braithwaite, E. K., R. Prasad, D. D. Shock, E. W. Hou, W. A. Beard and S. H. Wilson (2005). "DNA polymerase lambda mediates a back-up base excision repair activity in extracts of mouse embryonic fibroblasts." J Biol Chem **280**(18): 18469-18475.

Broughton, B. C., A. Cordonnier, W. J. Kleijer, N. G. Jaspers, H. Fawcett, A. Raams, V. H. Garritsen, A. Stary, M. F. Avril, F. Boudsocq, C. Masutani, F. Hanaoka, R. P. Fuchs, A. Sarasin and A. R. Lehmann (2002). "Molecular analysis of mutations in DNA polymerase eta in xeroderma pigmentosum-variant patients." Proc Natl Acad Sci U S A **99**(2): 815-820.

Brown, T. A., C. Cecconi, A. N. Tkachuk, C. Bustamante and D. A. Clayton (2005). "Replication of mitochondrial DNA occurs by strand displacement with alternative light-strand origins, not via a strand-coupled mechanism." Genes Dev **19**(20): 2466-2476.

Bryant, H. E., E. Petermann, N. Schultz, A. S. Jemth, O. Loseva, N. Issaeva, F. Johansson, S. Fernandez, P. McGlynn and T. Helleday (2009). "PARP is activated at stalled forks to mediate Mre11-dependent replication restart and recombination." EMBO J **28**(17): 2601-2615.

Buis, J., Y. Wu, Y. Deng, J. Leddon, G. Westfield, M. Eckersdorff, J. M. Sekiguchi, S. Chang and D. O. Ferguson (2008). "Mre11 nuclease activity has essential roles in DNA repair and genomic stability distinct from ATM activation." Cell **135**(1): 85-96.

Bullock, S. K., W. K. Kaufmann and M. Cordeiro-Stone (2001). "Enhanced S phase delay and inhibition of replication of an undamaged shuttle vector in UVC-irradiated xeroderma pigmentosum variant." Carcinogenesis **22**(2): 233-241.

Burns, T. F. and W. S. El-Deiry (2003). "Microarray analysis of p53 target gene expression patterns in the spleen and thymus in response to ionizing radiation." Cancer Biol Ther **2**(4): 431-443.

Burr, K. L., S. Velasco-Miguel, V. S. Duvvuri, L. D. McDaniel, E. C. Friedberg and Y. E. Dubrova (2006). "Elevated mutation rates in the germline of Polkappa mutant male mice." DNA Repair (Amst) **5**(7): 860-862.

Busuttil, R. A., Q. Lin, P. J. Stambrook, R. Kucherlapati and J. Vijg (2008). "Mutation frequencies and spectra in DNA polymerase eta-deficient mice." Cancer Res **68**(7): 2081-2084.

Byun, T. S., M. Pacek, M. C. Yee, J. C. Walter and K. A. Cimprich (2005). "Functional uncoupling of MCM helicase and DNA polymerase activities activates the ATR-dependent checkpoint." Genes Dev **19**(9): 1040-1052.

Carlson, K. D., R. E. Johnson, L. Prakash, S. Prakash and M. T. Washington (2006). "Human DNA polymerase kappa forms nonproductive complexes with matched primer termini but not with mismatched primer termini." Proc Natl Acad Sci U S A **103**(43): 15776-15781.

Casper, A. M., P. Nghiem, M. F. Arlt and T. W. Glover (2002). "ATR regulates fragile site stability." Cell **111**(6): 779-789.

Ceppi, P., S. Novello, A. Cambieri, M. Longo, V. Monica, M. Lo Iacono, M. Giaj-Levra, S. Saviozzi, M. Volante, M. Papotti and G. Scagliotti (2009). "Polymerase eta mRNA expression predicts survival of non-small cell lung cancer patients treated with platinum-based chemotherapy." Clin Cancer Res **15**(3): 1039-1045.

Chacinska, A., N. Pfanner and C. Meisinger (2002). "How mitochondria import hydrophilic and hydrophobic proteins." Trends Cell Biol **12**(7): 299-303.

Chan, S. S. and W. C. Copeland (2009). "DNA polymerase gamma and mitochondrial disease: understanding the consequence of POLG mutations." Biochim Biophys Acta **1787**(5): 312-319.

Choi, J. H., A. Besaratinia, D. H. Lee, C. S. Lee and G. P. Pfeifer (2006). "The role of DNA polymerase iota in UV mutational spectra." Mutat Res **599**(1-2): 58-65.

Choi, J. H. and G. P. Pfeifer (2005). "The role of DNA polymerase eta in UV mutational spectra." DNA Repair (Amst) **4**(2): 211-220.

Clarke, A. R., C. A. Purdie, D. J. Harrison, R. G. Morris, C. C. Bird, M. L. Hooper and A. H. Wyllie (1993). "Thymocyte apoptosis induced by p53-dependent and independent pathways." Nature **362**(6423): 849-852.

Clayton, D. A., J. N. Doda and E. C. Friedberg (1974). "The absence of a pyrimidine dimer repair mechanism in mammalian mitochondria." Proc Natl Acad Sci U S A **71**(7): 2777-2781.

Cooper, M. P., L. Qu, L. M. Rohas, J. Lin, W. Yang, H. Erdjument-Bromage, P. Tempst and B. M. Spiegelman (2006). "Defects in energy homeostasis in Leigh syndrome French Canadian variant through PGC-1alpha/LRP130 complex." Genes Dev **20**(21): 2996-3009.

Cooper, M. P., M. Uldry, S. Kajimura, Z. Arany and B. M. Spiegelman (2008). "Modulation of PGC-1 coactivator pathways in brown fat differentiation through LRP130." J Biol Chem **283**(46): 31960-31967.

Copeland, W. C. (2010). "The mitochondrial DNA polymerase in health and disease." Subcell Biochem **50**: 211-222.

Copeland, W. C. (2012). "Defects in mitochondrial DNA replication and human disease." Crit Rev Biochem Mol Biol **47**(1): 64-74.

Copeland, W. C. and X. Tan (1995). "Active site mapping of the catalytic mouse primase subunit by alanine scanning mutagenesis." J Biol Chem **270**(8): 3905-3913.

Cordeiro-Stone, M., A. Frank, M. Bryant, I. Oguejiofor, S. B. Hatch, L. D. McDaniel and W. K. Kaufmann (2002). "DNA damage responses protect xeroderma pigmentosum variant from UVC-induced clastogenesis." Carcinogenesis **23**(6): 959-965.

Cordonnier, A. M., A. R. Lehmann and R. P. Fuchs (1999). "Impaired translesion synthesis in xeroderma pigmentosum variant extracts." Mol Cell Biol **19**(3): 2206-2211.

Cruet-Hennequart, S., S. Coyne, M. T. Glynn, G. G. Oakley and M. P. Carty (2006). "UV-induced RPA phosphorylation is increased in the absence of DNA polymerase eta and requires DNA-PK." DNA Repair (Amst) **5**(4): 491-504.

D'Souza, S., L. S. Waters and G. C. Walker (2008). "Novel conserved motifs in Rev1 C-terminus are required for mutagenic DNA damage tolerance." DNA Repair (Amst) **7**(9): 1455-1470.

Dantzer, F., H. P. Nasheuer, J. L. Vonesch, G. de Murcia and J. Menissier-de Murcia (1998). "Functional association of poly(ADP-ribose) polymerase with DNA polymerase alpha-primase complex: a link between DNA strand break detection and DNA replication." Nucleic Acids Res **26**(8): 1891-1898.

Davidzon, G., P. Greene, M. Mancuso, K. J. Klos, J. E. Ahlskog, M. Hirano and S. DiMauro (2006). "Early-onset familial parkinsonism due to POLG mutations." Ann Neurol **59**(5): 859-862.

de Boer, J. and J. H. Hoeijmakers (2000). "Nucleotide excision repair and human syndromes." Carcinogenesis **21**(3): 453-460.

de Feraudy, S., C. L. Limoli, E. Giedzinski, D. Karentz, T. M. Marti, L. Feeney and J. E. Cleaver (2007). "Pol eta is required for DNA replication during nucleotide deprivation by hydroxyurea." Oncogene **26**(39): 5713-5721.

de Souza-Pinto, N. C., P. A. Mason, K. Hashiguchi, L. Weissman, J. Tian, D. Guay, M. Lebel, T. V. Stevnsner, L. J. Rasmussen and V. A. Bohr (2009). "Novel DNA mismatch-repair activity involving YB-1 in human mitochondria." DNA Repair (Amst) **8**(6): 704-719.

Debatisse, M., B. Le Tallec, A. Letessier, B. Dutrillaux and O. Brison (2012). "Common fragile sites: mechanisms of instability revisited." Trends Genet **28**(1): 22-32.

Delbos, F., A. De Smet, A. Faili, S. Aoufouchi, J. C. Weill and C. A. Reynaud (2005). "Contribution of DNA polymerase eta to immunoglobulin gene hypermutation in the mouse." J Exp Med **201**(8): 1191-1196.

Denison, S. R., G. Callahan, N. A. Becker, L. A. Phillips and D. I. Smith (2003). "Characterization of FRA6E and its potential role in autosomal recessive juvenile parkinsonism and ovarian cancer." Genes Chromosomes Cancer **38**(1): 40-52.

Denison, S. R., F. Wang, N. A. Becker, B. Schule, N. Kock, L. A. Phillips, C. Klein and D. I. Smith (2003). "Alterations in the common fragile site gene Parkin in ovarian and other cancers." Oncogene **22**(51): 8370-8378.

Despras, E., F. Daboussi, O. Hyrien, K. Marheineke and P. L. Kannouche (2010). "ATR/Chk1 pathway is essential for resumption of DNA synthesis and cell survival in UV-irradiated XP variant cells." Hum Mol Genet **19**(9): 1690-1701.

Diaz, M., L. K. Verkoczy, M. F. Flajnik and N. R. Klinman (2001). "Decreased frequency of somatic hypermutation and impaired affinity maturation but intact germinal center formation in mice expressing antisense RNA to DNA polymerase zeta." J Immunol **167**(1): 327-335.

Diede, S. J. and D. E. Gottschling (1999). "Telomerase-mediated telomere addition in vivo requires DNA primase and DNA polymerases alpha and delta." Cell **99**(7): 723-733.

Doherty, A. J., S. P. Jackson and G. R. Weller (2001). "Identification of bacterial homologues of the Ku DNA repair proteins." FEBS Lett **500**(3): 186-188.

Dumstorf, C. A., A. B. Clark, Q. Lin, G. E. Kissling, T. Yuan, R. Kucherlapati, W. G. McGregor and T. A. Kunkel (2006). "Participation of mouse DNA polymerase iota in strand-biased mutagenic bypass of UV photoproducts and suppression of skin cancer." Proc Natl Acad Sci U S A **103**(48): 18083-18088.

Durkin, S. G. and T. W. Glover (2007). "Chromosome fragile sites." Annu Rev Genet **41**: 169-192.

Emara, M. M., K. Fujimura, D. Sciaranghella, V. Ivanova, P. Ivanov and P. Anderson (2012). "Hydrogen peroxide induces stress granule formation independent of eIF2alpha phosphorylation." Biochem Biophys Res Commun **423**(4): 763-769.

Ensch-Simon, I., P. M. Burgers and J. S. Taylor (1998). "Bypass of a site-specific cis-Syn thymine dimer in an SV40 vector during in vitro replication by HeLa and XPV cell-free extracts." Biochemistry **37**(22): 8218-8226.

Esposito, G., I. Godindagger, U. Klein, M. L. Yaspo, A. Cumano and K. Rajewsky (2000). "Disruption of the Rev3l-encoded catalytic subunit of polymerase zeta in mice results in early embryonic lethality." Curr Biol **10**(19): 1221-1224.

Fachinetti, D., R. Bermejo, A. Cocito, S. Minardi, Y. Katou, Y. Kanoh, K. Shirahige, A. Azvolinsky, V. A. Zakian and M. Foiani (2010). "Replication termination at eukaryotic chromosomes is mediated by Top2 and occurs at genomic loci containing pausing elements." Mol Cell **39**(4): 595-605.

Faili, A., S. Aoufouchi, E. Flatter, Q. Gueranger, C. A. Reynaud and J. C. Weill (2002). "Induction of somatic hypermutation in immunoglobulin genes is dependent on DNA polymerase iota." Nature **419**(6910): 944-947.

Faili, A., S. Aoufouchi, S. Weller, F. Vuillier, A. Stary, A. Sarasin, C. A. Reynaud and J. C. Weill (2004). "DNA polymerase eta is involved in hypermutation occurring during immunoglobulin class switch recombination." J Exp Med **199**(2): 265-270.

Falck, J., J. V. Forment, J. Coates, M. Mistrik, J. Lukas, J. Bartek and S. P. Jackson (2012). "CDK targeting of NBS1 promotes DNA-end resection, replication restart and homologous recombination." EMBO Rep **13**(6): 561-568.

Fang, J. M., M. F. Arlt, A. C. Burgess, S. L. Dagenais, D. G. Beer and T. W. Glover (2001). "Translocation breakpoints in FHIT and FRA3B in both homologs of chromosome 3 in an esophageal adenocarcinoma." Genes Chromosomes Cancer **30**(3): 292-298.

Ferreira, M., A. Torraco, T. Rizza, F. Fattori, M. C. Meschini, C. Castana, N. E. Go, F. E. Nargang, M. Duarte, F. Piemonte, C. Dionisi-Vici, A. Videira, L. Vilarinho, F. M. Santorelli, R. Carrozzo and E. Bertini (2011). "Progressive cavitating leukoencephalopathy associated with respiratory chain complex I deficiency and a novel mutation in NDUFS1." Neurogenetics **12**(1): 9-17.

Foiani, M., G. Lucchini and P. Plevani (1997). "The DNA polymerase alpha-primase complex couples DNA replication, cell-cycle progression and DNA-damage response." Trends Biochem Sci **22**(11): 424-427.

Franklin, A., P. J. Milburn, R. V. Blanden and E. J. Steele (2004). "Human DNA polymerase-eta, an A-T mutator in somatic hypermutation of rearranged immunoglobulin genes, is a reverse transcriptase." Immunol Cell Biol **82**(2): 219-225.

Frick, D. N. and C. C. Richardson (2001). "DNA primases." Annu Rev Biochem **70**: 39-80.

Friedberg, E. C., A. R. Lehmann and R. P. Fuchs (2005). "Trading places: how do DNA polymerases switch during translesion DNA synthesis?" Mol Cell **18**(5): 499-505.

Fu, D., F. D. Dudimah, J. Zhang, A. Pickering, J. Paneerselvam, M. Palrasu, H. Wang and P. Fei (2013). "Recruitment of DNA polymerase eta by FANCD2 in the early response to DNA damage." Cell Cycle **12**(5): 803-809.

Fujii, S. and R. P. Fuchs (2004). "Defining the position of the switches between replicative and bypass DNA polymerases." EMBO J **23**(21): 4342-4352.

Furnari, B., A. Blasina, M. N. Boddy, C. H. McGowan and P. Russell (1999). "Cdc25 inhibited in vivo and in vitro by checkpoint kinases Cds1 and Chk1." Mol Biol Cell **10**(4): 833-845.

Fuste, J. M., S. Wanrooij, E. Jemt, C. E. Granycome, T. J. Cluett, Y. Shi, N. Atanassova, I. J. Holt, C. M. Gustafsson and M. Falkenberg (2010). "Mitochondrial RNA polymerase is needed for activation of the origin of light-strand DNA replication." Mol Cell **37**(1): 67-78.

Gadaleta, M. N., G. Rainaldi, A. M. Lezza, F. Milella, F. Fracasso and P. Cantatore (1992). "Mitochondrial DNA copy number and mitochondrial DNA deletion in adult and senescent rats." Mutat Res **275**(3-6): 181-193.

Gan, G. N., J. P. Wittschieben, B. O. Wittschieben and R. D. Wood (2008). "DNA polymerase zeta (pol zeta) in higher eukaryotes." Cell Res **18**(1): 174-183.

Garg, P. and P. M. Burgers (2005). "DNA polymerases that propagate the eukaryotic DNA replication fork." Crit Rev Biochem Mol Biol **40**(2): 115-128.

Garg, P., C. M. Stith, J. Majka and P. M. Burgers (2005). "Proliferating cell nuclear antigen promotes translesion synthesis by DNA polymerase zeta." J Biol Chem **280**(25): 23446-23450.

Gentleman, R. C., V. J. Carey, D. M. Bates, B. Bolstad, M. Dettling, S. Dudoit, B. Ellis, L. Gautier, Y. Ge, J. Gentry, K. Hornik, T. Hothorn, W. Huber, S. Iacus, R. Irizarry, F. Leisch, C. Li, M. Maechler, A. J. Rossini, G. Sawitzki, C. Smith, G. Smyth, L. Tierney, J. Y. Yang and J. Zhang (2004). "Bioconductor: open software

development for computational biology and bioinformatics." Genome Biol **5**(10): R80.

Gloeckner, C. J., K. Boldt, A. Schumacher and M. Ueffing (2009). "Tandem affinity purification of protein complexes from mammalian cells by the Strep/FLAG (SF)-TAP tag." Methods Mol Biol **564**: 359-372.

Gloeckner, C. J., K. Boldt and M. Ueffing (2009). "Strep/FLAG tandem affinity purification (SF-TAP) to study protein interactions." Curr Protoc Protein Sci **Chapter 19**: Unit19 20.

Glover, T. W., C. Berger, J. Coyle and B. Echo (1984). "DNA polymerase alpha inhibition by aphidicolin induces gaps and breaks at common fragile sites in human chromosomes." Hum Genet **67**(2): 136-142.

Glover, T. W. and C. K. Stein (1987). "Induction of sister chromatid exchanges at common fragile sites." Am J Hum Genet **41**(5): 882-890.

Gohler, T., S. Sabbioneda, C. M. Green and A. R. Lehmann (2011). "ATR-mediated phosphorylation of DNA polymerase eta is needed for efficient recovery from UV damage." J Cell Biol **192**(2): 219-227.

Goodman, M. F. (2002). "Error-prone repair DNA polymerases in prokaryotes and eukaryotes." Annu Rev Biochem **71**: 17-50.

Gorgoulis, V. G., L. V. Vassiliou, P. Karakaidos, P. Zacharatos, A. Kotsinas, T. Liloglou, M. Venere, R. A. Ditullio, Jr., N. G. Kastrinakis, B. Levy, D. Kletsas, A. Yoneta, M. Herlyn, C. Kittas and T. D. Halazonetis (2005). "Activation of the DNA damage checkpoint and genomic instability in human precancerous lesions." Nature **434**(7035): 907-913.

Gueranger, Q., A. Stary, S. Aoufouchi, A. Faili, A. Sarasin, C. A. Reynaud and J. C. Weill (2008). "Role of DNA polymerases eta, iota and zeta in UV resistance and UV-induced mutagenesis in a human cell line." DNA Repair (Amst) **7**(9): 1551-1562.

Guo, C., P. L. Fischhaber, M. J. Luk-Paszyc, Y. Masuda, J. Zhou, K. Kamiya, C. Kisker and E. C. Friedberg (2003). "Mouse Rev1 protein interacts with multiple DNA polymerases involved in translesion DNA synthesis." EMBO J **22**(24): 6621-6630.

Guo, C., E. Sonoda, T. S. Tang, J. L. Parker, A. B. Bielen, S. Takeda, H. D. Ulrich and E. C. Friedberg (2006). "REV1 protein interacts with PCNA: significance of the REV1 BRCT domain in vitro and in vivo." Mol Cell **23**(2): 265-271.

Hakonen, A. H., S. Heiskanen, V. Juvonen, I. Lappalainen, P. T. Luoma, M. Rantamaki, G. V. Goethem, A. Lofgren, P. Hackman, A. Paetau, S. Kaakkola, K. Majamaa, T. Varilo, B. Udd, H. Kaariainen, L. A. Bindoff and A. Suomalainen (2005). "Mitochondrial DNA polymerase W748S mutation: a common cause of autosomal recessive ataxia with ancient European origin." Am J Hum Genet **77**(3): 430-441.

Hecht, F. and T. W. Glover (1984). "Cancer chromosome breakpoints and common fragile sites induced by aphidicolin." Cancer Genet Cytogenet **13**(2): 185-188.

Hefferin, M. L. and A. E. Tomkinson (2005). "Mechanism of DNA double-strand break repair by non-homologous end joining." DNA Repair (Amst) **4**(6): 639-648.

Heller, R. C. and K. J. Marians (2006). "Replication fork reactivation downstream of a blocked nascent leading strand." Nature **439**(7076): 557-562.

Hellman, A., A. Rahat, S. W. Scherer, A. Darvasi, L. C. Tsui and B. Kerem (2000). "Replication delay along FRA7H, a common fragile site on human chromosome 7, leads to chromosomal instability." Mol Cell Biol **20**(12): 4420-4427.

Hellman, A., E. Zlotorynski, S. W. Scherer, J. Cheung, J. B. Vincent, D. I. Smith, L. Trakhtenbrot and B. Kerem (2002). "A role for common fragile site induction in amplification of human oncogenes." Cancer Cell **1**(1): 89-97.

Helmrich, A., M. Ballarino and L. Tora (2011). "Collisions between replication and transcription complexes cause common fragile site instability at the longest human genes." Mol Cell **44**(6): 966-977.

Hewett, D. R., O. Handt, L. Hobson, M. Mangelsdorf, H. J. Eyre, E. Baker, G. R. Sutherland, S. Schuffenhauer, J. I. Mao and R. I. Richards (1998). "FRA10B structure reveals common elements in repeat expansion and chromosomal fragile site genesis." Mol Cell **1**(6): 773-781.

Ho, T. V. and O. D. Scharer (2010). "Translesion DNA synthesis polymerases in DNA interstrand crosslink repair." Environ Mol Mutagen **51**(6): 552-566.

Hoefs, S. J., O. H. Skjeldal, R. J. Rodenburg, B. Nedregaard, E. P. van Kaauwen, U. Spiekerkotter, J. C. von Kleist-Retzow, J. A. Smeitink, L. G. Nijtmans and L. P. van den Heuvel (2010). "Novel mutations in the NDUFS1 gene cause low residual activities in human complex I deficiencies." Mol Genet Metab **100**(3): 251-256.

Holm, L. and C. Sander (1995). "DNA polymerase beta belongs to an ancient nucleotidyltransferase superfamily." Trends Biochem Sci **20**(9): 345-347.

Holt, I. J. (2009). "Mitochondrial DNA replication and repair: all a flap." Trends Biochem Sci **34**(7): 358-365.

Holt, I. J. and A. Reyes (2012). "Human mitochondrial DNA replication." Cold Spring Harb Perspect Biol **4**(12).

Hubscher, U., G. Maga and S. Spadari (2002). "Eukaryotic DNA polymerases." Annu Rev Biochem **71**: 133-163.

Inoue, K., K. Nakada, A. Ogura, K. Isobe, Y. Goto, I. Nonaka and J. I. Hayashi (2000). "Generation of mice with mitochondrial dysfunction by introducing mouse mtDNA carrying a deletion into zygotes." Nat Genet **26**(2): 176-181.

Irizarry, R. A., B. Hobbs, F. Collin, Y. D. Beazer-Barclay, K. J. Antonellis, U. Scherf and T. P. Speed (2003). "Exploration, normalization, and summaries of high density oligonucleotide array probe level data." Biostatistics **4**(2): 249-264.

Ito, J. and D. K. Braithwaite (1991). "Compilation and alignment of DNA polymerase sequences." Nucleic Acids Res **19**(15): 4045-4057.

Iyer, L. M., E. V. Koonin, D. D. Leipe and L. Aravind (2005). "Origin and evolution of the archaeo-eukaryotic primase superfamily and related palm-domain proteins: structural insights and new members." Nucleic Acids Res **33**(12): 3875-3896.

J, O. W., K. Kawamura, Y. Tada, H. Ohmori, H. Kimura, S. Sakiyama and M. Tagawa (2001). "DNA polymerase kappa, implicated in spontaneous and DNA damage-induced mutagenesis, is overexpressed in lung cancer." Cancer Res **61**(14): 5366-5369.

Jansen, J. G., P. Langerak, A. Tsaalbi-Shtylik, P. van den Berk, H. Jacobs and N. de Wind (2006). "Strand-biased defect in C/G transversions in hypermutating immunoglobulin genes in Rev1-deficient mice." J Exp Med **203**(2): 319-323.

Jansen, J. G., A. Tsaalbi-Shtylik, G. Hendriks, H. Gali, A. Hendel, F. Johansson, K. Erixon, Z. Livneh, L. H. Mullenders, L. Haracska and N. de Wind (2009). "Separate domains of Rev1 mediate two modes of DNA damage bypass in mammalian cells." Mol Cell Biol **29**(11): 3113-3123.

Jansen, J. G., A. Tsaalbi-Shtylik, P. Langerak, F. Calleja, C. M. Meijers, H. Jacobs and N. de Wind (2005). "The BRCT domain of mammalian Rev1 is involved in regulating DNA translesion synthesis." Nucleic Acids Res **33**(1): 356-365.

Jaruga, P. and M. Dizdaroglu (1996). "Repair of products of oxidative DNA base damage in human cells." Nucleic Acids Res **24**(8): 1389-1394.

Johnson, R. E., C. M. Kondratick, S. Prakash and L. Prakash (1999). "hRAD30 mutations in the variant form of xeroderma pigmentosum." Science **285**(5425): 263-265.

Johnson, R. E., M. T. Washington, L. Haracska, S. Prakash and L. Prakash (2000). "Eukaryotic polymerases iota and zeta act sequentially to bypass DNA lesions." Nature **406**(6799): 1015-1019.

Johnson, R. E., M. T. Washington, S. Prakash and L. Prakash (2000). "Fidelity of human DNA polymerase eta." J Biol Chem **275**(11): 7447-7450.

Johnson, R. E., S. L. Yu, S. Prakash and L. Prakash (2003). "Yeast DNA polymerase zeta (zeta) is essential for error-free replication past thymine glycol." Genes Dev **17**(1): 77-87.

Jung, E. G. (1970). "New form of molecular defect in xeroderma pigmentosum." Nature **228**(5269): 361-362.

Kaguni, L. S. (2004). "DNA polymerase gamma, the mitochondrial replicase." Annu Rev Biochem **73**: 293-320.

Kalifa, L. and E. A. Sia (2007). "Analysis of Rev1p and Pol zeta in mitochondrial mutagenesis suggests an alternative pathway of damage tolerance." DNA Repair (Amst) **6**(12): 1732-1739.

Kannouche, P., B. C. Broughton, M. Volker, F. Hanaoka, L. H. Mullenders and A. R. Lehmann (2001). "Domain structure, localization, and function of DNA polymerase eta, defective in xeroderma pigmentosum variant cells." Genes Dev **15**(2): 158-172.

Kannouche, P., A. R. Fernandez de Henestrosa, B. Coull, A. E. Vidal, C. Gray, D. Zicha, R. Woodgate and A. R. Lehmann (2002). "Localization of DNA polymerases eta and iota to the replication machinery is tightly co-ordinated in human cells." EMBO J **21**(22): 6246-6256.

Kannouche, P., A. R. Fernandez de Henestrosa, B. Coull, A. E. Vidal, C. Gray, D. Zicha, R. Woodgate and A. R. Lehmann (2003). "Localization of DNA polymerases eta and iota to the replication machinery is tightly co-ordinated in human cells." EMBO J **22**(5): 1223-1233.

Kannouche, P. and A. Stary (2003). "Xeroderma pigmentosum variant and error-prone DNA polymerases." Biochimie **85**(11): 1123-1132.

Kannouche, P. L., J. Wing and A. R. Lehmann (2004). "Interaction of human DNA polymerase eta with monoubiquitinated PCNA: a possible mechanism for the polymerase switch in response to DNA damage." Mol Cell **14**(4): 491-500.

Kano, C., F. Hanaoka and J. Y. Wang (2012). "Analysis of mice deficient in both REV1 catalytic activity and POLH reveals an unexpected role for POLH in the generation of C to G and G to C transversions during Ig gene hypermutation." Int Immunol **24**(3): 169-174.

Kasahara, A., K. Ishikawa, M. Yamaoka, M. Ito, N. Watanabe, M. Akimoto, A. Sato, K. Nakada, H. Endo, Y. Suda, S. Aizawa and J. Hayashi (2006). "Generation of trans-mitochondrial mice carrying homoplasmic mtDNAs with a missense mutation in a structural gene using ES cells." Hum Mol Genet **15**(6): 871-881.

Kasiviswanathan, R., M. A. Gustafson, W. C. Copeland and J. N. Meyer (2012). "Human mitochondrial DNA polymerase gamma exhibits potential for bypass and mutagenesis at UV-induced cyclobutane thymine dimers." J Biol Chem **287**(12): 9222-9229.

Kaufmann, W. K. (2010). "The human intra-S checkpoint response to UVC-induced DNA damage." Carcinogenesis **31**(5): 751-765.

Kawamoto, T., K. Araki, E. Sonoda, Y. M. Yamashita, K. Harada, K. Kikuchi, C. Masutani, F. Hanaoka, K. Nozaki, N. Hashimoto and S. Takeda (2005). "Dual roles for DNA polymerase eta in homologous DNA recombination and translesion DNA synthesis." Mol Cell **20**(5): 793-799.

Kawamura, K., O. W. J, R. Bahar, N. Koshikawa, T. Shishikura, A. Nakagawara, S. Sakiyama, K. Kajiwara, M. Kimura and M. Tagawa (2001). "The error-prone DNA polymerase zeta catalytic subunit (Rev3) gene is ubiquitously expressed in normal and malignant human tissues." Int J Oncol **18**(1): 97-103.

Kidane, D., A. S. Jonason, T. S. Gorton, I. Mihaylov, J. Pan, S. Keeney, D. G. de Rooij, T. Ashley, A. Keh, Y. Liu, U. Banerjee, D. Zelterman and J. B. Sweasy (2010). "DNA polymerase beta is critical for mouse meiotic synapsis." EMBO J **29**(2): 410-423.

Kielbassa, C., L. Roza and B. Epe (1997). "Wavelength dependence of oxidative DNA damage induced by UV and visible light." Carcinogenesis **18**(4): 811-816.

King, N. M., N. Nikolaishvili-Feinberg, M. F. Bryant, D. D. Luche, T. P. Heffernan, D. A. Simpson, F. Hanaoka, W. K. Kaufmann and M. Cordeiro-Stone (2005). "Overproduction of DNA polymerase eta does not raise the spontaneous mutation rate in diploid human fibroblasts." DNA Repair (Amst) **4**(6): 714-724.

Kirouac, K. N. and H. Ling (2011). "Unique active site promotes error-free replication opposite an 8-oxo-guanine lesion by human DNA polymerase iota." Proc Natl Acad Sci U S A **108**(8): 3210-3215.

Komarova, E. A., M. V. Chernov, R. Franks, K. Wang, G. Armin, C. R. Zelnick, D. M. Chin, S. S. Bacus, G. R. Stark and A. V. Gudkov (1997). "Transgenic mice with p53-responsive lacZ: p53 activity varies dramatically during normal development and determines radiation and drug sensitivity in vivo." EMBO J **16**(6): 1391-1400.

Kuchta, R. D. and G. Stengel (2010). "Mechanism and evolution of DNA primases." Biochim Biophys Acta **1804**(5): 1180-1189.

Kujoth, G. C., A. Hiona, T. D. Pugh, S. Someya, K. Panzer, S. E. Wohlgemuth, T. Hofer, A. Y. Seo, R. Sullivan, W. A. Jobling, J. D. Morrow, H. Van Remmen, J. M. Sedivy, T. Yamasoba, M. Tanokura, R. Weindruch, C. Leeuwenburgh and T. A. Prolla (2005). "Mitochondrial DNA mutations, oxidative stress, and apoptosis in mammalian aging." Science **309**(5733): 481-484.

Kukimoto, I., H. Igaki and T. Kanda (1999). "Human CDC45 protein binds to minichromosome maintenance 7 protein and the p70 subunit of DNA polymerase alpha." Eur J Biochem **265**(3): 936-943.

Kunkel, T. A. (2004). "DNA replication fidelity." J Biol Chem **279**(17): 16895-16898.

Labib, K., J. A. Tercero and J. F. Diffley (2000). "Uninterrupted MCM2-7 function required for DNA replication fork progression." Science **288**(5471): 1643-1647.

Lamperti, C. and M. Zeviani (2009). "Encephalomyopathies caused by abnormal nuclear-mitochondrial intergenomic cross-talk." Acta Myol **28**(1): 2-11.

Lange, S. S., E. Bedford, S. Reh, J. P. Wittschieben, S. Carbajal, D. F. Kusewitt, J. DiGiovanni and R. D. Wood (2013). "Dual role for mammalian DNA polymerase zeta in maintaining genome stability and proliferative responses." Proc Natl Acad Sci U S A **110**(8): E687-696.

Lange, S. S., K. Takata and R. D. Wood (2011). "DNA polymerases and cancer." Nat Rev Cancer **11**(2): 96-110.

Lao-Sirieix, S. H. and S. D. Bell (2004). "The heterodimeric primase of the hyperthermophilic archaeon Sulfolobus solfataricus possesses DNA and RNA primase, polymerase and 3'-terminal nucleotidyl transferase activities." J Mol Biol **344**(5): 1251-1263.

Latonen, L. and M. Laiho (2005). "Cellular UV damage responses--functions of tumor suppressor p53." Biochim Biophys Acta **1755**(2): 71-89.
Latonen, L., Y. Taya and M. Laiho (2001). "UV-radiation induces dose-dependent regulation of p53 response and modulates p53-HDM2 interaction in human fibroblasts." Oncogene **20**(46): 6784-6793.
Lawrence, C. W. (2004). "Cellular functions of DNA polymerase zeta and Rev1 protein." Adv Protein Chem **69**: 167-203.
Le Beau, M. M., F. V. Rassool, M. E. Neilly, R. Espinosa, 3rd, T. W. Glover, D. I. Smith and T. W. McKeithan (1998). "Replication of a common fragile site, FRA3B, occurs late in S phase and is delayed further upon induction: implications for the mechanism of fragile site induction." Hum Mol Genet **7**(4): 755-761.
Lee, D. H. and G. P. Pfeifer (2008). "Translesion synthesis of 7,8-dihydro-8-oxo-2'-deoxyguanosine by DNA polymerase eta in vivo." Mutat Res **641**(1-2): 19-26.
Lee, H. C. and Y. H. Wei (2000). "Mitochondrial role in life and death of the cell." J Biomed Sci **7**(1): 2-15.
Lehmann, A. R. (2000). "Replication of UV-damaged DNA: new insights into links between DNA polymerases, mutagenesis and human disease." Gene **253**(1): 1-12.
Lehmann, A. R. (2003). "DNA repair-deficient diseases, xeroderma pigmentosum, Cockayne syndrome and trichothiodystrophy." Biochimie **85**(11): 1101-1111.
Lehmann, A. R. (2005). "Replication of damaged DNA by translesion synthesis in human cells." FEBS Lett **579**(4): 873-876.
Lehmann, A. R., S. Kirk-Bell, C. F. Arlett, S. A. Harcourt, E. A. de Weerd-Kastelein, W. Keijzer and P. Hall-Smith (1977). "Repair of ultraviolet light damage in a variety of human fibroblast cell strains." Cancer Res **37**(3): 904-910.
Letessier, A., G. A. Millot, S. Koundrioukoff, A. M. Lachages, N. Vogt, R. S. Hansen, B. Malfoy, O. Brison and M. Debatisse (2011). "Cell-type-specific replication initiation programs set fragility of the FRA3B fragile site." Nature **470**(7332): 120-123.
Levine, R. L., H. Miller, A. Grollman, E. Ohashi, H. Ohmori, C. Masutani, F. Hanaoka and M. Moriya (2001). "Translesion DNA synthesis catalyzed by human pol eta and pol kappa across 1,N6-ethenodeoxyadenosine." J Biol Chem **276**(22): 18717-18721.
Li, Z., P. R. Musich, M. A. Serrano, Z. Dong and Y. Zou (2011). "XPA-mediated regulation of global nucleotide excision repair by ATR Is p53-dependent and occurs primarily in S-phase." PLoS One **6**(12): e28326.
Limoli, C. L., E. Giedzinski, W. M. Bonner and J. E. Cleaver (2002). "UV-induced replication arrest in the xeroderma pigmentosum variant leads to DNA double-strand breaks, gamma -H2AX formation, and Mre11 relocalization." Proc Natl Acad Sci U S A **99**(1): 233-238.
Lin, Q., A. B. Clark, S. D. McCulloch, T. Yuan, R. T. Bronson, T. A. Kunkel and R. Kucherlapati (2006). "Increased susceptibility to UV-induced skin carcinogenesis in polymerase eta-deficient mice." Cancer Res **66**(1): 87-94.
Liu, Q., S. Guntuku, X. S. Cui, S. Matsuoka, D. Cortez, K. Tamai, G. Luo, S. Carattini-Rivera, F. DeMayo, A. Bradley, L. A. Donehower and S. J. Elledge (2000). "Chk1 is an essential kinase that is regulated by Atr and required for the G(2)/M DNA damage checkpoint." Genes Dev **14**(12): 1448-1459.
Livneh, Z., O. Ziv and S. Shachar (2010). "Multiple two-polymerase mechanisms in mammalian translesion DNA synthesis." Cell Cycle **9**(4): 729-735.
Loeb, L. A., K. R. Loeb and J. P. Anderson (2003). "Multiple mutations and cancer." Proc Natl Acad Sci U S A **100**(3): 776-781.

Loeb, L. A. and R. J. Monnat, Jr. (2008). "DNA polymerases and human disease." Nat Rev Genet **9**(8): 594-604.

Lommel, L. and P. C. Hanawalt (1993). "Increased UV resistance of a xeroderma pigmentosum revertant cell line is correlated with selective repair of the transcribed strand of an expressed gene." Mol Cell Biol **13**(2): 970-976.

Lone, S., S. A. Townson, S. N. Uljon, R. E. Johnson, A. Brahma, D. T. Nair, S. Prakash, L. Prakash and A. K. Aggarwal (2007). "Human DNA polymerase kappa encircles DNA: implications for mismatch extension and lesion bypass." Mol Cell **25**(4): 601-614.

Longley, M. J., M. A. Graziewicz, R. J. Bienstock and W. C. Copeland (2005). "Consequences of mutations in human DNA polymerase gamma." Gene **354**: 125-131.

MacCallum, D. E., T. R. Hupp, C. A. Midgley, D. Stuart, S. J. Campbell, A. Harper, F. S. Walsh, E. G. Wright, A. Balmain, D. P. Lane and P. A. Hall (1996). "The p53 response to ionising radiation in adult and developing murine tissues." Oncogene **13**(12): 2575-2587.

Maher, V. M., L. M. Ouellette, R. D. Curren and J. J. McCormick (1976). "Frequency of ultraviolet light-induced mutations is higher in xeroderma pigmentosum variant cells than in normal human cells." Nature **261**(5561): 593-595.

Mailand, N., J. Falck, C. Lukas, R. G. Syljuasen, M. Welcker, J. Bartek and J. Lukas (2000). "Rapid destruction of human Cdc25A in response to DNA damage." Science **288**(5470): 1425-1429.

Mailand, N., A. V. Podtelejnikov, A. Groth, M. Mann, J. Bartek and J. Lukas (2002). "Regulation of G(2)/M events by Cdc25A through phosphorylation-dependent modulation of its stability." EMBO J **21**(21): 5911-5920.

Mangelsdorf, M., K. Ried, E. Woollatt, S. Dayan, H. Eyre, M. Finnis, L. Hobson, J. Nancarrow, D. Venter, E. Baker and R. I. Richards (2000). "Chromosomal fragile site FRA16D and DNA instability in cancer." Cancer Res **60**(6): 1683-1689.

Marini, F., A. Pellicioli, V. Paciotti, G. Lucchini, P. Plevani, D. F. Stern and M. Foiani (1997). "A role for DNA primase in coupling DNA replication to DNA damage response." EMBO J **16**(3): 639-650.

Marshall, A. J., N. Doyen, L. A. Bentolila, C. J. Paige and G. E. Wu (1998). "Terminal deoxynucleotidyl transferase expression during neonatal life alters D(H) reading frame usage and Ig-receptor-dependent selection of V regions." J Immunol **161**(12): 6657-6663.

Martomo, S. A., W. W. Yang, A. Vaisman, A. Maas, M. Yokoi, J. H. Hoeijmakers, F. Hanaoka, R. Woodgate and P. J. Gearhart (2006). "Normal hypermutation in antibody genes from congenic mice defective for DNA polymerase iota." DNA Repair (Amst) **5**(3): 392-398.

Martomo, S. A., W. W. Yang, R. P. Wersto, T. Ohkumo, Y. Kondo, M. Yokoi, C. Masutani, F. Hanaoka and P. J. Gearhart (2005). "Different mutation signatures in DNA polymerase eta- and MSH6-deficient mice suggest separate roles in antibody diversification." Proc Natl Acad Sci U S A **102**(24): 8656-8661.

Masutani, C., M. Araki, A. Yamada, R. Kusumoto, T. Nogimori, T. Maekawa, S. Iwai and F. Hanaoka (1999). "Xeroderma pigmentosum variant (XP-V) correcting protein from HeLa cells has a thymine dimer bypass DNA polymerase activity." EMBO J **18**(12): 3491-3501.

Matsuda, T., K. Bebenek, C. Masutani, F. Hanaoka and T. A. Kunkel (2000). "Low fidelity DNA synthesis by human DNA polymerase-eta." Nature **404**(6781): 1011-1013.

McCulloch, S. D. and T. A. Kunkel (2008). "The fidelity of DNA synthesis by eukaryotic replicative and translesion synthesis polymerases." Cell Res **18**(1): 148-161.

McDonald, J. P., E. G. Frank, B. S. Plosky, I. B. Rogozin, C. Masutani, F. Hanaoka, R. Woodgate and P. J. Gearhart (2003). "129-derived strains of mice are deficient in DNA polymerase iota and have normal immunoglobulin hypermutation." J Exp Med **198**(4): 635-643.

McDonald, J. P., V. Rapic-Otrin, J. A. Epstein, B. C. Broughton, X. Wang, A. R. Lehmann, D. J. Wolgemuth and R. Woodgate (1999). "Novel human and mouse homologs of Saccharomyces cerevisiae DNA polymerase eta." Genomics **60**(1): 20-30.

McHugh, P. J. and S. Sarkar (2006). "DNA interstrand cross-link repair in the cell cycle: a critical role for polymerase zeta in G1 phase." Cell Cycle **5**(10): 1044-1047.

McIlwraith, M. J., A. Vaisman, Y. Liu, E. Fanning, R. Woodgate and S. C. West (2005). "Human DNA polymerase eta promotes DNA synthesis from strand invasion intermediates of homologous recombination." Mol Cell **20**(5): 783-792.

Mechali, M. (2010). "Eukaryotic DNA replication origins: many choices for appropriate answers." Nat Rev Mol Cell Biol **11**(10): 728-738.

Michael, W. M., R. Ott, E. Fanning and J. Newport (2000). "Activation of the DNA replication checkpoint through RNA synthesis by primase." Science **289**(5487): 2133-2137.

Michalet, X., R. Ekong, F. Fougerousse, S. Rousseaux, C. Schurra, N. Hornigold, M. van Slegtenhorst, J. Wolfe, S. Povey, J. S. Beckmann and A. Bensimon (1997). "Dynamic molecular combing: stretching the whole human genome for high-resolution studies." Science **277**(5331): 1518-1523.

Mitchell, D. L. (1988). "The relative cytotoxicity of (6-4) photoproducts and cyclobutane dimers in mammalian cells." Photochem Photobiol **48**(1): 51-57.

Mrasek, K., C. Schoder, A. C. Teichmann, K. Behr, B. Franze, K. Wilhelm, N. Blaurock, U. Claussen, T. Liehr and A. Weise (2010). "Global screening and extended nomenclature for 230 aphidicolin-inducible fragile sites, including 61 yet unreported ones." Int J Oncol **36**(4): 929-940.

Mukhopadhyay, S., D. R. Clark, N. B. Watson, W. Zacharias and W. G. McGregor (2004). "REV1 accumulates in DNA damage-induced nuclear foci in human cells and is implicated in mutagenesis by benzo[a]pyrenediolepoxide." Nucleic Acids Res **32**(19): 5820-5826.

Murakumo, Y., S. Mizutani, M. Yamaguchi, M. Ichihara and M. Takahashi (2006). "Analyses of ultraviolet-induced focus formation of hREV1 protein." Genes Cells **11**(3): 193-205.

Murphy, M. P. (2009). "How mitochondria produce reactive oxygen species." Biochem J **417**(1): 1-13.

Musio, A., C. Montagna, T. Mariani, M. Tilenni, M. L. Focarelli, L. Brait, E. Indino, P. A. Benedetti, L. Chessa, A. Albertini, T. Ried and P. Vezzoni (2005). "SMC1 involvement in fragile site expression." Hum Mol Genet **14**(4): 525-533.

Muzi-Falconi, M., M. Giannattasio, M. Foiani and P. Plevani (2003). "The DNA polymerase alpha-primase complex: multiple functions and interactions." ScientificWorldJournal **3**: 21-33.

Myhr, B. C., D. Turnbull and J. A. DiPaolo (1979). "Ultraviolet mutagenesis of normal and xeroderma pigmentosum variant human fibroblasts." Mutat Res **62**(2): 341-353.

Nair, D. T., R. E. Johnson, L. Prakash, S. Prakash and A. K. Aggarwal (2005). "Rev1 employs a novel mechanism of DNA synthesis using a protein template." Science **309**(5744): 2219-2222.

Nakada, K., A. Sato, H. Sone, A. Kasahara, K. Ikeda, Y. Kagawa, H. Yonekawa and J. Hayashi (2004). "Accumulation of pathogenic DeltamtDNA induced deafness but not diabetic phenotypes in mito-mice." Biochem Biophys Res Commun **323**(1): 175-184.

Narayanan, D. L., R. N. Saladi and J. L. Fox (2010). "Ultraviolet radiation and skin cancer." Int J Dermatol **49**(9): 978-986.

Nasheuer, H. P., R. Smith, C. Bauerschmidt, F. Grosse and K. Weisshart (2002). "Initiation of eukaryotic DNA replication: regulation and mechanisms." Prog Nucleic Acid Res Mol Biol **72**: 41-94.

Naviaux, R. K. and K. V. Nguyen (2004). "POLG mutations associated with Alpers' syndrome and mitochondrial DNA depletion." Ann Neurol **55**(5): 706-712.

Naviaux, R. K., W. L. Nyhan, B. A. Barshop, J. Poulton, D. Markusic, N. C. Karpinski and R. H. Haas (1999). "Mitochondrial DNA polymerase gamma deficiency and mtDNA depletion in a child with Alpers' syndrome." Ann Neurol **45**(1): 54-58.

Nelson, J. R., P. E. Gibbs, A. M. Nowicka, D. C. Hinkle and C. W. Lawrence (2000). "Evidence for a second function for Saccharomyces cerevisiae Rev1p." Mol Microbiol **37**(3): 549-554.

Nelson, J. R., C. W. Lawrence and D. C. Hinkle (1996). "Thymine-thymine dimer bypass by yeast DNA polymerase zeta." Science **272**(5268): 1646-1649.

Nguyen, K. V., F. S. Sharief, S. S. Chan, W. C. Copeland and R. K. Naviaux (2006). "Molecular diagnosis of Alpers syndrome." J Hepatol **45**(1): 108-116.

Nick McElhinny, S. A., D. A. Gordenin, C. M. Stith, P. M. Burgers and T. A. Kunkel (2008). "Division of labor at the eukaryotic replication fork." Mol Cell **30**(2): 137-144.

Ogawa, T., T. A. Baker, A. van der Ende and A. Kornberg (1985). "Initiation of enzymatic replication at the origin of the Escherichia coli chromosome: contributions of RNA polymerase and primase." Proc Natl Acad Sci U S A **82**(11): 3562-3566.

Ogi, T. and A. R. Lehmann (2006). "The Y-family DNA polymerase kappa (pol kappa) functions in mammalian nucleotide-excision repair." Nat Cell Biol **8**(6): 640-642.

Ogi, T., S. Limsirichaikul, R. M. Overmeer, M. Volker, K. Takenaka, R. Cloney, Y. Nakazawa, A. Niimi, Y. Miki, N. G. Jaspers, L. H. Mullenders, S. Yamashita, M. I. Fousteri and A. R. Lehmann (2010). "Three DNA polymerases, recruited by different mechanisms, carry out NER repair synthesis in human cells." Mol Cell **37**(5): 714-727.

Ogi, T., J. Mimura, M. Hikida, H. Fujimoto, Y. Fujii-Kuriyama and H. Ohmori (2001). "Expression of human and mouse genes encoding polkappa: testis-specific developmental regulation and AhR-dependent inducible transcription." Genes Cells **6**(11): 943-953.

Ogi, T., Y. Shinkai, K. Tanaka and H. Ohmori (2002). "Polkappa protects mammalian cells against the lethal and mutagenic effects of benzo[a]pyrene." Proc Natl Acad Sci U S A **99**(24): 15548-15553.

Ohashi, E., K. Bebenek, T. Matsuda, W. J. Feaver, V. L. Gerlach, E. C. Friedberg, H. Ohmori and T. A. Kunkel (2000). "Fidelity and processivity of DNA synthesis by DNA polymerase kappa, the product of the human DINB1 gene." J Biol Chem **275**(50): 39678-39684.

Ohkumo, T., Y. Kondo, M. Yokoi, T. Tsukamoto, A. Yamada, T. Sugimoto, R. Kanao, Y. Higashi, H. Kondoh, M. Tatematsu, C. Masutani and F. Hanaoka (2006). "UV-B radiation induces epithelial tumors in mice lacking DNA polymerase eta and

mesenchymal tumors in mice deficient for DNA polymerase iota." Mol Cell Biol **26**(20): 7696-7706.
Ohmori, H., E. C. Friedberg, R. P. Fuchs, M. F. Goodman, F. Hanaoka, D. Hinkle, T. A. Kunkel, C. W. Lawrence, Z. Livneh, T. Nohmi, L. Prakash, S. Prakash, T. Todo, G. C. Walker, Z. Wang and R. Woodgate (2001). "The Y-family of DNA polymerases." Mol Cell **8**(1): 7-8.
Okazaki, R., T. Okazaki, K. Sakabe and K. Sugimoto (1967). "Mechanism of DNA replication possible discontinuity of DNA chain growth." Jpn J Med Sci Biol **20**(3): 255-260.
Otsuka, C., N. Kunitomi, S. Iwai, D. Loakes and K. Negishi (2005). "Roles of the polymerase and BRCT domains of Rev1 protein in translesion DNA synthesis in yeast in vivo." Mutat Res **578**(1-2): 79-87.
Ozeri-Galai, E., A. C. Bester and B. Kerem (2012). "The complex basis underlying common fragile site instability in cancer." Trends Genet **28**(6): 295-302.
Ozeri-Galai, E., R. Lebofsky, A. Rahat, A. C. Bester, A. Bensimon and B. Kerem (2011). "Failure of origin activation in response to fork stalling leads to chromosomal instability at fragile sites." Mol Cell **43**(1): 122-131.
Paige, A. J., K. J. Taylor, C. Taylor, S. G. Hillier, S. Farrington, D. Scott, D. J. Porteous, J. F. Smyth, H. Gabra and J. E. Watson (2001). "WWOX: a candidate tumor suppressor gene involved in multiple tumor types." Proc Natl Acad Sci U S A **98**(20): 11417-11422.
Palakodeti, A., Y. Han, Y. Jiang and M. M. Le Beau (2004). "The role of late/slow replication of the FRA16D in common fragile site induction." Genes Chromosomes Cancer **39**(1): 71-76.
Palakodeti, A., I. Lucas, Y. Jiang, D. J. Young, A. A. Fernald, T. Karrison and M. M. Le Beau (2010). "Impaired replication dynamics at the FRA3B common fragile site." Hum Mol Genet **19**(1): 99-110.
Palumbo, E., L. Matricardi, E. Tosoni, A. Bensimon and A. Russo (2010). "Replication dynamics at common fragile site FRA6E." Chromosoma **119**(6): 575-587.
Pan, H. and D. B. Wigley (2000). "Structure of the zinc-binding domain of Bacillus stearothermophilus DNA primase." Structure **8**(3): 231-239.
Pan, Q., Y. Fang, Y. Xu, K. Zhang and X. Hu (2005). "Down-regulation of DNA polymerases kappa, eta, iota, and zeta in human lung, stomach, and colorectal cancers." Cancer Lett **217**(2): 139-147.
Patrick, S. M., G. G. Oakley, K. Dixon and J. J. Turchi (2005). "DNA damage induced hyperphosphorylation of replication protein A. 2. Characterization of DNA binding activity, protein interactions, and activity in DNA replication and repair." Biochemistry **44**(23): 8438-8448.
Petta, T. B., S. Nakajima, A. Zlatanou, E. Despras, S. Couve-Privat, A. Ishchenko, A. Sarasin, A. Yasui and P. Kannouche (2008). "Human DNA polymerase iota protects cells against oxidative stress." EMBO J **27**(21): 2883-2895.
Pfeifer, G. P., Y. H. You and A. Besaratinia (2005). "Mutations induced by ultraviolet light." Mutat Res **571**(1-2): 19-31.
Picchio, M. C., E. S. Martin, R. Cesari, G. A. Calin, S. Yendamuri, T. Kuroki, F. Pentimalli, M. Sarti, K. Yoder, L. R. Kaiser, R. Fishel and C. M. Croce (2004). "Alterations of the tumor suppressor gene Parkin in non-small cell lung cancer." Clin Cancer Res **10**(8): 2720-2724.
Pillaire, M. J., R. Betous, C. Conti, J. Czaplicki, P. Pasero, A. Bensimon, C. Cazaux and J. S. Hoffmann (2007). "Upregulation of error-prone DNA polymerases beta and kappa

slows down fork progression without activating the replication checkpoint." Cell Cycle **6**(4): 471-477.

Pitcher, R. S., N. C. Brissett, A. J. Picher, P. Andrade, R. Juarez, D. Thompson, G. C. Fox, L. Blanco and A. J. Doherty (2007). "Structure and function of a mycobacterial NHEJ DNA repair polymerase." J Mol Biol **366**(2): 391-405.

Pitcher, R. S., L. M. Tonkin, J. M. Daley, P. L. Palmbos, A. J. Green, T. L. Velting, A. Brzostek, M. Korycka-Machala, S. Cresawn, J. Dziadek, G. F. Hatfull, T. E. Wilson and A. J. Doherty (2006). "Mycobacteriophage exploit NHEJ to facilitate genome circularization." Mol Cell **23**(5): 743-748.

Plosky, B. S., A. E. Vidal, A. R. Fernandez de Henestrosa, M. P. McLenigan, J. P. McDonald, S. Mead and R. Woodgate (2006). "Controlling the subcellular localization of DNA polymerases iota and eta via interactions with ubiquitin." EMBO J **25**(12): 2847-2855.

Poltoratsky, V., C. J. Woo, B. Tippin, A. Martin, M. F. Goodman and M. D. Scharff (2001). "Expression of error-prone polymerases in BL2 cells activated for Ig somatic hypermutation." Proc Natl Acad Sci U S A **98**(14): 7976-7981.

Prakash, S., R. E. Johnson and L. Prakash (2005). "Eukaryotic translesion synthesis DNA polymerases: specificity of structure and function." Annu Rev Biochem **74**: 317-353.

Prasad, R., M. J. Longley, F. S. Sharief, E. W. Hou, W. C. Copeland and S. H. Wilson (2009). "Human DNA polymerase theta possesses 5'-dRP lyase activity and functions in single-nucleotide base excision repair in vitro." Nucleic Acids Res **37**(6): 1868-1877.

Qin, X., S. Zhang, H. Oda, Y. Nakatsuru, S. Shimizu, Y. Yamazaki, O. Nikaido and T. Ishikawa (1995). "Quantitative detection of ultraviolet light-induced photoproducts in mouse skin by immunohistochemistry." Jpn J Cancer Res **86**(11): 1041-1048.

Rasmussen, A. K., A. Chatterjee, L. J. Rasmussen and K. K. Singh (2003). "Mitochondria-mediated nuclear mutator phenotype in Saccharomyces cerevisiae." Nucleic Acids Res **31**(14): 3909-3917.

Rastogi, R. P., Richa, A. Kumar, M. B. Tyagi and R. P. Sinha (2010). "Molecular mechanisms of ultraviolet radiation-induced DNA damage and repair." J Nucleic Acids **2010**: 592980.

Rey, L., J. M. Sidorova, N. Puget, F. Boudsocq, D. S. Biard, R. J. Monnat, Jr., C. Cazaux and J. S. Hoffmann (2009). "Human DNA polymerase eta is required for common fragile site stability during unperturbed DNA replication." Mol Cell Biol **29**(12): 3344-3354.

Robbins, J. H., K. H. Kraemer and B. A. Flaxman (1975). "DNA repair in tumor cells from the variant form of xeroderma pigmentosum." J Invest Dermatol **64**(3): 150-155.

Rogakou, E. P., D. R. Pilch, A. H. Orr, V. S. Ivanova and W. M. Bonner (1998). "DNA double-stranded breaks induce histone H2AX phosphorylation on serine 139." J Biol Chem **273**(10): 5858-5868.

Ross, A. L. and J. E. Sale (2006). "The catalytic activity of REV1 is employed during immunoglobulin gene diversification in DT40." Mol Immunol **43**(10): 1587-1594.

Roush, A. A., M. Suarez, E. C. Friedberg, M. Radman and W. Siede (1998). "Deletion of the Saccharomyces cerevisiae gene RAD30 encoding an Escherichia coli DinB homolog confers UV radiation sensitivity and altered mutability." Mol Gen Genet **257**(6): 686-692.

Rozier, L., E. El-Achkar, F. Apiou and M. Debatisse (2004). "Characterization of a conserved aphidicolin-sensitive common fragile site at human 4q22 and mouse

6C1: possible association with an inherited disease and cancer." Oncogene **23**(41): 6872-6880.
Sale, J. E., A. R. Lehmann and R. Woodgate (2012). "Y-family DNA polymerases and their role in tolerance of cellular DNA damage." Nat Rev Mol Cell Biol **13**(3): 141-152.
Santamaria, D., E. Viguera, M. L. Martinez-Robles, O. Hyrien, P. Hernandez, D. B. Krimer and J. B. Schvartzman (2000). "Bi-directional replication and random termination." Nucleic Acids Res **28**(10): 2099-2107.
Sarkaria, J. N., E. C. Busby, R. S. Tibbetts, P. Roos, Y. Taya, L. M. Karnitz and R. T. Abraham (1999). "Inhibition of ATM and ATR kinase activities by the radiosensitizing agent, caffeine." Cancer Res **59**(17): 4375-4382.
Sarkies, P., C. Reams, L. J. Simpson and J. E. Sale (2010). "Epigenetic instability due to defective replication of structured DNA." Mol Cell **40**(5): 703-713.
Schenten, D., V. L. Gerlach, C. Guo, S. Velasco-Miguel, C. L. Hladik, C. L. White, E. C. Friedberg, K. Rajewsky and G. Esposito (2002). "DNA polymerase kappa deficiency does not affect somatic hypermutation in mice." Eur J Immunol **32**(11): 3152-3160.
Schmitt, M. W., Y. Matsumoto and L. A. Loeb (2009). "High fidelity and lesion bypass capability of human DNA polymerase delta." Biochimie **91**(9): 1163-1172.
Shachar, S., O. Ziv, S. Avkin, S. Adar, J. Wittschieben, T. Reissner, S. Chaney, E. C. Friedberg, Z. Wang, T. Carell, N. Geacintov and Z. Livneh (2009). "Two-polymerase mechanisms dictate error-free and error-prone translesion DNA synthesis in mammals." EMBO J **28**(4): 383-393.
Sharma, S., J. K. Hicks, C. L. Chute, J. R. Brennan, J. Y. Ahn, T. W. Glover and C. E. Canman (2012). "REV1 and polymerase zeta facilitate homologous recombination repair." Nucleic Acids Res **40**(2): 682-691.
Sheaff, R., D. Ilsley and R. Kuchta (1991). "Mechanism of DNA polymerase alpha inhibition by aphidicolin." Biochemistry **30**(35): 8590-8597.
Sheaff, R. J. and R. D. Kuchta (1994). "Misincorporation of nucleotides by calf thymus DNA primase and elongation of primers containing multiple noncognate nucleotides by DNA polymerase alpha." J Biol Chem **269**(30): 19225-19231.
Shiloh, Y. (2003). "ATM and related protein kinases: safeguarding genome integrity." Nat Rev Cancer **3**(3): 155-168.
Shimizu, T., T. Azuma, M. Ishiguro, N. Kanjo, S. Yamada and H. Ohmori (2005). "Normal immunoglobulin gene somatic hypermutation in Pol kappa-Pol iota double-deficient mice." Immunol Lett **98**(2): 259-264.
Shimizu, T., Y. Shinkai, T. Ogi, H. Ohmori and T. Azuma (2003). "The absence of DNA polymerase kappa does not affect somatic hypermutation of the mouse immunoglobulin heavy chain gene." Immunol Lett **86**(3): 265-270.
Shmookler Reis, R. J. and S. Goldstein (1983). "Mitochondrial DNA in mortal and immortal human cells. Genome number, integrity, and methylation." J Biol Chem **258**(15): 9078-9085.
Simpson, L. J. and J. E. Sale (2003). "Rev1 is essential for DNA damage tolerance and non-templated immunoglobulin gene mutation in a vertebrate cell line." EMBO J **22**(7): 1654-1664.
Skoneczna, A., J. McIntyre, M. Skoneczny, Z. Policinska and E. Sledziewska-Gojska (2007). "Polymerase eta is a short-lived, proteasomally degraded protein that is temporarily stabilized following UV irradiation in Saccharomyces cerevisiae." J Mol Biol **366**(4): 1074-1086.

Smith, L. A., A. V. Makarova, L. Samson, K. E. Thiesen, A. Dhar and T. Bessho (2012). "Bypass of a psoralen DNA interstrand cross-link by DNA polymerases beta, iota, and kappa in vitro." Biochemistry **51**(44): 8931-8938.

Soria, G., L. Belluscio, W. A. van Cappellen, R. Kanaar, J. Essers and V. Gottifredi (2009). "DNA damage induced Pol eta recruitment takes place independently of the cell cycle phase." Cell Cycle **8**(20): 3340-3348.

Stancel, J. N., L. D. McDaniel, S. Velasco, J. Richardson, C. Guo and E. C. Friedberg (2009). "Polk mutant mice have a spontaneous mutator phenotype." DNA Repair (Amst) **8**(12): 1355-1362.

Stavnezer, J., J. E. Guikema and C. E. Schrader (2008). "Mechanism and regulation of class switch recombination." Annu Rev Immunol **26**: 261-292.

Stucki, M., B. Pascucci, E. Parlanti, P. Fortini, S. H. Wilson, U. Hubscher and E. Dogliotti (1998). "Mammalian base excision repair by DNA polymerases delta and epsilon." Oncogene **17**(7): 835-843.

Stumpf, J. D. and W. C. Copeland (2011). "Mitochondrial DNA replication and disease: insights from DNA polymerase gamma mutations." Cell Mol Life Sci **68**(2): 219-233.

Suomalainen, A., A. Majander, M. Wallin, K. Setala, K. Kontula, H. Leinonen, T. Salmi, A. Paetau, M. Haltia, L. Valanne, J. Lonnqvist, L. Peltonen and H. Somer (1997). "Autosomal dominant progressive external ophthalmoplegia with multiple deletions of mtDNA: clinical, biochemical, and molecular genetic features of the 10q-linked disease." Neurology **48**(5): 1244-1253.

Svoboda, D. L., L. P. Briley and J. M. Vos (1998). "Defective bypass replication of a leading strand cyclobutane thymine dimer in xeroderma pigmentosum variant cell extracts." Cancer Res **58**(11): 2445-2448.

Takenaka, K., T. Ogi, T. Okada, E. Sonoda, C. Guo, E. C. Friedberg and S. Takeda (2006). "Involvement of vertebrate Polkappa in translesion DNA synthesis across DNA monoalkylation damage." J Biol Chem **281**(4): 2000-2004.

Tauchi, H., J. Kobayashi, K. Morishima, D. C. van Gent, T. Shiraishi, N. S. Verkaik, D. vanHeems, E. Ito, A. Nakamura, E. Sonoda, M. Takata, S. Takeda, S. Matsuura and K. Komatsu (2002). "Nbs1 is essential for DNA repair by homologous recombination in higher vertebrate cells." Nature **420**(6911): 93-98.

Thorland, E. C., S. L. Myers, D. H. Persing, G. Sarkar, R. M. McGovern, B. S. Gostout and D. I. Smith (2000). "Human papillomavirus type 16 integrations in cervical tumors frequently occur in common fragile sites." Cancer Res **60**(21): 5916-5921.

Tibbetts, R. S., K. M. Brumbaugh, J. M. Williams, J. N. Sarkaria, W. A. Cliby, S. Y. Shieh, Y. Taya, C. Prives and R. T. Abraham (1999). "A role for ATR in the DNA damage-induced phosphorylation of p53." Genes Dev **13**(2): 152-157.

Tissier, A., E. G. Frank, J. P. McDonald, S. Iwai, F. Hanaoka and R. Woodgate (2000). "Misinsertion and bypass of thymine-thymine dimers by human DNA polymerase iota." EMBO J **19**(19): 5259-5266.

Tissier, A., P. Kannouche, M. P. Reck, A. R. Lehmann, R. P. Fuchs and A. Cordonnier (2004). "Co-localization in replication foci and interaction of human Y-family members, DNA polymerase pol eta and REVl protein." DNA Repair (Amst) **3**(11): 1503-1514.

Toledo, L. I., M. Murga, R. Zur, R. Soria, A. Rodriguez, S. Martinez, J. Oyarzabal, J. Pastor, J. R. Bischoff and O. Fernandez-Capetillo (2011). "A cell-based screen identifies ATR inhibitors with synthetic lethal properties for cancer-associated mutations." Nat Struct Mol Biol **18**(6): 721-727.

Trifunovic, A., A. Wredenberg, M. Falkenberg, J. N. Spelbrink, A. T. Rovio, C. E. Bruder, Y. M. Bohlooly, S. Gidlof, A. Oldfors, R. Wibom, J. Tornell, H. T. Jacobs and N. G. Larsson (2004). "Premature ageing in mice expressing defective mitochondrial DNA polymerase." Nature **429**(6990): 417-423.

Tsaalbi-Shtylik, A., J. W. Verspuy, J. G. Jansen, H. Rebel, L. M. Carlee, M. A. van der Valk, J. Jonkers, F. R. de Gruijl and N. de Wind (2009). "Error-prone translesion replication of damaged DNA suppresses skin carcinogenesis by controlling inflammatory hyperplasia." Proc Natl Acad Sci U S A **106**(51): 21836-21841.

Tsantoulis, P. K., A. Kotsinas, P. P. Sfikakis, K. Evangelou, M. Sideridou, B. Levy, L. Mo, C. Kittas, X. R. Wu, A. G. Papavassiliou and V. G. Gorgoulis (2008). "Oncogene-induced replication stress preferentially targets common fragile sites in preneoplastic lesions. A genome-wide study." Oncogene **27**(23): 3256-3264.

Vaisman, A., E. G. Frank, S. Iwai, E. Ohashi, H. Ohmori, F. Hanaoka and R. Woodgate (2003). "Sequence context-dependent replication of DNA templates containing UV-induced lesions by human DNA polymerase iota." DNA Repair (Amst) **2**(9): 991-1006.

van der Ende, A., T. A. Baker, T. Ogawa and A. Kornberg (1985). "Initiation of enzymatic replication at the origin of the Escherichia coli chromosome: primase as the sole priming enzyme." Proc Natl Acad Sci U S A **82**(12): 3954-3958.

Van Goethem, G., B. Dermaut, A. Lofgren, J. J. Martin and C. Van Broeckhoven (2001). "Mutation of POLG is associated with progressive external ophthalmoplegia characterized by mtDNA deletions." Nat Genet **28**(3): 211-212.

Van Goethem, G., P. Luoma, M. Rantamaki, A. Al Memar, S. Kaakkola, P. Hackman, R. Krahe, A. Lofgren, J. J. Martin, P. De Jonghe, A. Suomalainen, B. Udd and C. Van Broeckhoven (2004). "POLG mutations in neurodegenerative disorders with ataxia but no muscle involvement." Neurology **63**(7): 1251-1257.

Van Goethem, G., J. J. Martin, B. Dermaut, A. Lofgren, A. Wibail, D. Ververken, P. Tack, I. Dehaene, M. Van Zandijcke, M. Moonen, C. Ceuterick, P. De Jonghe and C. Van Broeckhoven (2003). "Recessive POLG mutations presenting with sensory and ataxic neuropathy in compound heterozygote patients with progressive external ophthalmoplegia." Neuromuscul Disord **13**(2): 133-142.

Veal, E. A., A. M. Day and B. A. Morgan (2007). "Hydrogen peroxide sensing and signaling." Mol Cell **26**(1): 1-14.

Velasco-Miguel, S., J. A. Richardson, V. L. Gerlach, W. C. Lai, T. Gao, L. D. Russell, C. L. Hladik, C. L. White and E. C. Friedberg (2003). "Constitutive and regulated expression of the mouse Dinb (Polkappa) gene encoding DNA polymerase kappa." DNA Repair (Amst) **2**(1): 91-106.

Vidal, A. E. and R. Woodgate (2009). "Insights into the cellular role of enigmatic DNA polymerase iota." DNA Repair (Amst) **8**(3): 420-423.

Villani, G., S. Boiteux and M. Radman (1978). "Mechanism of ultraviolet-induced mutagenesis: extent and fidelity of in vitro DNA synthesis on irradiated templates." Proc Natl Acad Sci U S A **75**(7): 3037-3041.

Volker, M., M. J. Mone, P. Karmakar, A. van Hoffen, W. Schul, W. Vermeulen, J. H. Hoeijmakers, R. van Driel, A. A. van Zeeland and L. H. Mullenders (2001). "Sequential assembly of the nucleotide excision repair factors in vivo." Mol Cell **8**(1): 213-224.

Vreeswijk, M. P., A. van Hoffen, B. E. Westland, H. Vrieling, A. A. van Zeeland and L. H. Mullenders (1994). "Analysis of repair of cyclobutane pyrimidine dimers and

pyrimidine 6-4 pyrimidone photoproducts in transcriptionally active and inactive genes in Chinese hamster cells." J Biol Chem **269**(50): 31858-31863.

Waga, S. and B. Stillman (1998). "The DNA replication fork in eukaryotic cells." Annu Rev Biochem **67**: 721-751.

Wakasugi, M. and A. Sancar (1999). "Order of assembly of human DNA repair excision nuclease." J Biol Chem **274**(26): 18759-18768.

Walsh, E., X. Wang, M. Y. Lee and K. A. Eckert (2013). "Mechanism of replicative DNA polymerase delta pausing and a potential role for DNA polymerase kappa in common fragile site replication." J Mol Biol **425**(2): 232-243.

Wang, C. H., S. B. Wu, Y. T. Wu and Y. H. Wei (2013). "Oxidative stress response elicited by mitochondrial dysfunction: implication in the pathophysiology of aging." Exp Biol Med (Maywood) **238**(5): 450-460.

Wang, H., W. Wu, H. W. Wang, S. Wang, Y. Chen, X. Zhang, J. Yang, S. Zhao, H. F. Ding and D. Lu (2010). "Analysis of specialized DNA polymerases expression in human gliomas: association with prognostic significance." Neuro Oncol **12**(7): 679-686.

Wang, H., S. Y. Zhang, S. Wang, J. Lu, W. Wu, L. Weng, D. Chen, Y. Zhang, Z. Lu, J. Yang, Y. Chen, X. Zhang, X. Chen, C. Xi, D. Lu and S. Zhao (2009). "REV3L confers chemoresistance to cisplatin in human gliomas: the potential of its RNAi for synergistic therapy." Neuro Oncol **11**(6): 790-802.

Wang, X., C. A. Peterson, H. Zheng, R. S. Nairn, R. J. Legerski and L. Li (2001). "Involvement of nucleotide excision repair in a recombination-independent and error-prone pathway of DNA interstrand cross-link repair." Mol Cell Biol **21**(3): 713-720.

Wang, Y., M. Seimiya, K. Kawamura, L. Yu, T. Ogi, K. Takenaga, T. Shishikura, A. Nakagawara, S. Sakiyama, M. Tagawa and O. W. J (2004). "Elevated expression of DNA polymerase kappa in human lung cancer is associated with p53 inactivation: Negative regulation of POLK promoter activity by p53." Int J Oncol **25**(1): 161-165.

Wang, Y., R. Woodgate, T. P. McManus, S. Mead, J. J. McCormick and V. M. Maher (2007). "Evidence that in xeroderma pigmentosum variant cells, which lack DNA polymerase eta, DNA polymerase iota causes the very high frequency and unique spectrum of UV-induced mutations." Cancer Res **67**(7): 3018-3026.

Wanrooij, S., J. M. Fuste, G. Farge, Y. Shi, C. M. Gustafsson and M. Falkenberg (2008). "Human mitochondrial RNA polymerase primes lagging-strand DNA synthesis in vitro." Proc Natl Acad Sci U S A **105**(32): 11122-11127.

Watanabe, K., S. Tateishi, M. Kawasuji, T. Tsurimoto, H. Inoue and M. Yamaizumi (2004). "Rad18 guides poleta to replication stalling sites through physical interaction and PCNA monoubiquitination." EMBO J **23**(19): 3886-3896.

Waters, L. S. and G. C. Walker (2006). "The critical mutagenic translesion DNA polymerase Rev1 is highly expressed during G(2)/M phase rather than S phase." Proc Natl Acad Sci U S A **103**(24): 8971-8976.

Weisshart, K., H. Forster, E. Kremmer, B. Schlott, F. Grosse and H. P. Nasheuer (2000). "Protein-protein interactions of the primase subunits p58 and p48 with simian virus 40 T antigen are required for efficient primer synthesis in a cell-free system." J Biol Chem **275**(23): 17328-17337.

Weller, G. R., B. Kysela, R. Roy, L. M. Tonkin, E. Scanlan, M. Della, S. K. Devine, J. P. Day, A. Wilkinson, F. d'Adda di Fagagna, K. M. Devine, R. P. Bowater, P. A. Jeggo, S. P. Jackson and A. J. Doherty (2002). "Identification of a DNA nonhomologous end-joining complex in bacteria." Science **297**(5587): 1686-1689.

Wernette, C. M., M. C. Conway and L. S. Kaguni (1988). "Mitochondrial DNA polymerase from Drosophila melanogaster embryos: kinetics, processivity, and fidelity of DNA polymerization." Biochemistry **27**(16): 6046-6054.

Winter, D. B., Q. H. Phung, R. D. Wood and P. J. Gearhart (2000). "Differential expression of DNA polymerase epsilon in resting and activated B lymphocytes is consistent with an in vivo role in replication and not repair." Mol Immunol **37**(3-4): 125-131.

Winterthun, S., G. Ferrari, L. He, R. W. Taylor, M. Zeviani, D. M. Turnbull, B. A. Engelsen, G. Moen and L. A. Bindoff (2005). "Autosomal recessive mitochondrial ataxic syndrome due to mitochondrial polymerase gamma mutations." Neurology **64**(7): 1204-1208.

Wittschieben, J., M. K. Shivji, E. Lalani, M. A. Jacobs, F. Marini, P. J. Gearhart, I. Rosewell, G. Stamp and R. D. Wood (2000). "Disruption of the developmentally regulated Rev3l gene causes embryonic lethality." Curr Biol **10**(19): 1217-1220.

Wong, T. W. and D. A. Clayton (1985). "Isolation and characterization of a DNA primase from human mitochondria." J Biol Chem **260**(21): 11530-11535.

Wong, T. W. and D. A. Clayton (1986). "DNA primase of human mitochondria is associated with structural RNA that is essential for enzymatic activity." Cell **45**(6): 817-825.

Xu, F., J. B. Addis, J. M. Cameron and B. H. Robinson (2012). "LRPPRC mutation suppresses cytochrome oxidase activity by altering mitochondrial RNA transcript stability in a mouse model." Biochem J **441**(1): 275-283.

Yagi, T., J. Tatsumi-Miyajima, M. Sato, K. H. Kraemer and H. Takebe (1991). "Analysis of point mutations in an ultraviolet-irradiated shuttle vector plasmid propagated in cells from Japanese xeroderma pigmentosum patients in complementation groups A and F." Cancer Res **51**(12): 3177-3182.

Yamada, A., C. Masutani, S. Iwai and F. Hanaoka (2000). "Complementation of defective translesion synthesis and UV light sensitivity in xeroderma pigmentosum variant cells by human and mouse DNA polymerase eta." Nucleic Acids Res **28**(13): 2473-2480.

Yamamoto, J., D. Loakes, C. Masutani, S. Simmyo, K. Urabe, F. Hanaoka, P. Holliger and S. Iwai (2008). "Translesion synthesis across the (6-4) photoproduct and its Dewar valence isomer by the Y-family and engineered DNA polymerases." Nucleic Acids Symp Ser (Oxf)(52): 339-340.

Yamamoto, M. and I. Nonaka (1988). "Skeletal muscle pathology in chronic progressive external ophthalmoplegia with ragged-red fibers." Acta Neuropathol **76**(6): 558-563.

Yamtich, J. and J. B. Sweasy (2010). "DNA polymerase family X: function, structure, and cellular roles." Biochim Biophys Acta **1804**(5): 1136-1150.

Yanagihara, H., J. Kobayashi, S. Tateishi, A. Kato, S. Matsuura, H. Tauchi, K. Yamada, J. Takezawa, K. Sugasawa, C. Masutani, F. Hanaoka, C. M. Weemaes, T. Mori, L. Zou and K. Komatsu (2011). "NBS1 recruits RAD18 via a RAD6-like domain and regulates Pol eta-dependent translesion DNA synthesis." Mol Cell **43**(5): 788-797.

Yang, J., Z. Chen, Y. Liu, R. J. Hickey and L. H. Malkas (2004). "Altered DNA polymerase iota expression in breast cancer cells leads to a reduction in DNA replication fidelity and a higher rate of mutagenesis." Cancer Res **64**(16): 5597-5607.

Yang, W. (2003). "Damage repair DNA polymerases Y." Curr Opin Struct Biol **13**(1): 23-30.

Yasukawa, T., A. Reyes, T. J. Cluett, M. Y. Yang, M. Bowmaker, H. T. Jacobs and I. J. Holt (2006). "Replication of vertebrate mitochondrial DNA entails transient ribonucleotide incorporation throughout the lagging strand." EMBO J **25**(22): 5358-5371.

Ying, S., F. C. Hamdy and T. Helleday (2012). "Mre11-dependent degradation of stalled DNA replication forks is prevented by BRCA2 and PARP1." Cancer Res **72**(11): 2814-2821.

Yoon, J. H., L. Prakash and S. Prakash (2009). "Highly error-free role of DNA polymerase eta in the replicative bypass of UV-induced pyrimidine dimers in mouse and human cells." Proc Natl Acad Sci U S A **106**(43): 18219-18224.

Yoon, J. H., L. Prakash and S. Prakash (2010). "Error-free replicative bypass of (6-4) photoproducts by DNA polymerase zeta in mouse and human cells." Genes Dev **24**(2): 123-128.

Yu, S., M. Mangelsdorf, D. Hewett, L. Hobson, E. Baker, H. J. Eyre, N. Lapsys, D. Le Paslier, N. A. Doggett, G. R. Sutherland and R. I. Richards (1997). "Human chromosomal fragile site FRA16B is an amplified AT-rich minisatellite repeat." Cell **88**(3): 367-374.

Yuasa, M. S., C. Masutani, A. Hirano, M. A. Cohn, M. Yamaizumi, Y. Nakatani and F. Hanaoka (2006). "A human DNA polymerase eta complex containing Rad18, Rad6 and Rev1; proteomic analysis and targeting of the complex to the chromatin-bound fraction of cells undergoing replication fork arrest." Genes Cells **11**(7): 731-744.

Zan, H., A. Komori, Z. Li, A. Cerutti, A. Schaffer, M. F. Flajnik, M. Diaz and P. Casali (2001). "The translesion DNA polymerase zeta plays a major role in Ig and bcl-6 somatic hypermutation." Immunity **14**(5): 643-653.

Zan, H., C. A. White, L. M. Thomas, T. Mai, G. Li, Z. Xu, J. Zhang and P. Casali (2012). "Rev1 recruits ung to switch regions and enhances du glycosylation for immunoglobulin class switch DNA recombination." Cell Rep **2**(5): 1220-1232.

Zeng, X., G. A. Negrete, C. Kasmer, W. W. Yang and P. J. Gearhart (2004). "Absence of DNA polymerase eta reveals targeting of C mutations on the nontranscribed strand in immunoglobulin switch regions." J Exp Med **199**(7): 917-924.

Zeng, X., D. B. Winter, C. Kasmer, K. H. Kraemer, A. R. Lehmann and P. J. Gearhart (2001). "DNA polymerase eta is an A-T mutator in somatic hypermutation of immunoglobulin variable genes." Nat Immunol **2**(6): 537-541.

Zeviani, M., S. Servidei, C. Gellera, E. Bertini, S. DiMauro and S. DiDonato (1989). "An autosomal dominant disorder with multiple deletions of mitochondrial DNA starting at the D-loop region." Nature **339**(6222): 309-311.

Zhang, H., A. Chatterjee and K. K. Singh (2006). "Saccharomyces cerevisiae polymerase zeta functions in mitochondria." Genetics **172**(4): 2683-2688.

Zhang, Y., X. Wu, D. Guo, O. Rechkoblit and Z. Wang (2002). "Activities of human DNA polymerase kappa in response to the major benzo[a]pyrene DNA adduct: error-free lesion bypass and extension synthesis from opposite the lesion." DNA Repair (Amst) **1**(7): 559-569.

Zhang, Y., X. Wu, O. Rechkoblit, N. E. Geacintov, J. S. Taylor and Z. Wang (2002). "Response of human REV1 to different DNA damage: preferential dCMP insertion opposite the lesion." Nucleic Acids Res **30**(7): 1630-1638.

Zhang, Y., F. Yuan, X. Wu, M. Wang, O. Rechkoblit, J. S. Taylor, N. E. Geacintov and Z. Wang (2000). "Error-free and error-prone lesion bypass by human DNA polymerase kappa in vitro." Nucleic Acids Res **28**(21): 4138-4146.

Zhu, H., H. Bhattarai, H. G. Yan, S. Shuman and M. S. Glickman (2012). "Characterization of Mycobacterium smegmatis PolD2 and PolD1 as RNA/DNA polymerases homologous to the POL domain of bacterial DNA ligase D." Biochemistry **51**(51): 10147-10158.

Zhu, H. and S. Shuman (2006). "Substrate specificity and structure-function analysis of the 3'-phosphoesterase component of the bacterial NHEJ protein, DNA ligase D." J Biol Chem **281**(20): 13873-13881.

Zlatanou, A., E. Despras, T. Braz-Petta, I. Boubakour-Azzouz, C. Pouvelle, G. S. Stewart, S. Nakajima, A. Yasui, A. A. Ishchenko and P. L. Kannouche (2011). "The hMsh2-hMsh6 complex acts in concert with monoubiquitinated PCNA and Pol eta in response to oxidative DNA damage in human cells." Mol Cell **43**(4): 649-662.

Zou, L., D. Cortez and S. J. Elledge (2002). "Regulation of ATR substrate selection by Rad17-dependent loading of Rad9 complexes onto chromatin." Genes Dev **16**(2): 198-208.

Zou, L. and S. J. Elledge (2003). "Sensing DNA damage through ATRIP recognition of RPA-ssDNA complexes." Science **300**(5625): 1542-1548.